Role of Cnot3 in gene regulation and cell cycle progression

Matteo Martufi

MRC Clinical Sciences Centre

Imperial College, Faculty of Medicine

Doctor of Philosophy

September 2014

Declaration of originality

The work presented in this PhD thesis is my own. The contributions of other people included in this work are indicated wherever presented or cited. Whenever the use of copyrighted material was needed, copyright holder's permission was obtained.

Copyright declaration

The copyright of this thesis rests with the author and is made available under a Creative Commons Attribution Non-Commercial No Derivatives licence. Researchers are free to copy, distribute or transmit the thesis on the condition that they attribute it, that they do not use it for commercial purposes and that they do not alter, transform or build upon it. For any reuse or redistribution, researchers must clear to others the licence terms of this work.

Abstract

Gene expression is a process that is tightly regulated by many factors. Different genes are transcribed not only in a cell specific manner but are also differentially expressed at different stages of the cell cycle. Cnot3 is part of the CCR4-NOT deadenylation complex, which is involved in the turnover of mRNAs in the cytoplasm and has also been shown to have roles in regulating transcription and cell proliferation and in maintaining ES cell pluripotency. Previous work demonstrated that Cnot3 interacts directly with Aurora B kinase and is phosphorylated by Aurora B in an i*n vitro* assay. Aurora B and Cnot3 co-localise at active gene promoters in resting B cells. Since Aurora B is a cell cycle kinase, I have developed a cell synchronization system to analyse the role of the Cnot3-Aurora B interaction at different stages of the cell cycle in primary B cells. Using this system, I have demonstrated that the interaction between Cnot3 and Aurora B varies during cell cycle progression*. In vitro* analysis showed that the interaction occurs through the NOT box domain of Cnot3. Mass spectrometry analysis of Cnot3 interactors, performed on nuclear extracts from B cells in the early G1 and G2 phases of the cell cycle, identified interactions with many factors that are known to have roles in transcription regulation and RNA processing. Interaction of Cnot3 with Histone H1 was confirmed using a peptide binding assay, suggesting a potential role in chromatin organization. Cnot3 was also shown to interact with Xrn2, a 5'-3' exoribonuclease that is involved in RNA turnover and termination of transcription. ChIP analysis demonstrated promoter binding of Cnot3 at a number of cell cycle stages. Cnot3 shows cell cycle dependent binding to promoters of a wide range of active genes, including promoters that are not directly involved in cell cycle regulation. Genome wide analysis using ChIP sequencing revealed changes in the binding profiles of Cnot3 at promoters and enhancers during cell cycle progression. A Cnot3 conditional knock out mouse has been generated, which will be used to test the functional importance of these observations.

Acknowledgments

I would like to thank Professor Niall Dillon who gave me the opportunity to work on this project and has given me a wise and great supervision during my PhD. I would also like to thank the MRC that funded my PhD. Thanks to Piera, Anne-Marie, Natalia, Inesa, Parvin, Rob, Alberto, Jonathan, Holger in the GRC group.

A massive thanks goes to Monica, mi hermana. This PhD could not be possible without you. A really clever scientist who taught me many things in these years. Thanks for always being there for me when I needed support, when I needed to find my way in life, when I needed a good friend or simply a breakito.

Thanks to Gopu and Tom for introducing me in the elaborate world of the bioinformatics and to Peter for the lessons on Mass Spec.

When four years ago I moved to London, the foreigner with the funny accent, I had many doubts. It was the most difficult decision in my life. The opportunity to live in this city was a dream for me. During this time I met many people that have made my experience here unforgettable. Since my first day here, I have been surrounded by lots of friends from all around the world. However, these years have been difficult as well. I fell many times, I went through difficult moments and I got over them thanks to many friends who always supported me. Thanks for all you have done for me!

A special thanks is for Silvia. Thanks for dealing with me not just in the lab but also at home, for laughing to my silly jokes, for enjoying my dirty stuff in your room, for understanding the crazy side of Matteo and make fun of it. I will always bring with me all the moments when we could not stop laughing. Thanks, you are special to me.

Thanks to Joana. I have always felt at home even if I was leaving at your place, thanks for welcoming me in your house and for all the “silly” comments you have always provided. Together we have shared very good moments. Thanks for being such a good friend, Obrigado!

Thanks to Hakan. Mate we made it there then!! Thanks for Glastonbury in first place!! We would have never made it without you. Thanks for your support, for cheering me up everytime that I was down with your funny jokes.

Thanks to Sadaf!!!!! Hats off to you miss for all your amazing pranks, for the coconut water, for your contagious happiness, for playing with me all the time. Thanks for the skittles when I was confused and for supporting me in those days.

Thanks to Niko for all the moments he made fun of me because of my way of being Italian. You have been a good friend and we had lots of fun together. Graçias Frato’!

Thanks to Thomas for being such a funny Fif and to Margie for respecting my timings and being supportive and funny with me.

Thanks to Georgia! Although my English still keeps a funny accent you always understood my Italian humour. We had lots of fun together. Thanks for sharing with me your joy of life.

Thanks to my Berlin friend Joao who left us to find glory in Germany. Frato' your support to make fun of Silvia was priceless and all the words you taught me in Portuguese will be very useful.

Thanks to Nicola for his way to be so "kind" with people that always made me laugh. Thanks to Preksha for being supportive all the time, to Olly who learned how not be tricked by an italian, to Ziwei, for sharing the thesis experience, to Marie-Therese for being a bit crazy. Thanks to Andy, Jorge, Vlad, Sergi and the other guys in Lymphocyte Development for the breaks from science.

Many thanks to Stefano, my first friend in London. Thanks for all the chatting until 2am, for always being positive and supportive, for laughing with me to our roman jokes. Thanks to Francesca, mia sorella. Thanks for all time spent together during these years, for your strong support and suggestions. You were always there when I needed. Thanks to all my friends in London.

Thanks to all my Italian friends, my biggest fans for this PhD, to my fiuggini friends for all your support, your craziness, your unique way of being funny. Thanks to my friends around Ciociaria and Rome.

Thanks to Manu, Alex and Danilo for the times spent together in Rome in lab and going out. You introduced me to science and all your suggestions have always made difference for me!

The biggest thank you is for my Ilaria. These years have been difficult, the distance has been a tough enemy to fight against. You have always been there for me, you have always supported me like no one else. Your smile, your way to cheer me up and make me laugh are things that made me a really lucky guy to have you in my life. More than everything thank you for being there when I did not deserve it.

L'ultimo ringraziamento va alla mia famiglia. Un'isola felice nella mia vita. Grazie a nonna Elfina, Grazie a nonno Pierino e nonna Giulia che mi hanno voluto un sacco bene e Grazie ai miei zii. Grazie a Pierino, Martina e alla bellissima Elena, a Paolo e Caterina, a Marco, Grazie per avermi fatto crescere in una famiglia splendida, unica al mondo.

Grazie a Mamma e Papa' per tutti i sacrifici che avete fatto per me, per tutto il vostro aiuto e supporto. Siete le persone piu' belle che io conosca ed ogni giorno cerco di mettere in pratica i vostri insegnamenti, vi voglio bene…. Durante questi anni io ci ho sempre creduto!!!

Table of Contents

Declaration of originality **2**
Copyright declaration **3**
Abstract **4**
Acknowledgments **5**

Table of Contents **7**
List of figures **10**
List of tables **12**
Supplementary table and figure **13**
Abbreviations **14**

Chapter 1 - Introduction **17**
1.1 Overview **17**
1.2 Cell cycle **17**
1.2.1 Cell cycle checkpoints 18
1.2.2 The restriction point 20
1.2.3 Regulation of quiescence 21
1.2.4 Mitosis and cytokinesis 23
1.2.5 The role of Aurora B in cell cycle progression 25
1.3 Transcriptional regulation **27**
1.3.1 Transcription is regulated by post-translational modifications and histone variants 27
1.3.2 Chromatin remodelers affect chromatin conformational state 30
1.3.3 Transcription performed by RNA polymerase II: initiation, elongation and termination 31
1.3.3.1 Initiation 32
1.3.3.2 Transcriptional elongation 34
1.3.3.3 Termination 36
1.4 Splicing is a two-step reaction **38**
1.4.1 Alternative splicing as a source of variation 41
1.5 RNA decay **43**
1.6 The CCR4-NOT complex is involved in many cellular processes **47**
1.7 The role of CNOT3 in gene expression and cell cycle control **50**
1.7.1 Involvement of CNOT3 in human disease 52
1.8 Development of B lymphocytes and regulation of the B cell cycle **53**
1.8.1 T-dependent and T-independent B cell activation 57
1.9 Aim of the study **59**

Chapter 2 Material and methods **60**
2.1 Resting B cell isolation **60**
2.2 B cell culture and synchronization **60**
2.3 ES cell culture, electroporation and crystal violet staining **61**
2.4 Aurora B conditional knockout mice **61**
2.5 FACS analysis **62**
2.5.1 PI staining 62
2.5.2 Staining of cell surface markers 62
2.5.3 EdU incorporation assay 62

2.6 DAPI staining 63
2.7 Proteomics 63
2.7.1 Nuclear protein extraction for IP 63
2.7.2 Co-immunoprecipitation and western blotting 64
2.7.3 GST Aurora B protein expression, extraction and purification 65
2.7.4 *In vitro* transcription/translation 66
2.7.5 GST pull down assay 67
2.7.6 Mass Spectrometry (MS) analysis 67
2.7.7 *In vitro* peptide binding assay 68
2.8 Chromatin Immunoprecipitation 69
2.8.1 Chromatin preparation 69
2.8.2 Immunoprecipitation 70
2.8.3 Quantitative real-time PCR 71
2.9 ChIP-sequencing (ChIP-seq) 72
2.9.1 Preparation of libraries 72
2.9.2 Data analysis and peak calling 72
2.9.3 Density plot generation 73
2.9.4 Gene ontology analysis 74
2.10 Transcriptional Analysis 74
2.10.1 Spike-in preparation 74
2.10.2 Isolation of nuclear RNA and preparation of cDNA 75
2.10.3 RNA quantification 76
2.11 Cnot3 conditional knockout mice 76
2.11.1 TALEN design and construction 76
2.11.2 TALEN mRNA and targeting vector preparation 80
2.11.3 Microinjection into mouse oocytes 80
2.11.4 Genotyping of mice 80

Chapter 3 -Interaction of Cnot3 with the AuroraB kinase during the B cell cycle 83
3.1 Introduction 83
3.2 Characterization of a B cell system to study different phases of the cell cycle 84
3.3 Characterisation of the interaction between Cnot3 and Aurora B during cell cycle progression 88
3.4 *In vitro* analysis of the interaction between Cnot3 and Aurora B 91
3.5 Summary 93

Chapter 4 - Analysis of Cnot3 interactors in early G1 and G2 94
4.1 Introduction 94
4.2 Mass spectrometry analysis of Cnot3 interactors 94
4.3 Cnot3 interacts with chromatin organization factors and splicing factors in early G1 cells 96
4.4 *In vitro* interaction Cnot3-histone H1 98
4.5 In G2 Cnot3 interacts with components of the CPC complex and proteins involved in RNA maturation 99
4.6 Cnot3 interacts with the Xrn2 5'-3'exoribonuclease 103
4.7 Summary 105

Chapter 5 - Cell cycle regulated binding of Cnot3 to gene promoters 106
5.1 Introduction 106
5.2 Aurora B and Cnot3 co-occupy promoters of active genes in resting B cells 106
5.3 Binding of Cnot3 to promoters in resting B cells is not affected by Aurora B depletion 108

5.4 Binding of Cnot3 to gene promoters during cell cycle progression 110
5.5 Analysis of Cnot3 binding to gene promoters during S phase 111
5.5.1 Pcna binds to gene promoters during S phase 114
5.6 Analysis of transcription levels during cell cycle progression 115
5.7 Xrn2 binds to promoters of active genes in resting and G2 cells 118
5.8 Summary 119

Chapter 6 - Genome wide binding profiles of Cnot3 during cell cycle progression 120
6.1 Introduction 120
6.2 Genome wide binding of Cnot3 to chromatin is cell cycle regulated 120
6.3 The binding profile of Cnot3 at the TSS changes during cell cycle 124
6.4 Comparison of peaks of Cnot3 binding during cell cycle progression 127
6.5 Summary 131

Chapter 7 - Design and generation of Cnot3 conditional knock out mouse 132
7.1 Introduction 132
7.2 TALEN targeting of the *Cnot3* gene 132
7.3 Testing of the TALEN constructs in ES cells 134
7.4 Generation of Cnot3 conditional knockout mouse 136
7.5 Summary 137

Chapter 8 - Discussion 139
8.1 Overview 139
8.2 Cnot3 interacts with the cell cycle regulator Aurora B 141
8.3 The interaction of Cnot3 with histones suggests a role in transcriptional regulation 143
8.4 Cnot3 binds chromatin in a cell cycle dependent manner 144
8.5 Involvement of Cnot3 with the RNA processing machinery 145
8.6 Future directions: characterization of Cnot3 knockout mouse 146
Bibliography 147
Appendix 171

List of figures

Figure 1.1: Representation of the cell cycle phases. 17
Figure 1.2: Transcriptional regulation of Rb and FoxM1 20
Figure 1.3: Chromosomal Passenger Complex (CPC). 24
Figure 1.4: Schematic representation of nucleosomal core histone variants and post-translational modifications 29
Figure 1.5: RNA polymerase II cycle of transcription. 32
Figure 1.6: Promoter proximal pausing of Pol II. 35
Figure 1.7: mRNA transcription termination. 38
Figure 1.8: Schematic representation of sequence elements within introns 39
Figure 1.9: Spliceosome complexes and splicing process. 41
Figure 1.10: Regulation of splicing by SR and hnRNP proteins. 43
Figure 1.11: RNA decay pathways. 44
Figure 1.12: Human CCR4-NOT complexes showing different compositions with respect to their deadenylases subunits. 48
Figure 1.13: Hematopietic stem cell differentiation. 55
Figure 1.14: Anatomy of the spleen. 57
Figure 3.1: Characterization of the B cell population. 84
Figure 3.2: Activation of resting B cells by treatment with anti-IgM antibody. 85
Figure 3.3: LPS response of anti-IgM treated cells. 86
Figure 3.4: Synchronization of B cells in S phase. 87
Figure 3.5: Populations of cells enriched in G2 and M phases. 88
Figure 3.6: Interaction between Aurora B and Cnot3 in resting B cells. 89
Figure 3.7: Interaction between Aurora B and Cnot3 during cell cycle progression in primary B cells. 91
Figure 3.8: Schematic representation of the domain structure of wild-type human CNOT3 and the deletions of mouse Cnot3 used in the GST pull down assays. 92
Figure 3.9: Mapping of Cnot3-Aurora B interaction. 93
Figure 4.1: Gene ontology analysis of Cnot3 interactors in early G1 and G2 cells. 95
Figure 4.3: Cnot3 *in vitro* interaction with histone H1 peptides. 99
Figure 4.4: Gene ontology analysis of Cnot3 interactors in G2. 101
Figure 4.6: Xrn2 interaction with Cnot3 in mid-late S phase and G2. 103
Figure 4.7: Interaction of Aurora B and Xrn2 in mid/late S phase and G2. 104
Figure 4.8: Xrn2 interaction with Aurora B and Cnot3 in resting B cells. 105
Figure 5.1: Aurora B and Cnot3 bind the same active gene promoters. 107
Figure 5.2: Cnot3 binds gene promoters in Aurora B knock out cells. 109
Figure 5.3: Binding of Cnot3 to gene promoters during cell cycle progression. 111

Figure 5.4: EdU incorporation in resting and anti-IgM+LPS treated B cells. 112
Figure 5.5: Binding of Cnot3 to gene promoters in resting B,
mid-late S phase and anti-IgM+LPS 14 hours. 113
Figure 5.6: Pcna binds gene promoters in S phase. 114
Figure 5.7: Analysis of primary transcripts during cell cycle progression
of activated B cells. 116
Figure 5.8: Analysis of nuclear mRNA during cell cycle progression
of activated B cells. 117
Figure 5.9: Xrn2 binding to gene promoters in resting and G2 B cells. 119
Figure 6.1: ChIP-seq analysis of Cnot3 binding at different stages
of the cell cycle during B cell activation. 123
Figure 6.2: Cnot3 binding around the TSS during cell cycle progression. 126
Figure 6.4: Distribution of Cnot3 binding peaks during cell cycle progression. 128
Figure 6.5: ChIP-seq analysis of Cnot3 binding at different stages
of the cell cycle during B cell activation on enhancer regions. 130
Figure 7.1: TALEN targeting. 133
Figure 7.2: Strategy to flox *Cnot3* gene. 134
Figure 7.3: Crystal violet staining of ES cells after neomycin selection. 135
Figure 7.4: Genotyping of the *Cnot3* gene. 137
Figure 8.1: Schematic representation of the domain structure of human CNOT3. 140

List of tables

Table 2.1: Antibodies. 81
Table 2.2: Primers for ChIP (promoter region). 81
Table 2.3: Primers for primary transcript analysis. 82
Table 2.4: Primers for mRNA analysis. 82
Table 4.2: Early G1 interactors of Cnot3. 97
Table 4.5: Cnot3 interactors in G2. 102
Table 6.3: Number of peaks of Cnot3 binding called for each cell cycle phase. 127

Supplementary table and figure

Table A: Cnot3 interactors in early G1 and G2. 171

Figure B: Snapshots of ChIP-seq tracks of Cnot3 binding during cell cycle progression. 183

Abbreviations

APC	Antigen Presenting Cell
BAFF	B-cell Activating Factor
BCR	B Cell Receptor
Bp	Base pair
BS	Branch Site
BSA	Bovine Serum Albumin
CBC	Cap-Binding Complex
CDK	Cyclin Dependent Kinase
CDKI	Cyclin Dependent Kinase Inhibitor
cDNA	Complementary DNA
CF	Cleavage Factor
ChIP	Chromatin Immunoprecipitation
ChIP-seq	Chromatin Immunoprecipitation sequencing
cKO	conditional Knockout
CLP	Common Lymphoid Progenitor
Co-IP	Co-Immunoprecipitation
CPC	Chromosomal Passenger Complex
CS	Connector Sequence
CTD	Carboxy Terminal Domain
CPSF	Cleavage and Polyadenylation Specificity Factor
CSTF	Cleavage stimulation factor
Dcp	Decapping
dpc	days post coytum
dNTP	deoxyribonucleotide
DS	Double Strand
DSIF	DRB Sensitivity Inducing Factor
eIF4F	translation initiation factor 4F
EJC	Exon Junction Complex
ER	Endoplasmatic Reticulum
ERa	Estrogen Receptor a
ESC	Embrionic Stem Cell
ESE	Exonic Splicing Enhancers
ESS	Exonic Splicing Silencers
FCS	Fetal Calf Serum
FW	Forward
G0	G zero phase
G1	Gap phase 1
G2	Gap phase 2
GAP	GTPase Activating Protein
GSH	Glutathione Sepharose High performance

GTF	General Transcription Factors
HDAC	Histone Deacetylase
HFD	Histone Fold Domain
hnRNP	heterogeneous nuclear ribonucleoproteins
HRP	horseradish peroxidase
HSC	Hematopioetic Stem Cell
HP1	Heterocromatin Protein 1
Ig	Immunoglobulin
Ig-H	Immunoglobulin Heavy chain
Ig-L	Immunoglobulin Light chain
IP	Immunoprecipitation
iPS	Induced Pluripotent Stem cell
IPTG	Isopropyl β-D-1-thiogalactopyranoside
ITAM	Immunoreceptor Tyrosine-based Activation Motis
Kb	kilobase
LPS	LipoPolySaccharide
MACS	Model-based Analysis for ChIP-seq
MHC	Major Histocompatibility Complex
MEF	Mouse Embryonic Fibroblast
miRNA	microRNA
MNase	Micrococcal Nuclease
MPP	MultiPotent-Progenitor cells
mRNA	mature RNA
MS	Mass Spectrometry
NAR	NOT1 Anchor Regions
ncRNA	Non coding RNA
NELF	Negative elongation factor
NGD	No-Go Decay
NLS	Nuclear Localization Signal
NMD	Non-sense Mediated Decay
NSD	Non-Stop Decay
P bodies	Processing bodies
PABP	Poly-A Binding Protein
PALS	PeriArteriolar Lymphoid Sheath
PAP	Poly-A Polymerase
PBS	Phosphate Buffered Saline
PIC	Pre Initiation Complex
Pol II	Rna Polimerase II
PTC	Premature Termination Codon
PTK	Protein Tyrosine Kinase
qRT-PCR	quantitative real time PCR
RARa	Retinoi acid receptor alfa
Rb	Retinoblastoma
RNA seq	RNA sequencing

RNP	Ribonucleoprotein
rNTP	ribonucleotide
RP	Retinitis Pigmentosa
RPM	Revolutions per minute
rRNA	Ribosomal RNA
RV	Reverse
RVD	Repeat Variable Di-residue
RXRb	Retinoid X Receptor beta
S phase	Synthesis phase
SAC	Spindle Assembly Checkpoint
SNP	Single Nucleotide Polymorphism
snRNA	small nuclear RNA
T-ALL	T-cell acute lymphoblastic leukemia
TALEN	Transcription Activator Like Effector Nucleases
TLR	Toll Like Receptor
TRa	Thyroid hormone receptor alpha
tRNA	Transfer RNA
TSA	Trichostatin A
TSS	Transcription Start Site
UTR	Un-translated region
V(D)J	Variable (Diversity) Joining
3'SS	3’ splice site
4-OHT	4-hydroxytamoxifen
5'SS	5’ splice site

Chapter 1- Introduction

1.1 Overview

Cnot3 is a member of the CCR4-NOT deadenylase complex, which controls mRNA turnover and has also been implicated in transcriptional and cell cycle control. Co-immunoprecipitation and mass spectrometry analysis identified Cnot3 as a major interactor with the chromosomal passenger complex (CPC), which has major roles in orchestrating mitosis and cytokinesis through the activity of its catalytic component, the Aurora B kinase. The interaction suggests that Cnot3 could be involved in some of the many functions that have been identified for the CPC. The aim of this project was to investigate the role of Cnot3 in gene regulation and cell cycle progression in B cells.

1.2 Cell cycle

The concept of a 'cell cycle' was first explored around 50 years ago when the mitotic cycle was described as having 4 phases. Cell cycle was therefore sub-divided into Gap phase 1 (G1), DNA synthesis (S phase), Gap phase 2 (G2) and Mitosis (M) (Figure 1.1). This study was the first one that gave a description of the length of the cell cycle (Sisken and Morasca, 1965).

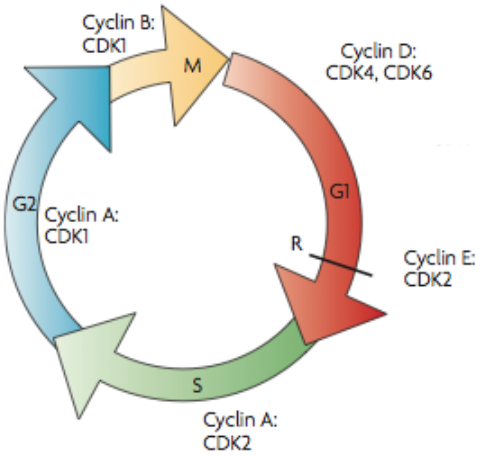


Figure 1.1: Representation of the cell cycle phases.
The chart shows the phases of the cell cycle. Each phase is charachterized by the presence of different active cyclin/CDK complexes. G1 is divided into two parts by the restriction point (Adapted from (Dehay and Kennedy, 2007)).

During the G phases, cells are actively transcribing the genome in order to prepare for correct DNA replication and cellular division. The process of cellular division occurs after G2, and represents a crucial moment for the formation of two daughter cells carrying identical genetic material. The duration of the cell cycle phases is different among species and cell types. There are a few examples where gap phases are very short and cells spend most of the time in S phase. Murine and human embryonic stem cells (Stead et al., 2002) and embryonal germ cells (Resnick et al., 1992) have a fast cell cycle composed mainly of S phase and a very short G1 and G2. In these cells the cell cycle structure resembles the one present in lower vertebrates, where the cell cycle is essentially composed by rounds of S phase and mitosis (Murray and Kirschner, 1989). Mammalian somatic cells usually complete a cell cycle in about 24 hours and cells spend most of the time in G1. During G1 and G2, cells grow in size and production of RNAs and proteins increases.

The progression through each phase of the cell cycle is governed by cellular checkpoints, which are regulated by different complexes. The proteins in charge of controlling phase transitions are complexes formed by Cyclin-Dependent Kinases (CDKs) and cyclins (Pavletich, 1999). During the cell cycle, the activity of CDK-cyclin complexes is regulated by the cell cycle dependent expression of cyclins. Several cyclins are expressed in mammals and once they have completed their functions in a specific cell cycle phase, they are degraded (Evans et al., 1983). The presence of complexes controlling different cellular checkpoints is necessary to achieve a fine regulation of the cell cycle.

1.2.1 Cell cycle checkpoints

Cell checkpoints are control mechanisms that the cell uses to ensure that processes such as DNA replication or mitosis are carried out properly. Cell cycle checkpoints are controlled by different CDK-cyclin complexes that are active at different times during cell cycle (Arellano and Moreno, 1997). CDK activity is controlled by binding to cyclins and by the action of two classes of inhibitors. These inhibitors are grouped into two families: the INK4 and the Cip/Kip families. The INK4 inhibitors are specific for CDK4 and CDK6, and regulate the G1/S transition. They impede the catalytic site of CDKs, blocking their activity

and inducing cell cycle arrest (Serrano et al., 1993). The other family of CDK inhibitors is represented by the Cip/Kip family and exert their functions in a broader manner throughout the cell cycle through inhibition of cyclins D, A, B, E. The CDKIs, p21 and p27 (Harper et al., 1993; Toyoshima and Hunter, 1994) are included in this group.

Cyclins represent the regulatory part of the cyclin-CDK complexes. They are expressed in a cell cycle dependent manner and mediate temporal regulation of the activity of CDKs. Their stability is controlled by proteasomal degradation via two different families of E3 ubiquitin ligases: the SCF complex, which is active from late G1 to mitosis, and the APC/C complex, which operates from anaphase to late G1 (Nakayama and Nakayama, 2006).

CDKs phosphorylate the Retinoblastoma (Rb) protein whose activity is regulated by its phosphorylation state. Rb regulates the G1/S transition by inhibiting S phase genes, including cyclin E (Weinberg, 1995). In early G1, cyclin D is expressed and forms a complex with CDK4 or CDK6. Rb is phosphorylated by CDK4/6 and it switches from a non-phosphorylated to a hypophosphorylated form (Connell-Crowley et al., 1997). In this state the transcriptional inhibition caused by Rb is only partial and consequently cyclin E can be transcribed. Cyclin E is expressed in late G1, due to the release of HDAC1 from its interaction with Rb and consequent activation of the cyclin E promoter (Harbour et al., 1999). However, the inhibitory power of Rb is not totally blocked because it can still bind to and repress E2F, which is responsible for transcription of S phase specific genes (Bagchi et al., 1991). Transcription of cyclin E leads to the activation of its binding partner CDK2, which generates a hyperphosphorylated form of Rb. This conformation of Rb cannot interact with E2F and consequently S phase-specific genes are transcribed due to E2F release (Morris et al., 2000).

One of the consequences of E2F transcriptional activity is also that it promotes the expression of cyclin A (Soucek et al., 1997). Cyclin A keeps CDK2 in an active state, which keeps Rb in a phosphorylated and inactive state (Akiyama et al., 1992). Moreover, cyclin A-CDK2 is present during S phase, while cyclin B–CDK1 is active in G2 and during mitosis. The hyperphosphorylated form of Rb is retained until the mitotic process is completed. Cyclin A-CDK2 and cyclin B-CDK1 phosphorylate the transcription factor FoxM1 during G2 promoting its

activation (Laoukili et al., 2008) (Chen et al., 2009). Phosphorylated FoxM1 is able to bind to its co-activator partner CBP and together they stimulate transcription of genes involved in mitosis (Major et al., 2004) (Figure 1.2).

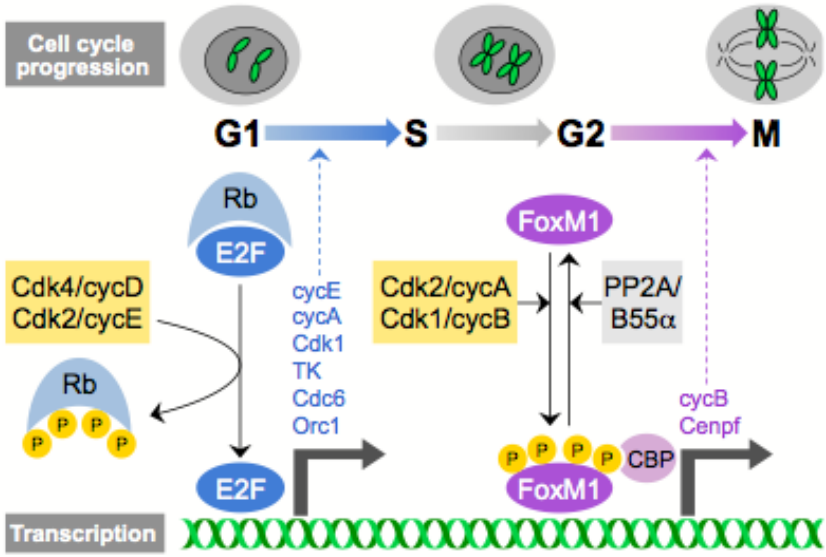


Figure 1.2: Transcriptional regulation of Rb and FoxM1.
Rb phosphorylation by the Cdk4/cycD and Cdk2/cycE complexes releases E2F from Rb inhibition. E2F is required for transcription of S phase genes. Phosphorylation of FoxM1 promotes its activity. During G2 it is phosphorylated by Cdk2/cycA and Cdk1/cycB. This leads to self-activation and promotes binding to CBP, which is a co-activator. Activation of FoxM1 leads to transcription of genes required during mitosis. The phosphorylation state of FoxM1 is counteracted by the action of the phosphotase PP2A/B55α.
(Adapted from (Lim and Kaldis, 2013)).

1.2.2 The restriction point

The existence of the restriction point was first hypothesized in 1974 when Pardee *et al.* showed that during G1, cells decide whether to proceed through the cell cycle or become quiescent (Pardee, 1974). A better characterization was provided by Zetterberg *et al.* who analysed the restriction point in serum starved Swiss 3T3 cells. They demonstrated that the restriction point was located 3.5 hours after cell cycle re-entry in response to mitogenic stimuli. Therefore, they divided G1 into two parts: G1 post-mitotic before the restriction point and G1-

pre-S after the restriction point. The presence of mitogenic stimuli during G1 was the determining factor for a cell to decide whether to go through S phase or not (Zetterberg and Larsson, 1985). However, a recent study has revealed new details about the decision to undergo cell cycle progression. Spencer *et al.* confirmed the data published by Zetterberg *et al.* by showing that serum starved cells, once back in the cell cycle, are susceptible to the presence of mitogenic stimuli before reaching the restriction point. This is mainly due to the low levels of CDK2 and the hypophosphorylated state of Rb (Spencer et al., 2013). They also showed that cycling MCF10A cells behave differently to serum-starved Swiss 3T3 cells. In cycling MCF10A cells the decision to proceed to S phase is dependent on levels of CDK2 in the previous cycle. Levels of CDK2 accumulate after formation of the nuclear envelope and are inversely proportional to CDKI p21. Withdrawal of mitogenic stimuli from these cells does not cause an immediate exit from the cell cycle. The deprivation of mitogenic stimuli will determine low levels of CDK2 in the next cell cycle due to high levels of p21. During the following G1, the presence or absence of mitogenic stimuli will determine whether cells will cycle or become quiescent (Spencer et al., 2013).

1.2.3 Regulation of quiescence

Quiescence is a reversible state of the cell, which is called G0, and can be activated due to different reasons, such as serum starvation, contact inhibition and loss of adhesion. The quiescent state is thought to preserve the genome from damage and to allow cells to respond to particular external stimuli. Cells in a G0 state present some distinctive features, such as low rate of transcription and translation, hypophoshorylated Rb, low levels of CDK2 and high levels of p21 (Spencer et al., 2013). Indeed, quiescent cells can re-enter the cell cycle following a mitogenic stimulus. They have unique characteristics and in the last decade increasing evidence has been obtained for the existence of a quiescence program. Quiescence does not correspond to dormancy, because cells are active. However, processes such as DNA replication and cell division that require a large amount of energy and the activation of biosynthetic pathways, are inhibited. The transcription and translation rates are also much lower than in cycling cells.

As described above, there are known molecular mechanisms and transcription programmes that drive cells towards quiescence. The restriction point was first described using mitogenic stimulation of quiescent serum starved fibroblasts (Zetterberg and Larsson, 1985). One of the first experiments to characterize quiescence in a more detailed way was carried out by Coller *et al.*. They studied the activation of quiescence transcription program in fetal human lung diploid fibroblasts following three different pathways. The G0 state was generated either by loss of adhesion, contact inhibition, serum starvation or by combining all three states. They revealed that each of these conditions activated a different pathway to achieve quiescence, and showed that synergy between the pathways resulted in a robust activation of a quiescence program (Coller et al., 2006). According to their work many genes were upregulated, including genes involved in suppressing apoptosis or differentiation, and many others were downregulated, for example genes required for cell cycle progression, DNA replication or mitosis. Moreover, they also showed that a cell cycle arrest due to CDK inhibitors activated a different set of genes, not resembling the quiescent program. They concluded that cell cycle arrest and quiescence are two separate events (Coller et al., 2006).

Quiescent cells are active cells that direct their metabolic processes in a different direction than the cell cycle. To reinforce the theory of a specific transcription program, Chen *et al.* generated serum starved human foreskin fibroblasts. They showed fibroblasts that undergo quiescence are more responsive to inflammatory responses, activating genes such as COX-2 and IL-2, which are downregulated in cycling fibroblasts (Chen et al., 2012). A very recent study comparing G0 and G1 mouse embryonic fibroblasts supports the idea of a specific quiescence program. The analysis showed that G1 cells transcribed genes involved in mitosis, cell cycle, proliferation whereas G0 cells expressed genes coding for epigenetic regulators, inflammatory responses and tumor suppressors (Oki et al., 2014). Studies in lymphocytes have shown a requirement of activating genes such as Gadd45 and repressing others such as Myc (Glynne et al., 2000). Two major groups of transcription factors that play an important role in lymphocyte quiescence are the KLF family proteins and the FOXO proteins.

These two class of proteins cause a reversible exit of the cell cycle by acting on cell cycle checkpoints and proliferative factors (Yusuf and Fruman, 2003).

1.2.4 Mitosis and cytokinesis

Mitosis is the stage of the cell cycle that follows immediately after G2 and is characterized by five stages: prophase, metaphase, anaphase, telophase and cytokinesis. During prophase, chromosomes condense and centrosomes at opposite poles create a mitotic spindle composed of microtubules. Each kinetochore structure on chromosomes binds to microtubules on the spindle. Once chromosomes are bound to spindle microtubules, they are aligned to form a metaphase plate. At this point, if there is aberrant binding of the microtubules to the kinetochores, the spindle assembly checkpoint (SAC) is activated to avoid aberrant segregation of chromosomes (Musacchio and Salmon, 2007). This involves many proteins and is needed to correct microtubule-kinetochore misalignment (Li and Nicklas, 1995). When the metaphase plate is set, chromosomes start to migrate at opposite poles during anaphase. Microtubules with different orientation that are present in the central part of the spindle start to form a structure called the spindle midzone (Glotzer, 2009). The spindle midzone gives rise to the contractile ring, which is needed for cell division. During telophase and cytokinesis the cell progresses through division with the formation of the cleavage furrow which results in division into two daughter cells (D'Avino et al., 2005).

The Chromosomal Passenger Complex (CPC) has been implicated in many steps during mitosis, particularly in the SAC and in cytokinesis (Sampath et al., 2004). The CPC complex is composed by four proteins: INCENP, Aurora B kinase, Borealin and Survivin (Figure 1.3). The scaffold protein in the complex is INCENP, which binds the other three proteins. INCENP is responsible for activating Aurora B, which is the catalytic component of the complex (Adams et al., 2001). Binding of the INCENP IN-Box motif to Aurora B activates the kinase, which in turn auto-phosphorylate at Thr232, to achieve full activation, and then phosphorylates INCENP (Honda et al., 2003).

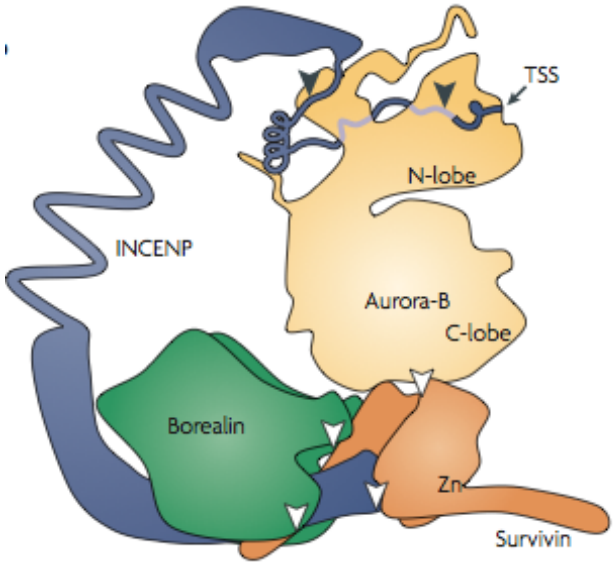


Figure: 1.3: Chromosomal Passenger Complex (CPC).
The CPC is composed by four subunits: Aurora B kinase, INCENP, Borealin, Survivin. INCENP is the scaffold protein that interacts with the other three subunits. Activation of the complex is triggered by binding of INCENP to Aurora B. This promotes autophosphorylation and phosphorylation of other components to achieve full activation.
(Adapted from (Ruchaud et al., 2007)).

In mitosis the CPC complex is first present on chromosome arms and then progressively migrates towards centromeric chromatin. Phosphorylation of histone H3S10 by Aurora B on the centromeric heterochromatin and binding of INCENP promote the displacement of the Heterochromatin Protein 1 (HP1) from histone H3K9me3 (Hirota et al., 2005). The migration of the CPC from the chromosomal arms towards the pericentromeric chromatin regulates the correct orientation of sister kinetochores attachment to opposite spindle poles (Tanaka et al., 2002). Furthermore, after the migration of CPC towards the centromere, Aurora B interacts with and phosphorylates the centromeric histone variant CENP-A (Zeitlin et al., 2001). The presence of minor satellite RNA also seems to have a role in recruiting the CPC to the centromeric region (Ferri et al., 2009). The RNA not only influences the Aurora B CENP-A interaction but also the binding of the kinase to Survivin. It has been reported that the kinase activity of Aurora B is considerably reduced in the absence of RNA (Ferri et al., 2009). These results have been confirmed very recently by Jambhekar *et al*. showing the presence of RNA in a complex with the CPC, and presenting evidence that the presence of RNA in the complex affects CPC localization (Jambhekar et al., 2014).

The presence of the CPC at the kinetochore is important to ensure formation of a correct SAC and to avoid problems with microtubule attachment. The CPC is localized at the inner kinetochore and is able to recognize incorrect or missing binding between kinetochores and microtubules (Kelly and Funabiki, 2009). Syntelic or merotelic binding of chromosomes to spindle poles would result in generation of aneuploid cells. When incorrect binding occurs, the CPC can sense the loss of tension in the attachment of microtubules. Consequently, the SAC is triggered to allow the cell to remedy the incorrect binding. This mechanism promotes phosphorylation of kinetochore proteins by Aurora B, causing release of the microtubules (Lampson et al., 2004). Once all of the chromosomes are bound to the spindle in a correct orientation, the SAC is repressed and chromosomes can migrate towards the spindle poles during anaphase (Sampath et al., 2004).

The CPC remains in the midbody during anaphase, where it promotes the formation of the cleavage furrow. During telophase a contractile ring in the midzone initiates cellular division, which will be completed in cytokinesis (Miller, 2011). The CPC is localized in the midzone during telophase and its components are important for completion of cytokinesis. INCENP localizes at the inner plasma membrane in the cleavage furrow (Earnshaw and Cooke, 1991). Aurora B has been shown to be required for normal cytokinesis. Expression of a kinase-dead Aurora B can cause abortive cytokinesis, leading to formation of diploid cells (Terada et al., 1998). One of the functions of Aurora B during cytokinesis is to phosphorylate components of the cytoskeleton. Vimentin is a target of Aurora B and is required for correct division (Goto et al., 2003). It has also been shown that another target of Aurora B is the GTPase activating protein (GAP) MgcRacGAP, which is essential for cytokinesis. Loss of phosphorylation of MgcRacGAP by Aurora B leads to polyploidy (Minoshima et al., 2003).

1.2.5 The role of Aurora B in cell cycle progression

The end of mitosis marks the beginning of a new cell cycle for the two new daughter cells. After peaking in mitosis, levels of Aurora B drop dramatically after mitotic exit. The kinase is a target for the anaphase promoting complex

(APC/C), which poly-ubiquitinates Aurora B and promotes its degradation via the proteasome (Stewart and Fang, 2005).

The role of Aurora B in the regulation of mitosis has been extensively described. Protein levels of Aurora B in G1 are much lower than in mitosis but are still detectable (Kimura et al., 2004). A study carried out by Song *et al.* provided evidence that Aurora B is in a complex together with mTOR and Survivin that controls G1/S progression in T lymphocytes. Inhibition of Aurora B or mTOR suppresses activation of cyclin A and therefore activation of CDK 1 and CDK2. Aurora B phosphorylates Survivin and mTOR and this complex controls cell cycle progress by regulation of Rb, activation of CDK1 and CDK2 and repression of cyclin A (Song et al., 2007). Furthermore, Aurora B activity is dependent on mTOR. When cells were treated with rapamicin, the mTOR inhibitor, Aurora B was expressed normally, however phosphorylation of Survivin, Rb, CDK1 and CDK2 were affected by the presence of rapamicin, showing that mTOR affects the activity of Aurora B (Song et al., 2007).

It has also been shown that Aurora B is involved in regulating the G1/S transition in many cancer cell lines. Aurora B interacts with and phosphorylates Rb in HCT-116 cells (Nair et al., 2009). This post-translational modification is necessary to avoid endoreduplication after aberrant mitosis. Hyperphosphoryated Rb normally releases E2F, which promotes transcription of S phase genes, as described in section 1.2.1. However, Aurora B phosphorylation of Rb has the opposite effect because it stabilizes the Rb-E2F1 interaction instead of promoting the release of E2F1. Thus, the cell cycle is arrested and endoreduplication is inhibited (Nair et al., 2009).

Recently it has been shown that Aurora B controls the transcriptional activity of p53. Aurora B is able to phosphorylate p53 targeting it for proteasome degradation in a breast cancer cell line (MCF-7). Inhibition of Aurora B promotes the upregulation of p53 target genes, such as p21 and MDM2 (Gully et al., 2012). Another study in mouse embryonic fibroblasts (MEFs) has revealed that Aurora B knock down generates a delay in entry into S phase rather then a G1/S arrest. The delay is due to high levels of p21, which is upregulated by p53. Furthermore, the high levels of p21 in Aurora B ablated cells do not affect entry in mitosis. However, due to the inhibition of CDK1 by p21, cells undergo a premature exit

from mitosis (Trakala et al., 2013). Additional Aurora B studies on cancer cell lines have confirmed that Aurora B controls p53 and p21 activity. Genes in the p53 pathway are upregulated in cells where Aurora B has been inhibited, while E2F-regulated genes have a decreased expression. Cell cycle arrest is generated by the presence of p21, hyperphosphorylation of Rb and consequent repression of E2F (Kumari et al., 2014).

1.3 Transcriptional regulation

1.3.1 Transcription is regulated by post-translational modifications and histone variants

Gene transcription is a highly regulated process that involves many different proteins, regulatory RNAs and the input of signalling pathways. The state of transcription is also affected by the composition of chromatin. A tightly packed chromatin conformation generally corresponds to a repressive transcriptional state, while in the case of active transcription the chromatin is more accessible. Chromatin is formed by strings of nucleosomes, which are composed of DNA and histones. Nucleosomes consist of an octamer formed from two molecules of each of histone H2A, H2B, H3 and H4. 146 base pairs (bp) of DNA is wrapped around the octamer (Luger et al., 1997). The linker histone H1 sits outside of the nucleosomal core on the linker DNA between the nucleosomes. The N-tails of the histones are exposed to the action of enzymes that generate post-translational modifications.

The function of histone modifications is to control the compaction of chromatin and therefore the accessibility to transcription factors. A large number of post-translational modifications have been studied, including methylation, acetylation, phosphorylation, ubiquitination, sumoylation, ADP ribosylation, deimination, proline isomerization (Kouzarides, 2007). The multiple combinations of different modifications that are found on histone tails have important roles in the regulation of gene transcription. A particular modification does not in itself imply a repressive or active state as it can have different effects depending on which residue is modified. For example,

methylation on histone H3K4me3 is considered to be an active marker for transcription (Santos-Rosa et al., 2002), whereas histone H3K9me3 has generally been thought to be repressive feature as it is a target for binding of heterochromatin protein-1 (HP1) (Bannister et al., 2001). Acetylation seems to be mostly associated with transcriptional activation but acetylation of H4K12 has been shown to be associated with heterochromatin formation in *Drosophila* (Turner et al., 1992).

Post-translational modifications can act in combinations to regulate transcription. For instance, when the H3K9me3 modification is combined with phosphorylation on H3S10 in the G2 stage of the cell cycle, there is a switch that leads to displacement of HP1 binding to H3K9me3 (Hirota et al., 2005). Another combination of modifications is represented by bivalent domains in ES cells, which are marked by H3K4me3 and H3K27me3. The presence of two modifications that are respectively active and repressive markers in the same chromatin domains has been hypothesised to keep developmentally regulated genes in a poised state, ready for activation when ES cells differentiate. (Bernstein et al., 2006).

Post-translational modifications on histone tails are not the only mechanism by which histones can affect gene transcription. Canonical histone proteins can be replaced by histone variants that have different functions in cellular processes. The histone H3 variant H3.3 is particularly enriched at transcriptionally active loci (Ahmad and Henikoff, 2002b). Nucleosome containing H3.3 are unstable and therefore chromatin is more accessible to transcription factors (Chow et al., 2005). CENP-A is another variant of histone H3 that is found at centromeres and is required for kinetochore assembly (Van Hooser et al., 2001) (Figure 1.4). Histone H2A, has 19 variants, among which are H2A.Z, H2AX, macroH2A and H2ABBD (Figure 1.4). H2A.Z has recently been the focus of much research, as it was shown to be present in promoters of active genes in mice (Bargaje et al., 2012). Promoter nucleosomes become unstable due to the presence of H2A.Z and H3.3, indicating that H2A.Z/H3.3 containing nucleosomes promote the access of transcription factors (Jin et al., 2009). The histone variant H2AX is recruited to the regions surrounding double strand breaks where it promote DNA repair (Paull et al., 2000). MacroH2A is found on

the inactive X chromosome and is involved in silencing (Costanzi and Pehrson, 1998). H2ABBD is the most recently discovered of the H2 variants and has been connected to transcriptional activation. A recent study has shown that its presence in the gene body is crucial for a correct splicing (Tolstorukov et al., 2012)

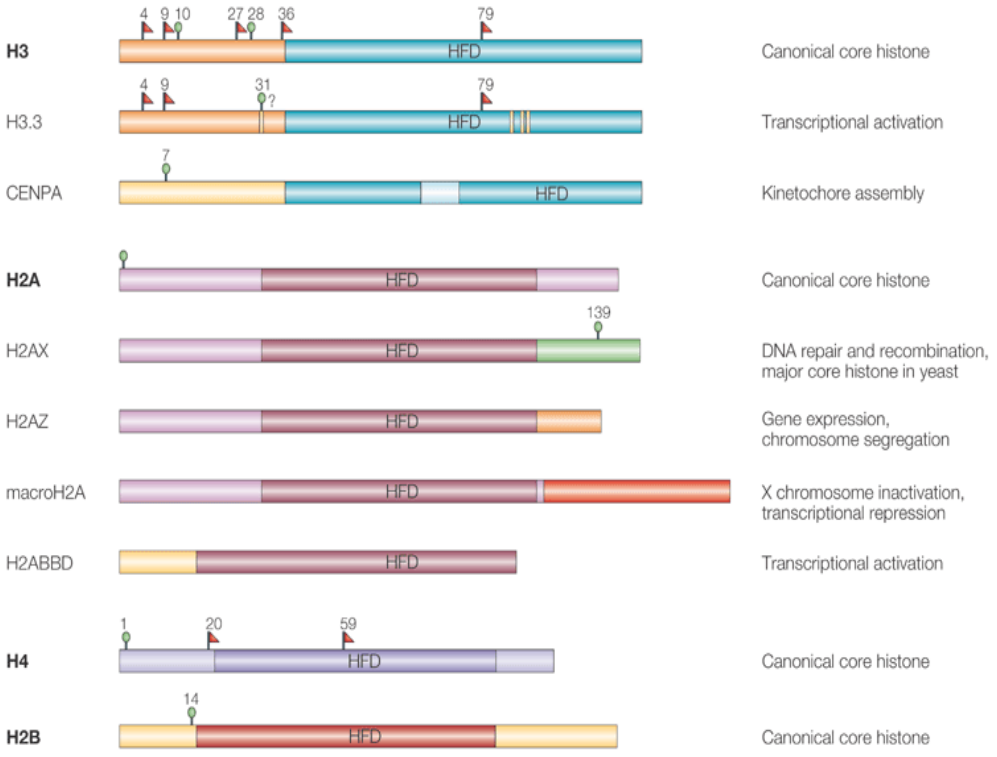


Figure 1.4: Schematic representation of nucleosomal core histone variants and post-tranlsational modifications.
The most studied histone variants are shown. Known functions are listed on the right. Each variant has a common Histone Fold Domain (HFD). Residues that are targets for modification are marked with green circles for phosphorylation and red flags for methylation.
(Adapted from (Sarma and Reinberg, 2005)).

Histone H1 is positioned outside of the nucleosomal core on the linker DNA between nucleosomes and is involved in controlling the compaction of chromatin. In mammals there are 11 known histone H1 variants, 5 of which are somatic. The other variants are either tissue-specific or expressed in the germ line. H1.1, H1.2, H1.3, H1.4 and H1.5 are expressed in somatic cells, while the variant H1.0 is expressed in terminally differentiated or growth arrested cells (Happel and Doenecke, 2009). There is only limited information about the variant H1.x. It has been reported to be an ubiquitous protein with repressive

proterties and is enriched in less accessible areas of genome (Shahhoseini et al., 2010). The remaining H1 variants, H1.oo, H1.t, Hils1, H1T2, are expressed in testis and oocytes or in the zygote (Happel and Doenecke, 2009).

The role of histone H1 in regulating transcription has been long debated. In general, histone H1 has been considered to be a repressor of transcription (Buttinelli et al., 1999). Studies have shown that H1 promotes the compaction of chromatin and its presence around genes does not allow transcription factors to bind (Robinson and Rhodes, 2006). Furthermore, the linker histones are often associated with areas of the genome that are in a repressive state. A study has reported that the interaction between histone H1 and Nucleolin is responsible for decondensing the chromatin as it displaces the linker histone (Erard et al., 1988). However, recent studies have shown that acetylation of histone H1.4 on the lysine 34 is connected with active transcription (Kamieniarz et al., 2012). Histone H1.4K34 is acetylated by GNC5 and it is present at promoters of active genes. Therefore, the chromatin is more open and accessible to transcription factors (Kamieniarz et al., 2012).

1.3.2 Chromatin remodelers affect chromatin conformational state

Chromatin conformation and accessibility at promoters and enhancers is affected by positioning of nucleosomes with respect to these elements. Nucleosomes can be positioned by local displacement by a bound transcription factor or by specific DNA sequences that favour or disfavour the formation of a nucleosome (Jiang and Pugh, 2009). DNA sequences of this type can create local nucleosome-free areas in important regulatory regions, such as promoters. Alternatively, they can promote the formation of nucleosome condensed areas, such as heterochromatic regions (Ahmad and Henikoff, 2002a).

Protein complexes called chromatin remodellers have been shown to be responsible of modifying the composition of chromatin. Remodelling complexes are ATP-dependent DNA translocases that affect the DNA-histone interactions. Chromatin remodellers can mediate either repositioning, sliding or removal of nucleosomes along the chromosome (Clapier and Cairns, 2009). There are four families of chromatin remodellers, characterized by an ATPase domain flanked

by different domains, which are specific for each family. The chromatin remodeller families are SWI/SNF, INO80, CHD and ISWI. The mechanism of action is common among these families as they all use ATP hydrolysis to mobilize DNA from the nucleosome octamer (Vignali et al., 2000).

The SWI/SNF complex has been shown to mediate nucleosome sliding or eviction of histones from nucleosomes. However, this remodeller cannot participate in the assembly of the nucleosome. Members of the SWI/SNF complex family can recognize acetylated histones and promote transcription activation. In humans, the complexes that belong to this family are BAF and PBAF (Sudarsanam and Winston, 2000). ISWI remodelers, such as ACF and CHRAC, are involved in promoting nucleosome spacing in order to facilitate chromatin assembly and repression (Langst and Becker, 2001). The NURF complex is part of the ISWI family however it promotes transcription activation (Mizuguchi et al., 1997). Another family called CHD is composed of complexes that can act as activators or repressors. CHD1 is known to be an activator because it promotes ejection or sliding of nucleosomes and it has been shown to participate in transcriptional elongation. A CHD family remodeler called Mi2-NuRD has been connected with repression and is formed by deacetylases and proteins that bind methyl CpG nucleotides (Hall and Georgel, 2007). The chromatin remodellers that belong to the INO80 family are mainly associated with transcriptional activation, but there is evidence that they can also be involved in repression in association with the polycomb proteins (Bhatia et al., 2010). The INO80 complex members can mediate the exchange of the H2A.Z/H2A dimer with H2B/H2A (Papamichos-Chronakis et al., 2011).

1.3.3 Transcription performed by RNA polymerase II: initiation, elongation and termination

RNA polymerases are the enzymes that are responsible for the transcription of RNA. In most eukaryotes, there are three RNA polymerases that transcribe different types of genes. RNA polymerase II (Pol II) is the most studied because it is involved in the transcription of all mRNAs and most snRNA and microRNA. RNA polymerase I transcribes ribosomal genes with the exception of the 5S rRNA

(Grummt, 2003), which is produced by RNA polymerase III. This enzyme exerts its functions by trancribing tRNAs, 5S rRNA and other non coding RNAs, including the SK7RNA that controls RNA Polymerase II activity (White, 2011).

Pol II is composed of 12 subunits called Rpb. The largest subunit, Rpb1, is important for regulation of Pol II enzyme activity (Kimura et al., 1997). In mammals the carboxy terminal domain (CTD) of this subunit is composed by 52 hepta-repetitions of YSPTSPS. Serine residues are located within each repetition in position 2, 5, 7 (Corden, 2007). These serine residues are phosphorylated during the process of transcription and are involved in regulating initiation, elongation and termination (Figure 1.5).

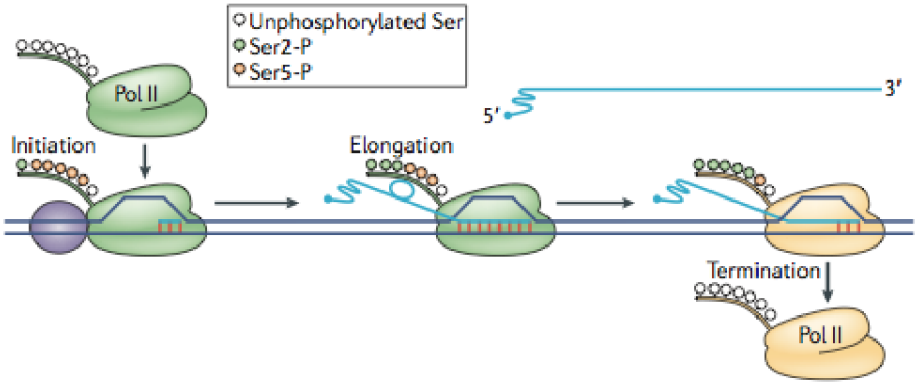


Figure 1.5: RNA polymerase II cycle of transcription.
The process of transcription can be divided into initiation, elongation and termination. These stages are regulated by phosphorylation of serines on the CTD of the Pol II. Upon binding to the promoter, the CTD is unphosphorylated. During initiation, it is phosphorylated at serine-5 and during elongation it becomes phoshorylated at serine-2.
(Adapted from (Kuehner et al., 2011)).

1.3.3.1 Initiation

The unphosphorylated form of Pol II binds to the promoter upstream the transcriptional start site. It is recruited in this regulatory part of the gene to form a complex called Pre-Initiation Complex (PIC) (Nikolov and Burley, 1997). PIC formation is important for transcription and is related to recognition of DNA sequences at the promoter by the PIC components (Orphanides et al., 1996). Promoters can have different features according to sequence elements that are included in them and can be broadly divided into AT-rich and CpG island promoters.

AT-rich promoters are characterized by the presence of specific sequences that are required for their recognition by general transcription factors. These types of promoters can have a TATA box located 30 bp upstream of the Transcription Start Site (TSS). The TATA box is bound by the general transcription factor TBP, which promotes the formation of the PIC (Wong and Bateman, 1994). TBP is part of the TFIID complex, which is also important for the recognition of other promoter elements (Inr and DPE) that are situated downstream from the TSS (Emami et al., 1997). Binding of TFIID to the promoter elements is important to promote the binding of TFIIA and TFIIB, thereby stabilizing the binding of TBP to the DNA. TFIIB binds to another promoter element called BRE, which is located upstream of the TATA box (Lagrange et al., 1998). An important function of TFIIB is to ensure the correct directionality of Pol II and to stimulate the activity of the enzyme by preventing short newly formed DNA-RNA hybrids from impeding RNA synthesis (Sainsbury et al., 2013). TFIIB is then stabilized by the presence of TFIIF, which is also required for transcription initiation (Cabart et al., 2011). Furthermore, TFIIF interacts with another factor, TFIIE, which in turn interacts with the unphosphorylated Pol II. Assembly of the PIC is completed after recruitment of TFIIH, which is the only GTF with enzymatic activity (Maxon et al., 1994). TFIIH is composed of the helicases XBP and XDP and the kinase Cdk7. The activity of TFIIH is required for the unwinding of DNA to create the transcription bubble that is needed for the polymerase to start transcribing (Bradsher et al., 2000). Cdk7 also is necessary for transcription initiation because it phosphorylates Serine 5 on the CTD (Tirode et al., 1999).

The Mediator complex also plays important roles in the formation of the PIC. Mediator can recruit TFIIH and this interaction facilitates phosphorylation of Pol II. Furthermore, Mediator interacts with co-activators to stimulate formation of the PIC (Esnault et al., 2008). Transcription factors are needed for the formation of the PIC because they recognize promoter elements. The TATA box is recognised by general transcription factors but genes lacking the presence of TATA box are bound by the general transcription factors (GTFs) via other promoter elements. TFIID is crucial for the formation of the PIC and is recruited

to TATA-less promoters via transcription factors, such as Sp1 (Pugh and Tjian, 1991).

CpG islands are regions that have a high frequency of CpG dinucleotides that are often found at gene promoters. The CpG dinucleotide is underrepresented in the genome because methylation of the cytosine results in deamination leading to conversion to thymidine. However, a high proportion of genes in mammals, including most housekeeping genes, have CpG islands at their promoters. These regions are characterized by the presence of multiple TSS and are nucleosome-deficient (Ramirez-Carrozzi et al., 2009). CpG island promoters often lack classical promoter elements such as TATA boxes and are regulated by the binding of ubiquitous transcription factors, such as Sp1 (Deaton and Bird, 2011).

1.3.3.2 Transcriptional elongation

Once assembly of the PIC is completed, escape from the promoter is triggered by phosphorylation of the CTD at Serine 5. This modification is mediated by Cdk7 and allows the polymerase to transcribe around 30 bp (Ramanathan et al., 2001). At this point transcription is paused due to the presence of DRB Sensitivity Inducing Factor (DSIF) and Negative elongation factor (NELF), which are inhibitors of transcription (Yamaguchi et al., 1999). This might also be a checkpoint to promote the addition of a methylguanosine cap. The cap is needed to protect the newly produced RNA from degradation as well as promoting mRNA export and enhance translation (Lewis and Izaurralde, 1997). The RNA capping is a three step reaction that starts with the digestion of the 5' triphosphate, followed by the addition of a guanine and it is terminated with by methylation of the added guanine. The reaction is exerted catalysed by a single capping enzyme, which is recruited by the phosphorylation on serine-5 of the CTD and also by DSIF, and a cap guanine-N7 methyltransferase (Mandal et al., 2004). In the case of production of aberrant pre-mRNA due to splicing defects, the cap of the RNA is removed by decapping enzymes and the RNA is degraded by Xrn2. This leads to premature transcription termination and represents a mechanism of transcription regulation (Davidson et al., 2012).

Release from the paused state is mediated by the protein P-TEFb. This protein is usually sequestrated by the complex 7sk RNP (Nguyen et al., 2001). After

transcription initiation, P-TEFb is released either by Mediator or Brda4, allowing it to phosphorylate target proteins (Jang et al., 2005). P-TEFb phosphorylates serine-2 on the CTD of Pol II. CTD phosphorylation at serine-2 is the hallmark of promoter escape and promotes elongation (Ramanathan et al., 2001). Following release of the polymerase from the promoter, the level of serine-5 phosphorylation decreases to reach low levels at the 3' end of the gene. P-TEFb is also responsible for phosphorylation of the pausing factors DSIF and NELF. This causes release of NELF, while DSFI is kept in the elongation complex (Peterlin and Price, 2006) (Figure 1.6).

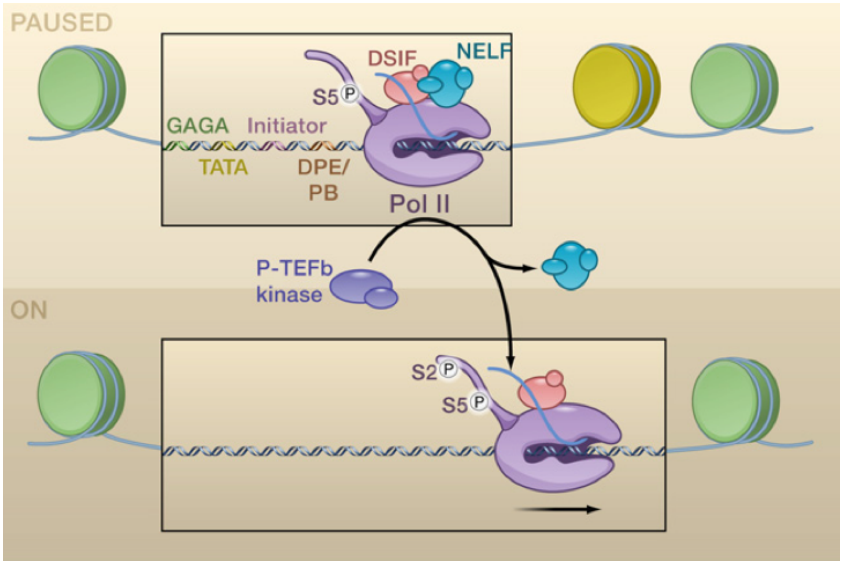


Figure 1.6: Promoter proximal pausing of Pol II.
Pol II is hold in pausing state around 30 bp by the factors DSIF and NELF. Upon the P-TEFb activation, the two factors are phosphorylated as well as Serine 2 on the Pol II CTD. These phosphorylations cause the release of NELF and generate the elongating Pol II.
(Adapted from (Levine, 2011)).

In order to escape from the paused state, Pol II needs to recruit factors to overcome the barrier of nucleosomes. One of these is the PAF complex, which does not have any enzymatic activity. However, this complex acts as a platform for recruiting proteins that are needed to generate a loose conformation of the nucleosome that can be transcribed by Pol II (Kim et al., 2010). In particular, the FACT complex has an important role as it removes the H2A-H2B dimer from the nucleosome. The ejection of H2A-H2B creates a nucleosomal conformation that allows the polymerase to transcribe along nucleosomal DNA. After the passage of

the enzyme, FACT re-deposites the H2A-H2B dimer back into the nucleosome (Belotserkovskaya et al., 2003).

1.3.3.3 Termination

Factors involved in 3'end RNA formation constitute a complex that is composed of more than 14 proteins (Mandel et al., 2008). Serine-2 phosphorylation at the Pol II CTD is important to recruit proteins that are required for 3'end cleavage of the nascent RNA (Gu et al., 2013). Once Pol II reaches the 3' end of the gene, recognition of a poly-A site sequence mediates pausing of the enzyme. The Cleavage and Polyadenylation Specificity Factor (CPSF), which is composed of five subunits and interacts with the body of Pol II, is present in the elongating complex and recognizes the poly-A sequence (Dantonel et al., 1997). This is constituted by the sequence AAUAAA, which is located around 10-30 nucleotides upstream of the cleavage site. A G-U rich sequence downstream of the cleavage site is important for 3' end processing (Chou et al., 1994) (Figure 1.7-1). The binding of CPSF to the AAUAAA sequence causes pausing of the polymerase and promotes interaction between Pol II and the cleavage stimulation factor (Cstf) (Nag et al., 2007). Moreover, binding of Cstf to the G-U rich sequence is facilitated by the interaction with Pol II (Figure 1.7-2) (Nag et al., 2007). The binding of CPSF and Cstf, respectively upstream and downstream of the cleavage site, promotes formation of the pre-mRNA 3' end. For correct completion of the process two other factors, called CFI and CFII, are needed (Takagaki et al., 1989). CFI promotes recognition of the poly-A site (Brown and Gilmartin, 2003), while CFII mediates the interaction between CFI and CPSF (de Vries et al., 2000). A protein called symplekin acts as a scaffold for the interaction of these factors (Takagaki and Manley, 2000).

Once all of the proteins that are involved in 3'end formation are recruited, the CPSF-73 subunit carries out the cleavage of the pre-mRNA (Ryan et al., 2004). However, the cut generates a free a 3'end that needs to be protected from the action of ribonucleases. The CPSF subunit Fip1 stimulates the activity of the poly-A polymerase (Pap) (Kaufmann et al., 2004). Pap is present in the termination complex machinery and has the function of adding a poly-A tail composed of around 200 Adenines to the 3' end of the RNA (Bardwell et al.,

1990). Pap activity is stimulated and regulated by the interaction with poly-A binding proteins (PABPs). Moreover, the poly-A tail is protected by the binding of multiple PABPs that are needed to regulate the length and stability of the poly-A tail (Kuhn et al., 2009).

After the cleavage of the nascent RNA, Pol II keeps on transcribing along the DNA. It has been proposed that the termination of transcription involves the protein Xrn2, following a termination model called the Torpedo Model (West et al., 2004). Upon formation of the 3' end of the RNA, Pol II does not come off the DNA, leading to production of new RNA downstream of the cleavage site. However, the newly transcribed RNA is not capped and therefore has a 5' end that is exposed to the action of exoribonucleases. Xrn2 can recognize the uncapped transcript and start degrading it. The degradation of the RNA ultimately brings Xrn2 in contact with Pol II and interaction results in displacement of Pol II from the DNA, probably due to conformational changes at the catalytic site (Figure 1.7-3) (West et al., 2004). However, the torpedo model does not fully explain how Pol II is mechanistically displaced from the DNA. It has been recently shown that the CTD of Pol II plays a role in termination (Mayer et al., 2012). A study conducted in yeast has revealed that dephosphorylation of CTD Tyrosine 1 by Gcl7 is required at the poly-A sequence to promote the recruitment of termination factors. The phosphorylation state of Tyrosine 1 impairs termination factors and is therefore required to avoid premature termination during elongation (Schreieck et al., 2014).

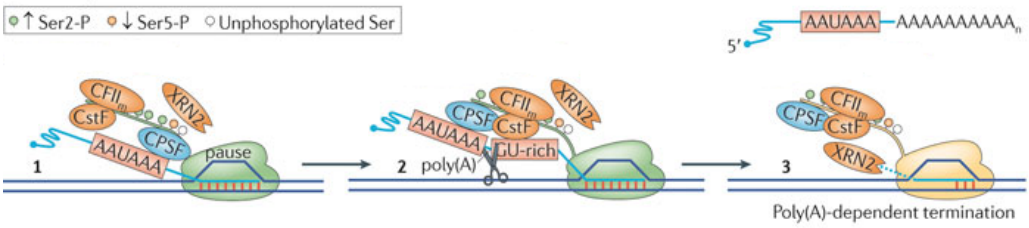


Figure 1.7: mRNA transcription termination.
1) The elongating complex recognizes the AAUAAA sequence through the CPSF complex. 2) Pol II pauses after the stop signal and the Cstf complex binds the GU rich sequence downstream of the cleavage site. 3) After cleavage and release of the mRNA, Xrn2 degrades the new uncapped RNA that Pol II transcribes after the cleavage site. The action of Xrn2 causes the release of Pol II from DNA.
(Adapted from (Kuehner et al., 2011)).

1.4 Splicing is a two-step reaction

Splicing is an essential process that is required for removal of introns from primary transcripts to generate a mature RNA. The mRNA is then exported to the cytoplasm where it is translated into proteins. Splicing is carried out by a large group of proteins that contribute to the formation of the spliceosome (Will and Luhrmann, 2011). This is a heterogeneous complex formed by ribonucleoprotein (RNP) complexes. The composition of RNP complexes is based on the interaction of small nuclear RNA (snRNA) with Sm proteins. The snRNAs are characterized by the presence of secondary structures that are crucial for the interaction with proteins and DNA. The snRNAs are U1, U2, U5, U4/U6 and each RNA interacts with a ring shaped complex formed by seven Sm proteins (Wahl et al., 2009). An exception is represented by the snRNAs U4 and U6 that are base-paired forming a single RNA molecule. The unwinding of U4/U6 by the RNA helicase Prp8 is necessary for the formation of an active U6 molecule during splicing (Kuhn et al., 1999).

Splicing is a two-step process that consists of two transesterification reactions for the excision of the intron. Excision is achieved by an intermediate lariat conformation of the intron (Moore and Sharp, 1993). Removal of the intron is mediated by the snRNP complexes, which are able to recognize sequences within the intron. These consist of the 5' splice site (5'SS), the Adenine of the branch site (BS) and the 3' splice site (3'SS) (Figure 1.8).

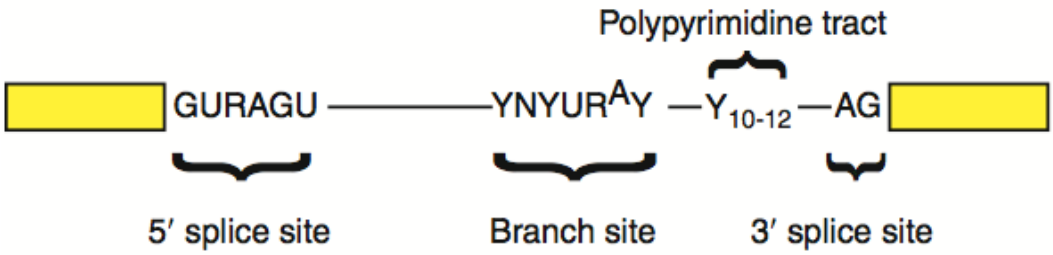


Figure 1.8: Schematic representation of sequence elements within introns. The intron is characterized by a 5' splice site (5'SS), a branch site (BS), a polypyrimidine tract and the 3' splice site (3'SS). The first transesterification reaction is between the adenine in the BS and the 5'SS to achieve the lariat formation. The 3' hydroxyl of the cleaved 5' exon then attacks the phosphodiester bond at the 3' splice site. This results in ligation of the 5' and 3' splice sites and excision of the lariat (Adapted from (Semlow and Staley, 2012)).

The splicing reactions are characterized by the presence of different spliceosome complexes formed by different combinations of snRNPs. The snRNAs and pre-mRNA interact weakly and therefore the presence of accessory proteins is required to stabilize the interactions. First, the 5'SS downstream of an exon is recognized by the U1 70K snRNP. This binding is stabilized by interaction of the U1 sRNP with the Serine-Arginine (SR)-rich splicing factor 1 (SRSF1). The Sm and SR proteins are required to stabilize the binding of U1 snRNA to the 5'SS (Cho et al., 2011). Furthermore, the binding of U2AF65 and U2AF35, respectively to the polypyrimidine tract and the dinucleotide AG at the 3'SS, are needed for the formation of the first spliceosome complex, called E (Zamore and Green, 1989). Complex E also contains the protein SF1/BBP, which interacts with the Branch Site (Figure 1.9). The formation of complex E is important for the recognition of the 5'SS and 3'SS within the intron (Michaud and Reed, 1993).

From this point, the presence of eight RNA helicases in different steps is required to deliver energy to the spliceosome in an ATP-dependent manner. These helicases belong to DEAD-box, DEAH-box and Ski-2 like families and can perform ATP binding and hydrolysis as well as nucleic acid interactions (Cordin and Beggs, 2013). The DEAD-box RNA helicase Sub2/UAP56 displaces the SF1/BBP complex, which is bound to the BS. On the other hand, the helicase Prp5 is important for the binding and remodelling of U2 snRNA. Prp5 promotes the interaction between U2 snRNP and the polypyrimidine tract (Xu et al., 2004). U2 snRNP then interacts with U2AF65 and consequently promotes the binding of

proteins SF3a and b at the BS. The assembled complex is called the pre-spliceosome or complex A (Figure 1.9) (Kramer and Utans, 1991).

At this point a tripartite snRNP containing U5 and U4/U6 interacts with complex A. The spliceosome is loaded with all the snRNPs, but it is inactive and is called complex B^{ina}. The RNA helicase Prp28 is required for the removal of U1, which is replaced at the 5'SS by U6 (Staley and Guthrie, 1999). Therefore, Prpr28 promotes the binding of U6 to U2. The release of U1 is also accompanied by the release of the U4, due to the action of the helicases Brr2 and Snu114 that unwind the base-paired U4/U6 RNAs (Raghunathan and Guthrie, 1998). The spliceosome complex B becomes active and contains U6, U5 and U2 (Figure 1.9). Moreover, the double interaction of U6 with U2 and at the same time with the 5'SS, promotes the formation of the lariat as it brings the 5'SS closer to the 3'SS (Valadkhan and Manley, 2000). During the switch from the inactive to the active B complex, the structure of U6 is rearranged to achieve a conformation that promotes lariat formation. Before the first transesterification reaction of the splicing process, the DEAH-box RNA helicase Prp2 is involved in the destabilization of the proteins SF3a and SF3b to cause their displacement from the BS(Lardelli et al., 2010). Furthermore, the 2'OH of the Adenine at the BS is aligned to carry out a nucleophilic attack at the 5'SS. This transesterification reaction generates a lariat that is bound to the 3' exon. The spliceosome after the first nucleophilic reaction is called complex C that consequently carries out the second transesterification reaction. This is mediated by the action of the helicase Prp16 and the binding of U5 to the 3'end and the 5'end of the two exons (Figure 1.9). Prpr16 together with Prp43 exerts a proofreading activity before the cleavage to ensure a correct splicing process (Koodathingal et al., 2010). Moreover, in order to complete the excision of the intron, the 3'OH of the 5'exon carries out a nucleophilic attack at the 3'exon producing the fusion between two exons, in a process controlled by the RNA helicase Prp22 (Mayas et al., 2006). Furthermore, the release of the lariat is mediated by the RNA helicase Prp43 (Martin et al., 2002) (Figure 1.9).

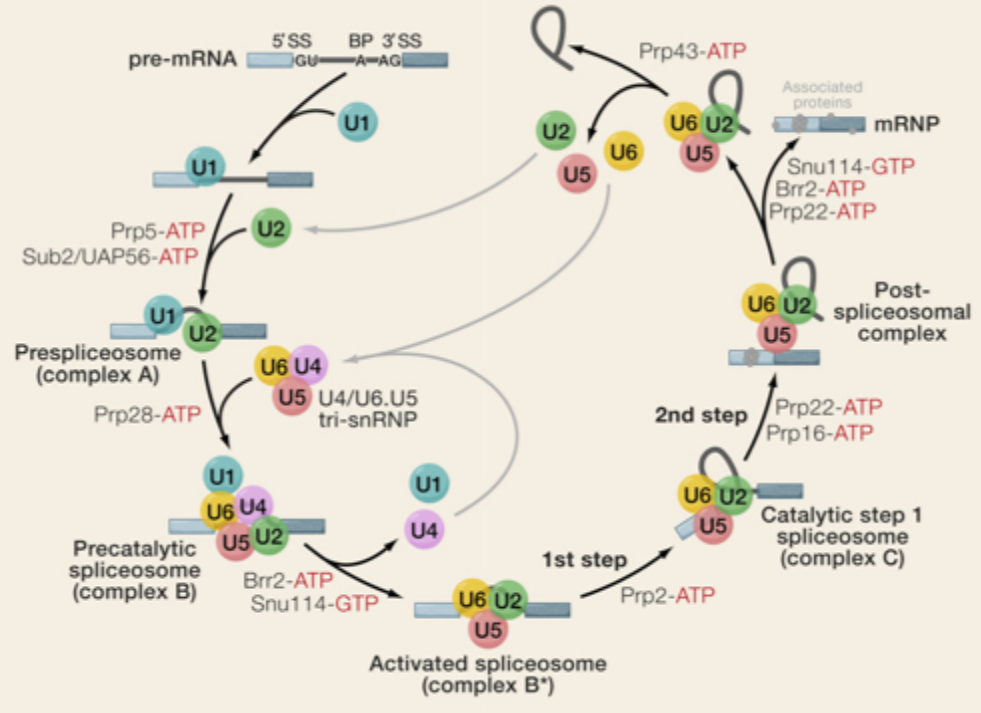


Figure 1.9: Spliceosome complexes and splicing process.
The splicing processes is carried out by the snRNP complexes that mediate recognition of the intron sequences and the two transesterification reactions. RNA helicases play a crucial role during the splicing process.
(Adapted from (Wahl et al., 2009)).

1.4.1 Alternative splicing as a source of variation

The processing of pre-mRNA results in the formation of a mature transcript. However, alternative splicing has been shown to be a means for generating different isoforms of the same protein. This process has been estimated to affect around 95% of human genes (Pan et al., 2008). The difference in composition of the mRNA is driven by the presence or absence of exons through regulation of exon inclusion or exclusion by proteins connected to splicing. Two models, which are not mutually exclusive, have been proposed to explain the presence of different isoforms generated by alternative splicing. The first of these is called the recruitment model, according to which Pol II recruits splicing factors during transcription that determine the fate of the primary transcript. Interaction with SR proteins promotes exon inclusion whereas hnRNP proteins have an inhibitory effect that results in exon skipping. For example, it has been reported that interaction of the CTD of Pol II with SRp20 promotes alternative splicing by including alternative exons (de la Mata and Kornblihtt, 2006). The binding

partners of Pol II during transcription are responsible for the choice of exon inclusion/skipping. A second model to explain alternative splicing is the kinetic model. According to this model, Pol II regulates the inclusion/exclusion of exons. Alternative splicing in the kinetic model is dependent on the rate of transcription of Pol II and the strength of the splice sites in the pre-mRNA. Usually, strong and upstream splice sites are included while weak and downstream splice sites are skipped (Ip et al., 2011). Sequence elements residing within the exon are targets for binding of proteins involved in splicing regulation. These elements are Exonic Splicing Enhancers (ESE) and Exonic Splicing Silencers (ESS). The same elements can control splicing processing by their presence within introns (Wang and Burge, 2008)(Figure 1.10).

Splicing is regulated by accessory proteins that affect the binding of snRNP complexes. The SR proteins are known to promote the formation of the spliceosome after recognition of an exon. These proteins bind to the ESE and are known to bind with UAF35 and UAF65 to stabilize their binding to the 3'SS of the intron and also with U1 snRNP at the 5'SS (Long and Caceres, 2009). However, competition between SR proteins proteins and heterogeneous nuclear ribonucleoproteins (hnRNPs) has a role in alternative splicing regulation (Zhu et al., 2001). hnRNPs are a large family of 20 proteins that are involved in RNA processing as well as mRNA export to the cytoplasm. HnRNPs contain a Nuclear Localization Signal (NLS) that allows them to shuttle between nucleus and cytoplasm (Pinol-Roma and Dreyfuss, 1992). These proteins can bind RNA either through an RRM or KH domain. Many of the hnRNP proteins have been involved in repression of splicing by binding of ESS elements in exons or introns (Han et al., 2010). Furthermore, hnRNP proteins promote exon skipping either by inhibiting binding of snRNP factors or by promoting the looping out of the exon. An example of exon looping out is represented by the mechanism of action of hnRNP A1, which promotes extrusion of the exon (Blanchette and Chabot, 1999). hnRNP proteins can also promote splicing. An example of this is the role of hnRNP H in the alternative splicing of c-src in neuronal cells (Chou et al., 1999).

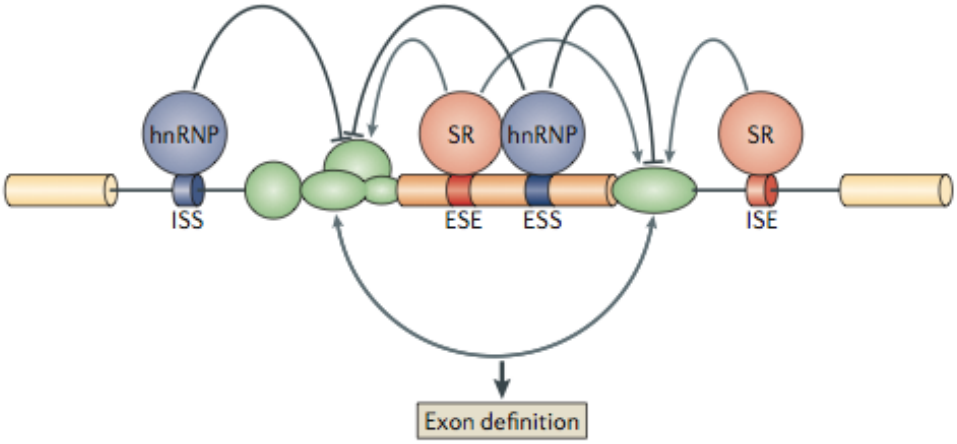


Figure 1.10: Regulation of splicing by SR and hnRNP proteins.
Regulatory elements are present in the exon and are called Exonic Splicing Enhancers (ESE) and Exonic Splicing Silencers (ESS). Usually the SR proteins bind to the ESE promoting exon inclusion, whereas hnRNP proteins bind the ESS to exert exon exclusion. Similar elements are present in the intron and are called ISS and ISE (Adapted from (Kornblihtt et al., 2013)).

1.5 RNA decay

The formation of mature RNA requires a correct splicing process. Furthermore, export of mRNA to the cytoplasm and translation to generate a functional protein are dependent on the production of a functional mRNA, which is formed by a 5' 7-methylguanosine cap and poly-A tail bound by several PABPs. These structures at the ends of the RNA are required for correct initiation of translation and to protect the molecule from nuclease degradation.

The steps from transcription to the formation of a polypetpide require accurate RNA processing. However, RNAs can be misprocessed, leading to the production of aberrant proteins. In order to avoid production of these proteins, several mechanisms of RNA decay have been developed in the cell (Garneau et al., 2007). The major mechanisms of RNA degradation relate to the exposure of either the 5' or the 3' end of the mRNA. Decapping enzymes and deadenylases are required respectively for the removal of the 5' cap and the poly-A tail. Alternatively, RNA decay can be carried out by endonucleases able to cut inside

the RNA molecule. This cut generates two free ends that can be recognized by exonucleases to perform the degradation (Figure 1.11)

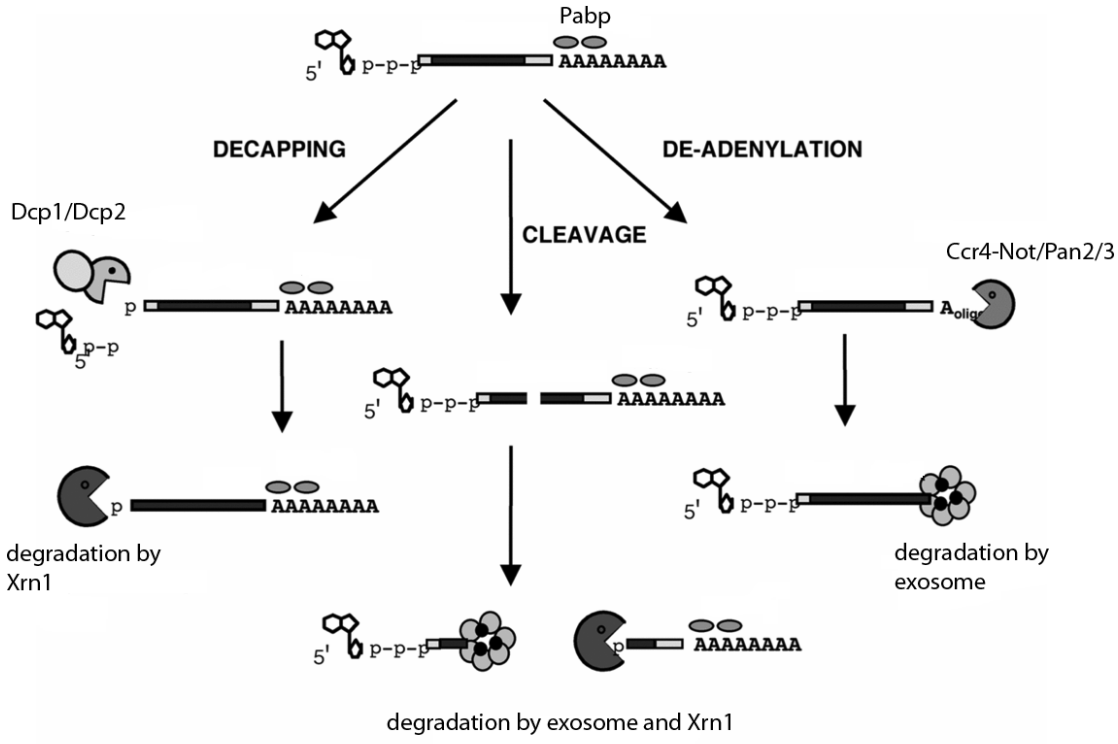


Figure 1.11: RNA decay pathways.
In the decapping mediated degradation, decapping enzymes are responsible for removing the cap at the 5'end of the RNA. Xrn1 can then degrade the RNA from the exposed 5'end. The endonucleolitic cleavage of the RNA triggers the degradation by the exosome and Xrn1. In the 3'end mediated degradation, the deadenylases CCR4-NOT, PARN or Pan2/3 start degrading the poly-A tail. Trimming of the tail allows the 3'-5' decay mediate by the exosome (Adapted from (Jones and Newbury, 2010)).

RNA stability at the 5' end is provided by the cap. During post-transcriptional maturation, the RNA cap is protected by the cap-binding complex (CBC) in the nucleus, while in the cytoplasm it is bound by the translation initiation factor 4F (eIF4F). The CBC has been shown to be important for pre-mRNA splicing and 3' end formation (Izaurralde et al., 1994). It also mediates mRNA export to the cytoplasm. In the cytoplasmic compartment, it is replaced by eIF4F, which binds the cap and promotes translation (Lewis and Izaurralde, 1997). The decapping complex is responsible for removing the cap, leaving an unprotected 5' end. This complex is composed by Dcp1, Dcp2, Ecd4 and Xrn1 (Chang et al., 2014). Ecd4 acts as platform and is crucial because it is needed for recruitment of the other factors and to mediate their interactions. The contact between Dcp1 and Dcp2 is

facilitated by Ecd4. Dcp1 then generates a conformational change in Dcp2, which carries out the cap removal. Once the cap has been removed, the 5' end of the RNA is recognized by Xrn1 and degraded (Chang et al., 2014).

RNA decay can be triggered by a deadenylation process, which removes the poly-A tail, exposing the 3'end of the RNA molecule. In mammals there are 26 enzymes responsible for deadenylation. The large number of enzymes was possibly generated by gene duplication events (Goldstrohm and Wickens, 2008). Three major mediators of deadenylation are Poly-A-specific ribonuclease (Parn), the Pan2/3 complex and the CCR4-NOT complex. The mechanisms used by these enzymes to carry out shortening of the poly-A tail are different and mRNA specific. Parn is a deadenylase that is cap dependent and it has been shown that its activity is inhibited by the presence of the CBC and Pabp (Balatsos et al., 2006). A different induction is required for the Pan enzymes that are stimulated by the presence of the Pabps. Pan2 is the deadenylase subunit of the Pan complex and is responsible for trimming of the poly-A tail, reducing the length of the tail from around 200 nucleotides to around 80 (Wolf and Passmore, 2014). Decapping enzymes are inhibited by the Pabps and therefore in the presence of an intact poly-A tail, the decapping process does not happen (Khanna and Kiledjian, 2004). Poly-A shortening facilitates binding at the 3'end of Lsm proteins that interact with Dcp2 promoting decapping (van Dijk et al., 2002). When the poly-A tail is shorter the CCR4-NOT complex degrades the remaining part leaving a free 3' RNA end. The RNA is then degraded by the action of the exosome, which is 3'-5' exoribonuclease. Therefore, this type of deadenylation is a biphasic process (Yamashita et al., 2005). Following deadenylation and the 3'-5' degradation by the exosome, another enzyme called scavenger decapping (Dcps) is recruited to degrade the cap at the 5'end of the RNA. The Dcps is required because Dcp2 cannot act on RNA shorter than 9 nucleotides (van Dijk et al., 2003).

RNA decay in the cytoplasm is mediated by the mechanisms described above. However, this process of RNA control has been confined to granules that have been found in the cytoplasm. These structures are called P bodies and are formed by RNAs and proteins involved in RNA decay and translation. Within these granules are proteins involved in 5'-3' RNA degradation (Anderson and

Kedersha, 2006). The decapping enzymes, Xrn1, and Lsm proteins were found in P bodies, as well as the deadenylases Pan2/3 and CCR4-NOT. Interestingly, the exosome proteins are not in the P bodies, meaning that two mechanisms of RNA decay are present in separated factories in the cytoplasm (Kulkarni et al., 2010).
RNA surveillance is needed as a quality control for the newly processed RNA. There are three pathways in the cytoplasm that trigger RNA decay: non-sense mediated decay (NMD), non-stop decay (NSD) and no-go decay (NGD). The NMD is able to detect transcripts with a premature termination codon (PTD). The NMD is triggered by the presence of an exon junction complex (EJC) after a termination codon. The EJC is usually deposited 20-24 nucleotides upstream of the junction between two exons. In the case of premature termination, the EJC is retained on junctions downstream from the PTD (Le Hir et al., 2000). Moreover, the PTD causes stalling of the ribosome, which is recognized by proteins of the Surf complex. The Surf complex subunit Upf1 is able to interact with the protein Upf2 present in the EJC downstream. Therefore, the interaction between the Surf complex and the EJC triggers RNA decay (Kashima et al., 2006).

Another mechanism of RNA surveillance is non-stop decay. Unlike the previous pathway, this leads to RNA decay due to lack of a stop codon. The ribosome translates the RNA, but the lack of a stop codon causes stalling of the ribosome at the 3' end. The stalled ribosome is recognized by the Ski complex, which displaces the ribosome and recruits the exosome to degrade the RNA (Frischmeyer et al., 2002).

Finally, the last mechanism of RNA surveillance is represented by the NGD. This has been studied in yeast and has been shown to be responsible for RNA decay triggered by ribosome stalling. The presence of the stalled ribosome signals recruitment of the Dom34-Hbs1 proteins, which generate an endonucleolytic cleavage in the RNA molecule. The new formed fragments are then degraded by the exosome and Xrn1 (Doma and Parker, 2006).

1.6 The CCR4-NOT complex is involved in many cellular processes

The CCR4-NOT complex is a large complex of proteins that has been implicated in many cellular processes in both nuclear and cytoplasmic compartments. The complex was first isolated and characterized in yeast. There are a large number of proteins associated with CCR4-NOT, but the proteins that are considered to be the core subunits are Not1, Not2, Not3, Not4, Not5, Caf40, Caf130 and the deadenylase subunits Ccr4 and Pop2/Caf1 (Liu et al., 1998). The first description of a human complex was reported by Albert *et al.*, who looked for yeast homologues in the human genome. They were able to identify the proteins hNOT2, hNOT3, hNOT4 and the deadenylases hCAF1 (CNOT7) and hCALIF/hPOP2 (CNOT8) as subunits of the human CCR4-NOT complex (Albert et al., 2000). It was then shown that the protein CNOT4 is an E3 ubiquitin ligase that interacts with CNOT1 (Albert et al., 2002). The study of the CCR4-NOT complex in mammals revealed the presence of multiple deadenylase subunits, indicating the existence of different sub-complexes. The deadenylase hCAF1 was also shown to be in different locations at different the cell cycle stages. In G0 and G1 the protein was mainly detected in the nucleus, whereas during S phase there was a switch to the cytoplasm (Morel et al., 2003). The yeast CCR4 subunit has been shown to have two homologs in mammals initially called CCR4a (CNOT6) and CCR4b (CNOT6L) (Yamashita et al., 2005).

Lau *et al.* provided more detailed characterization of different CCR4-NOT complexes in HeLa and 293T cells (Lau et al., 2009). They reported that in human cells, different CCR4-NOT complexes have different deadenylase components. CNOT10 and CNOT9, which is homologous to yeast Caf40, were shown to be part of the complex. CNOT7 and CNOT8 compete for the same binding site on CNOT1, which is the scaffold subunit of the complex. Therefore, the presence of CNOT7 and CNOT8 was reported to be mutually exclusive (Lau et al., 2009). The same result was obtained for CNOT6 and CNOT6L, as they were not found in the same complex. However, a more stable complex was isolated in the presence of CNOT8 than with CNOT7. Moreover, it was demonstrated that CNOT4 is not a stable part of the complex. In the same study, two new proteins were identified as new components of the CCR4-NOT complex, TAB182 and

C2ORF29 (Figure 1.12) (Lau et al., 2009). Another study in 293T cells confirmed the presence of C2ORF29, which was called CNOT11, and revealed a new module within the complex formed by interaction of CNOT11 with CNOT10 (Mauxion et al., 2013). Recently, a crystal structure for a module composed by CNOT1, CNOT2 and CNOT3 has been published. CNOT2 and CNOT3 form an heterodimer through their C-terminal NOT-box and interact with CNOT1 via their NOT1 anchor regions (Boland et al., 2013).

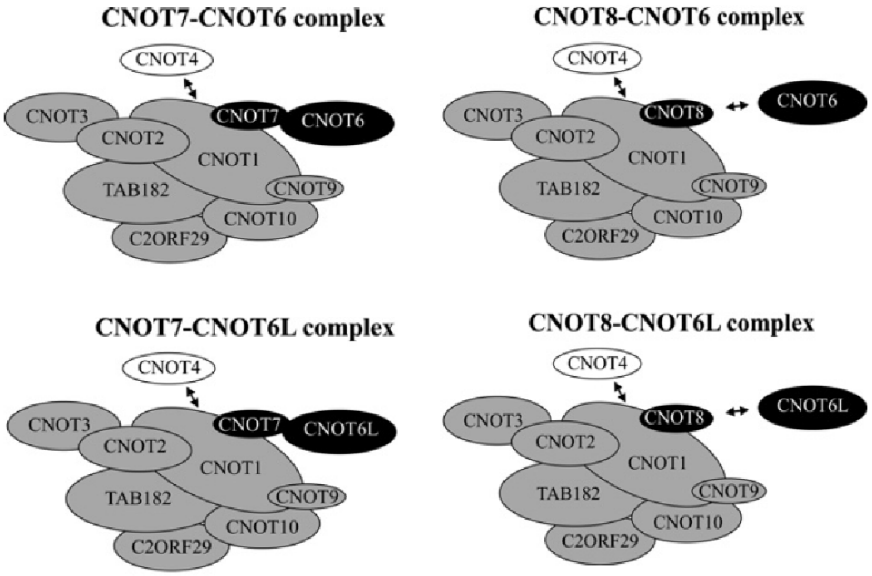


Figure 1.12: Human CCR4-NOT complexes showing different compositions with respect to their deadenylases subunits.
The deadenylases subunit CNOT7 and CNOT8 are considered mutually exclusive as well as CNOT6 and CNOT6L. The ubiquitin ligase CNOT4 is considered to be a transient interactor with the complex.
(Adapted from (Lau et al., 2009)).

As described above, CCR4-NOT is a deadenylase complex that is involved in RNA decay. However, many studies have reported functions for the complex in a number of different cellular processes. Most of the papers that have been published regarding CCR4-NOT functions were generated in yeast and revealed a role for the complex in controlling gene expression and RNA processing and stability. For example, it has been reported that CCR4-NOT is important in transcriptional initiation and can promote elongation of stalled Pol II by interacting with the body of Pol II (Kruk et al., 2011). CCR4-NOT interacts with the TRAMP polyadenylation complex and the nuclear exosome and is likely to be

a platform for the recruitment of the two complexes. This might be connected to a role in controlling RNA quality in the nucleus (Azzouz et al., 2009). Moreover, the involvement of CCR4-NOT in the export of RNA has been shown, as it was unveiled a physical interaction with the hnRNP proteins and the nuclear pore complex (Kerr et al., 2011). It was also shown that deletion of the gene encoding the Cnot4 E3 ligase in *Saccharomyces cerevisiae* results in a decrease in the active H3K4me3 mark (Laribee et al., 2007).

Studies carried out in mammals have confirmed the importance of CCR4-NOT in transcription regulation and cell cycle progression. A number of studies have identified roles for CCR4-NOT subunits in controlling the activation of nuclear hormone receptors. Cnot7 binds the retinoid X receptor beta (Rxrb) and acts as co-activator to promote normal spermatogenesis in mice (Nakamura et al., 2004). CNOT6 and CNOT9 were reported to enhance the transcriptional activity of several nuclear hormone receptors, such as TRα, RARα and RXRα, acting as co-activators in conjunction with NIF-1 (Garapaty et al., 2008). However, these studies have been performed by transient transfections or protein knock down of single subunits. Therefore, the results obtained for single subunits cannot be extended to the whole complex. For example, CNOT1 was shown to repress the activity of ERα resulting in downregulation of the transcription levels of genes controlled by ERα in MCF-7 cells. In the presence of the HDAC inhibitor Trichostatin A (TSA), the inhibition caused by CNOT1 was diminished suggesting that the inhibitory effects of CNOT1 could be due to recruitment of histone deacetylases (HDACs). In the same study CNOT3 was also shown to have an inhibitory influence on genes controlled by ERα (Winkler et al., 2006). A similar behaviour was also reported for CNOT2, which had a repressive effect in a gene reporter assay performed in human osteosarcoma cell line (U2OS). The inhibition was sensitive to TSA and mediated by the NOT-box (Zwartjes et al., 2004). The HDAC dependent mechanism of CNOT2 was further supported by the observation that CNOT2 interacts with the SMRT/NCoR–HDAC3 complex. Overexpression of CNOT2 and the HDAC3 complex augmented the repression activity mediated by CNOT2 (Jayne et al., 2006). CNOT2 is important for the integrity of the CCR4-NOT complex and it mediates the interaction of CNOT3 with the rest of the complex. Depletion of CNOT2 leads to an over-production of

misfolded proteins that induces apoptosis triggered by endoplasmatic reticulum (ER) stress (Ito et al., 2011).

The CCR4-NOT complex has also been implicated in miRNA repression. CCR4-NOT interacts with GW182 proteins at the 3' end of mRNAs promoting deadenylation. Interestingly, the interaction between GW182 and CCR4-NOT is needed to repress not only poly-A^+ but also poly-A^- mRNA. In the case of poly-A^- RNA, repression of translation is not mediated by RNA decay as the mRNA levels do not change (Chekulaeva et al., 2011).

A small number of studies have reported that CCR4-NOT subunits are important for controlling cell proliferation. CNOT6L ablation provides insights that could play a role in cell growth in NIH 3T3 mouse fibroblast through the stabilization of a crucial cell cycle gene such as p27 (Morita et al., 2007). It has been reported that in MCF-7 cells, depletion of both CNOT6 and CNOT6L leads to decreased cell proliferation as well as decreased cell survival. Knockdown of CNOT6 and CNOT6L showed that the two deadenylases are involved in controlling not only cell cycle progression but also have roles in the prevention of cell death and senescence. Moreover, it was found that depletion of CNOT6/CNOT6L or CNOT7/CNOT8 affects different sets of genes (Mittal et al., 2011). A similar mechanism has been described for the action of CNOT7 and CNOT8 in MCF-7 cells. The knockdown of these deadenylases causes cells to accumulate in G1 due to up-regulation of genes that are involved in cell cycle control (Aslam et al., 2009). The role in cell proliferation reported in many studies of CCR4-NOT components seems to be cell specific. The different roles of complexes that have different deadenylase subunits might be explained by the specificity of each enzyme for different mRNA targets.

1.7 The role of CNOT3 in gene expression and cell cycle control

CNOT3 is part of the CCR4-NOT complex and has recently been shown to form a module with CNOT1 and CNOT2 through the NOT box domain (Boland et al., 2013). However, the presence of CNOT3 within the CCR4-NOT complex is mediated by CNOT2 because depletion of CNOT2 causes loss of CNOT3 from the

complex (Ito et al., 2011). CNOT3 has been implicated in many cellular processes mainly through post-transcriptional effects on the stability of target mRNA. However, several studies have reported an involvement in controlling gene transcription. Expression studies carried out in 293T and U2OS cells have shown that full length CNOT3 does not affect transcription while the NOT box domain acts as a repressor of reporter gene activity (Zwartjes et al., 2004). Another study in MCF-7 cells showed that CNOT3 represses transcription dependent on ERα. Transcripts of ERα target genes were upregulated following CNOT3 knockdown (Winkler et al., 2006).

An RNAi screen performed in mouse ES cells has provided evidence of a role for Cnot3 in the self-renewal program of pluripotent cells. Cnot3 acts in concert with Trim28, Zfx and c-myc by binding promoters of a cohort of genes that is distinct from the genes that are controlled by the canonical transcription factors Nanog, Sox2 and Oct4 (Hu et al., 2009). The genes that are controlled by this newly identified module are mainly involved in cell cycle control and cell survival. Knockdown of Cnot3 in mouse ES cells leads to the loss of pluripotency and the acquisition of a phenotype that resembles cells of trophoectoderm lineage (Hu et al., 2009). Furthermore, Cnot3 keeps the self-renewal program active together with Cnot1 and Cnot2 (Zheng et al., 2012). They form a module that is required for the repression of the trophoectoderm factors. Silencing of Cnot1-3 leads to upregulation of transcription factors such as Cdx2 or Gata3 that are important for trophoectoderm lineage specification (Zheng et al., 2012). This module of Cnot proteins was also shown to be responsible of the conversion from partial iPS state to a genuine iPS. The mechanism by which the Cnot proteins mediate the conversion involves repression of factors that are involved in developmental process (Kamon et al., 2014).

CNOT3 has also been reported to be important for cell cycle progression and has been shown to be, necessary for proliferation of MCF-7 cells. Knockdown of Cnot3 leads to accumulation of the cells in G1, indicating that is required for entry into S phase. However, CNOT3 is not necessary for cell survival (Mittal et al., 2011). Another study has highlighted the importance of CNOT3 during mitotic progression (Takahashi et al., 2012). Knockdown of CNOT3 in HeLa cells resulted in mitotic arrest. Evidence was presented that CNOT3 controls mRNA

levels of MAD1, which is a protein involved in mitotic spindle assembly. CNOT3 might therefore represent a player in controlling the spindle assembly checkpoint (Takahashi et al., 2012).

1.7.1 Involvement of CNOT3 in human disease

An important study published recently reported that CNOT3 is a tumor suppressor in T-cell acute lymphoblastic leukemia (T-ALL) (De Keersmaecker et al., 2013). The study was performed by exome sequencing of T-ALL samples. The analysis of patients affected by T-ALL reported that around 8% of the cases carried mutations on CNOT3 gene. Arg57 in the N terminal region was identified as a mutation hot-spot for missense mutations that also seemed to result in splicing defects, leading to low expression of Cnot3 mRNA. The study was extended to a Drosophila eye cancer model and it was reported that loss of CNOT3 greatly increased the incidence of tumor onset (De Keersmaecker et al., 2013).

Potential roles for CNOT3 have been identified in a number of other diseases. CNOT3 has been shown to affect penetrance of the autosomal dominant eye disease Retinitis Pigmentosa (RP). Heterozygous mutations on the PRPF31 are responsible for the disease. However, the penetrance of the disease changes according to the expression levels of PRPF31 and asymptomatic carriers have been shown to compensate for the mutation in one allele by expressing high levels of PRPF31 from the other allele (Venturini et al., 2012). It has been reported that CNOT3 negatively affects the expression of the gene PRPF31. Therefore, high levels of CNOT3 promote onset of the disease, whereas asymptomatic carriers express low levels of CNOT3, allowing high expression of PRPF31 (Venturini et al., 2012).

Studies on osteoporosis in mice have revealed a role for Cnot3 in causing osteopenia. Deficiency of Cnot3 was reported to diminish bone mass volume and promoted bone resorption by increasing osteoclast number (Watanabe et al., 2014). However, depletion of Cnot3 did not affect bone formation. Cnot3 absence augmented stability of the 3'UTR of the receptor activator of NF-κB (RANK) mRNA, which is responsible for differentiation of osteoclasts. Cnot3 controls the onset of osteoporosis, as it has been shown that absence of Cnot3 worsens the

disease in aged osteoporotic mice by promoting osteoclast formation. Therefore, Cnot3 has a protective effect in maintaining the bone mass in mice (Watanabe et al., 2014).

Cnot3 has also been shown to be involved in regulating metabolism. Studies carried out in Cnot3$^{+/-}$ mice have reported a new function for protein in controlling metabolism-related genes. The mice have an increased glucose tolerance and are resistant to a high fat diet. The body size and weight of body and tissues are also lower than in wild type mice. The reduction in Cnot3 levels corresponds to an increase in the expression of genes that are involved in lipid catabolism, while genes that are responsible for lipogenesis are downregulated. Cnot3 has been shown to control the stability of specific mRNAs that are involved in lipid and glucose catabolism (Morita et al., 2011).

Lastly, a role in heart function was unveiled in Cnot3$^{+/-}$mice. The analysis showed that heart functionality was impaired with development of cardiac contractile abnormalities. It was also shown that Cnot3$^{+/-}$ mice that were subjected to cardiac stress underwent heart failure. Analysis of histone modifications in heart extracts revealed a decreased presence of histone H3K4me3 and H3K9ac. Treatment with the HDAC inhibitor VPA restored normal heart function, even in the presence of cardiac stress, avoiding heart failure. This study also showed that a Single Nucleotide Polymorphism (SNP) in the promoter of human CNOT3 is associated with cardiac malfunctions (Neely et al., 2010).

1.8 Development of B lymphocytes and regulation of the B cell cycle

Development of B cells is defined by a number of stages that occur initially in the bone marrow and are then completed in the secondary lymphoid organs. B cells arise from the hematopoietic stem cells (HSCs), which reside in the bone marrow and have two major features: the ability to generate all of the blood cell lineages and the capacity for self-renewal. HSCs are multipotent cells that can be identified by the absence of lineage specific markers (Lin-) and the presence of the stem cell factor receptor, c-kit (CD117) (Bryder et al., 2006).

The first step of HSC differentiation into multipotent-progenitor cells (MPP) is driven by the expression of Flt3. Lymphoid differentiation is accompanied by upregulation of Rag genes (Igarashi et al., 2002) and transcription factors, such as E2A (Dias et al., 2008) and Ikaros (Yoshida et al., 2006). Consequently, the expression of the interleukin 7 receptor-α is upregulated in these cells. This determines the loss of potential to generate myeloid cells, thus promoting the development of Common Lymphoid Progenitors (CLPs). The last phase for the final commitment of lymphoid cells is the choice between B or T lymphocytes specification. Commitment to become a B cell is achieved by the upregulation of B cell transcription factors including Pax5, Ebf1 and E2A (Nutt and Kee, 2007). Pax5 is needed to down-regulate the expression of Notch1, a factor required for T cell commitment. Pax 5 is also required for repression of myeloid lineage genes (Delogu et al., 2006). Moreover, Ebf1 promotes transcription of Pax5, which in turn upregulates expression of Ebf1, creating positive feedback (Busslinger, 2004). Expression of Pax5 during the final stage of B-cell lineage commitment is necessary for expression of the B cell programme and to promote the upregulation of CD19, a B cell marker. CD19 is important for the development of the mature B cells that reside in the secondary lymphoid organs (Kovesdi et al., 2010)(Figure 1.13).

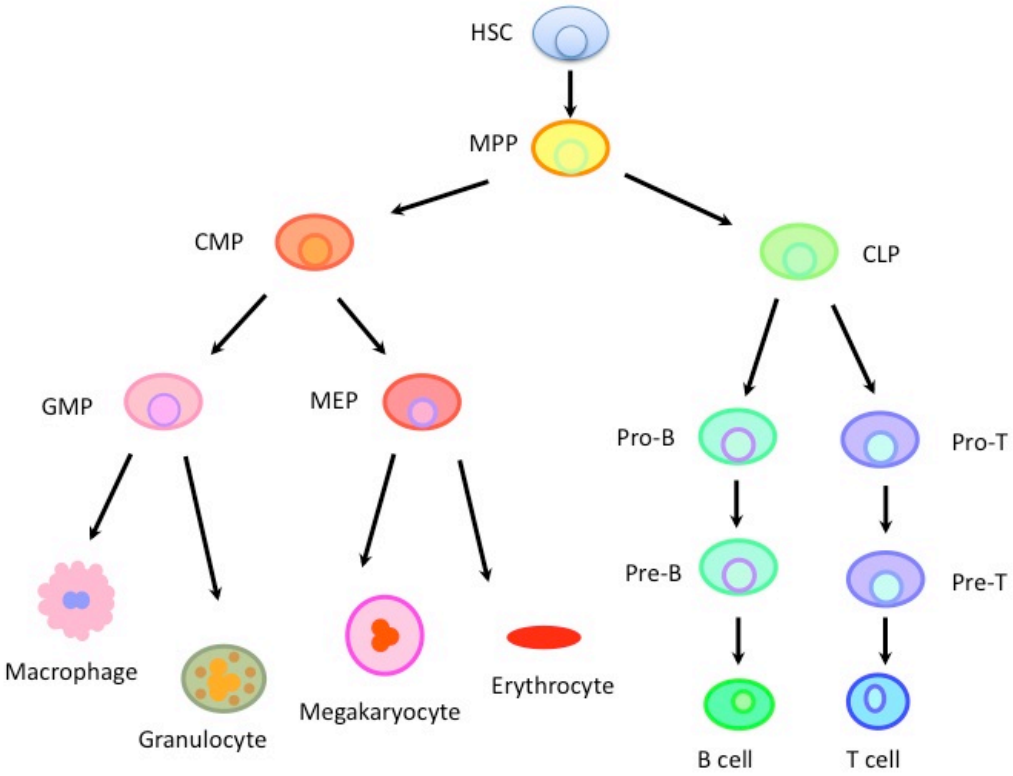


Figure 1.13: Hematopietic stem cell differentiation.
Hematopoietic stem cells (HSC) differentiate to become multipotent-progenitor cells (MPP). The next step towards lymphocyte differentiation is the repression of genes defining the Common Myeloid Progenitor (CMP) cells and the upregulation of Common Lymphoid Progenitor (CLP) specific genes. The expression of B cell specific genes in CLPs drives commitment and differentiation into pro-B, pre-B and B cells.

At this stage of development, after expression of CD19, cells are called pro-B. They next undergo V(D)J recombination of the immunoglobulin heavy-chain genes in order to generate the antibody repertoire. This involves recombination of the (variable), D (diversity), J (joining) regions in the Ig heavy-chain locus (Bassing et al., 2002). The transition from pro-B to pre-B cells is accompanied by formation of the pre B Cell Receptor (BCR) complex. The pre-BCR complex is formed by two surrogate light chains (Martensson et al., 2007). Large cycling pre-B cells exit the cell cycle to become small non-cycling pre-B cells. At this point recombination of the Igκ or Igλ light chain loci, formation of a functional IgM and downregulation of the pre-BCR marks the transition to the immature B cell stage.

The expression of the BCR on the cell membrane is important for control of migration from the bone marrow to the peripheral lymphoid organs. Before migrating to secondary lymphoid organs, the BCR of immature B cells is tested to

verify the affinity for self-elements. If there is high reactivity the cells trigger induction of apoptosis by the BCR (Chen et al., 1995). In the case of absence of response after BCR stimulation, B cells undergo a state of unresponsiveness called anergy (Cambier et al., 2007). B cells that are highly reactive to self-elements can also edit the BCR (Hertz and Nemazee, 1997). If the affinity for self-elements is low, the cells migrate out of the bone marrow to the secondary lymphoid organs, such as the spleen and lymph nodes (Niiro and Clark, 2002).

The spleen is composed of the red pulp and the white pulp. The red pulp contains splenic sinuses enriched in macrophages. The red pulp filters blood and cleanses it of bacteria, pathogens and old erythrocytes. The white pulp is composed by the periarteriolar lymphoid sheath (PALS), which is enriched in T lymphocytes, follicles containing B cells and the marginal zone (Cesta, 2006). B cells that arrive in the spleen are called T1 (transitional-1) and are characterized by $IgM^{high}CD21^{-}CD23^{-}$ expression on their membrane. Immature T1 B cells migrate from the red pulp to the follicles in the white pulp. Before reaching the mature B cell stage, they go through two transitional states that are characterized by expression of different cellular markers: $IgM^{high}CD21^{+}CD23^{+}$(T2) and IgM^{low} $CD21^{+}CD23^{+}$(T3) (Allman et al., 2001). B cell activation factor (BAFF), which is a member of the TNF family, is important for the transition to mature B cells in synergy with BCR signalling (Batten et al., 2000).

In the spleen, B cells can reside in the follicles or in the marginal zone. The decision to reside in either of these locations is driven by differences in the strength of BCR signalling. High BCR stimulation determines the follicular localization of B cells, whereas weak BCR stimulation promotes the formation of marginal zone B cells (Allman and Pillai, 2008). B cells in the marginal zone are mainly involved in the T-cell independent response, acting against non-protein antigens, such as lipids from bacterial cell wall components (Cerutti et al., 2013). The B cells in the spleen follicles are involved in the T-dependent immune response. Activation of B cell in the follicles leads to formation of either long-lived plasma cells or a pool of memory B cells (Goodnow et al., 2010). In the spleen, B cells can be in a quiescent state for months and are characterized by low levels of transcription and low metabolic rate. Resting B cells need low-level

BCR stimulation to enhance survival (Kraus et al., 2004). This does not represent a mitogenic stimulus and cells do not proliferate in response to it. However, resting B cells can become active when they encounter antigens (Figure 1.14).

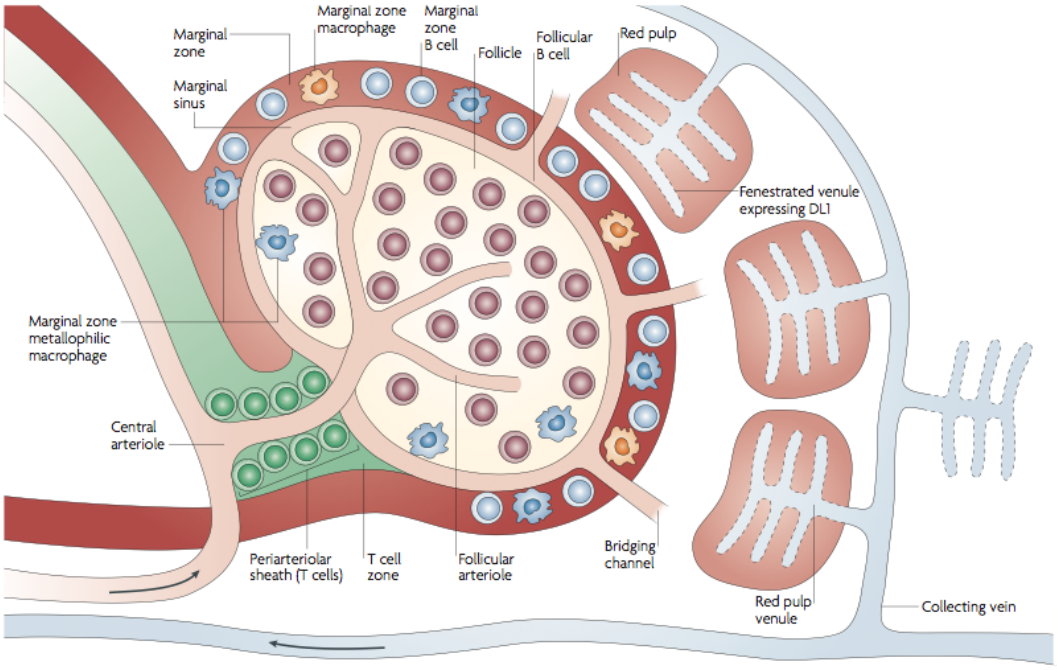


Figure1.14: Anatomy of the spleen.
Two different areas form the spleen: white pulp and red pulp. The white pulp is involved in the immune response while the main function of the red pulp instead is the filtration of red blood cells. In the white pulp there are two types of B cells: the follicular ones in the inner part and the marginal zone B cells in the part in contact with the red pulp. The white pulp is in contact with the periarteriolar sheath enriched in T cells.
(Adapted from (Pillai and Cariappa, 2009).

1.8.1 T-dependent and T-independent B cell activation

B cells are one of the most important effectors of the immune response. They are involved in the identification of antigen and, respond to it in a manner that is either T cell-dependent or T-cell independent. In T cell-dependent activation, the antigen binds to and activates the BCR. However, to achieve full activation, B cells need other signals from T helper cells (Noelle and Snow, 1991). T helper cells are activated by antigen presenting cells (APC) and are able to bind the major histocompatibility complex (MHC) and CD40 on B cells (Kupfer et al., 1994). APC can be dendritic cells, macrophages or B cells. Therefore, T helper cells are able to release cytokines to promote the development of B cells into

antibody-secreting long lived plasma cells or memory B cells. T dependent activation targets B cells that are present in the spleen follicles (Berek et al., 1991). This activation leads to production of germinal centres where B cells divide in order to then differentiate into long-lived plasma cells (Vernino et al., 1992). However, in an alternative pathway, a pool of follicular activated B cells enters into a quiescent state to form memory B cells, which will be able to recognize the same antigen in case of a second exposure (McHeyzer-Williams and Ahmed, 1999).

In the T-dependent response, binding of antigen to the BCR has a central role in the activation of B cells. The BCR is composed of two immunoglobulin heavy and light chains and two signalling components Igα and Igβ (Schamel and Reth, 2000). The antigen binding causes translocation of the BCR complex into specific areas of the cellular membrane called lipid rafts, which have a peculiar composition of sphingolipids and phospholipids (Gupta and DeFranco, 2007). Furthermore, lipid rafts are enriched for the presence of the kinase Lyn, which phosphorylates the immunoreceptor tyrosine-based activation motifs (ITAMs) on the Igα and Igβ (Pierce, 2002). The phosphorylated ITAM is recognized by the protein tyrosine kinase (PTK) SYK, which triggers the signalling pathway and activates transcription factors such as NFkb and NFAT (Niiro and Clark, 2002).

In the T cell-independent response bacterial wall lipids or non proteic bacterial components bind to the Toll Like Receptors (TLR) on marginal zone B cells. The marginal zone B cells are in close contact with antigens present in the blood of the spleen marginal sinus (Martin and Kearney, 2000). These cells can respond to the presence of antigens in two ways: they can develop short lived plasma cells or they can shuttle to the follicles to present the antigen either to T or B cells to trigger a more specific immune response (Cinamon et al., 2008).

TLRs are membrane glycoproteins that can bind different ligands to initiate an immune response. One of the most studied TLRs is TLR4, which can mediate the response to LipoPolySaccharide (LPS) (Poltorak et al., 1998). Stimulation of TLR leads to activation of the transduction signal that is driven by the myeloid differentiation primary-response protein 88 (MyD88) and IL-1R-associated kinase 4 (IRAK4). The pathway that is triggered by the binding of antigens to TLR drives the transcription of NF-kb regulated genes (Takeda and Akira, 2004).

1.9 Aim of the study

The aim of this project was to study the role of Cnot3 in gene regulation and cell cycle progression. Preliminary data collected in our lab revealed a strong interaction of Cnot3 with the Aurora B kinase, which has been shown to be involved in controlling transcription in resting B cells. Cnot3 was found to co-localise with Aurora B at many active gene promoters in these cells. Moreover, recent published studies have demonstrated a role for Cnot3 in transcriptional regulation in ES cells and in several human pathologies. These results formed the basis for a detailed investigation of the role of Cnot3 in gene regulation and the cell cycle, using quiescent and activated mouse splenic B cells as a model system.

Chapter 2 Material and methods

2.1 Resting B cell isolation

Resting B cells were isolated from 6 to 8 week old C57BL/6 mouse spleens. Cells were isolated using EasySep B cell enrichment kit (STEMCELL Technology) according to manufacturer's instructions. Spleens were homogenized and centrifuged for 10 minutes at 2,000 rpm without break in a Ficoll-Paque (GE Healthcare) gradient to separate lymphocytes from erythroid cells. Cells were incubated 15 minutes at 4°C with a cocktail that included monoclonal biotinylated antibodies that recognize surface markers of mouse cells of hemapoietic origin (CD4, CD8, CD11b, CD43, CD49b, Ly-6G (Gr-1), TER119). In the cocktail is also present an FcR blocker that recognizes mouse CD16/CD32 (Fcγ III/II Receptor), which is present on B cells and other FcR^+ cells. Cells were then incubated 15 minutes at 4°C with a cocktail containing Tetrameric Antibody Complexes (TAC) that recognizes the biotin of the antibodies bound to the cell surface. A suspension of magnetic dextran iron beads was used for 5 minutes at 4°C to bind the TAC on cells carrying biotinylated antibodies on the surface. A magnet was then used to deplete the suspension of unwanted cells leaving a pure resting B cell population in suspension.

2.2 B cell culture and synchronization

Resting B cells were cultured in RPMI-1640 supplemented with 15% Fetal Calf Serum (FCS) (Sigma), 0.1 U/ml penicillin (Lonza), 0.1 μg/ml streptomycin (Lonza), 2 mM L-Glutamine (Lonza), 50μM beta-mercapthoethanol (Gibco). The resting B cells were treated with 25 μg/ml of anti-IgM antibody (Millipore) for 20 hours to obtain cells in early G1. LPS (Sigma) was added at a concentration of 25 μg/ml and cells were left in culture for 6 hours to reach late G1. In order to synchronize cells, Aphidicolin (Sigma) was added to the culture at 1 μg/ml followed by incubation for 16 hours. After the treatment, aphidicolin blocked cells were washed once in medium at 1,800 rpm for 5 minutes at room

temperature to remove the inhibitor. The cells were then cultured in fresh medium. They were collected 30 minutes and 1, 2, 4 and 6 hours after the release.

2.3 ES cell culture, electroporation and crystal violet staining

Mouse A7 ES cells expressing Cre recombinase (kindly provided by Prof. Merkenschlager, MRC CSC London) were cultured on lamin coated plates in the following medium: Neurobasal (Gibco) and DMEM:F12 1:1 (Lonza) medium supplemented with N2 (Gibco), B27 (Gibco), 2 mM L-glutamine (Gibco), 100 uds/ml Penicillin-Streptomycin (Gibco), 0.1 mM β-mercaptoethanol (Gibco), 1 μM PDO3 (Stemgent), 3 μM CHIRON (Stemgent), 200 uds/ml LIF (Millipore).

$3x10^6$ cells were used for the electroporation of the TALEN plasmids and the linearized donor vector. The final amount of DNA that was electroporated was 10 μg, which included 3 μg of each TALEN plasmid and 4 μg of the linearized donor vector containing a neomycin resistance. Cells were washed three times with cold Phosphate-Buffered Saline (PBS) by centrifugation at 80g for 5 minutes at 4°C. They were then resuspended in 90μl of nucleofector solution and mixed with 10μl of the DNA mix. The cells and DNA mix were transferred to a cuvette and electroporated using the program A24 in the Nucleofector™ Device (Lonza). 0.5 ml of warm medium was then added to cells to plate them. Cells were growth in medium containing neomycin in order to select cells that integrated the donor vector.

Crystal violet was performed to stain the presence of colonies in the plates. After one week of selection, plates were washed and fixed in 4% paraformaldheyde (PFA) for 10 minutes. They were washed three times in PBS for 5 minutes. Cells were then stained with 0.5% Crystal violet/water for 15 minutes. Plates were washed with water and let air-dry.

2.4 Aurora B conditional knockout mice

Aurora B conditional knockout (cKO) mice were generated by Dr. Mónica Román Trufero by crossing homozygous Rosa26-CreER^{T2} mice with a strain of

mice in which exons 2 and 6 of the Aurora B gene flanked by *loxP* sites ($Aurkb^{fl/fl}$, kindly provided by Dr. Marcos Malumbres, CNIO, Madrid). The mice generated from this cross express the cre-estrogen receptor fusion protein, $CreER^{T2}$, under the control of the ubiquitous Rosa26 promoter. After treatment with 4-hydroxytamoxifen (4-OHT), $CreER^{T2}$ migrates into the nucleus and the Cre recombinase excises the floxed region and shuts down expression the Aurora B gene.

2.5 FACS analysis

2.5.1 PI staining

For Propidium Iodide (PI) staining, $1x10^6$ cells were collected by centrifugation at 2,500 rpm for 5 minutes at 4°C. Cells were washed in 1ml of 2% FCS/PBS. Fixation was performed by resuspending cells in 70% ethanol and leaving them for 10 minutes at -20°C. Two further washes in 2% FCS/PBS were carried out before incubating cells for 30 minutes at room temperature in PBS containing 0.05 mg/ml PI (Sigma), 0.05% Igepal CA-630 and 1 μg/ml RNase A (Sigma). Cells were analyzed on a FACSCalibur machine (BD Pharmigen).

2.5.2 Staining of cell surface markers

To determine the expression of cell surface markers, $1x10^6$ cells were washed in 2% FCS/PBS. Cells were then blocked using 5% goat serum and anti-CD16 antibody for 5 minutes at 4°C. A 1:100 dilution of anti-CD69 and anti-B220 antibodies were used. After two washes with 2% FCS/PBS, cells were resuspended in PBS and analyzed on a LSRII FACS machine.

2.5.3 EdU incorporation assay

EdU incorporation experiments were carried out using the kit Click-iT® EdU Flow Cytometry Assay Kits (Invitrogen) according to manufacturer's instructions. The experiments were performed using $1x10^6$ cells. EdU was added at a concentration of 10 μM for 30 minutes at 37°C before harvesting. Cells were collected and washed in 3 ml of 1% Bovine Serum Albumin (BSA) in PBS. After

centrifugation at room temperature for 5 minutes at 1,800rpm, they were resuspended in 100 µl of Click-iT fixative and incubated for 15 minutes at room temperature, protected from light. Cells were then washed once with 3 ml of 1% BSA/PBS and spun for 5 minutes at 1,800rpm. They were resuspended in 100 µl of Click-iT saponin-based permeabilization and wash reagent and incubated at room temperature for 15 minutes. 0.5 ml of Click-iT reaction cocktail were added and cells were incubated 30 minutes at room temperature. Cells were then washed once in 3 ml of Click-iT saponin based permeabilization buffer and resuspended in 0.5 ml of the same buffer for analysis on a LSR II FACS machine.

2.6 DAPI staining

Coverslips were coated with 400 µl of poly-Lysine at room temperature for 15 minutes. They were then washed once with PBS and once with RPMI medium for 3 minutes at room temperature. $5x10^5$ cells were spread over the coverslip. Cells were left 5 minutes to attach to the coverslip and incubated for 15 minutes at room temperature with 3 ml of 4% PFA. The coverslip was washed three times for 3 minutes with 3ml of PBS at room temperature. In order to stain for DNA content, cells were incubated 1 minute with 1 µg/ml of DAPI solution at room temperature. To mount the coverslip on a slide 20 µl of Mowiol were used. The slides were analysed using the Leica SP5 confocal microscope.

2.7 Proteomics

2.7.1 Nuclear protein extraction for IP

In order to extract proteins from the nuclear soluble and chromatin bound fraction, 15 million cells/IP were collected and washed 2 times in 1 ml of ice cold PBS. Cells were then resuspended in 1 ml of Sucrose buffer (10 mM Tris pH 8.0, 320 mM sucrose, 3 mM $CaCl_2$, 2 mM, Magnesium acetate, 1 mM DTT, 0.1 mM EDTA, 0.5% Igepal CA-630, supplemented with Complete MINI, EDTA-free protease inhibitors (Roche Diagnostics)) and incubated for 5 minutes on ice. The tube was spun at 500 g for 5 minutes at 4°C. In order to get rid of the cytoplasmic fraction, the supernatant was discarded and the nuclei resuspended in 200 µl of

high salt buffer (50 mM Tris pH 7.5, 400 mM NaCl, 1mM $MgCl_2$, 10% glycerol, 0.5 mM EDTA, Igepal CA-630 (Sigma), supplemented with Complete MINI, EDTA-free protease inhibitors). The samples were placed on a shaker at 1,400rpm for 30 minutes at 4°C. They were then centrifuged at 14,000 rpm for 15 minutes at 4°C. The supernatant representing the nuclear soluble fraction was kept on ice.

The pellet of chromatin was digested following two different protocols. Samples from resting B, 20 hours anti-IgM and 20 hours anti-IgM + 6 hours LPS cells were incubated with 6 units of micrococcal nuclease (MNase) (Sigma) and 15 units of benzonase (Novagen) at 4°C for 1 hour on a rotating wheel at 20 rpm. The salt concentration was then increased to 340 mM and the tubes were incubated for 1 hour at 20 rpm on a rotating wheel at 4°C. The samples were then centrifuged at 8,000 g for 10 minutes at 4°C to remove all the insoluble material. The supernatant was recovered and combined with the nuclear soluble fraction. The salt concentration was adjusted to 150 mM NaCl.

Aphidicolin blocked and 30 minutes, 1 hour, 4 hours and 6 hours aphidicolin released cells were treated with 1,000 gel units of MNase (NEB) at 1,400 rpm for 15 minutes at 37°C on a thermoshaker. The tubes were then spun at 8,000 g for 10 minutes at 4°C to remove the insoluble material. The supernatant was recovered and combined with the nuclear soluble fraction. The salt concentration was adjusted to 150 mM NaCl.

2.7.2 Co-immunoprecipitation and western blotting

All IPs for Co-immunoprecipitation (Co-IP) experiments were performed using nuclear soluble and chromatin bound fraction proteins extracted from 15 million cells. The protein extract was incubated for 16 hours with 50 µl of Dynabeads protein G (Invitrogen), pre-coupled with 2.5 µg of antibody. The beads were then washed three times with 500 µl of 0.1% Tween 20 at 4°C for 5 minutes at 12 rpm. The immunocomplexes were eluted by boiling the beads at 70°C for 15 minutes at 1,400 rpm in 60 µl of 2X loading buffer (125 mM Tris-HCl pH 6.8, 5% SDS, 0.004 % Bromophenol Blue, 0.2 M DTT, 10% glycerol). To carry out the western blot, half of the eluted material was diluted 1:2 in water and then loaded on acrylamide/bis-acrylamide gel. Proteins were transferred onto

nitrocellulose membranes (GE) using transfer buffer (25 mM Tris pH 8.3, 192 mM glycine, 0,1% SDS, 20 % methanol (VWR)). The membrane was blocked for 2 hours at room temperature in 5% milk/0.05% Igepal CA-630 in TBS. The primary and secondary antibodies were both diluted in blocking solution, in which the milk was replaced by 0.5 % BSA. The membrane was incubated over night with the primary antibody at 4°C and 45 minutes with the secondary at room temperature. The secondary antibodies were horseradish peroxidase (HRP)-conjugated and the Western Lightning Chemiluminescence Reagent Plus (Perkin Elmer) was used as chemiluminescent substrate for visualization of bands.

2.7.3 GST Aurora B protein expression, extraction and purification

Full-length mouse Aurora B cDNA (Addgene) was cloned in pGEX-4T-1, containing an ampicillin resistance gene, and then transformed in BL21 competent E.Coli cells. Bacteria were then grown in LB ampicillin agar plates over night at 37°C. A colony of bacteria was inoculated over night at 37°C in 2 ml of LB broth containing Ampicillin. The pre-inoculum was added to 98 ml of LB broth containing ampicillin and grown at 37°C to reach OD_{600} density of 0.6. Isopropyl β-D-1-thiogalactopyranoside (IPTG) (Sigma) was added at a concentration of 0.4 mM to induce protein expression. Cells were grown for 3 hours at 37°C and centrifuged at 6,000 rpm for 10 minutes at 4°C.

The pellet was resuspended in 6 ml of lysis buffer (50 mM Tris-HCl pH 8.0, 0.15 M NaCl, 1 mM EDTA, supplemented with Complete MINI, EDTA-free protease inhibitors). Lysozome was added to a final concentration of 100 μg/ml and cells were incubated 20 minutes on ice. DTT was then added at a concentration of 1 mM together with 1.5% sarcosyl and the tube was inverted several times. The lysate was then sonicated at intervals of 15 seconds on and 45 seconds off for 5 minutes. The lysate was then centrifuged at 10,000 rpm for 10 minutes at 4°C. The supernatant was collected and TritonX-100 was added to a final concentration of 1% and the lysate was filtered through a 45 μm filter. 100 μl of Glutathione Sepharose High performance (GSH) beads (GE Healthcare) were pre-washed in lysis buffer and incubated overnight at 4°C at 8 rpm on a

rotating wheel with the bacterial lysate. Beads were washed three times at 4°C for 10 minutes at 12 rpm with 500 µl of washing buffer (0.5% TritonX-100 in lysis buffer). The GST fused proteins were eluted twice in 1 volume of elution buffer (10 mM glutathione reduced, 5% glycerol in lysis buffer supplemented with Complete MINI, EDTA-free protease inhibitors) for 30 minutes at room temperature on a rotating wheel at 8 rpm.

2.7.4 *In vitro* transcription/translation

Cnot3 full length cDNA (Addgene) was cloned in pCDNA 3.2/V5/GW/D-TOPO® by PCR addition of restriction sites SmaI/NotI following the manufacturer's instructions. The cloning was carried out using pCDNA plasmid to take advantage of the T7 promoter for the *in vitro* transcription/translation. For the cloning of the full length Cnot3 the following primers were used: Fw 5'-CACCATGGCGGACAAGCGCAAACT-3', Rv 5'- CTGGAGGTCCCGGTCCTCCAGGTA-3'.

In order to generate Cnot3 mutants, mutant cDNAs were produced by PCR and then cloned in pCDNA 3.2/V5/GW/D-TOPO®. For the cloning of the Cnot3 mutant Δ1-200 the following primers were used: Fw 5'-CACCATGGAGATTAAGAAGCTACA-3', Rv 5'-CTGGAGGTCCCGGTCCTCCAGGTA-3'. For the cloning of the Cnot3 mutant Δ701-751 the following primers were used: Fw 5'-CACCATGGCGGACAAGCGCAAACT -3', Rv 5'-CATCATATACTTGGTGTGGAATCG -3'. For the cloning of the Cnot3 mutant Δ651-751 the following primers were used: Fw 5'- CACCATGGCGGACAAGCGCAAACT-3', Rv 5'-GGGTGGCATCTGGTGGTGGTAGGG-3'.

In order to perform a GST pull down assay with GST Aurora B, Cnot3 full length and the mutants were *in vitro* transcribed/translated using a TNT® Quick Coupled Transcription/Translation kit (Promega) according to manufacturer's instructions. 0.5 µg of plasmid were incubated with 20 µl of TNT T7 quick Master Mix, 1 µl of ^{35}S Methionine 10µCi and H_2O to reach a final volume of 25 µl. The reaction of transcription/translation was performed for 90 minutes at 30°C.

2.7.5 GST pull down assay

50 µl of GSH beads were washed three times at 4°C for 5 minutes at 12 rpm with the 200 µl of binding buffer (50 mM Tris HCl pH 8.0, 150 mM monopotassium glutamate, 1mM EDTA, 0.1 % Igepal CA-630, 5% glycerol, 0,2% BSA and supplemented with Complete MINI, EDTA-free protease inhibitors). 1 µg of GST or GST Aurora B was added to the beads and incubated at 4°C for 2 hours at 8 rpm rotation. The beads were then washed two times at 4°C for 5 minutes at 12 rpm rotation with 500 µl of binding buffer. 5 µl of the *in vitro* transcribed/translated Cnot3, generated as described in section 2.7.4, was incubated with the beads at 4°C over night at 8 rpm rotation. The beads were then washed three times at 4°C for 5 minutes at 12 rpm rotation with 500 µl of binding buffer without BSA. The beads were resuspended in 40 µl of loading buffer and incubated for 5 minutes at 95°C. The eluted proteins were loaded on acrylamide/bis-acrylamide gel. The gel was stained for 15 minutes in a staining solution (0.1% coomassie blue, 50% methanol, 10% acetic acid, 40% H_2O) and destained for 2 hours in destaining solution (50% methanol, 10% acetic acid, 40% H_2O). The gel was dried for 1 hour at 80°C and consequently exposed to X-ray film over night at room temperature.

2.7.6 Mass Spectrometry (MS) analysis

Co-IP experiments of Cnot3 IP in nuclear extracts were performed using early G1 and G2 cells as described in sections 2.7.1 and 2.7.2. To perform the IP a mix of two Cnot3 antibodies was used to a final amount of 2.5 µg. An anti-IgG control was used to carry out an IP in both samples and used as a negative control.

Eluted samples from the co-IP experiments were run on acrylamide/bis-acrylamide gel. The gel was then incubated with a staining solution (0.1% coomassie blue, 50% methanol, 10% acetic acid, 40% H_2O) for 1 hour at room temperature. The stained gel was processed for MS analysis by the Proteomics facility at the MRC CSC.

The samples were injected in a Thermo Scientific (Dionex) Ultimate 3000 nano liquid chromatography system to separate peptides prior to mass

spectrometric analysis. Peptides were then eluted on-line to an analytical column (Thermo Scientific Acclaim Pepmap RSLC). Eluted peptides were analysed using a Thermo LTQ-Orbitrap Velos operating in positive polarity, top 10 MSA CID (multistage activation collision induced dissociation mode) method. Ions for dissociation were determined from an initial 15,000 resolution MS survey scan (event 1) followed by MSA on the top 10 most abundant ions.

The analysis generated raw files that were searched against UniprotKB/Swiss-Prot database (version March 2012) restricted to mouse entries using Mascot v2.3.1 and Mascot Distiller v2.4.1. A fixed modification of carbamidomethylation (cysteine) was used, with variable modifications of oxidation (methionine), acetylation (protein N-terminal) and phosphorylation (serine, threonine, tyrosine). Precursor mass tolerance of 10ppm and fragment tolerance (MS/MS) of 600 mmu were used.

In the Co-IP MS analysis all the proteins with Normalised MS intensities (fold over max) above 0.1 in the control lane were discarded. The gene ontology analysis was performed using the free on-line software GOrilla.

2.7.7 *In vitro* peptide binding assay

Two peptides were synthesized by GL Biochem Shangai with the sequence of the mouse histone H1.3. They included amino acids 25 to 41 of H1.3. One peptide carried an acetylation on the lysine corresponding to the H1.3K35, while the other peptide had the same sequence without modification. Both peptides were synthesized with an N terminal acetylation and C terminal biotinylation. The N terminal was acetylated to enhance the solubility and stability of the peptide. The sequences are as it follows: Ac-KKTGAAAGKRK(Acetyl)ASGPPVSELIGK-(Biotin) and Ac-KKTGAAAGKRKASGPPVSELIGK- (Biotin). 25 µl of NeutrAvidin Agarose Resin were washed three times at 12 rpm rotation for 5 minutes at 4°C in 0.2% Triton-X/PBS. 2.5 µg of peptide were added to the beads and incubated at 4°C overnight at 8 rpm rotation.

Cnot3 full length and mutants were transcribed/translated as reported in section 2.7.4. A 5 µl aliquot of the reaction was incubated with 25 µl of the resin in a final volume of 500 µl of binding buffer (50 mM Tris HCl pH 8.0, 150 mM

monopotassium glutamate, 1mM EDTA, 0.1 % Igepal CA-630, 5% glycerol, 0,2% BSA and supplemented with Complete MINI, EDTA-free protease inhibitors) and incubated at 8 rpm rotation for 4 hours at 4°C. The resin was washed three times in binding buffer without BSA at 4°C for 10 minutes at 12 rpm rotation. Proteins were eluted by adding 30 µl of loading buffer and boiling at 95°C for 5 minutes. The eluted material was loaded onto a acrylamide/bis-acrylamide gel. The gel was stained for 15 minutes in a staining solution (0.1% coomassie blue, 50% methanol, 10% acetic acid, 40% H_2O) and destained for 2 hours in destaining solution (50% methanol, 10% acetic acid, 40% H_2O). The gel was dried for 1 hour at 80°C and exposed to X-ray film overnight at room temperature.

2.8 Chromatin Immunoprecipitation

2.8.1 Chromatin preparation

B cells were treated with formaldehyde (Sigma) to a final concentration of 1% to crosslink proteins to DNA. Cells were incubated at room temperature for 10 minutes with gentle tumbling. The reaction was then stopped by adding glycine (Sigma) to the medium to a final concentration of 0.125 M and incubating cells for 10 minutes at room temperature with gentle tumbling.

The crosslinked cells were spun for 7 minutes at 780 g and 4°C. Cells were washed twice with 10 ml of ice cold PBS. They were resuspended in 1.5 ml of swelling buffer/25x10^6 cells (25 mM Hepes pH 7.9 (Sigma), 10 mM KCl (Sigma), 1.5 mM $MgCl_2$, 0.1 % Igepal CA-630 (Sigma)) supplemented with Complete MINI, EDTA-free protease inhibitors (Roche Diagnostics). The cells were incubated for 10 minutes on ice and then homogenized using a tight dounce homogeniser with 50 strokes.

The nuclei were centrifuged at 3,000 g for 5 minutes at 4°C and resuspended to a final concentration of 2.5x10^7cells/ml in sonication buffer (50 mM Hepes pH 7.5, 140 mM NaCl (Sigma), 0,1 % sodium deoxycholate (Sigma), 0.1 % SDS (Sigma), 1% Triton-X 100 (Sigma), 1 mM EDTA (VWR)) supplemented with Complete MINI-EDTA free protease inhibitors (Roche Diagnostics). Aphidicolin treated cells and anti-IgM+ 14 hours LPS were resuspended to a final

concentration of $2x10^7$cells/ml in sonication buffer. 1 ml of suspension was transferred to 15 ml falcon tubes containing a probe for sonication. The falcon tubes were placed in a carousel of a Bioruptor sonicator (Diagenode) connected to a water bath (Thermo Scientifics), which kept the temperature of the water in the sonicator basin constantly at 4°C. The nuclei were sonicated at 30-second on/off intervals for 1.5 hours at high intensity to obtain a fragment size of approximately 500-3,000 bp.

The sonicated material was centrifuged at 10,000 g for 10 minutes at 4°C to remove the insoluble material. The purified chromatin was quantified after a 5 minute alkaline lysis (1:10 dilution of chromatin in 0.1 M NaOH (Sigma)) by measuring the DNA concentration using a ND-1000 spectrophotometer (Nanodrop). A 5 μg aliquot of chromatin was saved as input material.

2.8.2 Immunoprecipitation

Antibodies were pre-bound to paramagnetic Protein G Dynabeads (Invitrogen). For the immunoprecipitation (IP), 5 μg of antibody was incubated with 15 μl of magnetic beads at 4°C for 4 hours at 8 rpm rotation. The beads were then washed with 200 μl of sonication buffer by incubating at 4°C for 7 minutes at 8 rpm rotation.

For each ChIP assay, 100 μg of chromatin were added to the antibody-bound beads. The samples were incubated overnight at 4°C with 8 rpm rotation. The beads were sequentially washed with 200 μl of each of the following buffers: sonication buffer, high salt buffer (50 mM Hepes pH 7.5, 500 mM NaCl, 0.1% sodium deoxycholate, 0.1% SDS, 1% Triton-X 100, 1 mM EDTA), LiCl buffer (20 mM Tris pH 8 (Sigma), 250 mM LiCl (VWR), 0.5% sodium deoxycholate, 0.5% Igepal CA-630 (Sigma), 1 mM EDTA) and TE buffer (10 mM Tris pH 8, 1mM EDTA).

To elute the chromatin from the beads and reverse the formaldehyde crosslinking, the beads and the input DNA were resuspended in 150 μl of elution buffer (50 mM Tris pH 8, 50 mM NaCl, 1% SDS, 1 mM EDTA, 20 μg/ml DNase-free RNase (Roche Diagnostics)) and incubated at 68°C for 6 hours at 1,400 rpm on a thermoshaker. The supernatant was collected and the beads were further

eluted for 1 hour with 150 µl of elution buffer at 68°C at 1,400 rpm. For input samples, a final volume of 200 µl of elution was added to 5 µg of input and crosslink reversal was carried out for a total of 7 hours.

The resulting mixture of DNA and proteins was incubated at 42°C overnight at 300 rpm in the presence of 200 µg/ml proteinase K (Sigma) to cleave proteins. The DNA was further purified using QIAQuick PCR purification kit (Qiagen), according to manufacturer's instructions. The DNA from IP experiments and input was eluted in 100 µl of AnalaR grade water (VWR).

2.8.3 Quantitative real-time PCR

Quantitative real-time PCR (qRT-PCR) were performed to determine the binding levels of each factor using the same volume (2 µl) for the immunoprecipitated and input samples per reaction. The enrichment of the amplified sequence was reported as the percentage of the input that was pulled down by the specific antibody and calculated by the equation:

$$\% \text{ of INPUT} = ((2^{-\text{average CT IP}} / 2^{-\text{average CT input}})X100)/\text{input dilution factor}$$

The input dilution factor is the ratio between the amount of chromatin used for the IP and the volume input chromatin. qRT-PCR was performed either on Chromo 4 (Biorad) or DNA Engine Opticon system (MJ research) following these conditions: initial denaturation at 95°C for 10 minutes followed by 37 cycles at 95°C for 15 seconds, annealing at 60°C for 15 seconds, extension at 72°C for 15 seconds and final extension at 72°C for 5 minutes. The threshold for every experiment was set to meet a point at which the amplification was linear.

For every primer pair, the Ct values for the IP DNA and the input were generated in duplicate PCRs (technical duplicates). For each primer pair, each well on qRT-PCR plates (Biorad) was loaded with 2 µl of DNA and 23 µl of primer mix (10.3 µl of water, 0.1 µl of 100 µM forward primer, 0.1 µl f 100 µM reverse primer, 12.5 µl of SYBR Green JumpStart Taq Ready Mix (Sigma)).

2.9 ChIP-sequencing (ChIP-seq)

2.9.1 Preparation of libraries

ChIP-seq libraries were prepared from 10 ng of DNA that was immunoprecipitated using the ChIP protocol described in section 2.8.2. The DNA was first tested by qRT-PCR and then used to prepare libraries using the Library Prep Master Mix Set for Illumina (NEB) with minor variations on the manufacturer's protocol. The quantity of DNA adaptors was a 1:60 dilution of the recommended amount, to reduce the amount of unligated adaptors that would compete with and reduce the sequenced specific DNA fragments. Short fragments (such as those generated by unligated fragments) tend to be sequenced more than long ones. To sequence more than one library per lane in the Illumina HiSeq2000 (Illumina), DNA Illumina adapters and indexes from the Multiplexing Sample Preparation Oligonucleotide Kit (Illumina) were used to allow sample multiplexing.

Following PCR enrichment of adaptor ligated DNA fragments, the libraries were resolved on a 2% agarose gel to get rid of primer dimers and gel purified with Qiaquick Gel extraction kit (Qiagen) according to manufacturer's guidelines. The purified libraries were analysed on the Bioanalyser (Agilent) with a High Sensitivity DNA kit (Agilent) for the determination of the average fragment size and to assess the integrity of the library. ChIP-seq libraries were given to the analyzed on an Illumina HiSeq2000 sequencer by the Genomics Laboratory at the MRC CSC. Libraries were always subjected to single ended sequencing and the output size was 50 bp. Dr. Gopuraja Dharmalingam and Dr. Thomas Carroll from the CSC Core Bioinformatic Facility provided post-sequencing bioinformatic analysis of all the output files.

2.9.2 Data analysis and peak calling

The data analysis was carried out in collaboration with Dr. Gopuraja Dharmalingam and Dr. Thomas Carroll. The overall quality of the sequencing reads including per base quality distribution, duplicate level, GC content and adapter contamination were assessed by fastqc version 0.10.0. The reads were aligned to Mouse genome mm9 using Bowtie version 0.12.8 using "-S –n 2 –I 25 –

m 1' parameters. Only reads aligned uniquely to the genome were considered for further analysis. The SAM files generated by Bowtie were converted to BAM files using Samtools version 0.1.18, sorted according to chromosomal co-ordinates and orientation (duplicates) were filtered using Picard version 1.65. To visualize the genomic coverage of samples in UCSC genome browser, the reads were extended to estimate fragment size and converted to BigWig format. The fragment size was computationally estimated using SISSR method for each sample (Jothi et al., 2008) and the reads were extended using R script. Coverage for each base was computed using the extended the reads visualised using UCSC server. ChIP-seq experiments from resting B, 20 hours anti-IgM and 20 hours anti-IgM + 6 hours LPS were done in biological duplicate. The tracks generated from the duplicates were pooled together. ChIP-seq experiments from 30 minutes, 4 hours and 6 hours aphidicolin released cell were performed once.

Peaks were identified using MACS2 (https://github.com/taoliu/MACS/) with parameters "callpeak --broad --qvalue 0.05" and peaks with fold enrichment less than 20 were excluded from the analysis (Zhang et al., 2008). Peaks were filtered for mm9 blacklists and annotated to genic regions and distance to nearest TSSs using Chipseeker Bioconductor package.

2.9.3 Density plot generation

To visualize the ChIP-seq enrichment for each factor/modification around TSS, we divided TSS +/- 1kb region in to 50 base bins (total 40 bins). Gene co-ordinates were retrieved from Ensembl version67 using 'biomRT' bioconductor package. The genes were ordered by Cnot3 binding strength. The number of reads overlapping with each bin was counted and Reads per Million per bin (RPM) was calculated.

For the heatmaps generation, the area of the TSS +/- 3kb was divided in 50 base bins (120 bins). Me V version 4.8 was used to generate the heatmap images and visualize the enrichment.

2.9.4 Gene ontology analysis

Gene ontology analysis was carried using peaks coordinates called in every cell cycle phase. The analysis was performed using a free software available on-line and developed by the Bejerano lab (McLean et al., 2010).

2.10 Transcriptional Analysis

2.10.1 Spike-in preparation

The necessity of studying RNA levels during cells cycle requires having an accurate control to study gene expression variation. Due to the difficulty to find a housekeeping gene that does not change during the cell cycle, we generated a random DNA sequence that is not present in any genome. The sequence was created by using a free online software (http://www.bioinformatics.org/sms2/random_dna.html).

The sequence is the following:

5'-
CACCATGGTACTCTGGGGTGATATCTTTCCGGCATTTTGGGCAATGACCGGAACAGA
TAGGCATTGTGGGACCGGACGCGAGGGCCATACATGGTGGTGCCGACATACCACCCG
AGGCGCACCACGAGAATCATTTATTCTGTGTGTGGCATGTACGCTGACCATAAGGCG
CCAGTGGTTAGAGCTTTCCTTTCGGCATT-3'.

The DNA was cloned into pCDNA 3.2/V5/GW/D-TOPO® by PCR addition of restriction sites SmaI/NotI.

The part of the plasmid containing the spike sequence and the T7 promoter was then amplified by PCR. The PCR was performed using a Forward biotinylated primer in order to get a biotinylated linear DNA. The primer sequences used were the following: Fw 5'-BtnATGCGGTTTTGGCAGTACAT-3', Rv 5'- AAGGGCGAAAAACCGTCTAT-3'. The DNA was biotinylated to allow it to be immobilized on streptavidin beads during the process of transcription of the spike RNA. This procedure was carried out to allow high purity recovery of the RNA after the *in vitro* transcription.

DNA was purified using a PCR purification kit to remove the biotinylated primers. 10 μg of biotinilated DNA were incubated over night at 25°C with 40 μl of Dynabeads® MyOne™ Streptavidin T1 (Invitrogen) in wash and binding buffer (10 mM Tris-HCl pH 7.5, 1 mM EDTA, 2 M NaCl). The beads were then washed

with the same buffer three times at 25°C for 10 minutes at 300 rpm to remove the unbound DNA. The transcription reaction was carried out while the DNA was bound to the beads. The experiment was carried out using T7 Polymerase (Promega) according to manufacturer's instructions. 100 μl of transcription reaction mix Transcription optimized buffer, 10 mM DTT, 0.5 μM rNTP mix, Phage RNA Polymerase 40 units) were added to the DNA-beads and incubated at 300 rpm for 2 hours at 37°C. The supernatant containing the RNA was separated from the beads using a magnet. To ensure that there was no contaminating DNA in the supernatant, a DNase digestion was carried out using the RNeasy kit (Qiagen). The RNA was quantified on an ND-1000 spectrophotometer.

2.10.2 Isolation of nuclear RNA and preparation of cDNA

Cells from different phases of the cell cycle were collected and counted. $5x10^6$ cells were resuspended in 500 μl of buffer A (10 mM Hepes pH 7.9, 10 mM KCl, 1.5 mM $MgCl_2$, 0.5 mM DTT, 10% glycerol, 0.2% Triton-X 100). Cells were incubated on ice for 10 minutes. Nuclei were centrifuged at 4°C for 15 seconds at 14,000 rpm and the supernatant was discarded. The same volume of buffer A was added to the nuclei and they were spun at 4°C for 15 seconds at 14,000 rpm. Nuclei were resuspended in 1 ml of Trizol and spike RNA was added to a concentration of 0.1 ng/million cells. The lysate was incubated at room temperature for 5 minutes. 200 μl of Chloroform were added to the samples and vortexed for 10 seconds. Samples were left for 3 minutes at room temperature and centrifuged at 4°C for 15 minutes at 15,000 g. The aqueous phase was transferred to a new tube and 500 μl of isopropanol were added. The samples were incubated 10 minutes at room temperature and then centrifuged at 4°C for 10 minutes at 15,000 g. The pellet was washed once in 75% ethanol and then resuspended in 30 μl of DEPC-treated water.

The RNA was subjected to DNase digestion and RNA clean up by using the RNeasy kit according to manufacturer's instructions. The RNA was then quantified with a ND-1000 spectrophotometer and used for reverse transcription with random Hexamers (Applied Biosystems) and SuperScript II (Invitrogen). The protocol was performed as follows:

	RT+	RT- (Negative control)
RNA (ng)	100	100
Random Hexamers (µl)	1	1
10 mM dNTP (µl)	1	1
H_2O	up to 12 µl	up to 12 µl
Incubate 5' at 65°C		
5x buffer (µl)	4	4
0.1 M DTT (µl)	2	2
Rnase OUT inhibitor	1	1
SuperScript II (µl)	0.5	0
H_2O	up to 21 µl	up to 21 µl

The reverse transcription reaction was carried out as follows: 10 minutes at 25°C, 50 minutes at 42°C, 10 minutes at 94°C. 0.5 µl of RNase H was added to the sample to digest the RNA in RNA-DNA hybrids. Samples were then diluted 1:20 and 1 µl was used for each qRT-PCR reaction. For each primer pair the Ct values were generated in duplicate, while in the No RT the Ct values were produced in single. The qRT-PCR was carried out as described in Section 2.8.3 with except that the PCR was carried out for 40 cycles instead of 37.

2.10.3 RNA quantification

Specific primers were designed for the spike-in RNA and they were used to detect the level of the spike-in in every sample. To calculate the expression level of each gene relative to the spike-in RNA, the following formula was used:

RNA expression Gene X = $2^{Ct(Spike\text{-}in)-Ct(X)}$.

2.11 Cnot3 conditional knockout mice

2.11.1 TALEN design and construction

TALEN genomic binding sites were chosen using the online software published by Cermak *et al*, 2011. Input sequences were both introns 1 and 7. From all possibilities, we chose TALEN pairs that cut 200 bp or further from the exon to avoid interference with transcription and splicing as much as possible.

The protein sequences of the final TALENs used are as follows: (the repeat variable di-residues (RVDs) are shown underlined).

Intron 1
5' TALEN
MASSPPKKKRKVSWKDASGWSRMHADPIRPRRPSPARELLPGPQPDRVQPTADRGV
SAPAGSPLDGLPARRTVSRTRLPSPPAPSPAFSAGSFSDLLRPFDPSLLDTSLLDSMPAV
GTPHTAAAPAEWDEAQSALRAADDPPPTVRVAVTAARPPRAKPAPRRRAAQPSDAS
PAAQVDLRTLGYSQQQQEKIKPKVRSTVAQHHEALVGHGFTHAHIVALSQHPAALGT
VAVTYQHIITALPEATHEDIVGVGKQWSGARALEALLTDAGELRGPPLQLDTGQLVKI
AKRGGVTAMEAVHASRNALTGAPLNLTPDQVVAIASNGGGKQALETVQRLLPVLCQD
HGLTPDQVVAIASNNGGKQALETVQRLLPVLCQDHGLTPDQVVAIASNIGGKQALETV
QRLLPVLCQDHGLTPDQVVAIASNNGGKQALETVQRLLPVLCQDHGLTPDQVVAIASN
IGGKQALETVQRLLPVLCQDHGLTPDQVVAIASNGGGKQALETVQRLLPVLCQDHGLT
PDQVVAIASNGGGKQALETVQRLLPVLCQDHGLTPDQVVAIASNGGGKQALETVQRLL
PVLCQDHGLTPDQVVAIASHDGGKQALETVQRLLPVLCQDHGLTPDQVVAIASNGGG
KQALETVQRLLPVLCQDHGLTPDQVVAIASNIGGKQALETVQRLLPVLCQDHGLTPDQ
VVAIASNGGGKQALETVQRLLPVLCQDHGLTPDQVVAIASHDGGKQALETVQRLLPVL
CQDHGLTPDQVVAIASNGGGKQALETVQRLLPVLCQDHGLTPDQVVAIASNGGGKQA
LESIVAQLSRPDPALAALTNDHLVALACLGGRPAMDAVKKGLPHAPELIRRVNRRIGE
RTSHRVADYAQVVRVLEFFQCHSHPAYAFDEAMTQFGMSRNGLVQLFRRVGVTELEA
RGGTLPPASQRWDRILQASGMKRAKPSPTSAQTPDQASLHAFADSLERDLDAPSPMH
EGDQTRASSRKRSRSDRAVTGPSAQQAVEVRVPEQRDALHLPLSWRVKRPRTRIWGG
LPDPISRSQLVKSELEEKKSELRHKLKYVPHEYIELIEIARNSTQDRILEMKVMEFFMK
VYGYRGKHLGGSRKPDGAIYTVGSPIDYGVIVDTKAYSGGYNLPIGQADEMQRYVEEN
QTRNKHINPNEWWKVYPSSVTEFKFLFVSGHFKGNYKAQLTRLNHITNCNGAVLSVE
ELLIGGEMIKAGTLTLEEVRRKFNNGEINF

3' TALEN
MASSPPKKKRKVSWKDASGWSRMHADPIRPRRPSPARELLPGPQPDRVQPTADRGV
SAPAGSPLDGLPARRTVSRTRLPSPPAPSPAFSAGSFSDLLRPFDPSLLDTSLLDSMPAV
GTPHTAAAPAEWDEAQSALRAADDPPPTVRVAVTAARPPRAKPAPRRRAAQPSDAS
PAAQVDLRTLGYSQQQQEKIKPKVRSTVAQHHEALVGHGFTHAHIVALSQHPAALGT
VAVTYQHIITALPEATHEDIVGVGKQWSGARALEALLTDAGELRGPPLQLDTGQLVKI
AKRGGVTAMEAVHASRNALTGAPLNLTPDQVVAIASNNGGKQALETVQRLLPVLCQD
HGLTPDQVVAIASNNGGKQALETVQRLLPVLCQDHGLTPDQVVAIASNIGGKQALETV
QRLLPVLCQDHGLTPDQVVAIASNIGGKQALETVQRLLPVLCQDHGLTPDQVVAIASN
NGGKQALETVQRLLPVLCQDHGLTPDQVVAIASHDGGKQALETVQRLLPVLCQDHGL
TPDQVVAIASNIGGKQALETVQRLLPVLCQDHGLTPDQVVAIASNNGGKQALETVQRL
LPVLCQDHGLTPDQVVAIASNNGGKQALETVQRLLPVLCQDHGLTPDQVVAIASNIGG
KQALETVQRLLPVLCQDHGLTPDQVVAIASNIGGKQALETVQRLLPVLCQDHGLTPDQ
VVAIASNNGGKQALETVQRLLPVLCQDHGLTPDQVVAIASHDGGKQALETVQRLLPVL
CQDHGLTPDQVVAIASNIGGKQALETVQRLLPVLCQDHGLTPDQVVAIASNNGGKQAL
ETVQRLLPVLCQDHGLTPDQVVAIASHDGGKQALETVQRLLPVLCQDHGLTPDQVVAI
ASNIGGKQALETVQRLLPVLCQDHGLTPDQVVAIASHDGGKQALETVQRLLPVLCQDH
GLTPDQVVAIASNGGGKQALETVQRLLPVLCQDHGLTPDQVVAIASHDGGKQALESIV
AQLSRPDPALAALTNDHLVALACLGGRPAMDAVKKGLPHAPELIRRVNRRIGERTSH
RVADYAQVVRVLEFFQCHSHPAYAFDEAMTQFGMSRNGLVQLFRRVGVTELEARGGT
LPPASQRWDRILQASGMKRAKPSPTSAQTPDQASLHAFADSLERDLDAPSPMHEGDQ
TRASSRKRSRSDRAVTGPSAQQAVEVRVPEQRDALHLPLSWRVKRPRTRIWGGLPDP

ISRSQLVKSELEEKKSELRHKLKYVPHEYIELIEIARNSTQDRILEMKVMEFFMKVYGY
RGKHLGGSRKPDGAIYTVGSPIDYGVIVDTKAYSGGYNLPIGQADEMQRYVEENQTRN
KHINPNEWWKVYPSSVTEFKFLFVSGHFKGNYKAQLTRLNHITNCNGAVLSVEELLIG
GEMIKAGTLTLEEVRRKFNNGEINF

Intron 7
5' TALEN
MASSPPKKKRKVSWKDASGWSRMHADPIRPRRPSPARELLPGPQPDRVQPTADRGV
SAPAGSPLDGLPARRTVSRTRLPSPPAPSPAFSAGSFSDLLRPFDPSLLDTSLLDSMPAV
GTPHTAAAPAEWDEAQSALRAADDPPPTVRVAVTAARPPRAKPAPRRRAAQPSDAS
PAAQVDLRTLGYSQQQQEKIKPKVRSTVAQHHEALVGHGFTHAHIVALSQHPAALGT
VAVTYQHIITALPEATHEDIVGVGKQWSGARALEALLTDAGELRGPPLQLDTGQLVKI
AKRGGVTAMEAVHASRNALTGAPLNLTPDQVVAIASNGGGKQALETVQRLLPVLCQD
HGLTPDQVVAIASHDGGKQALETVQRLLPVLCQDHGLTPDQVVAIASNIGGKQALETV
QRLLPVLCQDHGLTPDQVVAIASNNGGKQALETVQRLLPVLCQDHGLTPDQVVAIASH
DGGKQALETVQRLLPVLCQDHGLTPDQVVAIASNGGGKQALETVQRLLPVLCQDHGL
TPDQVVAIASNNGGKQALETVQRLLPVLCQDHGLTPDQVVAIASNNGGKQALETVQR
LLPVLCQDHGLTPDQVVAIASHDGGKQALETVQRLLPVLCQDHGLTPDQVVAIASNIG
GKQALETVQRLLPVLCQDHGLTPDQVVAIASHDGGKQALETVQRLLPVLCQDHGLTP
DQVVAIASHDGGKQALETVQRLLPVLCQDHGLTPDQVVAIASNIGGKQALETVQRLLP
VLCQDHGLTPDQVVAIASHDGGKQALETVQRLLPVLCQDHGLTPDQVVAIASNIGGKQ
ALESIVAQLSRPDPALAALTNDHLVALACLGGRPAMDAVKKGLPHAPELIRRVNRRIG
ERTSHRVADYAQVVRVLEFFQCHSHPAYAFDEAMTQFGMSRNGLVQLFRRVGVTELE
ARGGTLPPASQRWDRILQASGMKRAKPSPTSAQTPDQASLHAFADSLERDLDAPSPM
HEGDQTRASSRKRSRSDRAVTGPSAQQAVEVRVPEQRDALHLPLSWRVKRPRTRIWG
GLPDPISRSQLVKSELEEKKSELRHKLKYVPHEYIELIEIARNSTQDRILEMKVMEFFM
KVYGYRGKHLGGSRKPDGAIYTVGSPIDYGVIVDTKAYSGGYNLPIGQADEMQRYVEE
NQTRNKHINPNEWWKVYPSSVTEFKFLFVSGHFKGNYKAQLTRLNHITNCNGAVLSV
EELLIGGEMIKAGTLTLEEVRRKFNNGEINF

3' TALEN
MASSPPKKKRKVSWKDASGWSRMHADPIRPRRPSPARELLPGPQPDRVQPTADRGV
SAPAGSPLDGLPARRTVSRTRLPSPPAPSPAFSAGSFSDLLRPFDPSLLDTSLLDSMPAV
GTPHTAAAPAEWDEAQSALRAADDPPPTVRVAVTAARPPRAKPAPRRRAAQPSDAS
PAAQVDLRTLGYSQQQQEKIKPKVRSTVAQHHEALVGHGFTHAHIVALSQHPAALGT
VAVTYQHIITALPEATHEDIVGVGKQWSGARALEALLTDAGELRGPPLQLDTGQLVKI
AKRGGVTAMEAVHASRNALTGAPLNLTPDQVVAIASHDGGKQALETVQRLLPVLCQD
HGLTPDQVVAIASNGGGKQALETVQRLLPVLCQDHGLTPDQVVAIASNGGGKQALETV
QRLLPVLCQDHGLTPDQVVAIASHDGGKQALETVQRLLPVLCQDHGLTPDQVVAIASH
DGGKQALETVQRLLPVLCQDHGLTPDQVVAIASHDGGKQALETVQRLLPVLCQDHGL
TPDQVVAIASNIGGKQALETVQRLLPVLCQDHGLTPDQVVAIASNIGGKQALETVQRLL
PVLCQDHGLTPDQVVAIASNGGGKQALETVQRLLPVLCQDHGLTPDQVVAIASNGGGK
QALETVQRLLPVLCQDHGLTPDQVVAIASNGGGKQALETVQRLLPVLCQDHGLTPDQ
VVAIASNNGGKQALETVQRLLPVLCQDHGLTPDQVVAIASNNGGKQALETVQRLLPVL
CQDHGLTPDQVVAIASNGGGKQALETVQRLLPVLCQDHGLTPDQVVAIASHDGGKQA
LETVQRLLPVLCQDHGLTPDQVVAIASHDGGKQALETVQRLLPVLCQDHGLTPDQVV
AIASNGGGKQALETVQRLLPVLCQDHGLTPDQVVAIASNGGGKQALETVQRLLPVLCQ
DHGLTPDQVVAIASNGGGKQALESIVAQLSRPDPALAALTNDHLVALACLGGRPAMD
AVKKGLPHAPELIRRVNRRIGERTSHRVADYAQVVRVLEFFQCHSHPAYAFDEAMTQ
FGMSRNGLVQLFRRVGVTELEARGGTLPPASQRWDRILQASGMKRAKPSPTSAQTPD

QASLHAFADSLERDLDAPSPMHEGDQTRASSRKRSRSDRAVTGPSAQQAVEVRVPEQ
RDALHLPLSWRVKRPRTRIWGGLPDPISRSQLVKSELEEKKSELRHKLKYVPHEYIELI
EIARNSTQDRILEMKVMEFFMKVYGYRGKHLGGSRKPDGAIYTVGSPIDYGVIVDTKA
YSGGYNLPIGQADEMQRYVEENQTRNKHINPNEWWKVYPSSVTEFKFLFVSGHFKGN
YKAQLTRLNHITNCNGAVLSVEELLIGGEMIKAGTLTLEEVRRKFNNGEINF

All TALEN plasmids were synthesized using the Golden Gate method developed by Cermak *et al.* 2011 (Addgene) following the protocol indicated by the authors. The final cloning step was done using the pTAL4 vector that allows subclone of TALEN sequences into mammalian expression vectors.

The targeting vectors comprised two homology regions of 300 bp flanking each LoxP sequence. GenScript synthesized both vectors. The sequences are the following:

Intron 1: 5'-
ACTCATAAACCCTCTTAGGGTCTTCCTCTCCAGGATGCCCTGTTTCGGGGTCAACTTT
TGTAGTGTGGATTTCCCTGCCAACCGACCTCCTCTCCTCAGTCCTTTGTCCTCAGGCC
CTTCTGAATTAAACTCTGCTTCCTTCAGAATAAAAATAGGTGTCTTTGACCTCCCTG
ATGGGTTCATGTTTCTGAGTCTAAATTGCCAGTCTATCTGATGTGGAACTCCTCCAT
GTGTGCAGATCTGTTCACTCATAGCTAAGGTTCTTCTCTTTATCTTTTTGAGATTTCT
ATCTTCTCATCGATAACTTCGTATAGCATACATTATACGAAGTTATATTCTA
CCCTCCTTGAGTGCTGCTTCCTGCTTCCAAGTTTCTATAGCCATTTTTAGTGTCGGGC
TTCTGCTGTGGAATAAATTTCTCGAAAGTGTAAGACCCTCTTGTTTGATATCCTGCC
TTGTCCTGTATGAATGGGCCTTGATCTTCATATCTCTCTTCCCCTTCAGCTCACACCT
CTTAGCCTTTCCAGGAGCTGCCAGCCTCATGTATTCTGTGACTTACCTAGAGTGGCCT
CTCTCAGTCACCTCTGCTCTCAGCCCCTCAGTTTAGAAAGTACCAT-3'.

Intron 7:

5'-
TGGGGGCACCATCACCCACAGGGTAAGGGTGGAGGTGGCCTGTGAACAGAGGGCATC
TGGAGGCTCATAGGAGTCTGGTCCTGGATACACCTGGGGCAGAGATTGAAAAGGCAG
AACAAGGCAGCTTAGCTGGCTGAGTTGTGGTATAGGGAGGAAGTGAGAGAGGATATT
GGGATATTTGGGTAGACAGTGTAGCCATTGTTAGGGGCAGTTTGGGTGAAGATGGAC
TTAGGTTCAGCTGGCACCACATAGTGAGACCTGAAGAAAGGACCAAATTATAACTTC
GTATAGCATACATTATACGAAGTTATGGGAAGATACACAGCACTCCAAAAATTCCCA
GGATCTCAGGAGGGGGTTGGTATGTCTCTAAGAACCAGTTGCTGTTGGAAACCTGGA
AATGGTTTGGGCCAAAGTCATATGATAGGGTCCCGAATCTTACACCTTTAGGATTGT
AAGGGTGTGAGTTCAAAGGGATGTCGACTCTGTCTCGTTAATGGTGTCACCAGGGAA
GGAAGTTCTGATGGGATGGAAAGAAAGAAAGATGTCACTGGGAGGGAAAAGAGTAG
ATCCTTGATAAAAGGAGGAATTTGGAGCTGGCACTAAGGCAT-3'.

2.11.2 TALEN mRNA and targeting vector preparation

TALENs were subcloned into pCDNA3.1. The new plasmids were linearised and transcribed in vitro using the mMessage mMachine T7 Ultra kit and the Megaclear kit (Life Technologies) according to the manufacturer's instructions. The targeting vectors were linearised, precipitated and resuspended in injection buffer (10 mM TrisHCl, 0.1 mM EDTA).

The final injection mix consisted of the four TALEN mRNAs each one at a final concentration of 5 ng/µl and both targeting vectors at final concentration of 2 ng/µl each in injection buffer.

2.11.3 Microinjection into mouse oocytes

All procedures for injection of the TALEN construcs into mouse oocytes were carried out by the MRC CSC Transgenic Facility. C57BL/6 females were superovulated and mated with Rosa26-ER^{T2}Cre homozygous males. TALEN mRNA-targeting vector mix described above was injected into pronuclei of 0.5d-post-coitum oocytes.

2.11.4 Genotyping of mice

Genomic DNA was obtained from ear notches. The tissue was incubated at 95°C for 10 minutes in 50 µl of NaOH and spun for 5 min at 16,000 g. Supernatant was then mixed with 50 µl of 0.5 M TrisHCl pH 8.0. 1 µl of the DNA solution was subjected to PCR with primers amplifying around both targeting sites in introns.

Intron 1 (FW 5'-ATCTGTTCACTCATAGCTAAG-3', RV 5'-GAAGAGAGATATGAAGATCAAG-3').

Intron 7 (FW 5'-GAGATTGAAAAGGCAGAACAAG-3' and RV 5'-CAGAACTTCCTTCCCTGGTG-3').

Table 2.1: Antibodies

Antibody	Manufacturer	Host	Application
Aurora B (ab2254)	Abcam	Rabbit	ChIP
Aurora B (sc-14327)	Santa Cruz	Goat	Co-IP, Western Blot
B220-APC conjugated (553092)	BD	Rat	FACS
CD69-PE conjugated (553237)	BD	Hamster	FACS
Cnot3 (A302-156A)	Bethyl	Rabbit	ChIP, Co-IP,Western Blot
Cnot3 (V-20) (sc-82824)	Santa Cruz	Goat	Co-IP
IgM (AP128)	Millipore	Goat	B cell activation
Mouse IgG-HRP conjugated (sc-2031)	Santa Cruz	Goat	Western Blot
Goat IgG-HRP conjugated (sc-2020)	Santa Cruz	Donkey	Western Blot
Rabbit IgG-HRP conjugated (sc-2030)	Santa Cruz	Goat	Western Blot
Normal goat IgG (sc-2028)	Santa Cruz	Goat	Co-IP
Normal rabbit IgG (kch-504-250)	Diagenode	Rabbit	ChIP, Co-IP
Pcna (ab18197)	Abcam	Rabbit	ChIP
Xrn2 (ab72181)	Abcam	Rabbit	ChIP, Western Blot

Table 2.2: Primers for ChIP (promoter region)

Arhgef2 FW	AGAGCTGAGCTGGGTTACCA
Arhgef2 RV	ATCCCTTACCGGAGCAACTT
b-Actin FW	GCAGGCCTAGTAACCGAGACA
b-Actin RV	AGTTTTGGCGATGGGTGCT
Bcan FW	GCAAGATTTCCTACCGACCA
Bcan RV	TGCTTAGCAGGGGAGTCTGT
Cct3 FW	ACATACGCACAGGCAAAACA
Cct3 RV	TAGACGCGCTGGTTTTCTTT
Fcrl1 FW	TGAACACTGGACAAGGTTGCT
Fcrl1 RV	CTTGAAGGTGCCTCTCACCA
Insrr FW	GCGTAAACCAATCCGTTTCT
Insrr RV	GACCTCCTGGACATGCAGAC
Lmna FW	GATGCCAGCAAGAGAAAAGG
Lmna RV	GTTCCAGGCCTCACAAACAT
Mtx1 FW	GTCTCGGTTCTCGGCAAAG
Mtx1 RV	GAGCTGTTCTGCTGGTCAGG
Nestin FW	GGGCTGTCTGGCTGTATCTC
Nestin RV	CCCAGCTCAGCAGAGAAGAA
Pmf1 FW	GCGACTAGCTTCTGGAGGAA
Pmf1 RV	GCTGAGGTGAGCCGAGATAG
Prcc FW	GCCTCCTGCTCCGTGCTCTA
Prcc RV	AGTGACTCGGCGGCCATTAG

Table 2.3: Primers for primary transcript analysis

Arhgef11 RT FW	AACCATGAGCATACGGTTGC
Arhgef11 RT RV	AGGCAAACACAACACTTCCC
Cct3 RT FW	TGCTCAGTGAGTTCAGGGAAG
Cct3 RT RV	AGGCGAAAAGACCACTGGAAG
CD19 RT FW	TACCATGCCATCTCCTCTCC
CD19 RT RV	ACATACCTTCTACCTCCACCAG
Fcrl1 RT FW	AGGCACCTTCAAGTTACCATCC
Fcrl1 RT RV	TTTAAGATCCCCGTTCCCAGAC
Gba RT FW	AACTTCAGCCTCCCAGAAGAAG
Gba RT RV	TCCATGTTGCTCTAGAGACAGC
Nes RT FW	AGGCGCTGGAACAGAGATT
Nes RT RV	TGAAGGTCTCTTGCCATCCT
Pmf1 RT FW	TGAAACTCCTGGACGCCATAG
Pmf1 RT RV	ACTTACGATCCTGCGACAGAC
Prcc RT FW	GCCTTCCCAAGCCAAAGAAG
Prcc RT RV	ATGGTTACAAGTCCCTCCTACC
Spike RT FW	GAGGGCCATACATGGTGGT
Spike RT RV	CTCTAACCACTGGCGCCTTA

Table 2.4: Primers for mRNA analysis

Arhgef11 RT FW	CATTGGTGAATCGGAACTCAG
Arhgef11 RT RV	GCTGCATCTGAGCCCTGT
Cct3 RT FW	CCGTGAGATGATGTTGAGCA
Cct3 RT RV	CTGCCATTCTCTTCAAACTGC
CD19 RT FW	AGGCAAGGGGTGATGATGT
CD19 RT RV	GCTAACAGGCCAGTACCCTC
Fcrl1 RT FW	TCCTCATCTGCTCGGTTGAT
Fcrl1 RT RV	AGCATCGCTCTGCTTCATGT
Gba RT FW	TCCCCAAAAGCTTTGGCTAC
Gba RT RV	AGTGCTCTCGTAACGGCTGA
Nes RT FW	CTGCAGGCCACTGAAAAGTT
Nes RT RV	TTCCAGGATCTGAGCGATCT
Pmf1 RT FW	CTCCTCTCCGGAAGCTGTG
Pmf1 RT RV	CCTGTCGGCGACTAGCTTCT
Prcc RT FW	TGGGTACCACAACCACCACT
Prcc RT RV	CTCAACTCCAGGTGGCTCAG
Spike RT FW	GAGGGCCATACATGGTGGT
Spike RT RV	CTCTAACCACTGGCGCCTTA

Chapter 3 -Interaction of Cnot3 with the AuroraB kinase during the B cell cycle

3.1 Introduction

Our lab is interested in studying roles for the Aurora B kinase outside of mitosis. Aurora B is widely described as having its main function during mitosis and cytokinesis (Adams et al., 2001). However, emerging evidence has suggested involvement in other cellular processes such as cell cycle progression (Song et al., 2007) and gene regulation (Tardaguila et al., 2011). Recent results from the group showed that Aurora B is part of the transcriptional machinery controlling the program of quiescence in resting B cells (Frangini et al., 2013). Previous work in the lab identified interactors of the kinase in resting and elutriated G1 LPS-activated B cells by mass spectrometry. Among many proteins that were identified as potential interactors in the analysis, one of the strongest hits was subunit 3 of the CCR4-NOT deadenylase complex (Cnot3).

CNOT3 was recently shown to be a tumor suppressor, which is mutated in T-cell acute lymphoblastic leukemia (T-ALL) (De Keersmaecker et al., 2013). It has also been shown to play a role in maintaining the self-renewal program in ES cells by transcriptional activation of pluripotent genes (Hu et al., 2009). Preliminary data generated by Dr. Alberto Frangini revealed the presence of Cnot3 on promoters of active genes in resting B cells, showing co-localization with Aurora B at many genes.

The aim of this PhD project was to investigate the interaction between Cnot3 and Aurora B and the role of Cnot3 in gene regulation and cell cycle progression. In order to achieve this goal, I have developed a B cell system that has made it possible to study population of cells enriched in different cell cycle phases.

3.2 Characterization of a B cell system to study different phases of the cell cycle

To study the behaviour of Cnot3 during the cell cycle, a B cell system was developed based on activation of resting B cells isolated from adult mouse spleen. Resting B cells are mature cells in a quiescent state that can re-enter the cell cycle by stimulation of the B cell receptor on the cellular membrane. More than three decades ago, De Franco et al. showed that resting B cells can be partially activated and induced to enter the blast stage by incubation anti-IgM antibody, which binds to the BCR. The cells become larger and production of RNA and proteins increases, although even 24 hours after activation, no cells entered S phase. Cells did, however, respond rapidly to mitogenic stimuli, such as LPS, to proceed through S phase (Defranco et al., 1982).

We decided to use this method as a starting point for obtaining synchronised populations of cells in different cell cycle phases. Resting B cells were isolated from adult mouse spleen using a negative selection procedure. A cocktail of biotinylated antibodies (EasySep kit from STEMCELL technology), that bind receptors on different types of hematopoietic cells, was used to deplete unwanted cells from the splenocyte suspension leaving a high purity resting B cell population (see Material and Methods Section 2.1 for details). Staining with antibodies against a marker of mature B cells (B220) and a marker for activation (CD69) showed that the isolated cells were more then 98% $B220^+$ and less than 0.2% $CD69^+$ (Figure 3.1).

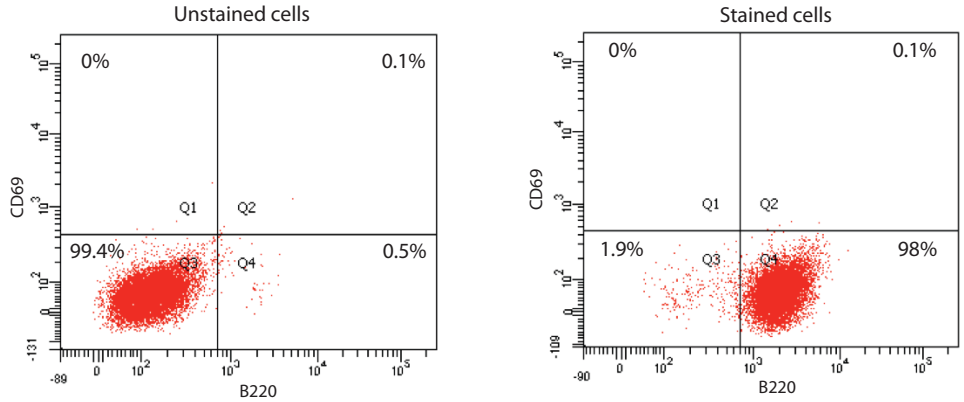


Figure 3.1: Characterization of the B cell population.
Resting B cells purified from adult mouse spleen were stained with anti-B220 and anti-CD69 antibodies and analyzed by FACS.

Purified resting B cells were incubated with anti-IgM antibody, which binds to the BCR, activating it and causing cell size to increase. In corroboration of De Franco's work I did not observe a significant number of cells in S phase, confirming that the antibody binding to the BCR for 20 hours causes entry into the blast stage, but not full activation (Figure. 3.2). When the anti-IgM activated cells were left in culture for 48 hours, a small percentage (around 30% of cells), were present in S or G2/M (data not shown). Therefore, all incubations with anti-IgM were carried out for 20 hours.

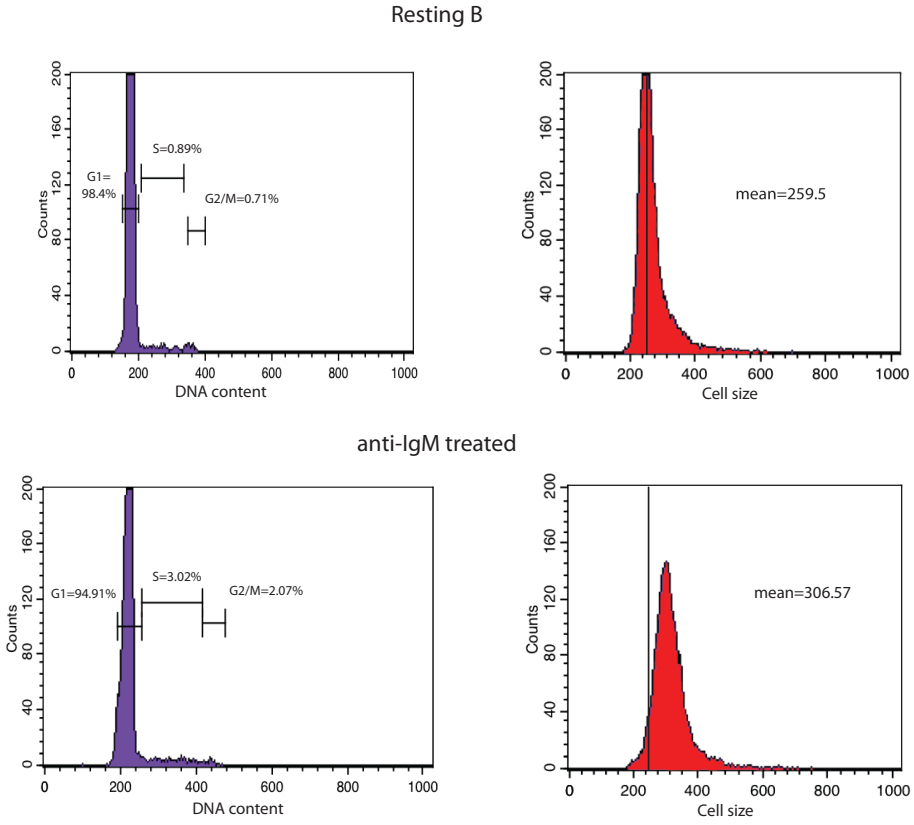


Figure 3.2: Activation of resting B cells by treatment with anti-IgM antibody. FACS analysis of propidium iodide stained resting and anti-IgM treated B cells. The left panels show the DNA content, with percentages relative to the proportion of cells in each cell cycle phase. The right panels show the distribution of cell size for resting and anti-IgM treated B cells.

In order to obtain synchronous entry into S phase using the anti-IgM treated cells, the cells were stimulated with LPS, which acts through the Toll like receptor 4 (TLR4) (Poltorak et al., 1998). Cells were collected at different time points after the LPS addition and analysed for cell cycle stage by PI staining.

However, this approach did not yield a population of cells that were fully synchronised in S phase (data not shown).

To further enhance the synchronization of the cells, we adopted a strategy of blocking the cells at the beginning of S-phase using the reversible DNA polymerase-α and -δ inhibitor aphidicolin. This compound acts as a nucleotide competitor for the active site of DNA polymerase and can be used to block cells at the onset of DNA replication (Krokan et al., 1981). To establish the most appropriate time point for applying aphidicolin, the timing of DNA replication after LPS addition to anti-IgM treated cells was determined. To achieve this, an EdU incorporation time course was performed to precisely detect when cells begin to incorporate the nucleotide analogue following activation with LPS. Samples were analysed 4, 6 or 8 hours after addition of LPS to anti-IgM treated cells. FACs analysis showed that around 5% of the cells were in S-phase at the 6 hours time point, suggesting that cells were starting to enter S phase (Figure 3.3). Hence, the decision was taken that aphidicolin should be added after 6 hours incubation with LPS.

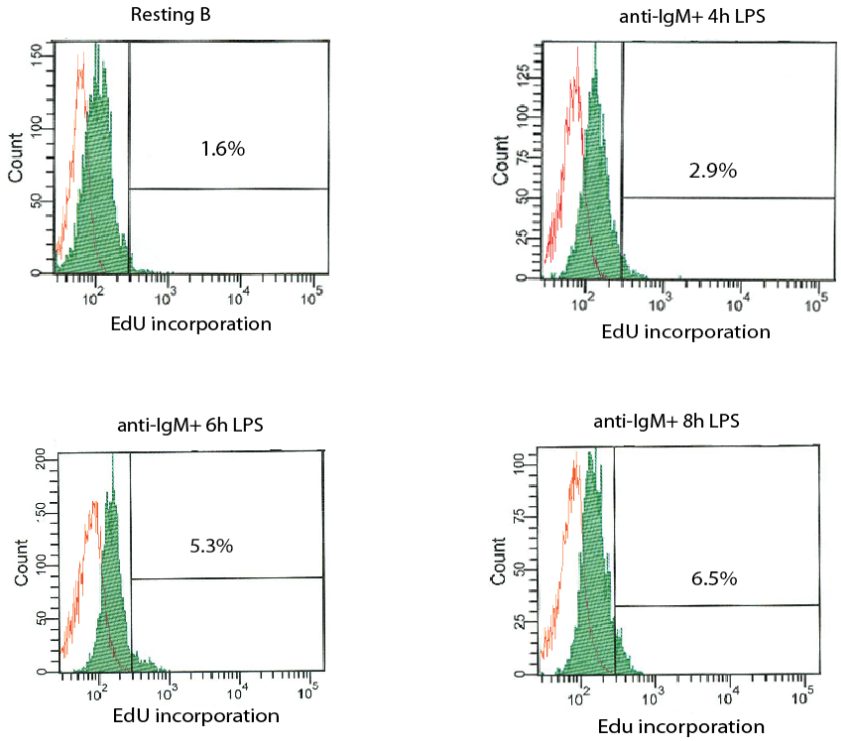


Figure 3.3: LPS response of anti-IgM treated cells.
FACS profile of EdU incorporation assay performed in resting and anti-IgM treated B cells at different time points after LPS addition. The green profile represents cells that were incubated for 30 minutes with EdU before harvesting, while the red profile shows the cells that have not been incubated with EdU. The value in the top right quadrangle of each FACS plot represents the percentage of EdU that has been incorporated.

The cells were incubated with aphidicolin for 16 hours and the inhibitor was washed out and the cells were cultured in fresh medium. The cell viability was measured after the treatment with the aphidicolin by trypan blue exclusion. The treatment with the DNA polymerase inhibitor caused around 40% of cell death. The cells were analysed by PI staining and FACS analysis immediately after release from the aphidicolin block and at different time points following release. Entry into S phase was observed to occur in a synchronous manner. After 30 minutes a shift was detected from G1 to a DNA content that is characteristic of S-phase, indicating that these cells were at the early stage of the replication process. The population of cells was enriched in S phase two hours from the wash-out of the aphidicolin. At this point around 80% of cells were in the replication phase of the cell cycle (Figure. 3.4A). This observation was confirmed by EdU incorporation, which gave very similar results for the percentage of cells in S phase (Figure 3.4B).

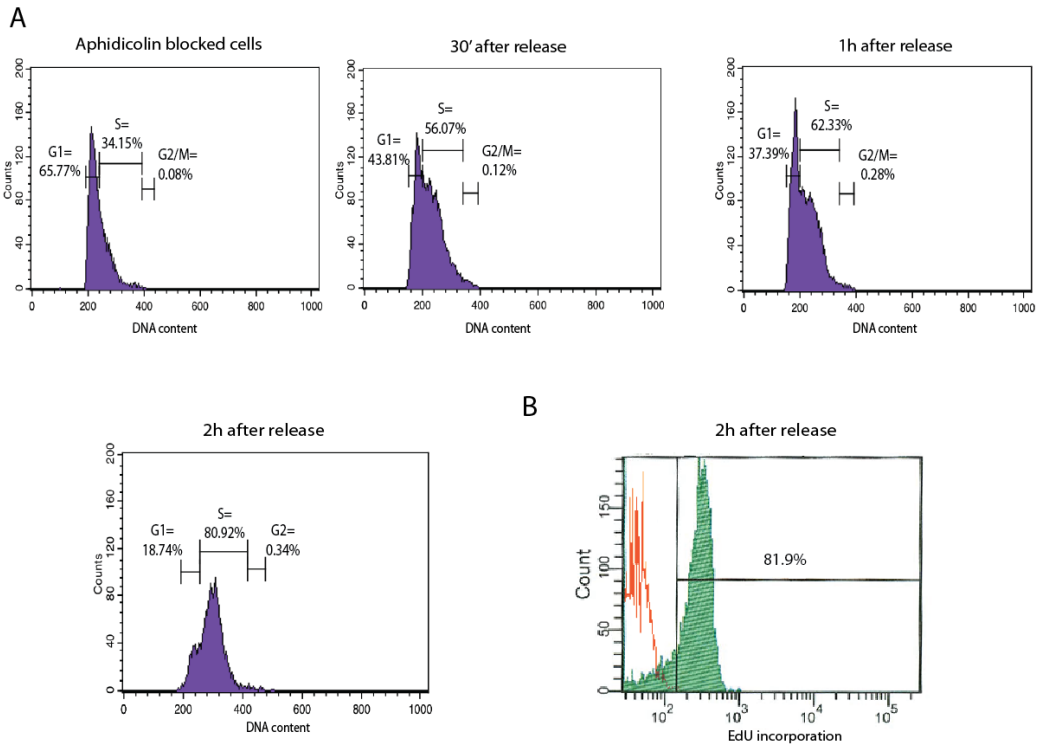


Figure 3.4: Synchronization of B cells in S phase.
A) FACS profile of propidium iodide staining of aphidicolin-blocked cells 30 minutes, 1 hour and 2 hours after wash-out of out the inhibitor. The numbers indicate the percentage of cells present in each cell cycle phase. B) FACS profile of EdU incorporation 2 hours after the aphidicolin wash-out. The gate has been set using the resting B cell profile.

In order to obtain a population of cells enriched in G2 and mitosis, the cells were released for 4 hours after the aphidicolin blocking. Visualisation by

confocal microscopy revealed an absence of mitotic cells, indicating that the cells were still in G2. After 6 hours, the cells were starting to divide, as shown in Figure 3.5 where characteristic metaphase plates can be clearly identified (Figure 3.5).

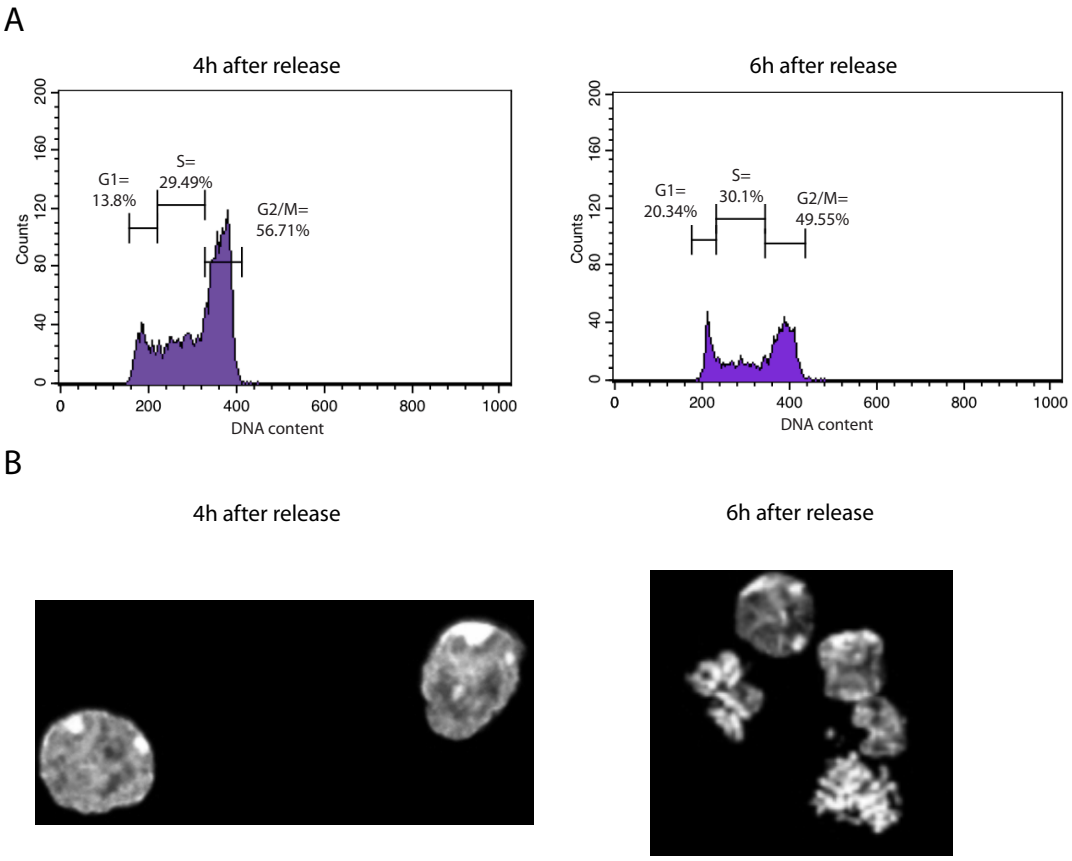


Figure 3.5: Populations of cells enriched in G2 and M phases.
A) FACS profile of propidium iodide staining showing the DNA content of cells collected 4 hours after aphidicolin release (G2) and after 6 hours (G2/M). The percentage of cells present in each cell cycle phase is shown. B) DAPI staining of the same population of cells to show the difference between G2 and G2/M populations.

3.3 Characterisation of the interaction between Cnot3 and Aurora B during cell cycle progression

The aim of this section of the project was to further characterize the interaction between Aurora B and Cnot3 that was identified by Dr. Alberto Frangini and to the extend the analysis to all stages of the cell cycle. Anti-Aurora B and anti-Cnot3

antibodies were used to immunoprecipitate the two proteins from the nuclear soluble and chromatin bound fractions of resting B nuclear protein extract. Western blot analysis was then used to probe for the presence of Aurora B and Cnot3 in the immunoprecipitated material. IP using an anti-IgG antibody was used as a negative control to guard against spurious IPs resulting from general stickiness or non-specific binding. A strong band for Cnot3 was observed for the Aurora B IP, confirming the interaction between the proteins (Figure 3.6). The Cnot3 IP gave a relatively weak IP of Aurora B, this may be due to the difference in abundance of the two proteins or to differences between the efficiency of pulldown by different antibodies.

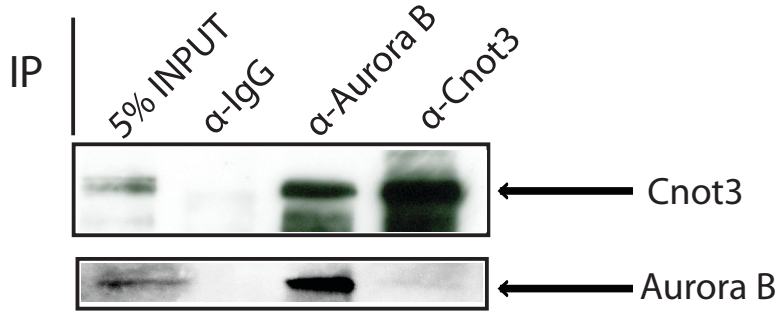


Figure 3.6: Interaction between Aurora B and Cnot3 in resting B cells.
Anti-Aurora B, anti-Cnot3 and anti-IgG antibodies were pre-bound to magnetic beads and incubated with nuclear protein extract from resting B cells. Western blot was carried out to detect the presence of Cnot3 and Aurora B. Input = 5% of the amount of extract used for the IP.

The co-IP analysis was extended to other phases of the cell cycle to establish whether the interaction is cell cycle dependent or not. Based on the co-IP result that was obtained in resting B cells, the remaining immunoprecipitations were carried out with anti-Aurora B antibody and the presence of Cnot3 in the immunprecipitated material was detected by western blot.

The results show that the interaction between Cnot3 and Aurora B varies during the cell cycle (Figure 3.7 A). Following anti-IgM treatment, when the cells are in early G1 and are starting to increase in size, it was still possible to detect a pulldown of Cnot3 but comparison with the results obtained in resting B cells, showed a decrease in the amount of Cnot3 in the IPd material. A similar level of pulldown was observed in late G1. (Figure 3.7 B).

In aphidicolin-blocked cells, Cnot3 interacts strongly with Aurora B when compared with early and late G1, suggesting that the interaction between the two proteins might play a role in the G1/S transition. There is already published evidence suggesting that this might be the case. Aurora B is part of a complex that controls the G1/S transition in T cells (Song et al., 2007) Cnot3 has been shown to be required for proliferation of MCF-7 breast cancer cells with reduced numbers of S-phase cells observed following knockdown of Cnot3 (Mittal et al., 2011). In early and mid S phase, 30 minutes and one hour after aphidicolin release, the Cnot3 and Aurora B interaction was reduced. When the cells were enriched for G2 cells, 4 hours after aphidicolin release, or in M-phase, 6 hours after release, a very strong interaction was detected. (Figure 3.7 D). The strong interaction in G2 and G2/M is particularly striking because the level of Aurora B is very high at this stage. The fact that similar levels of Aurora B and Cnot3 are detected in the pulldown with anti-Aurora B suggests that a large fraction of Aurora B is interacting with Cnot3 at these stages of the cell cycle.

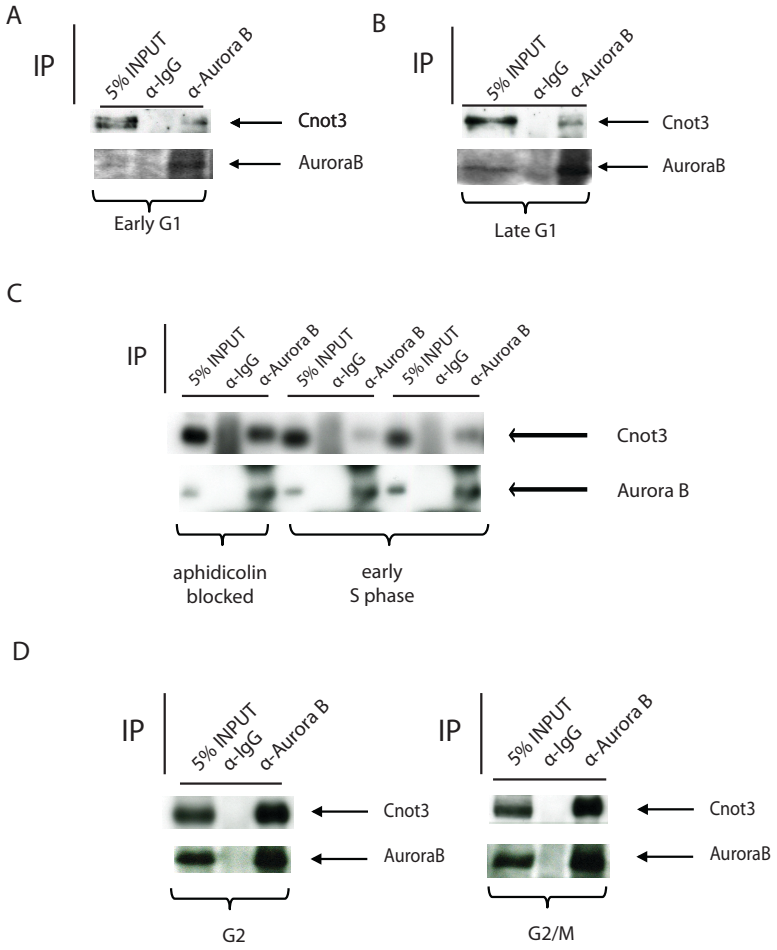


Figure 3.7: Interaction between Aurora B and Cnot3 during cell cycle progression in primary B cells
Anti-Aurora B and anti-IgG antibodies were pre-bound to magnetic beads and incubated with nuclear protein extracts from different cell cycle phases: anti-IgM 20 hours (A), anti-IgM+LPS 6 hours (B), aphidicolin blocked cells, 30 minutes and one hour after release (C), 4 and 6 hours after release (D). 5% of the extract used for the IP was analysed as INPUT.

3.4 *In vitro* analysis of the interaction between Cnot3 and Aurora B

The co-IP experiments described above reveal the existence of an interaction between Cnot3 and Aurora B during cell cycle progression. In order to map the region of Cnot3 that is responsible for the interaction, an *in vitro* GST pull down assay was performed using a GST tagged Aurora B and *in vitro* translated full length Cnot3 protein. Truncated Cnot3 proteins were also generated containing deletions at the N-terminus (Cnot3 Δ 1-200) or at the C-terminus (Cnot3 Δ 651-751, Cnot3 Δ 701-751). At the time when the mutants were generated, a crystal

structure of Cnot3 was not available, so the production of Cnot3 truncated proteins was based on structure prediction. At the end of 2013 a crystal structure for human CNOT3 was published (Boland et al., 2013). Human CNOT3 and mouse Cnot3 proteins share 95% of the sequence identity, with some differences present in the middle linker region. The N-terminus and the C-terminus are conserved, so we were able to use the crystal structure of the human CNOT3 protein to validate our mapping. The N terminus of Cnot3 consists of a coiled coil domain, while the C-terminus of the protein is called the NOT box domain and also includes the NOT1 anchor region (NAR) and the connector sequence (CS) (Figure 3.8).

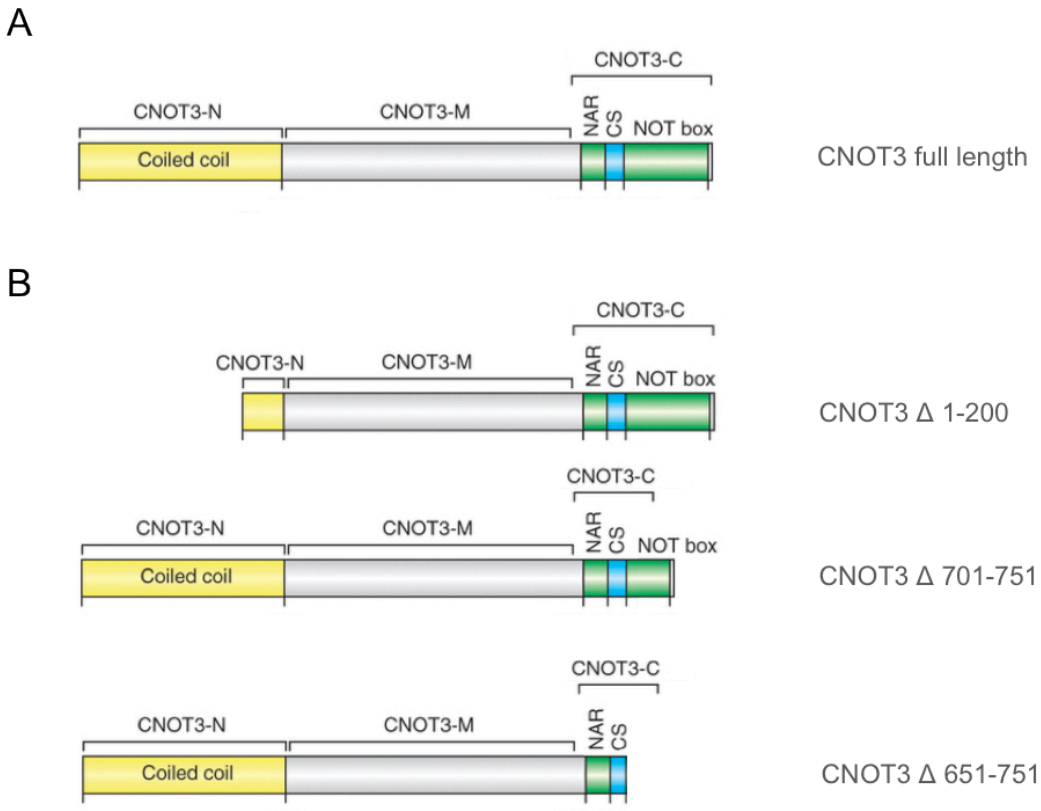


Figure 3.8: Schematic representation of the domain structure of wild-type human CNOT3 and the deletions of mouse Cnot3 used in the GST pull down assays.
A) Domains of human CNOT3, which is characterized by a coiled coil N-terminal domain, a central linker region and a C-terminal region that includes the NOT box domain, a Not1 anchor region (NAR) and a connector sequence (CS) (Adapted from (Boland et al., 2013)).
B) Deletions of mouse Cnot3 that were used for the GST pulldowns.

The results of the analysis (Figure 3.9) show that *in vitro* translated full length Cnot3 interacts directly with Aurora B. Of the three truncated Cnot3 proteins that were analysed, neither the N-terminal deletion of 200 amino acids or the Δ701-751 C-terminal deletion seem to have a significant effect on the binding of Cnot3 to Aurora B. Notably, the interaction was completely abolished when the NOT box was absent, indicating that the NOT box region of Cnot3 extending from 651 to 701 is required for the interaction with Aurora B.

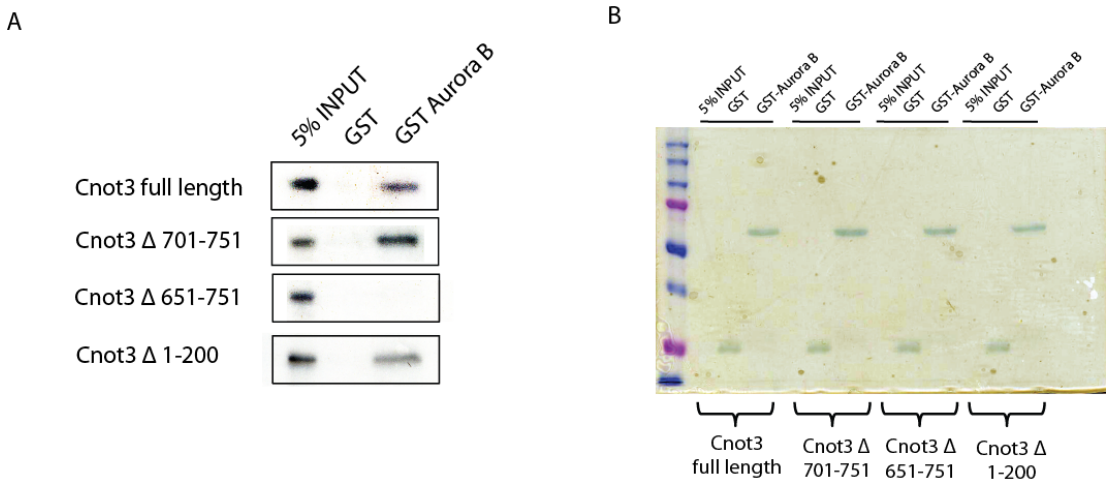


Figure 3.9: Mapping of Cnot3-Aurora B interaction.
GST pull-down using a purified bacterial expressed GST tagged Aurora B and *in vitro* translated Cnot3 proteins. GST Aurora B was pre-bound to GST agarose beads and then incubated with in vitro translated Cnot3, which was previously labeled with $^{S}35$ methionine. A) Autoradiography of gel samples. GST Aurora B was incubated with *in vitro* translated proteins: Cnot3 full length, Cnot3Δ 701-751, Cnot3Δ 651-751, Cnot3 Δ 1-200. B) Coomassie staining of the gel in the experiment in A to show the loading of the GST Aurora B.

3.5 Summary

In this chapter I have described a B cell system that makes it possible to study populations of primary B cells that are enriched in different cell cycle phases. I have used this system first to confirm the interaction previously revealed in our lab between Aurora B and Cnot3 in resting B cells, and then to extend the analysis to different phases of the cell cycle. The interaction between Aurora B and Cnot3 is dynamic and varies during cell cycle progression. Furthermore, I have demonstrated that the two proteins interact directly and I have mapped the region responsible for this to residues 651-701 of the NOT box of the Cnot3 protein.

Chapter 4- Analysis of Cnot3 interactors in early G1 and G2

4.1 Introduction

In order to analyse the role of Cnot3 during cell cycle in B cells, a co-immunoprecipitation analysis was carried out using anti-Cnot3 antibodies to identify Cnot3 interactors. The Cnot3 IP was followed by mass spectometry (MS) analysis. The analysis was performed on early G1 and G2 cells to identify proteins that interact with Cnot3 in these phases of the cell cycle.

Data that was described in Chapter 3 indicated a difference in the interaction of Cnot3 with Aurora B between early G1 and G2. These results raised the possibility that Cnot3 interacting proteins might be different between these two phases and suggest that Cnot3 could be part of different complexes at different cell cycle stages.

4.2 Mass spectrometry analysis of Cnot3 interactors

The Cnot3 IP was performed on a nuclear protein extract, including nuclear soluble and insoluble fractions. To maximise pulldown, a mix of two antibodies that recognise different part of the protein was used. IP done with an anti-IgG antibody was used as a negative control. The recovered proteins were then separated on a polyacrylamide gel and analysed by MS. The total number of proteins that were co-IPd in either or both samples was approximately 1,500. After quality control analysis, a total of 591 proteins was obtained that gave high confidence of recognition and were not present in the anti-IgG sample (see 2.7.6 for details of quality control). An initial gene ontology analysis was carried out all of the proteins that were co-IPd in early G1 and G2. Figure 4.1 shows a chart of the classes of proteins that interact with Cnot3 in the two stages. The class of proteins with the highest significance is RNA processing, but proteins involved in RNA metabolism and maturation also show low p-values. A good p-value score was also obtained for mRNA processing and splicing proteins. The analysis

shows that Cnot3 interacts with many splicing factors and RNA helicases that are involved in the mRNA production process. Proteins with functions related to RNA termination, turnover and export were also detected. From the global analysis of Cnot3 interactors in early G1 and G2, it appears that the largest category of Cnot3 interactions are with proteins that are involved in multiple aspects of RNA metabolism.

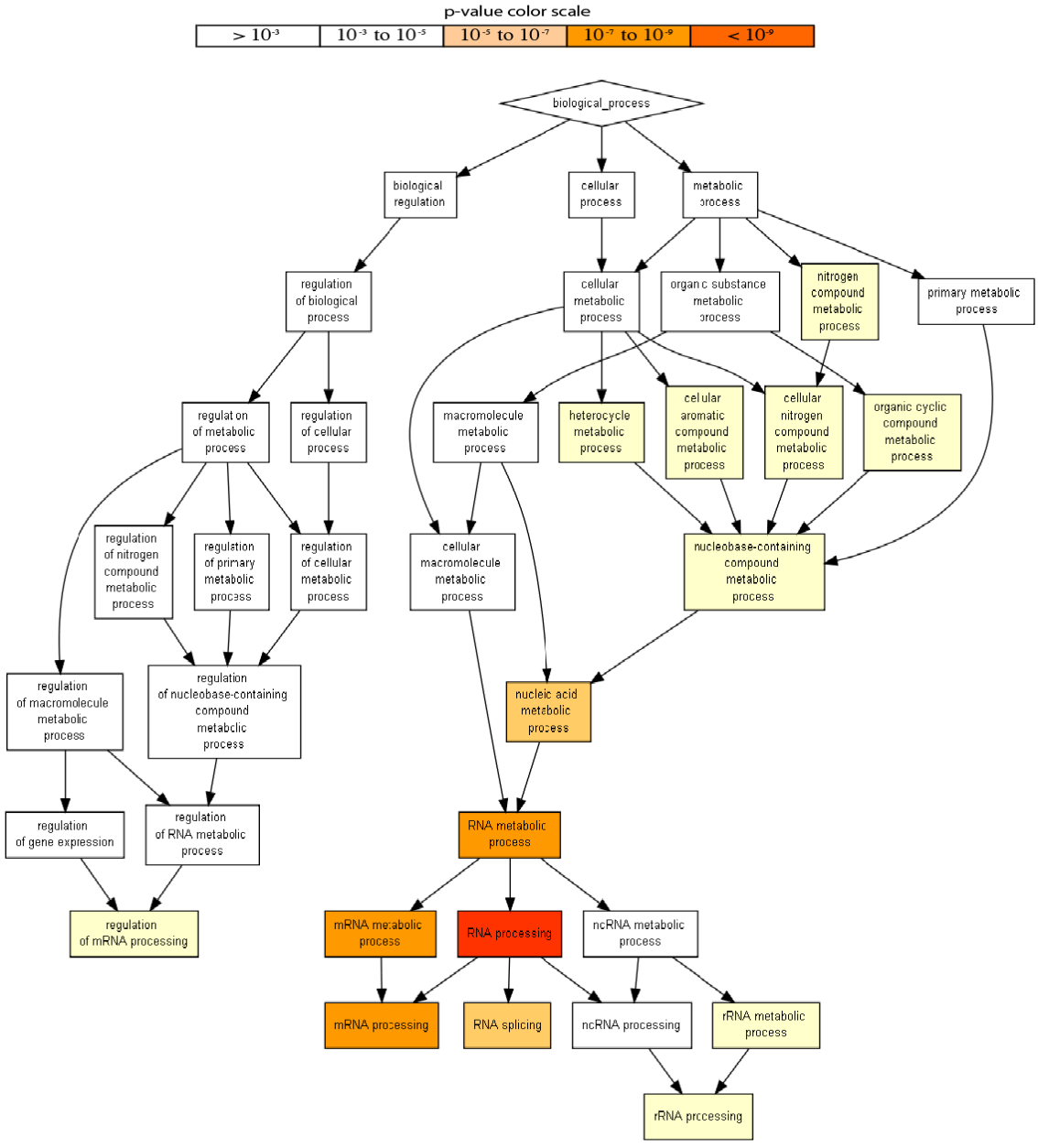


Figure 4.1: Gene ontology analysis of Cnot3 interactors in early G1 and G2 cells.
The GO analysis was carried out on 591 proteins identified by the MS analysis. Proteins that were included in the analysis were co-IPd by the anti-Cnot3 antibodies either in early G1 or in G2 or in both stages. The list of proteins obtained from the MS data was run on GOrilla software. A color scale from white to red represents the p-values for each category with red representing the most significant and white the least.

4.3 Cnot3 interacts with chromatin organization factors and splicing factors in early G1 cells

The aim of the analysis was to identify differences between Cnot3 interactions in early G1 and G2. Therefore, proteins have been divided to create two sub-groups relative to proteins present in one phase. Overlapping proteins that are present in both G1 and G2 were included in both lists. One major difference was the number of interacting proteins detected in each stage. In early G1, 239 proteins were detected by MS with high confidence whereas 425 proteins were detected in G2. This difference in the number of protein interactors in early G1 and G2 might reflect a different activation state of the cell and suggests that Cnot3 might be involved in more cellular processes in G2.

Among the most enriched classes of proteins in the G1 pulldown are chromatin organization proteins. They represent 13.1% of the proteins that are co-IPd with Cnot3 in early G1. Included in the chromatin organization protein group are histones, nucleolar proteins and transcription factors. Histone H1 was particularly enriched among the top hits in the list (Table 4.2). Five isoforms of histone H1 were co-IP'd (H1.1, H1.2, H1.3, H1.4, H1.5 and H1.t). Other histones are detected as well as histone H1, for instance histone H3.3 and many isoforms of the histone H2A. One of these is H2.AZ, which has recently been shown to be involved in recruitment of RNA polymerase II to active gene promoters (Bargaje et al., 2012).

Another Cnot3 interactor that was identified in early G1 was Nucleolin (Table 4.2). This protein acts together with histone H1 to regulate the accessibility of chromatin (Erard et al., 1988). Nucleolin is an ATPase and is one of the most abundant proteins in the nucleus. Nucleolin is involved in rRNA synthesis and ribosome biogenesis (Cong et al., 2012). Furthermore, it has been shown to have a role in regulating transcription in activated B cells (Hanakahi et al., 1997).

The role of Cnot3 in RNA regulation has been widely studied. The MS analysis has reported the interaction with proteins involved in splicing. In early G1 Cnot3 interacts with different classes of proteins involved in RNA maturation. They represent around 12.3% of the G1 proteins. Examples of these proteins are RNA helicases, small nuclear riboproteins and heterogeneous nuclear ribonucleoproteins (hnRNP proteins). The hnRNP proteins are involved in RNA

splicing, 3'end processing and regulation of transcription, as well as mediating the transfer of the mRNAs from the nucleus to the cytoplasm (Chaudhury et al., 2010).

Table 4.2: Early G1 interactors of Cnot3.
The table shows the first 40 out of 239 hits present in early G1 with a high protein score. The protein score is relative to the abundance and the quality of the peptide. The function for each protein is also shown.

Protein name	Protein score	Function
Nucleolin	1228.040559	Nucleolar Protein
Histone H1.2	922.245237	Chromatin organization
U5 small nuclear ribonucleoprotein 200 kDa helicase	882.3503041	Splicing
Histone H4	869.47	Chromatin organization
Rootletin	866.5340332	Cytoskeleton
Histone H2.AY	827.2599151	Chromatin organization
Histone H1.4	824.4873388	Chromatin organization
Histone H1.3	787.573305	Chromatin organization
Myotubularin related protein 5	731.785321	GTP releasing factor
Actin, gamma-enteric smooth muscle	708.2053219	Cytoskeleton
Histone H1.5	666.033305	Chromatin organization
Histone H1.1	654.6265251	Chromatin organization
Cytochrome b-c1 complex subunit 2	644.63	Metal ion binding
Heterogeneous nuclear ribonucleoprotein U	631.1532201	Splicing
Ras GTPase-activating-like protein IQGAP1	612.5225758	Signal transduction
Histone H2.B1H	550.163305	Chromatin organization
Histone H3.3	489.8753219	Chromatin organization
Smarca5	458.4164402	Chromatin organization
Putative ATP-dependent RNA helicase Pl10	444.943305	Splicing
Nucleolar transcription factor 1	435.2599151	Transcription factor
Regulator of non-sense transcripts 1	417.17	RNA Non-sense mediated decay
Histone H1.t	413.903305	Chromatin organization
Myosin-11	391.211932	Cytoskeleton
Histone H3.3C	388.793305	Chromatin organization
Actin related protein 3	384.7099151	Cytoskeleton
Elongation factor 2	362.3820169	Traslation
Histone H2.AX	361.4	Chromatin organization
Heat shock protein HSP 90-beta	355.8066101	Heat shock protein
Coronin1A	340.11	Cytoskeleton
Unconventional myosin Ig	334.9953219	Motor activity
Histone H2.B2E	326.87	Chromatin organization
Heterogeneous nuclear ribonucleoprotein U-like protein 2	325.64	Splicing
Heterochromatin protein 1-binding protein 3	324.3687118	Chromatin organization
RuvB-like 1	315.453305	Chromatin organization
Poly [ADP-ribose] polymerase 1	305.2366101	Transcription regulation
Apoptotic chromatin condensation inducer in the nucleus	303.6687118	Splicing
Filamin-A	296.8186269	Cytoskeleton
Gemin 5	283.7153219	Splicing
Rho guanine nucleotide exchange factor 6	283.563305	Signal transduction
Unconventional myosin-Ic	276.9486269	RNA transport

4.4 *In vitro* interaction Cnot3-histone H1

Among of the most abundant proteins found in the analysis were isoforms of histone H1. Cnot3 appeared to interact with many of histone H1 isoforms mainly in early G1. Histone H1 has eleven isoforms in mammals and is known to bind linker DNA, thus residing outside of the nucleosome. The main role for this protein is to regulate the condensation of chromatin by changing the structure of the chromatin fibres (Robinson and Rhodes, 2006). Moreover, the main function attributed to this histone variant was to control the accessibility of chromatin to transcription factors. However, there has been some controversy in the last decade about the role of H1 in regulating gene transcription. The first evidence obtained from studies on H1 suggested that it has a repressive role, promoting a closed state of the chromatin (Buttinelli et al., 1999). Nonetheless, there are some examples where H1 is involved in activation of transcription. This is mainly dependent on post-translational modifications. It has been reported that acetylation on lysine 34 of histone H1.4 can promote transcription, as it is enriched at promoters of active genes (Kamieniarz et al., 2012).

From the list of Cnot3 interactors, six isoforms of histone H1 were identified: H.1, H1.2, H1.3, H.4, H1.5 and H1.t. Furthermore, a post-translational modification analysis on the histone H1 isoforms has been done to check whether Cnot3 was preferentially binding any modifications on these proteins. The result revealed an interaction between Cnot3 and the isoform H1.3 that is acetylated at K35 (data not shown). Moreover, the N terminal part of the isoform H1.3, in which K35 resides, has 80% of homology with the isoform H1.4. Acetylation of H1.4K34 has been linked to transcriptional activation. From the alignment of the two proteins, H1.4K34 corresponds to H1.3K35.

To validate this interaction, an *in vitro* assay was performed using *in vitro* translated Cnot3 and a histone H1.3 peptide modified at the lysine 35. The assay was carried out by incubating *in vitro* translated Cnot3 either with an un-modified histone H1.3 peptide or the K35Ac peptide. The experiment used *in vitro* translated Cnot3 full length and Cnot3 mutants that were used previously to map the Cnot3-Aurora B interaction. As a negative control streptavidin beads were incubated with *in vitro* translated Cnot3 proteins to verify the presence of non-specific binding. The Cnot3-H1 interaction was confirmed but it was not

possible to detect a strong difference in binding between the modified and the unmodified peptide. A difference was observed in the interaction of the two peptides with the Cnot3 mutant lacking the 701-751 region of the NOT box domain. This truncated protein had a higher affinity for the un-modified peptide. The peptide did not interact with the mutants that lacked either the NOT box at the C terminal or a 200 amino acid region at the N terminal (Figure 4.3).

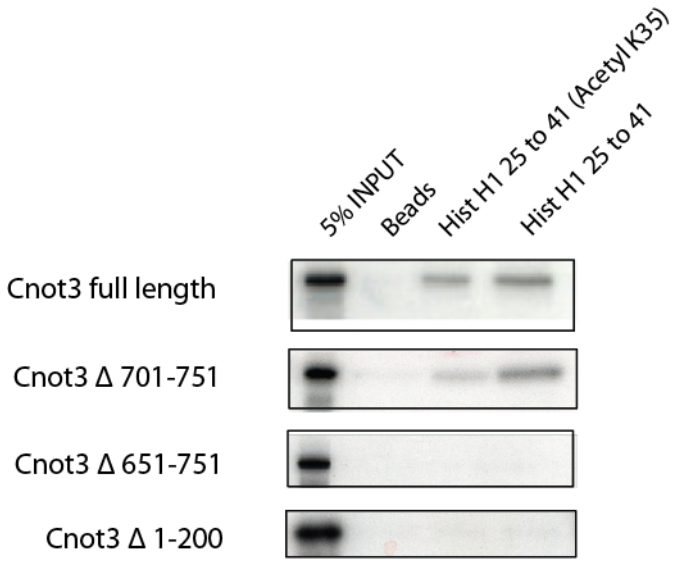


Figure 4.3: Cnot3 *in vitro* interaction with histone H1 peptides.
Histone H1.3 biotinylated peptides were synthesised by GenScript. The peptides contained the amino acids from the residue 25 to the residue 41 of the mouse histone H1.3. In the assay has been used a peptide carrying an acetylated lysine 35 and an unmodified peptide. The peptides were immobilized on streptavidin beads and then incubated either with *in vitro* translated Cnot3 full length, Cnot3 Δ1-200, Cnot3 Δ701-751 or Cnot3 Δ651-751. The *in vitro* translated proteins were previously labelled with S^{35} methionine. In the figure it is shown an autoradiography of the experiment.

4.5 In G2 Cnot3 interacts with components of the CPC complex and proteins involved in RNA maturation

The co-IP and MS revealed a large group of proteins that were pulled down by Cnot3 in G2. As described in Section 4.3, 425 interacting proteins were detected in this cell cycle phase. The results of co-IP and western blotting presented in Chapter 3 showed a strong interaction between Cnot3 and Aurora B in G2,

whereas in early G1 the interaction was much weaker. In accord with this result, the MS analysis of the Cnot3 pulldown detected Aurora B in G2, but not in early G1. The MS analysis also revealed the presence of the CPC complex members Incenp and Borealin among the Cnot3 interactors (Table A, Appendix). This suggests that Cnot3 interacts with the intact CPC.

Gene ontology was performed on the proteins that interact with Cnot3 in G2. The chart in Figure 4.4 shows the results of the analysis. The categories of proteins that were more enriched and with high significance represented processes such as splicing, RNA processing, mRNA metabolism. Many hnRNP proteins were detected as well as RNA helicases, which are known to play an important role in promoting splicing. Ddx1, Ddx18 and Ddx20 are RNA helicases that have been reported to be involved in RNA maturation, export and degradation (Rocak and Linder, 2004). Cnot3 interactors that have roles in transcription termination were also detected, including Cpsf1 and Fip1l1. Cpsf1 participates in transcription termination by recognizing a specific sequence at the 3' end of the pre-mRNA. Cpsf1 not only promotes termination, but also interacts with Fip1l1, which recruits the Poly-A polymerase for the addition of a poly-A tail to pre-mRNAs (Keller et al., 1991) (Kaufmann et al., 2004). Cnot3 interacts with both proteins in G2 as well as with Pabp1 (Table 4.5). Pabp1 binds the nascent pre-mRNA poly-A tail in order to stabilize the RNA and avoid degradation (Kuhn et al., 2009).

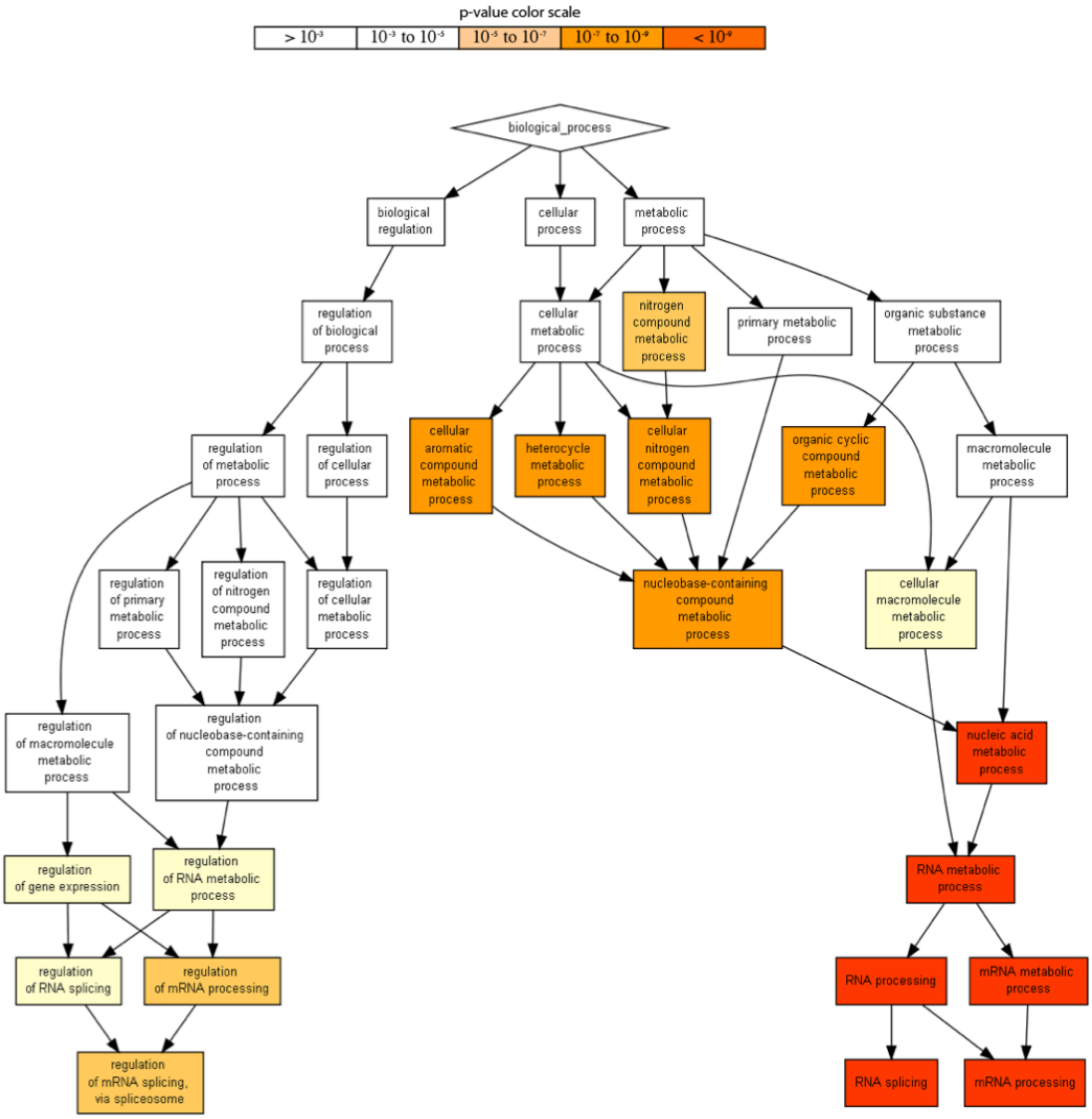


Figure 4.4: Gene ontology analysis of Cnot3 interactors in G2.
The chart was generated by using the software GOrilla. 425 proteins were included to perform the gene ontology analysis. A color scale indicates p-values.

Cnot3 is part of the CCR4-NOT complex, so it is not surprising that the protein that was most abundant among the Cnot3 interactors in G2 was Cnot1, which has already been shown to be part of a ternary complex with Cnot2 and Cnot3 (Boland et al., 2013). Cnot2 was also identified among the Cnot3 interactors identified in G2. The MS data also showed interaction with other components of the CCR4-NOT complex, including Cnot6, Cnot6L, Cnot7, Cnot8, Cnot10, Cnot11 (Table 4.5 and Table A, Appendix). However, not all of the subunits of the CCR4-NOT complex were found among the Cnot3 interacting proteins. This could be

due to the presence of sub-complexes of the CCR4-NOT, as described by (Lau et al., 2009).

The CCR4-NOT complex is the major eukaryotic deadenylase. In the process of RNA turnover, it interacts with other cellular complexes such as the exosome and the TRAMP complex (Azzouz et al., 2009). In accordance to this, the mass spectrometry analysis showed that Cnot3 interacts with Rrp46 that is a subunit of the exosome, which is known to be part of the apparatus for the RNA degradation (Mitchell et al., 1997).

Table 4.5: Cnot3 interactors in G2.
In the table are reported the first 40 out of 425 hits present in G2 with a high protein score. The protein score is relative to the abundance and the quality of the peptide. It is reported the function for each protein.

Protein name	Protein score	Function
CCR4-NOT transcription complex subunit 1	3528.449744	RNA turnover
Nucleolar RNA helicase 2	1393.945489	RNA unfolding
DNA topoisomerase 2-alpha	1289.480389	Chromatin organization
Protein RRP5 homolog	1163.337728	RNA processing
Protein NPAT	1107.526525	Transcription regulation
60S ribosomal protein L3	191.42	Translation
Polyadenylate-binding protein 1	992.6687118	RNA stability
Pre-mRNA-processing-splicing factor 8	857.4147619	Splicing
60S ribosomal protein L4	841.2299151	Translation
Nucleolar protein 56	795.9828795	rRNA processing
Putative ribosomal RNA methyltransferase NOP2	778.011932	rRNA processing
Nuclease-sensitive element-binding protein 1	299.223305	RNA processing
Myb-binding protein 1A	732.608542	Transcription regulation
Myotubularin-related protein 5	731.7853219	Signal transduction
ATP-dependent RNA helicase A	717.1753219	RNA processing
Protein SON	675.4480675	Splicing
Heterogeneous nuclear ribonucleoproteins C1/C2	674.5953219	Splicing
Heterogeneous nuclear ribonucleoprotein A3	658.563305	Splicing
60S ribosomal protein L6	646.7066101	Translation
Nucleoprotein TPR	628.8886264	RNA export
CCR4-NOT transcription complex subunit 10	612.8521862	RNA turnover
60S ribosomal protein L7a	596.8166101	Translation
DNA topoisomerase 2-beta	577.7766095	DNA organization
Heterogeneous nuclear ribonucleoproteins A2/B1	576.3	Splicing
60S acidic ribosomal protein P0	567.8166101	Translation
40S ribosomal protein S3a	566.2373388	Translation
60S ribosomal protein L5	556.8166101	Translation
RNA binding motif protein, X-linked-like-1	552.5598302	Splicing
RNA-binding motif protein, X chromosome	545.1432201	Splicing
Serine/arginine repetitive matrix protein 2	507.1702521	Splicing
60S ribosomal protein L7	503.9760506	Translation
Ankyrin repeat domain-containing protein 17	490.6826607	RNA binding
40S ribosomal protein S18	466.9266101	rRNA processing
WD repeat-containing protein 62	465.7066101	Nuclear membrane
Nucleolar protein 58	463.443305	rRNA processing
Ribosome-binding protein 1	456.4061305	Signal transduction
Heterogeneous nuclear ribonucleoprotein A1	454.3286269	Splicing
Histone H2.A2C	439.1966101	Chromatin organization
Eukaryotic initiation factor 4A-III	434.5366101	RNA processing
60S ribosomal protein L8	422.7	Translation
rRNA 2'-O-methyltransferase fibrillarin	413.583305	rRNA processing

4.6 Cnot3 interacts with the Xrn2 5'-3'exoribonuclease

The 5'-3'exoribonuclease, Xrn2, is involved in transcriptional termination and RNA degradation in the nucleus. Xrn2 degrades RNA at the 3' end of the gene after cleavage of the RNA at the poly-A site. According to the torpedo model of transcriptional termination, 5'-3' degradation of RNA downstream from the poly-A site displaces RNA polymerase II from DNA and promotes termination (Proudfoot, 2011). Xrn2 has been shown to be involved in degrading prematurely terminated transcripts around the transcription start site and may be involved in controlling transcription levels by displacing RNA polymerase II from DNA (Brannan et al., 2012). Xrn2 also promotes the maturation of rRNAs by degrading aberrant mRNAs together with the nuclear exosome (Davidson et al., 2012) as well as regulating the length of telomeres by degrading the RNA transcribed at termini of the chromosomes (Luke et al., 2008).

Because of the important roles played by Xrn2 in transcriptional termination and RNA processing, I focused on the interaction between Cnot3 and Xrn2. The interaction was initially detected in G2 cells by MS and was subsequently validated by co-IP and western blotting. Co-IP was also used to verify whether Xrn2 and Aurora B interact. The co-IP experiments were performed with nuclear extracts from mid-late S phase and G2 cells. The experiment revealed a strong interaction between these two proteins in both phases (Figure 4.6).

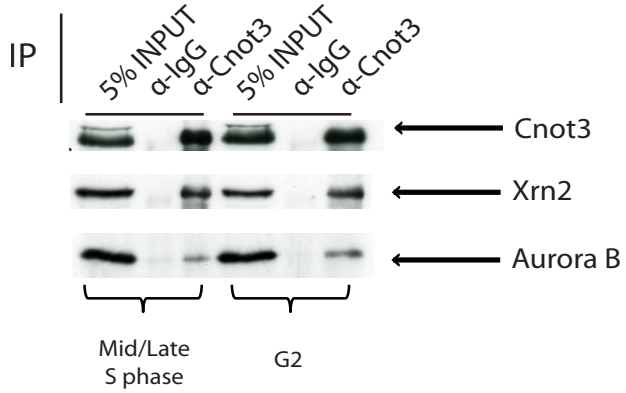


Figure 4.6: Xrn2 interaction with Cnot3 in mid-late S phase and G2.
Anti-Cnot3 and anti-IgG antibodies were pre-bound to magnetic beads and incubated with nuclear protein extracts from mid/late S phase and G2 cells. The proteins obtained after the IP were analyzed by western blot to reveal the presence of Cnot3, Xrn2 and Aurora B. 5% of the extract used for the IP has been used as INPUT.

A co-IP experiment was performed using mid/late S and G2 cells to test whether Aurora B interacts with Xrn2. The results show a clear pulldown of Xrn2 by anti-Aurora B. A difference in the amount of IPd Xrn2 was detected, with stronger pulldown observed in G2 than in mid/late S phase (Figure 4.7). This variation in the amount of interaction was similar to the difference observed for Aurora B-Cnot3 during the same phases of the cell cycle.

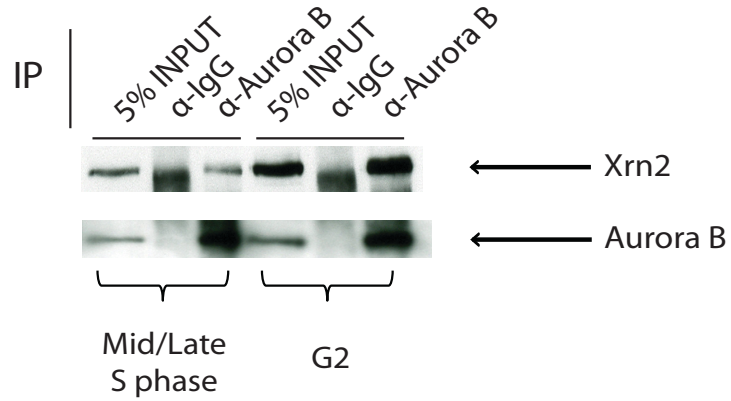


Figure 4.7: Interaction of Aurora B and Xrn2 in mid/late S phase and G2.
Anti-Aurora B and anti-IgG antibodies were pre-bound to magnetic beads and incubated with nuclear protein extracts from mid/late S phase and G2 cells. The proteins obtained after the IP were analyzed by western blot to reveal the presence of Cnot3, Xrn2 and Aurora B. 5% of the amount of extract used for the IPs was run as INPUT.

The Xrn2-Cnot3 interaction was also analysed in resting B cells. The interaction was detected in resting B cells but not at the same level relative to input as in G2 or mid/late S cells. Pulldown of Xrn2 by anti-Aurora B also showed a weak interaction (Figure 4.8). These results lead to the conclusion that the Xrn2-Aurora B and Xrn2-Cnot3 interactions vary at different stages of the cell cycle with a peak in the strength of the interactions in G2. In quiescent cells Xrn2 interacts weakly with both proteins.

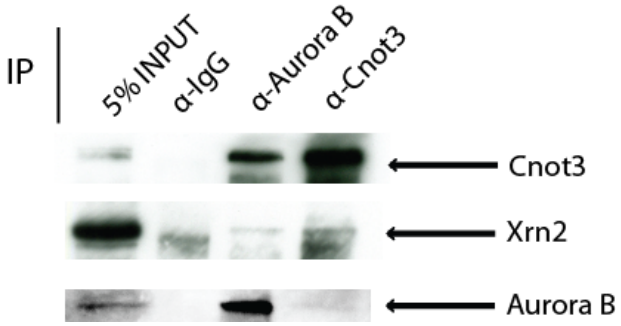


Figure 4.8: Xrn2 interaction with Aurora B and Cnot3 in resting B cells.
Anti-Aurora B and anti-IgG antibodies were pre-bound to magnetic beads and incubated with nuclear protein extracts from mid/late S phase and G2 cells. The proteins obtained after the IP were analyzed by western blot with antibodies that recognise Cnot3, Xrn2 and Aurora B. 5% of the extract used for the IP has been used as INPUT.

4.7 Summary

Analysis of the profile of Cnot3 interactors in early G1 and G2 cells showed that Cnot3 interacts during early G1 with chromatin organization factors, such as histones and transcription factors. Five isoforms of histone H1 were detected by the MS analysis in early G1 and the interaction with H1 was validated using an *in vitro* peptide binding assay. The second most enriched group of interacting proteins contained proteins that are involved in RNA processing, transcription regulation, splicing, RNA export and degradation. Among these classes of proteins, Cnot3 also interacts with many hnRNPs that are components of the spliceosome.

A higher number of interactors was observed in G2 compared with early G1. Components of the CPC, (Aurora B, Incenp and Borealin), were shown to interact with Cnot3. Factors involved in splicing and RNA maturation interact with Cnot3 in G2, as well as proteins with a role in transcription termination. Fipl1l, Spsf1 and Papb are Cnot3 interactors and function respectively to recognize the stop signal, recruit cleavage factors and bind the poly-A tail. The 5'-3' exoribonuclease Xrn2 was also detected as a Cnot3 interactor in the MS analysis. The interaction with Xrn2 with Cnot3 and Aurora B was confirmed by co-IP experiments in resting, mid/late S phase and G2. The Xrn2 interaction with both proteins was highest in G2, somewhat reduced in mid/late S phase and lowest in resting b cells.

Chapter 5- Cell cycle regulated binding of Cnot3 to gene promoters

5.1 Introduction

A number of lines of evidence obtained in the lab point to a role for Cnot3 in gene regulation. Cnot3 interacts with Aurora B in resting B cells and the two proteins are present on the same active gene promoters in these cells. Cnot3 also interacts in resting B cells with Ring1B, which is another protein involved in transcriptional regulation in resting B cells (Frangini et al., 2013). Cnot3 was found to be phosphorylated by Aurora B in an in vitro kinase assay. A published study reported that Cnot3 binds to promoters of active genes in ES cells, suggesting a role for Cnot3 in controlling self-renewal in these cells (Hu et al., 2009).

In this chapter the results of a ChIP analysis of Cnot3 binding to promoters of active genes at different phases of the cell cycle will be described. The description of Cnot3 occupancy on promoters will be studied in conjunction with the presence of the 5'-3' exoribonuclease Xrn2. Binding of Cnot3 to promoters will be then related to the transcriptional state of the cell.

5.2 Aurora B and Cnot3 co-occupy promoters of active genes in resting B cells

The interaction between Cnot3 and the Aurora B kinase during cell cycle progression was described in Chapter 3. Data generated in the lab showed that Aurora B binds to promoters of active genes in resting B cells. After activation by LPS, Aurora B does not bind to promoters and is replaced by the MSK 1 and MSK2 kinases (Frangini et al., 2013).

Cnot3 binds to the same active gene promoters where Aurora B was detected, while very little binding was observed at inactive genes (Figure 5.1). Levels of enrichment of Cnot3 and Aurora B were not the same for the two proteins. Although it is not possible to directly compare ChIP enrichments obtained with

different antibodies, enrichments obtained for Cnot3 at active genes were substantially higher than Aurora B. This could be due to the fact to differences in the levels of the two proteins in the nucleus and/or the fact that Aurora B is a kinase and therefore binds more dynamically than Cnot3.

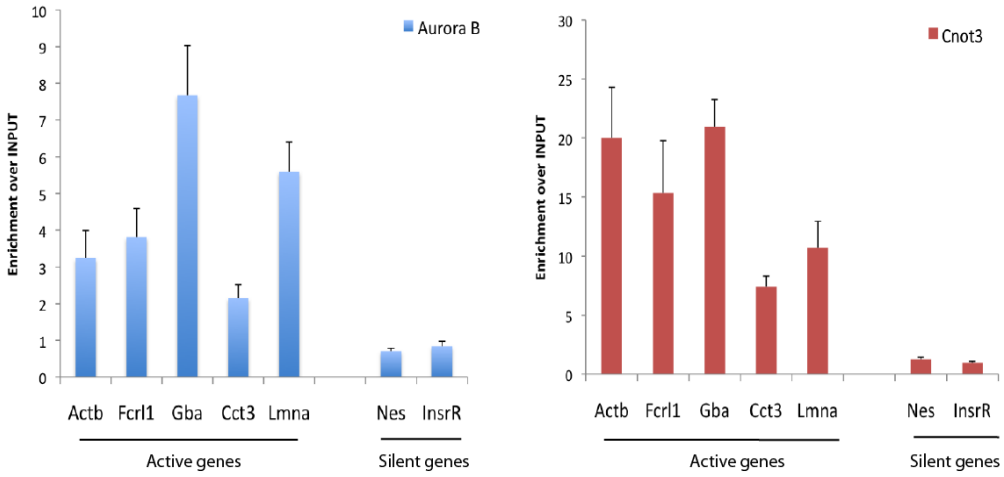


Figure 5.1: Aurora B and Cnot3 bind the same active gene promoters.
Anti-Aurora B and anti Cnot3 antibodies were bound to magnetic beads. Chromatin extracted from resting B cells was then incubated with the antibody-beads complex. The binding of Cnot3 and Aurora B to gene promoters was assessed by qRT-PCR using pair of primers that amplify promoter regions. Error bars represent standard deviation of the mean (n=4 biological replicates). The Aurora B ChIP data was generated by A. Frangini.

To follow up the results that were obtained for Aurora B and Cnot3, the B cell system described in Chapter 3 was used to analyse the binding of Cnot3 throughout the cell cycle. ChIP experiments for Aurora B did not show enrichment on gene promoters (data not shown). It is known that protein levels of Aurora B rise dramatically in S phase to reach a peak in G2/M. In G2 especially, Aurora B is spread all over the chromosomes (Terada et al., 1998). The effect of this generalized spreading would be to prevent detection of specific enrichment on gene promoters, since the IP of Aurora B would pull down DNA sequences that are localized not only on promoters but everywhere else in the chromosome. Therefore, there would not be any sequence enriched in respect to the ones present in the INPUT. Because of these issues, it was not possible to analyse binding of Aurora B to gene promoters in G2 by ChIP.

5.3 Binding of Cnot3 to promoters in resting B cells is not affected by Aurora B depletion

Attempts to knock down Cnot3 to obtain functional data about the role of Cnot3 did not achieve positive results. Our efforts to infect resting B cells using lentiviral vectors (Scott, 2011) (Su et al., 2011), were unsuccessful (data not shown). Furthermore, there are no molecules available that can inhibit Cnot3 activity and there have not been any reports of a Cnot3 conditional knockout mouse that would allow depletion of Cnot3 in B cells. The germline of Cnot3 knockout has been shown to be pre-implantation embryonic lethal, with the zygote unable to develop beyond the blastocyst (Neely et al., 2010). To study the functions of Cnot3 using the systems that I have set up, a strategy has been developed for the generation of a Cnot3 conditional knockout mouse. This will allow characterization of the functional role of Cnot3 in B cells. The strategy and progress of the generation of the Cnot3 conditional knockout mouse will be discussed in the Chapter 7.

Because Aurora B was shown to interact with Cnot3 and to phosphorylate it *in vitro*, I set out to verify whether the absence of the kinase could interfere with the binding of Cnot3 to chromatin. The analysis was carried out using mice that are homozygous for a floxed *Aurora B* allele (*Aurkb*^{fl}) and a tamoxifen inducible Cre-ER^{T2} gene under the control of constitutive Rosa 26 promoter. ChIP experiments were carried out in Aurora B knockout resting B cells. The resting B cells were isolated from *Aurkb*$^{fl/fl}$/Cre-ER^{T2}/Cre-ER^{T2} mice and incubated for 48 hours with tamoxifen, to promote entry of the Cre recombinase into the nucleus. The cre enzyme in the nucleus deletes genomic sequence present between the two LoxP sites. As control cells, resting B cells were also isolated from mice homozygous for Cre-ER^{T2} only and treated for 48 hours with tamoxifen. The level of Aurora B protein was analysed by western blot to confirm knockdown of the protein (Figure 5.2 A).

ChIP experiments were performed with an anti-Cnot3 antibody using chromatin isolated from Aurora B knockout and Cre-ER^{T2} only cells. No indicative change was found in Cnot3 binding at any of the active genes in the Aurora B knockout cells (Figure 5.2 B). This led to the conclusion that neither

interaction with nor phosphorylation by Aurora B are needed for Cnot3 to bind to chromatin in resting B cells.

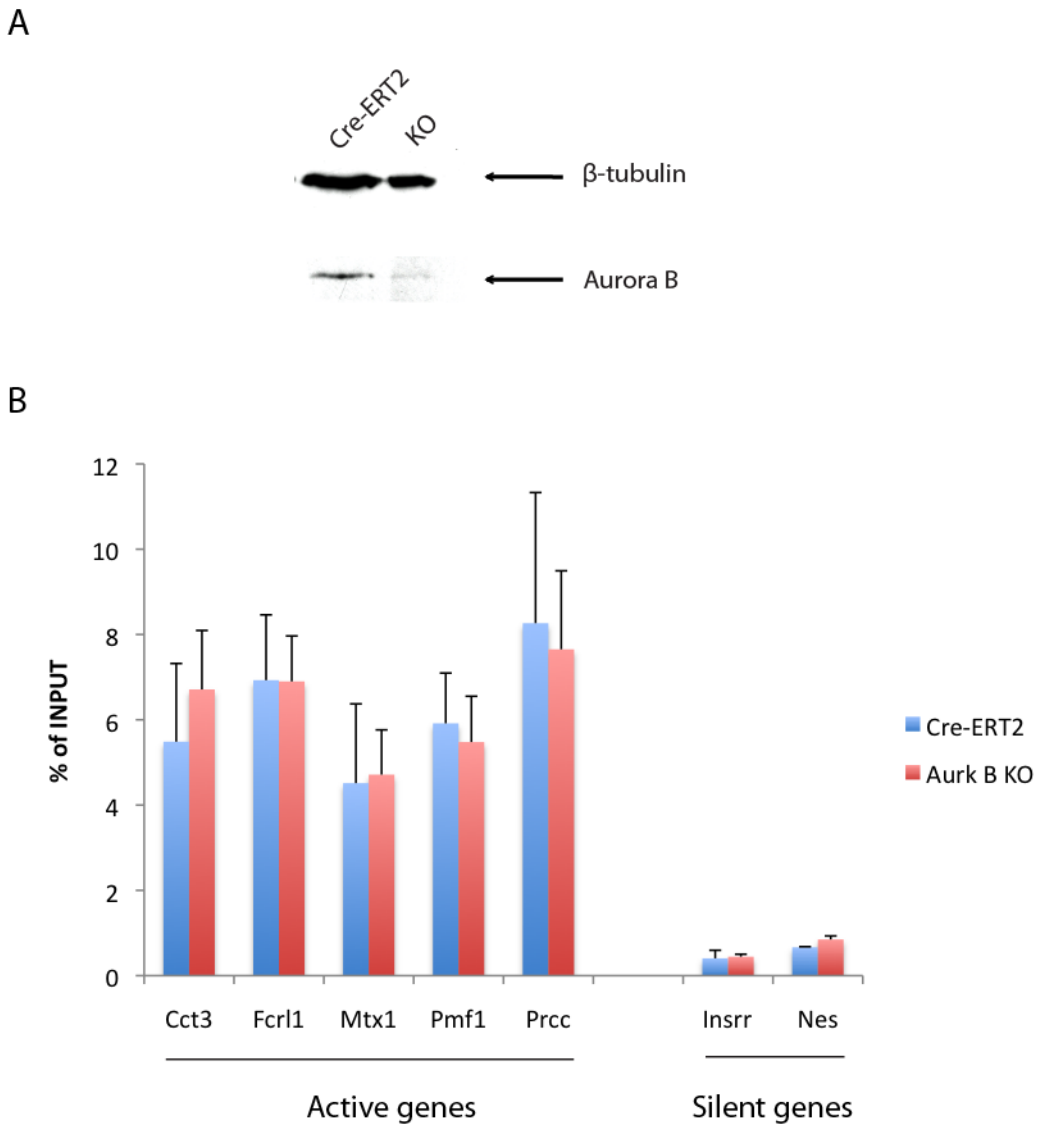


Figure 5.2: Cnot3 binds gene promoters in Aurora B knock out cells.
A) Confirmation of Aurora B knockout. Resting B cells were isolated from mice homozygous for *Aurkb*^{fl} and Cre-ER^{T2} (AurkB-KO) and from mice homozygous for Cre-ER^{T2} only (Cre-ER^{T2}). The cells were incubated for 48 hours with tamoxifen and chromatin was extracted and used for the ChIP shown in (B). Protein extracted from 10^6 AurkB-KO and Cre-ER^{T2} cells was loaded onto a 10% polyacrilamide gel and analysed by western blot. β-tubulin, was used as a loading control.
B) qRT-PCR ChIP analysis of Cnot3 binding using chromatin from resting B cells isolated from Cre-ER^{T2} and AurkB-KO mice and incubated with tamoxifen. Immunoprecipitated DNA was analysed using primers specific for the promoters of the indicated genes. Error bars represent the standard deviation of the mean (n=2 biological replicates).

5.4 Binding of Cnot3 to gene promoters during cell cycle progression

Cnot3 binding to gene promoters was analysed by ChIP to assess possible changes during cell cycle progression. The analysis focused on genes that are known to be active in B cells. They included the B cell-specific Fc receptor-like 1 (*Fcrl1)* gene as well as more widely expressed genes that mediate a variety of cellular processes including cell cycle progression and cell growth (*Arhgef2*, *Prcc*, *Pmf1*) protein chaperones (*Cct3*) and mitochondrial transport proteins (*Mtx1*). Binding of Cnot3 was also analysed on gene promoters that are not expressed in B cells such as *Insrr* and *Nestin*. These genes are located in a gene-dense region of mouse chromosome 3 that the lab has studied for a number of years.

The result of the ChIP confirmed that Cnot3 binds to active promoters in resting B cells. The highest binding was detected on the promoter of *Fcrl1*, which is a B cell gene involved in activation and cell growth. Substantial binding of Cnot3 was also found at other active promoters. Conversely, Cnot3 was barely detected on the promoters of inactive genes. Following activation of the cells with LPS, the binding of Cnot3 did not change significantly on active genes during early and late G1 (Figure 5.3).

When ChIP was carried out on cells that were blocked at the G1/S boundary by incubation with aphidicolin a change in binding was evident. The binding of Cnot3 at active genes decreased sharply compared with late G1 cells. An even larger drop in binding was observed 2 hours after washout of aphidicolin when the cells were in mid to late S phase. The level of Cnot3 binding on promoters of active genes increased again in G2/M. However, the levels of binding detected in this phase were lower than the levels observed in resting B cells. A possible reason for this might be a shift in the binding profile of Cnot3 at gene promoters. As will be described in Section 6.3, the Cnot3 binding peak is displaced towards the body of the gene in G2 cells. Therefore, the analysis by qRT-PCR of the same area of the promoter might be expected to deliver a weaker signal. A modest decrease in Cnot3 binding was observed in the G2/M population of cells compared to the G2 cells (Figure 5.3). This could be due to displacement of Cnot3

from the chromatin in the proportion of the cells in this population that were in metaphase.

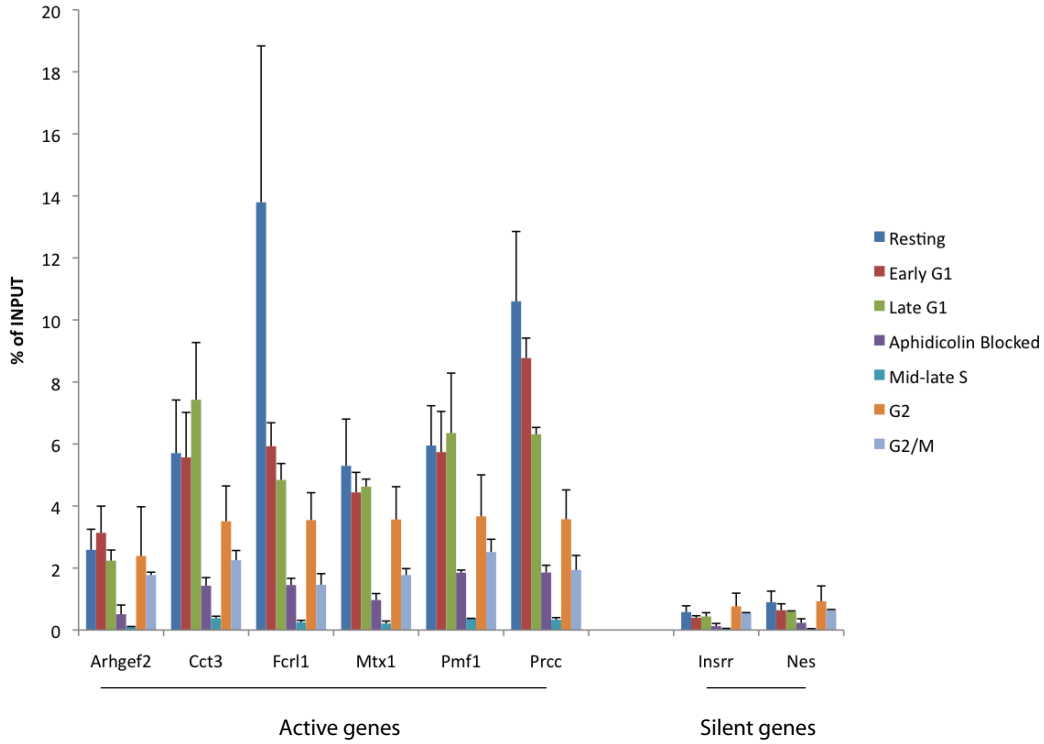


Figure 5.3: Binding of Cnot3 to gene promoters during cell cycle progression. qRT-PCR ChIP was carried out with anti-Cnot3 antibodies on chromatin from resting, anti-IgM treated (early G1), anti-IgM+LPS6h (late G1), aphidicolin blocked, 2 hours (mid-late S-phase), 4 hours (G2) and 6 hours (G2/M) aphidicolin released B cells. PCR primers detected immunoprecipitated DNA from the promoters of the indicated genes. Error bars represent the standard deviation of the mean (n=3 biological replicates).

5.5 Analysis of Cnot3 binding to gene promoters during S phase

The result shown in Figure 5.3 provide evidence that binding of Cnot3 to gene promoters changes during the cell cycle. The largest change in binding was observed in mid to late S phase, where Cnot3 binding was very low compared to resting cells. In order to exclude the possibility of artefacts caused by the DNA polymerase inhibitor, a ChIP experiment was performed in an aphidicolin-free system. Because it is not possible to obtain a B cell population that is fully synchronised in S-phase without using a DNA polymerase inhibitor, we decided to perform a ChIP experiment on a cell population prepared using a drug-free

method, that is enriched for cells in S phase. If the results shown in Figure 5.3 are correct, the binding of Cnot3 to active promoters should decrease in this population.

The strategy used involved incubation of resting B cells with anti-IgM for 20 hours, followed by incubation with LPS (see Section 3.2). In order to determine the optimal time of LPS incubation for obtaining a high percentage of cells in S phase, anti-IgM treated cells were incubated with LPS for 6, 8, 10, 12 or 14 hours and cells were incubated with EdU for 30 minutes before harvesting to determine the number of cells in S-phase. As previously shown in Section 3.2, the percentage of cells incorporating EdU after 6 hours was around 5%. A gradual increase in number of cells entering S phase was detected from 8 hours to 10 hours, with the percentage rising from 5.8% to 9.7%. At the 12 hour time point, around 18.3% of cells incorporated the nucleotide analogue. Cells that were treated for 14 hours with LPS were used for the ChIP experiment, as around 30% of them incorporated EdU (Figure 5.4).

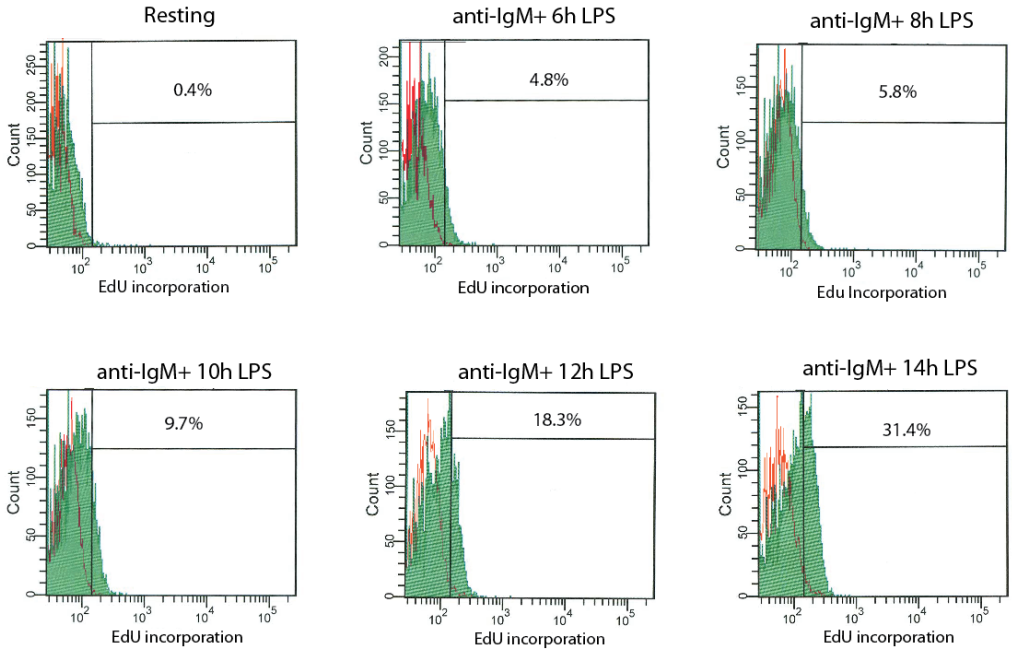


Figure 5.4: EdU incorporation in resting and anti-IgM+LPS treated B cells.
FACS profile of EdU incorporation assay performed in resting and anti-IgM treated B cells at different time points after the LPS addition. The green profile represents cells that were incubated for 30 minutes with EdU before harvesting, while the red profile shows the cells that have not been incubated with EdU. The numbers in each histogram represent the percentage of EdU that was incorporated by the cells.

ChIP was carried out to compare Cnot3 binding in anti-IgM+14h LPS cells and the mid to late S-phase cells obtained 2 hours after washout of aphidicolin.

Resting B cells were also included in the analysis. The binding of Cnot3 in anti-IgM+14h LPS cells was very low on gene promoters and was similar to the levels detected in the mid to late S phase cells obtained with aphidicolin. Moreover, in both samples Cnot3 binding was very low relative to the binding observed in resting B cells (Figure 5.5). This was surprising because around 30% of cells incorporated EdU in the anti-IgM+14h LPS cells. However, this figure might be an underestimation of the proportion of cells that are replicating their DNA. Due to their asynchronous behavior, we could have a representation of different points in S phase in these cells. EdU incorporation might also be not sufficiently sensitive to detect cells at very early and late stages of S phase. Based on the results obtained using the two methods, it is possible to conclude that Cnot3 binding to promoters of active genes is strongly reduced during S phase and that this phenomenon is not caused by synchronization with aphidicolin.

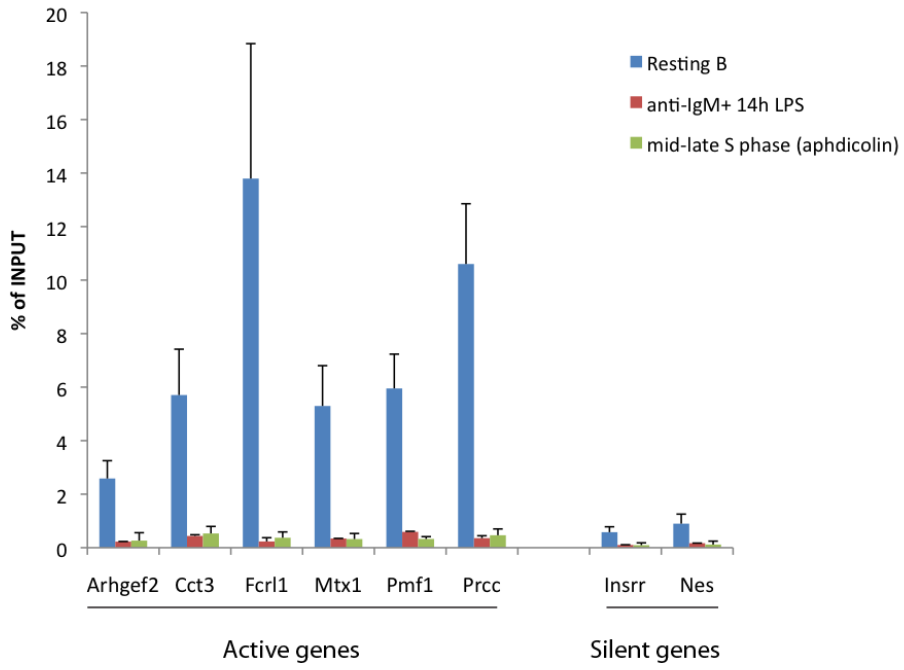


Figure 5.5: Binding of Cnot3 to gene promoters in resting B, mid-late S phase and anti-IgM+LPS 14 hours.
qRT-PCR ChIP with anti-Cnot3 antibody was carried out as described in the legend to Figure 5.3. The experiment was performed using chromatin from resting, anti-IgM+14h LPS and aphidicolin-treated B cells analysed 2 hours after aphidicolin washout. Error bars represent the standard deviation of the mean (n=3 biological replicates).

5.5.1 Pcna binds to gene promoters during S phase

To determine whether the loss of binding of Cnot3 during S-phase might be a ChIP artifact arising from global changes in chromatin structure during S-phase, ChIP was used to analyse the binding of Pcna at promoters of active and inactive genes in S-phase cells. Pcna is a DNA polymerase delta co-factor that participates in the process of elongation during DNA replication and promotes DNA polymerase activity (Prelich et al., 1987). ChIP experiments with an anti-Pcna antibody were performed using chromatin extracted from, early and mid to late S phase cells generated by aphidicolin block and washout. Resting B cells were also included in the analysis. Low levels of PCNA binding were observed in resting B cells and the level of binding was strongly increased at all stages of S-phase examined (Figure 5.6). The highest level of binding was observed in early S-phase 30 minutes hours after aphidicolin washout and binding decreased in mid to late S-phase. The level of binding of Pcna to gene promoters was similar at active and inactive genes.

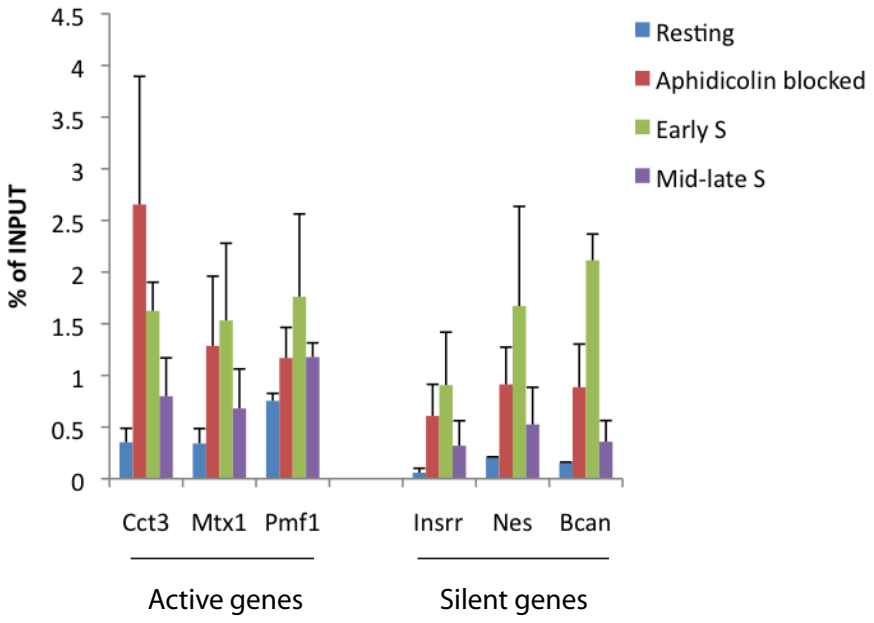


Figure 5.6: Pcna binds gene promoters in S phase.
qRT-PCR ChIP analysis of PCNA binding to gene promoters in resting and S-phase B cells. The experiment was performed using chromatin from resting and aphidicolin blocked B cells and 30 minutes (early S) or 2 hours (mid to late S) after aphidicolin washout. Error bars represent standard deviation of the mean (n=3 biological replicates).

5.6 Analysis of transcription levels during cell cycle progression

To correlate the binding of Cnot3 to promoters with transcription status at different stages of the cell cycle, nuclear RNA was isolated from cells and analysed by qRT-PCR using primers that were designed to amplify sequences containing intron-exon junctions. This approach made it possible to selectively analyse the levels of primary transcripts. Due to the difficulty of having a housekeeping gene that does not fluctuate during the cell cycle, a spike RNA was added to the nuclear lysate before RNA purification. The spike RNA was generated by the transcription of a unique random sequence (see Materials and Methods, section 2.10.1). The Ct values obtained for each gene were normalized to the spike RNA.

All of the genes analysed had similar primary transcript profiles, with little change in transcript level observed during progression from resting to early and late G1 stages (Figure 5.7). A sharp increase in primary transcripts was seen in early S phase and these levels were maintained in G2 and G2/M cells. The B cell-specific genes had significantly higher transcript levels at all cell cycle stages compared with the housekeeping genes. No transcripts were detected for Nestin which is repressed in B cells (Figure 5.7).

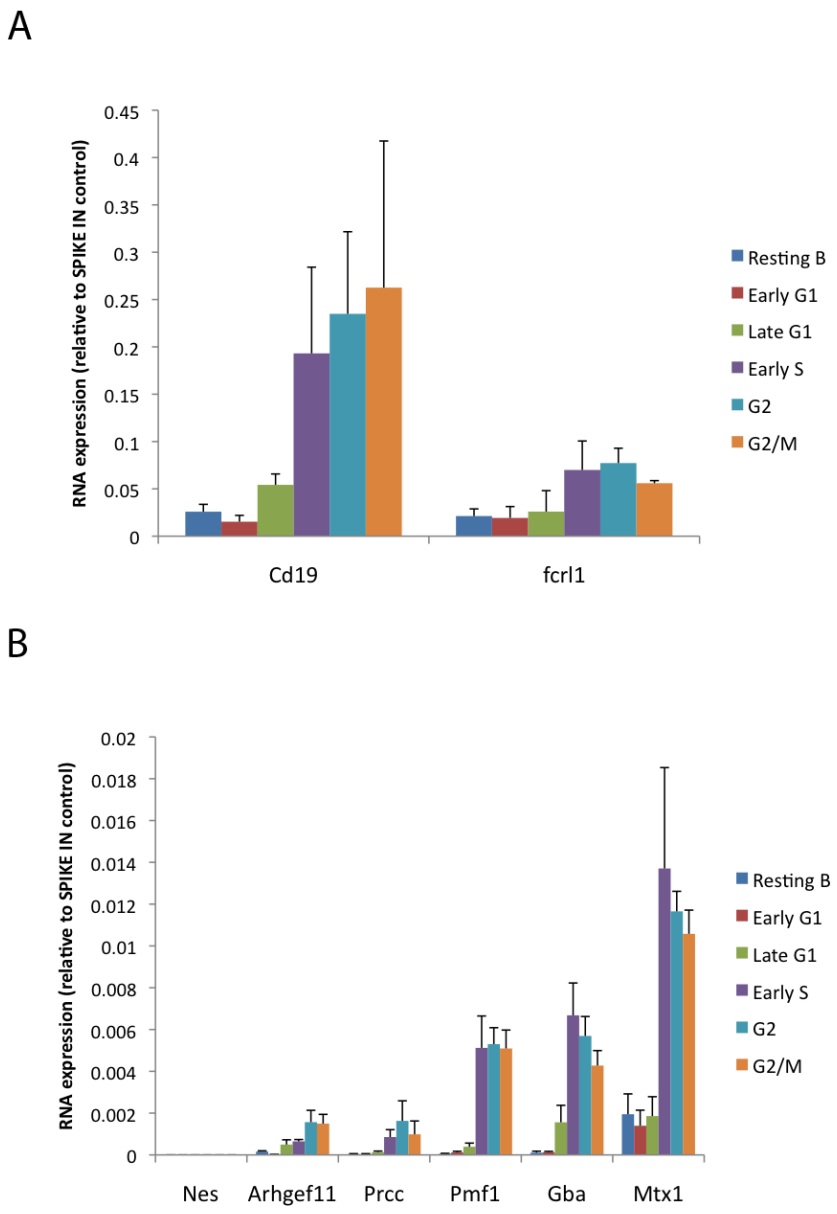


Figure 5.7: Analysis of primary transcripts during cell cycle progression of activated B cells
Nuclear RNA was extracted from cells collected in resting, early G1, late G1, early S phase, G2 and G2/M B cells and analysed by qRT-PCR. Gene expression was calculated relative to a spike-in RNA that was added to the nuclear lysate immediately after lysis (see Material and methods section 2.10.2). To detect only primary transcripts, primers that amplify sequences containing intron-exon junctions were used for the analysis. Levels for B cell genes are shown separately due to their higher transcript levels. A) B cell genes primary transcripts. B) Primary transcripts of genes covering different cellular processes. n=4 biological replicates for A and B.

The same nuclear RNA was also analysed using primers with complementary sequences located within exons in order to quantify mRNA levels in the nucleus. Similar to the primary transcripts, RNA levels were lower in quiescent, early and late G1 cells and then increased in early S, G2 and G2/M. Some differences were

observed between the relative levels of primary transcripts and mRNA for individual genes (see for example Prcc and Mtx1 transcript levels in Figure 5.7 and 5.8). Overall, the results of the primary transcript analysis indicate that there is a large increase in transcription and mRNA production from the onset of S-phase through G2.

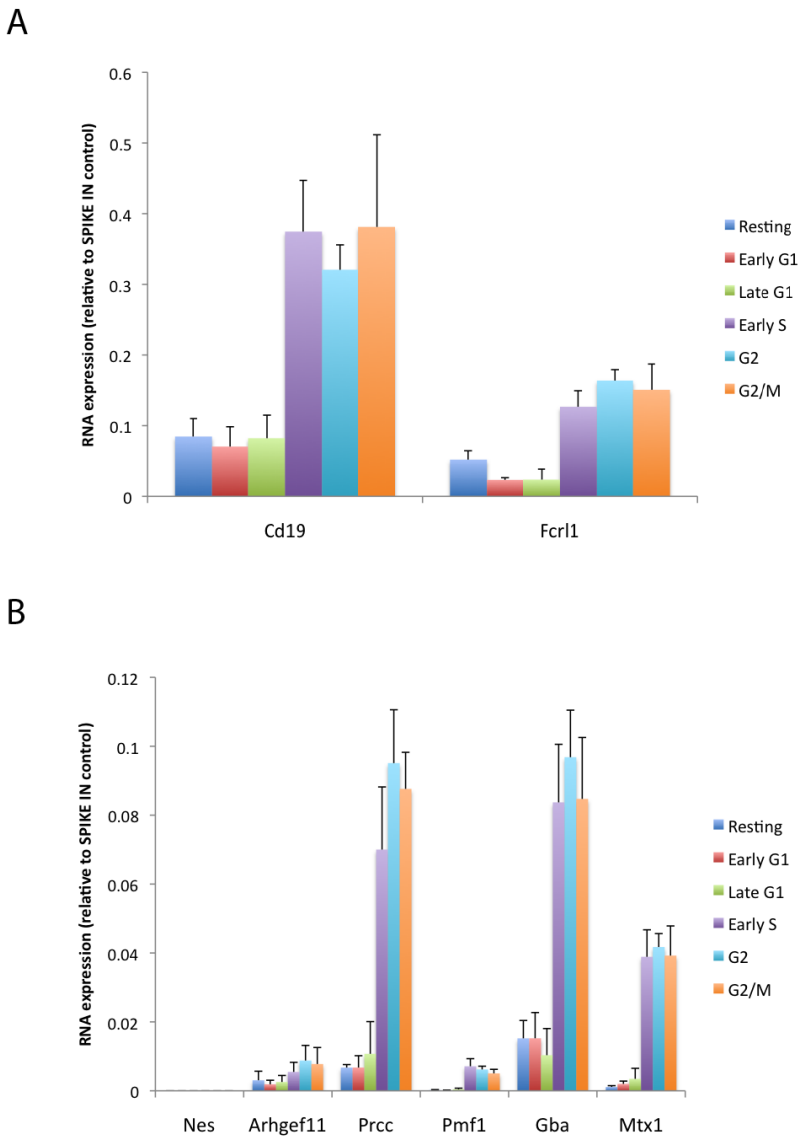


Figure 5.8: Analysis of nuclear mRNA during cell cycle progression of activated B cells.
Nuclear RNA was extracted from cells collected in resting, early G1, late G1, early S phase, G2 and G2/M B cells. Gene expression was calculated relative to a spike-in RNA that was added to the nuclear lysate immediately after lysis (see Material and methods section 2.10.2). Primers that recognize complementary sequences within the exon were used. B cell genes are shown separately due to their higher transcript levels. A) B cell genes primary transcripts. B) Primary transcripts of genes covering different cellular processes. n=4 biological replicates for A and B.

5.7 Xrn2 binds to promoters of active genes in resting and G2 cells

Data obtained from co-IP and mass spectrometry and subsequent validation by western blotting showed interaction between Xrn2, Cnot3 and Aurora B (Section 4.6). After having shown binding of Cnot3 and Aurora B to the same active gene promoters in resting B cells, I wanted to test whether Xrn2 binds to these promoters. Xrn2 is not only found at the 3' end of the gene but also binds to the region around the transcription start site where it has been shown to have a role in premature termination of RNA Pol II transcription (Brannan et al., 2012).

ChIP experiments were performed using an anti-Xrn2 antibody in resting B cells and in G2 cells. Xrn2 binding was observed on active promoters in resting and G2 B cells (Figure 5.9), but the binding showed some differences from the profile for Cnot3. The level of binding of Xrn2 in resting and G2 B cells was comparable whereas binding of Cnot3 was lower in G2 (Figure 5.3). A possible explanation for this might be that the region that is bound by Cnot3 is located more within the body of the gene in G2 cells, while Xrn2 binding might be localized to the promoter in both phases. If this is correct, it would suggest that Cnot3 is associated with transcription elongation in G2 cells while Xrn2 continues to associate with the initiation pausing regions at the 5' ends of genes (Figure 5.9).

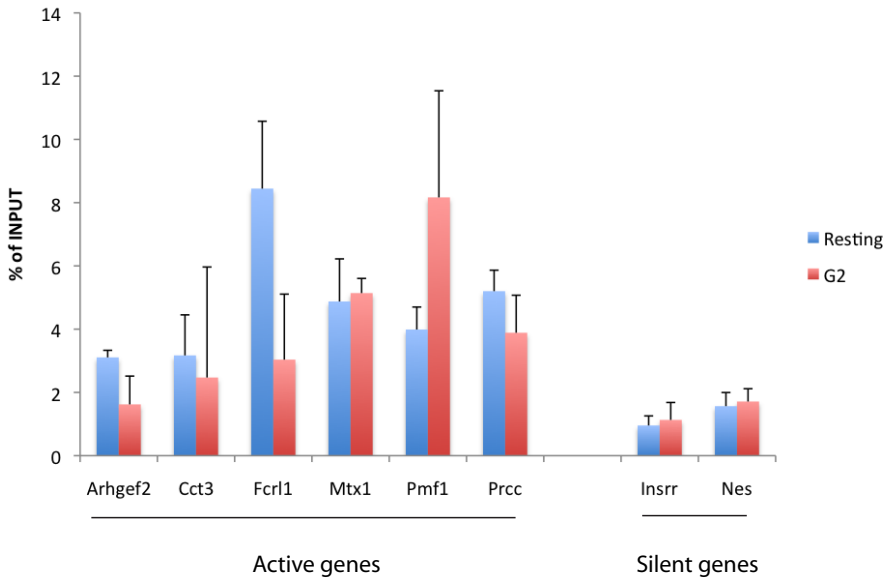


Figure 5.9: Xrn2 binding to gene promoters in resting and G2 B cells.
ChIP with anti-Cnot3 antibody was carried out on chromatin from resting and G2 B cells. The immunoprecipitated DNA was analysed by qRT-PCR using primer pairs that amplify in the promoter region. Error bars represent standard deviation of the mean (n=3 biological replicates).

5.8 Summary

The data presented in this chapter demonstrates that binding of Cnot3 to gene promoters is subject to cell cycle regulation. Cnot3 co-localises with Aurora B at some active gene promoters in resting B cells, but Cnot3 is still able to bind to these promoters in the absence of the kinase. Binding of Cnot3 to promoters is high in resting and G1 B cells drops sharply during S-phase and increases again in G2, although it does not reach the same levels as in resting cells. This effect might be due to a shift of Cnot3 binding towards the body of the gene. Pcna is bound to active and inactive gene promoters in S-phase cells, with binding reaching a maximum during early S phase. Analysis of primary unspliced transcripts and spliced nuclear mRNA showed that the level of transcription is similar in resting B cells and in early and late G1 cells. Transcription rises sharply at the onset of S phase and is maintained through G2. Finally, it was shown that the 5'-3' RNA exonuclease, Xrn2, binds at similar levels to promoters of active genes in resting and G2 B cells.

Chapter 6- Genome wide binding profiles of Cnot3 during cell cycle progression

6.1 Introduction

The ChIP experiments described in Chapter 5 revealed binding of Cnot3 to gene promoters that is regulated during the cell cycle. However, conventional qRT-PCR ChIP has limitations because it is only possible to analyse protein binding at few genes or specific genomic regions. Therefore, the analysis of binding to chromatin was extended genome wide using ChIP-sequencing (ChIP-seq). The technology for ChIP-seq has developed significantly over the last decade and has replaced the ChIP on ChIP approach as a method for analysing factor binding across large genomic regions. In this chapter, I will describe ChIP-seq analysis of Cnot3 binding at several different stages of the cell cycle.

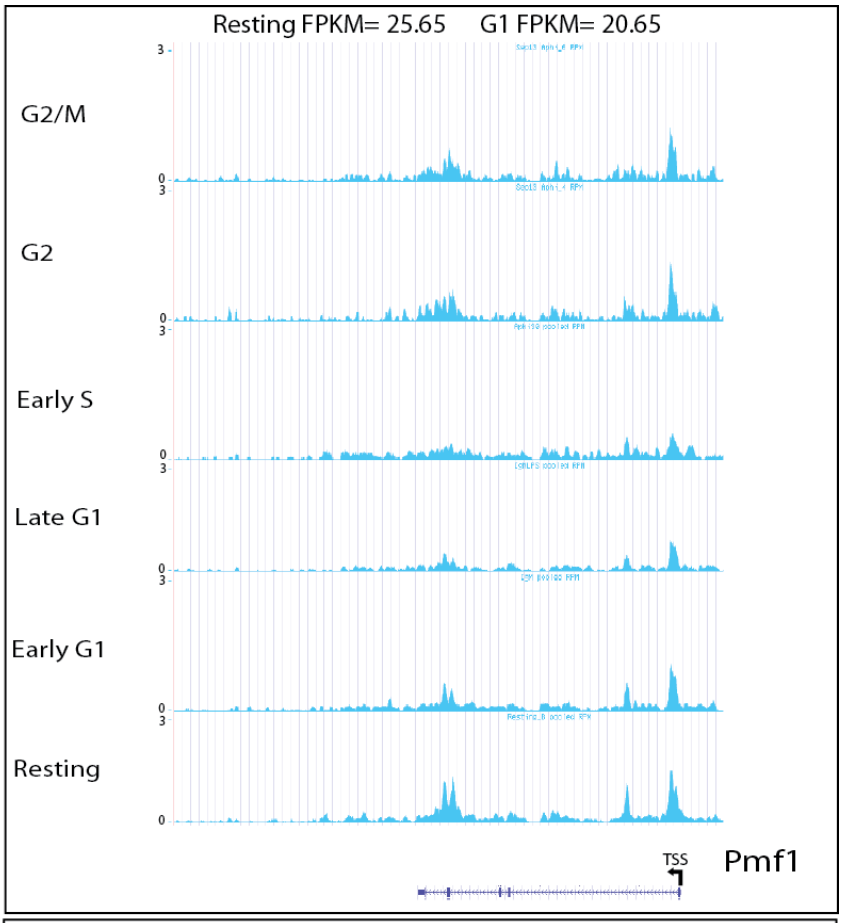
6.2 Genome wide binding of Cnot3 to chromatin is cell cycle regulated

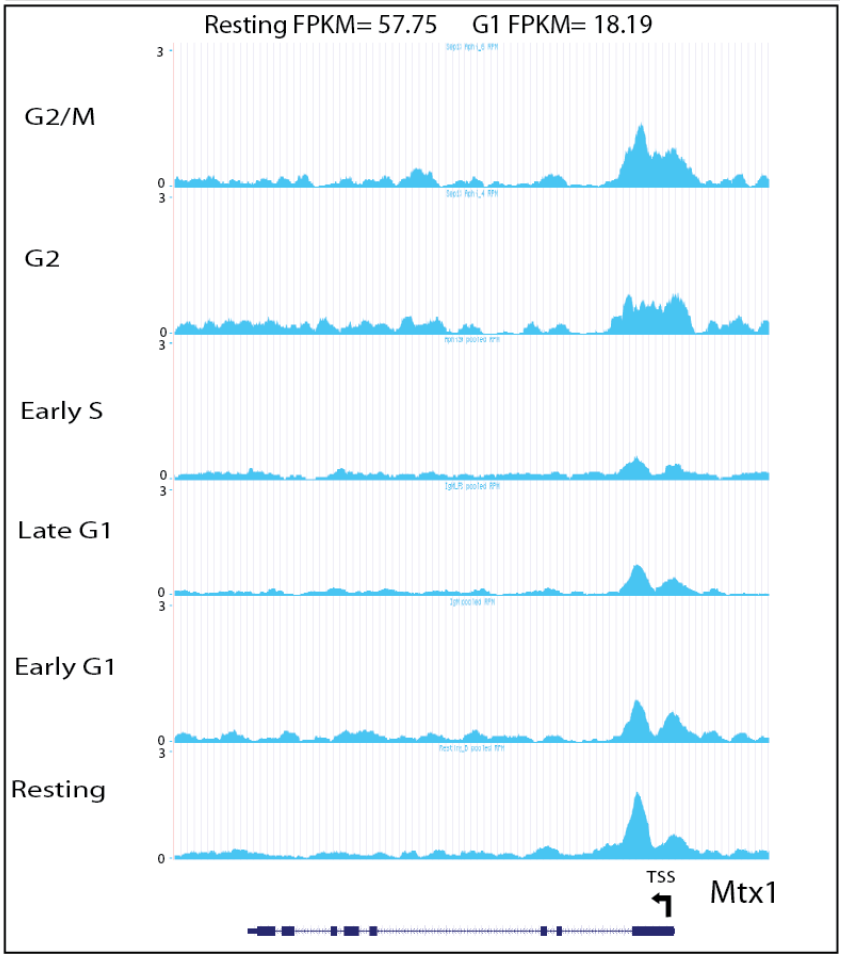
ChIP-seq analysis was performed on DNA samples recovered from resting, early and late G1, early S, G2 and G2/M cells. ChIP experiments for Cnot3 were carried out on these cell cycle stages and the recovered DNA was then sequenced on a next generation high throughput sequencer. The cells from different cell cycle stages were prepared using the methods described in Chapter 3. Early G1 cells were obtained by treating cells with anti-IgM for 20 hours and late G1 cells by treating these cells for a further 6 hours with LPS. Early S, G2 and G2/M cells were generated by blocking the cells with apihidicolin and then harvesting them at 30 minutes, 4 hours and 6 hours respectively after washout of the drug (see Section 3.2)

Preparation of libraries for sequencing of ChIP DNA requires a starting material of 10ng of ChIP DNA (see Section 2.9.1). For most of the phases of the cell cycle, it was possible to obtain this amount of DNA. However, it was not possible to recover enough DNA for the mid-late S phase. The results in Chapter 5 showed that the lowest binding of Cnot3 to chromatin was during this stage of the cell cycle.

The bioinformatic analysis of the ChIP-seq data was carried out in collaboration with Dr. Gopuraja Dharmalingam and Dr. Thomas Carroll (CSC Core Bioinformatics Facility). ChIP-seq tracks for each cell cycle phase were normalized to the total sequencing depth of the sample. Figure 6.1 shows the ChIP-seq tracks for four active genes (*Pmf1* and *Mtx1*, *Cd83* and *Cd37*). Additional tracks are shown in the Appendix (Figure B). Binding of Cnot3 to active genes is detected mainly at the promoters. However, the protein was also detected at the 3'end of *Pmf1 and Cd37* (Figure 6.1). This observation suggests that Cnot3 might participate in mRNA 3'end formation and transcriptional termination. Comparison of the results obtained from the ChIP-seq analysis for *Pmf1* and *Mtx1* with the results from the qRT-PCR ChIP of the same genes (Section 5.4, Figure 5.3) shows a strong similarity in the relative levels of bound Cnot3 measured at each the different cell cycle stages using the two methods. The binding of Cnot3 was high in resting B cells, decreased gradually through early and late G1 to a low level in early S phase and increased again in G2 and G2/M. Broadly similar binding profiles were observed for the B cell-specific genes *Cd83* and *Cd37* (Figure 6.1), although the decrease in binding was more pronounced during activation in early and late G1.

A


Resting FPKM= 25.65
G1 FPKM= 20.65
G2/M
G2
Early S
Late G1
Early G1
Resting
TSS
Pmf1


Resting FPKM= 57.75
G1 FPKM= 18.19
G2/M
G2
Early S
Late G1
Early G1
Resting
TSS
Mtx1

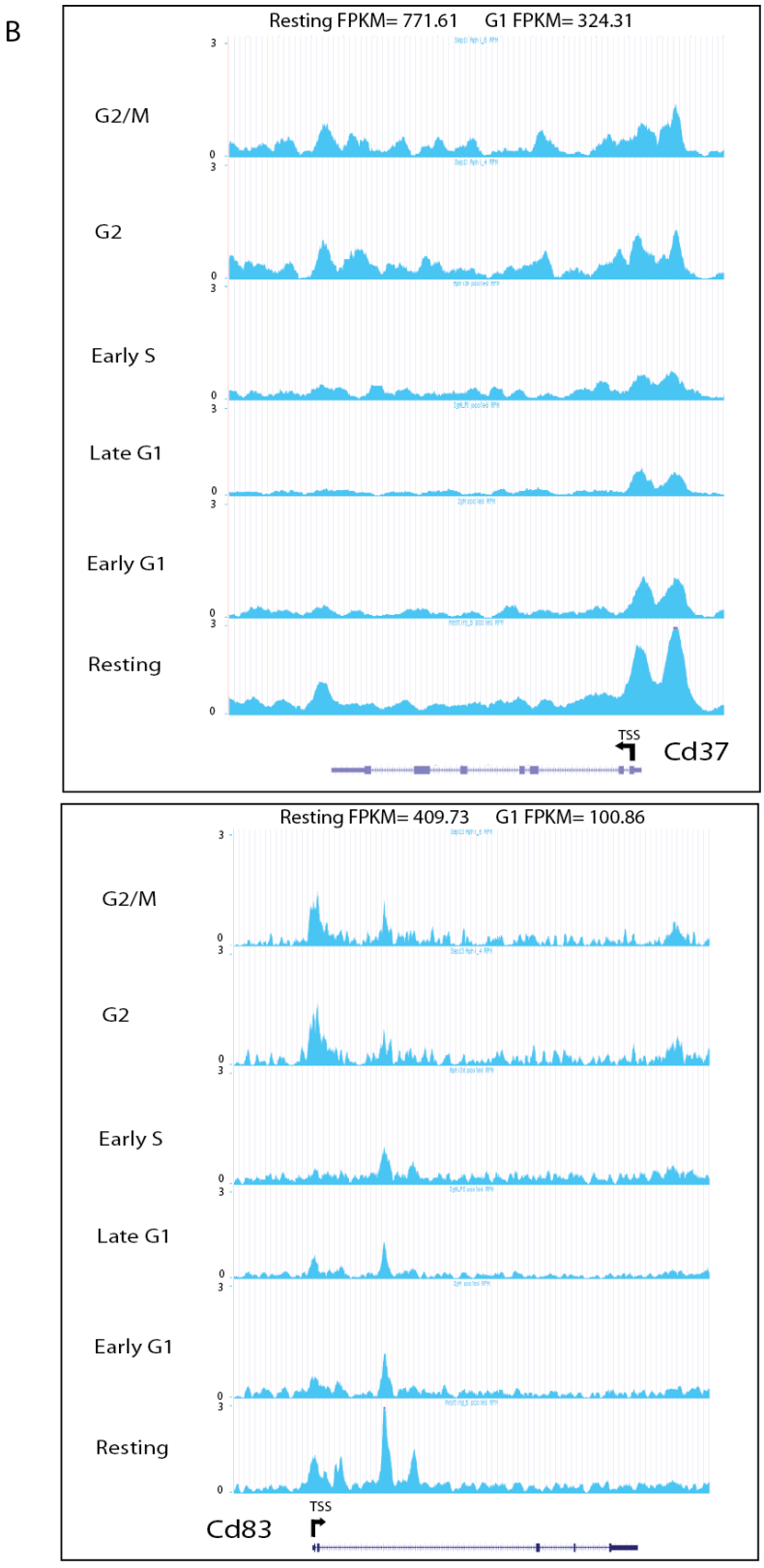


Figure 6.1: ChIP-seq analysis of Cnot3 binding at different stages of the cell cycle during B cell activation.
Snapshots are shown of Cnot3 binding across four genes. The tracks show binding profiles in resting, early and late G1, early S, G2 and G2/M B cells. In **A** are reported *Pmf1* and *Mtx1*. In **B** are reported *Cd37* and *Cd83*. The FPKM values in resting and G1 elutriated LPS activated B cells are shown. FPKM values report the gene expression levels.

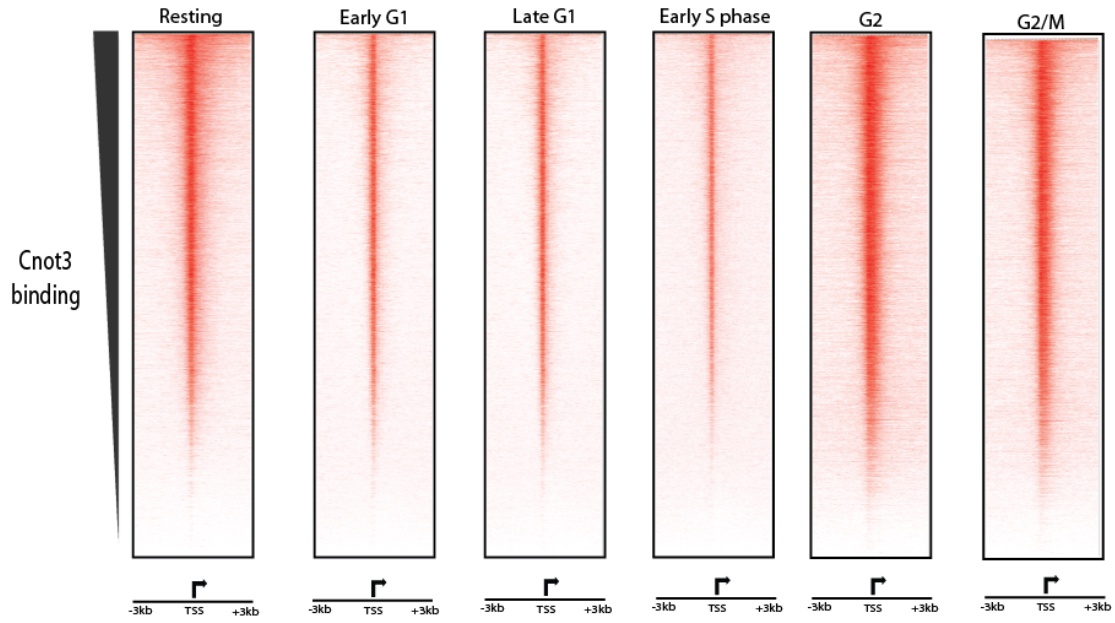
6.3 The binding profile of Cnot3 at the TSS changes during cell cycle

To gain additional information on the role of Cnot3 in gene regulation, the area around the TSS was analysed in more detail. Heat maps showing Cnot3 binding were generated for all of the cell cycle stages covering the area upstream and downstream from the TSS of 14,788 genes that are transcribed in resting B cells. The list of genes was generated based on RNA-seq data generated by A. Frangini. Genes were judged to be transcribed if their expression exceeded a threshold FPKM of 0.118. Genes were ranked in the heat map according to decreasing Cnot3 binding. Initally, the area of the TSS from +3kb to -3kb was plotted. The overall binding pattern is generally similar to the patterns observed at individual genes with high levels of binding detected in resting B cells, decreased binding through early and late G1, low levels in early S phase and then increased binding in G2 and G2/M (Figure 6.2-A).

To analyse Cnot3 binding in more detail, the area that was studied around the TSS was reduced to +1kb to -1kb. In order to have a quantitative chart of binding, line plots of the average Cnot3 binding across the TSS regions of the 14,788 genes were generated. The line plots revealed a change in both intensity and shape of average Cnot3 binding profiles during cell cycle progression (Figure 6.2B). In resting early and late G1 B cells, there was a peak of Cnot3 binding was centred upstream the TSS. The peaks have the same shape at all three stages, albeit with reduced binding levels in early and late G1. The minimum binding was detected in early S phase, but the shape of the peak was similar to the previous phases. Plotting Cnot3 average binding in resting and G2 B cells in the same chart, the shape of the curve was different in the two stages (Figure 6.2B). The binding of Cnot3 in resting cells was a sharp peak with a maximum upstream the TSS. In G2 the peak was not as sharp as in resting B cells and was more spread along the body of the gene. The height of the peak was slightly less in G2. This could be due to the fact that the gene cohort that was analysed represented genes that are expressed in resting B cells and some of these genes might be switched off in G2 cells. G2/M cells had a very similar average profile to the one that was observed in G2. (Figure 6.2B).

The shift in the Cnot3 binding peak suggests increased binding of Cnot3 in the 500bp region downstream from the TSS. The fact that this increase is accompanied by a strong increase in transcription, compared with resting B cells (Section 5.6), raises the possibility that Cnot3 is involved in controlling transit of RNA Pol II through the pause region downstream from the TSS. This is supported by the finding in this study that Cnot3 interacts with Xrn2, which has been shown to be involved in premature termination of transcription (Brannan et al., 2012).

A



B

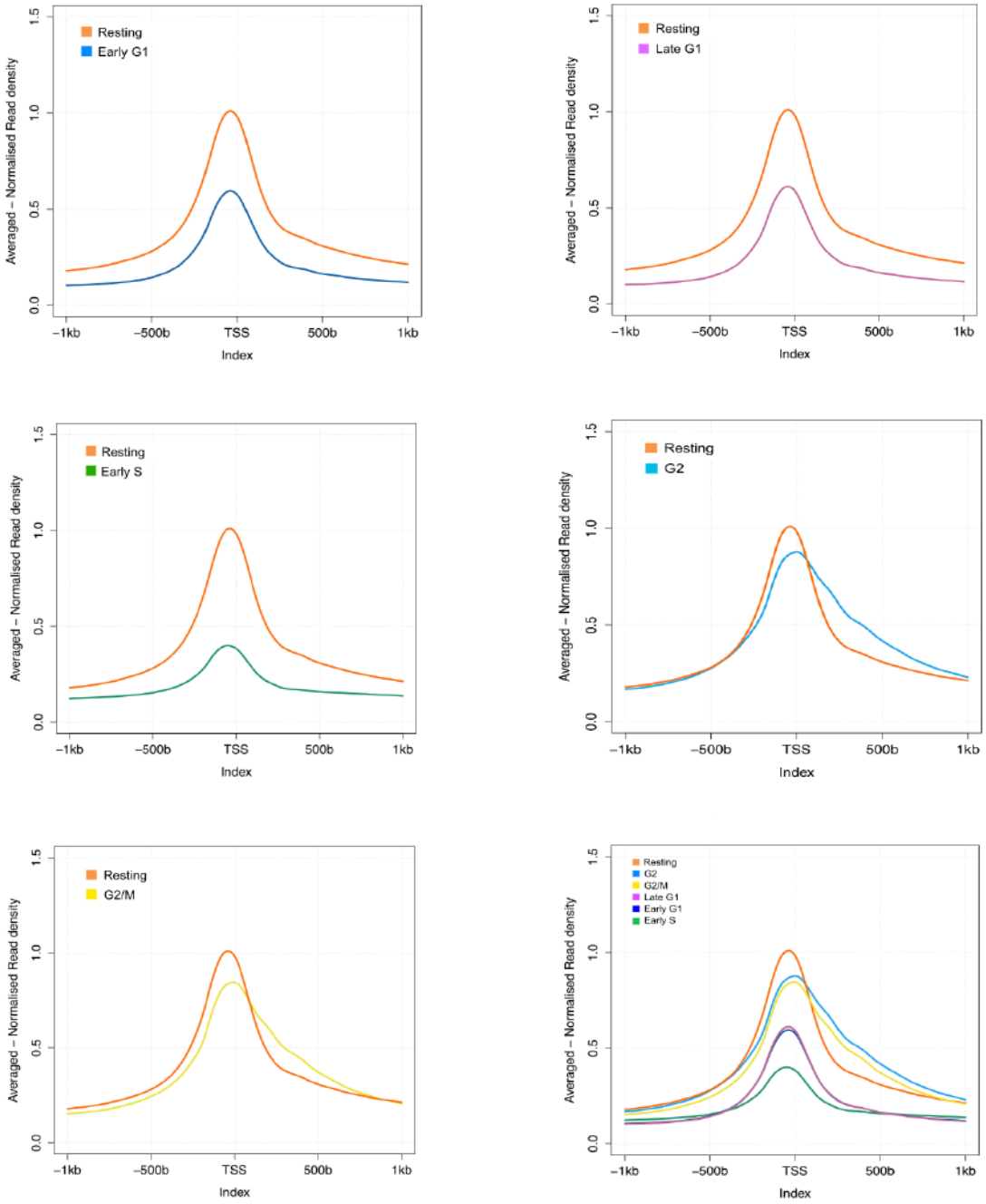


Figure 6.2: Cnot3 binding around the TSS during cell cycle progression.
A) Heat maps showing the area of the TSS from +3kb to -3kb for 14,788 genes during cell cycle progression. The genes were shown by RNAseq analysis to be expressed in resting B cells and were ranked based on decreasing binding of Cnot3 to the region analysed (see Materials and Methods, Section 2.9.3). The colour scale settings used to generate the heat maps were kept at the same settings for each cell cycle phase.
B) Line plots were generated by calculating the average binding of Cnot3 to the set of genes as in A, using a window of 2kb around the TSS. The resting B cell plot was compared to the other phases. The bottom right panel shows the plots for all of the cell cycle stages that were analysed.

6.4 Comparison of peaks of Cnot3 binding during cell cycle progression

In order to compare the overall distribution of Cnot3 binding at different stages of the cell cycle, peak calling was carried out for each cell cycle phase using the Model-based Analysis for ChIP-seq (MACS2) programme, (see Materials and Methods section 2.9.2). The highest number of peaks (51,964) was found in resting B cells. Approximately half of that number was present early and late G1 (25,591 and 23,636 respectively). In early S phase, 13,223 peaks were detected. The number increased again in G2 with 33,208 and in G2/M with 32,452 peaks identified (Table 6.3).

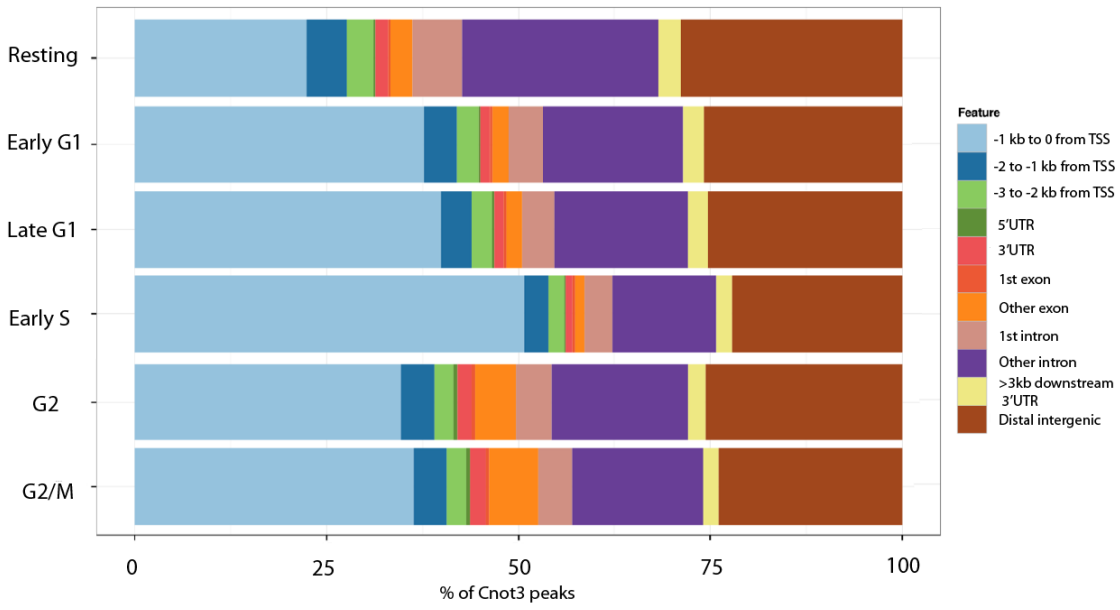
	Number of peaks
Resting	51,964
Early G1	25,591
Late G1	23,636
Early S	13,223
G2	33,208
G2/M	32,452

Table 6.3: Number of peaks of Cnot3 binding called for each cell cycle phase. The peak calling analysis was carried out using Model-based Analysis for ChIP-seq (MACS2).

Analaysis of the distribution of the peaks was performed using the Chipseeker Bioconductor package. Figure 6.4 shows the proportion of the total peak count that was located in different regions of the genome during cell cycle progression. In resting B cells around 23% of the total Cnot3 peaks were in the area of the promoter less than 1 kb upstream from the TSS. The distal part of the promoter from -1 to -3kb is not particularly enriched in peaks. The introns (1st intron + other introns) and the distal intergenic regions together constitute around 60% of the total (Figure 6.4). In early and late G1 and early S, as the overall number of Cnot3 drops, the proportion that are present in the area of the promoter near the TSS increases. In these cell cycle phases Cnot3 peaks located within the -1kb region upstream from the TSS represent around 40% of total peaks in early and

late G1. The percentage of peaks within -1 kb of the TSS is around 50% of total peaks in early S. From resting to early S the proportion of peaks that are located whithin introns shows a sharp decrease. The percentage goes from 32% in resting to 17% in early S. In the distal intergenic regions there is slight drop, the percentage of 28% of total peaks decreases to 22% in early S phase (Figure 6.4). In G2 this trend is reversed with around 50% of Cnot3 peaks residing in introns and distal intergenic regions, while around 35% are present within -1kb upstream from the promoter (Figure 6.4).

A



B

	-1 kb to 0 from TSS	Introns	Distal Intergenic
Resting	11,629	16,669	14,958
Early G1	9,633	5,838	5,969
Late G1	9,414	5,141	6,596
Early S	6,704	2,266	2,928
G2	11,517	7,490	8,496
G2/M	11,782	7,024	7,735

Figure 6.4. Distribution of Cnot3 binding peaks during cell cycle progression. A) The chart shows the distribution of called Cnot3 peaks in six different cell cycle phases. The colour key for the segments of each bar is shown on the right. The area of each segment is proportional to the number of peaks detected in that region of the genome. B) The table shows the number of peaks that were called in each cell cycle phase for the region within -1kb upstream from the TSS, in the introns and in the distal intergenic regions.

It is important to note that Figure 6.4 represents the relative abundance of peaks in different regions of the genomes. Since the overall number of peaks drops sharply in G1 and S-phase, the percentage between 40% and 50% of peaks within -1kb region upstream from the TSS in early and late G1 and early S phase is not due to gain of peaks on promoters, but is instead caused by a more pronounced loss of peaks in distal intergenic regions and introns (see numbers in Figure 6.4B and ChIP-seq snapshots in Figure 6.5). During G2 and G2/M a higher percentage of peaks are observed at the region -1kb upstream from the TSS compared to resting. However, the absolute number of peaks is very similar (Figure 6.4 B). The percentage is higher in G2 and G2/M because the absolute number of peaks decreases in distal enhancer elements and within introns (Figure 6.4 B). Therefore, the proportion of peaks in the region -1kb upstream from the TSS in G2 and G2/M is higher because there is a loss in introns and distal regions.

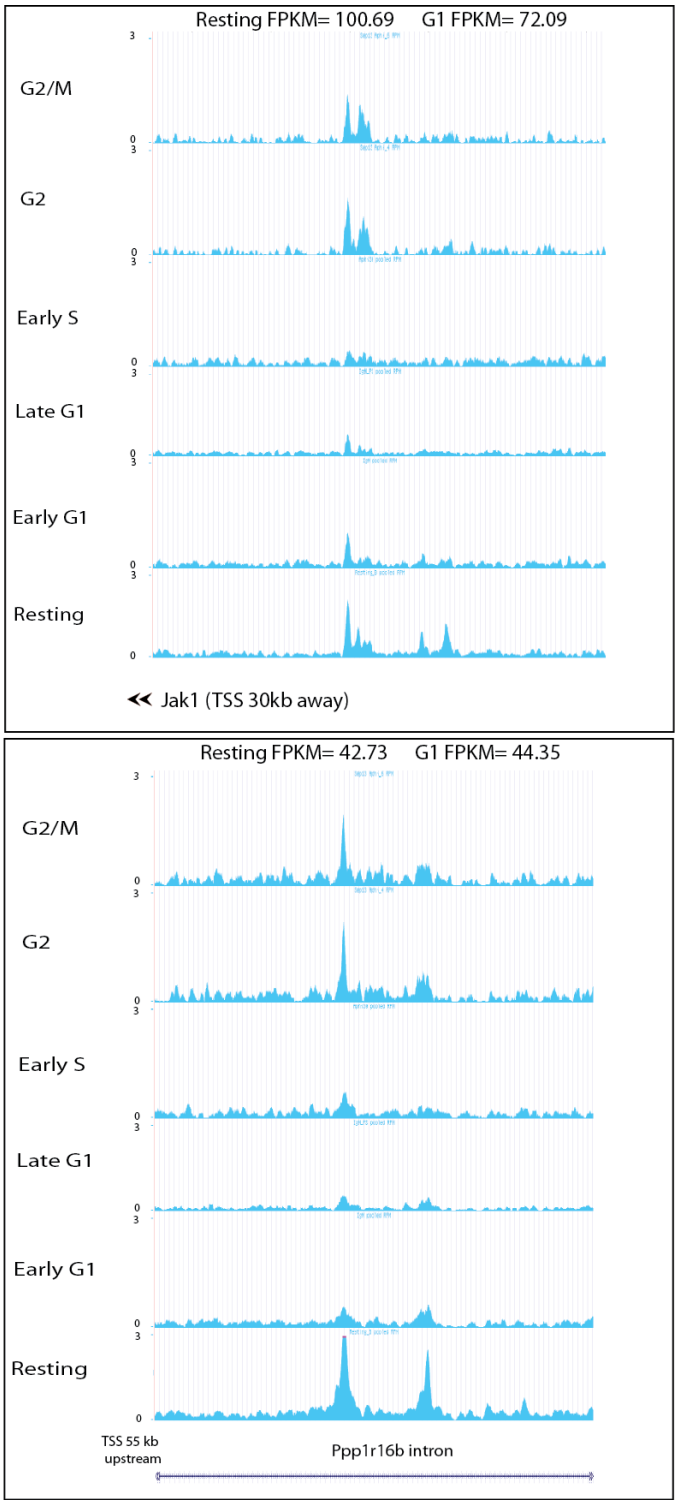


Figure 6.5. ChIP-seq analysis of Cnot3 binding at different stages of the cell cycle during B cell activation on enhancer regions.
Snapshots show ChIP-seq tracks of Cnot3 binding on enhancer regions in resting, early and late G1, early S, G2 and G2/M. The top panel shows the enhancer 30kb upstream from *Jak1.* The bottom panel shows the enhancer region in the intron 2 of the *Ppp1r16b* gene. FPKM values shown in each panel represent the expression levels of the genes in resting B cells and G1 B cells purified by elutriation 3 days after activation with LPS. The RNA-seq data was generated by A. Frangini. Enhancers coordinates were taken from (Kieffer-Kwon et al., 2013).

6.5 Summary

In this chapter, I have described the genome wide binding of Cnot3 to chromatin during cell cycle progression. The genome wide binding of Cnot3 at gene promoters varies during the cell cycle. The analysis of the region - 1kb to +1kb from the TSS has revealed differences during cell cycle progression. The average binding of Cnot3 on expressed genes shows a peak that decreases in intensity from resting to early S phase. In G2 the peak is similar to resting for intensity but the shape of the curve is different, meaning that Cnot3 binding is shifted towards the body of the gene. The peaks are enriched in the region of the TSS and distal regions in resting B cells. In early and late G1 and early S, when the overall number of Cnot3 peaks is reduced compared to resting B cells, peaks are retained at promoters but the number of peaks in intronic and distal intergenic regions is sharply reduced. During G2 and G2/M a higher proportion of peaks are found in introns and distal intergenic regions than on promoters. Overall the results suggest that significant changes in the location of Cnot3 binding take place during cell cycle progression. These results could reflect global changes in the functioning of distal enhancers at different stages of the cell cycle.

Chapter 7- Design and generation of Cnot3 conditional knock out mouse

7.1 Introduction

The results presented in the previous chapters described the behaviour of Cnot3 during the cell cycle in B cells. However, it was not possible to directly probe the functional role of Cnot3 in gene regulation using siRNA or shRNA approaches to deplete the protein. Primary B cells have many advantages because they are non-transformed cells that can be readily isolated and cultured. However genetic studies are difficult to perform in these cells because they cannot be easily transfected or infected with retroviruses. The solution to this problem was to generate a conditional Cnot3 knockout mouse to study the effects of knocking down the protein. Germline Cnot3 knockout mice have been described in literature, but the homozygous knockout animals are embryonic lethal at the implantation stage (Neely *et al.*, 2010). The design and production of a conditional Cnot3 knockout mouse using TALEN targeting will be described in this chapter.

7.2 TALEN targeting of the *Cnot3* gene

TALEN targeting is based on the principle that the introduction of a double strand (DS) break leads to repair of the break, either by non-homologous end-joining (NHEJ) or, alternatively, by homologous recombination (HR) if a suitable target sequence is available. Efficient introduction of a DS break results in HR at an efficiency that is much higher than the levels achieved by conventional gene targeting methods in ES cells. One of the systems that has been developed for efficient introduction of DS breaks at specific sites uses the transcription activator like effector nucleases (TALENs). TALENs consist of synthetic arrays of TAL effectors, which were discovered in plants as products of the pathogenic bacteria Xanthomonas. They are DNA binding proteins able to promote transcription in host organisms (Bogdanove et al., 2010). TAL effectors contain a

DNA binding domain that is formed by repeat-variable di-residue (RVD) repeats. Each RVD is able to bind to a specific nucleotide in the DNA sequence. In TALEN targeting the RVD repeats are arranged in a specific order that allows them to target the desired sequence. The TAL effectors have been modified by fusing a FokI endonuclease at the C-terminal of the TAL sequence. In order to be active and generate a cut, FokI needs to dimerize. Two TAL effectors recognize opposite strands on DNA target sequences to promote FokI dimerization. The active nuclease is therefore able to cause a double strand break that can be used to promote efficient homologous recombination (Figure 7.1).

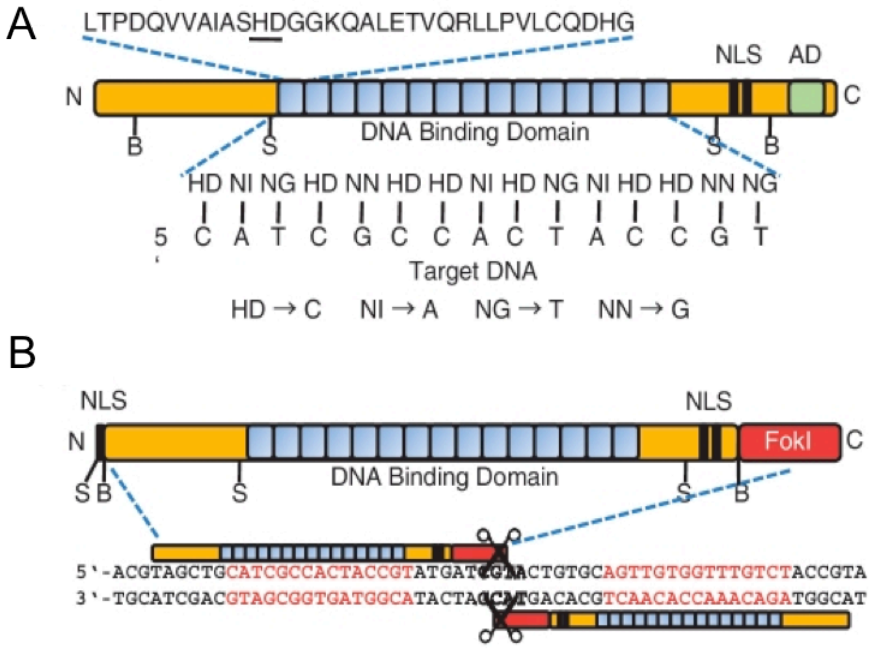


Figure 7.1: TALEN targeting.
A) TAL effector composed of N terminal domain, a central DNA binding domain and a C terminal domain with the NLS signal. The DNA binding domain is composed by RVDs. Each RVD recognizes a nucleotide. B) TALEN dimer of single TAL effectors fused to FokI monomers (adapted from (Cermak et al., 2011)).

We have developed a strategy to generate a mouse conditional knockout for Cnot3. The design of the TALEN plasmids and the experimental procedures to generate them were carried out in collaboration with Dr. Mónica Román Trufero. The TALEN targeting was used to insert two LoxP sequences within the *Cnot3* gene. In order to insert LoxP sequences into the genome with as little disruption

ofthe gene as possible, promoters and 5'UTR regions should be avoided and the distance from intron-exon junctions must be at least 200 bp. For the design of the DNA binding domain of the TALEN sequence, we took advantage of free software designed by Cermak *et al.* (TAL Effector Nucleotide Targeter 2.0; TALE-NT) (Cermak *et al.*, 2011). The software predicts the sequence of the TALEN that is needed to generate a double strand break in a desired position. Two pairs of TALEN were designed to induce double strand breaks in intron 1 and 7. The first LoxP sequence was inserted into intron 1 of the *Cnot3* gene and the second one in intron 7 (see Materials and Methods section 2.11.1). The two targeting constructs that contained 300bp of homology on each side of the cut site. After Cre recombination, this strategy will allow the deletion of 6 exons (Figure 7.2).

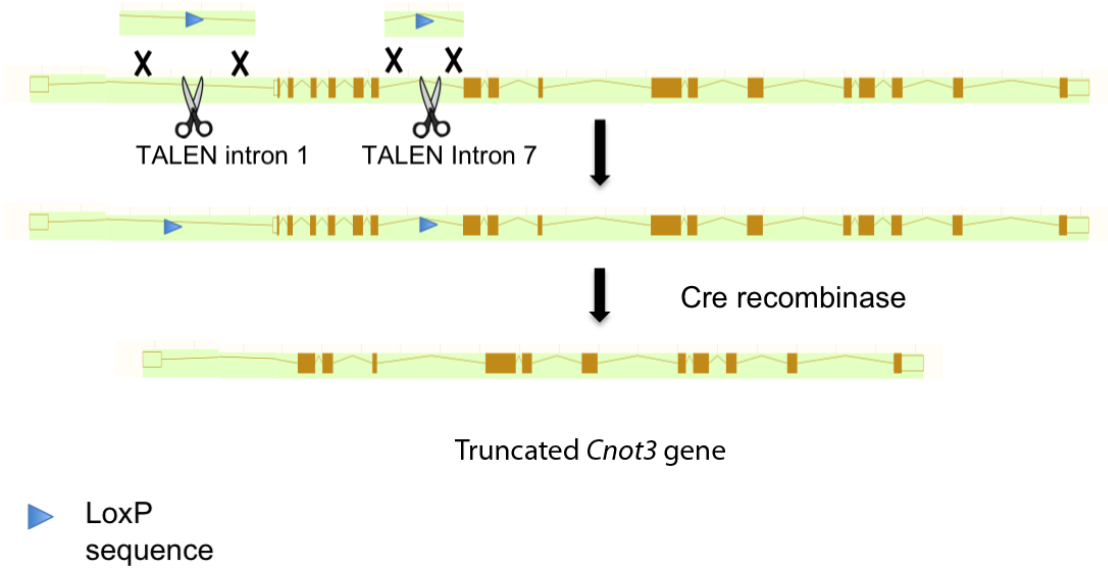


Figure 7.2: Strategy to flox *Cnot3* gene.
TALENs were designed to generate cuts in introns 1 and 7 of *Cnot3* gene. Targeting constructs containing the LoxP sequences carried 300 bp of homology arms on each side of the cut site.

7.3 Testing of the TALEN constructs in ES cells

The aim of the TALEN targeting was to edit the genome in the zygote in order to transmit the floxed gene to the whole mouse. To test the efficiency of this approach, we decided to apply this genome editing technique to ES cells. To

perform the test, the editing of the exon 1 was carried out. The targeting construct contained 300 bp of homology with the endogenous sequence on both sides of the cut site. The construct also contained a Neomycin resistance gene, under the control of the Pgk promoter, which was used to perform a positive selection on the cells. To carry out this experiment, ES cells were electroporated with two circular plasmids expressing TALENs and a linearized targeting construct to replace the genomic sequence. A separate ES cell plate was electroporated with only the targeting construct. After the electroporation, a selection was performed by culturing cells in medium containing neomycin. Only cells with the targeting construct integrated in the genome would survive after this selection. Cells were stained with crystal violet to visualize the number of neomycin resistant colonies. Figure 7.3 shows that the number of cells alive in the plate electroporated with TALENs and the targeting construct is much higher than the one for the plate that was electroporated with the targeting construct only (Figure 7.3). The much higher frequency obtained when the TALEN is included indicated that it was promoting a specific integration event, which was presumed to be homologous recombination at the DS break. The small number of colonies obtained without the TALEN would be the result of random integration of the construct, which would be much less efficient. Successful targeting was also achieved in ES cells with the other TALEN pair (data not shown).

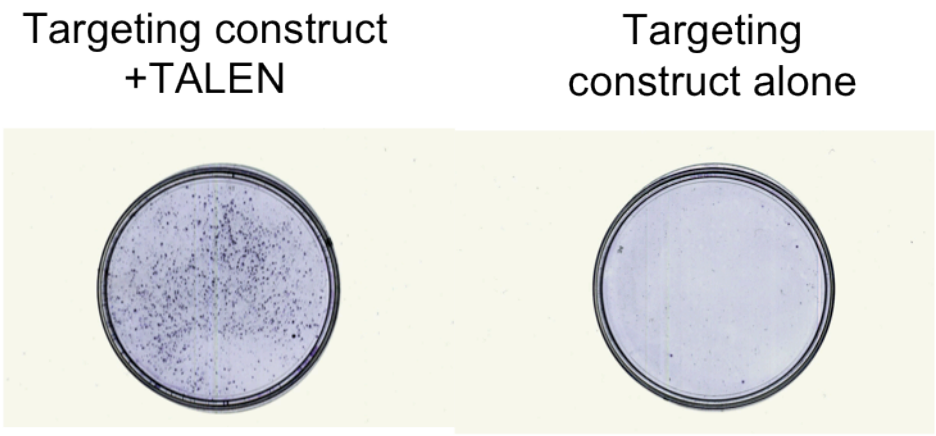


Figure 7.3: Crystal violet staining of ES cells after neomycin selection.
ES cells were electroporated either with TALEN and targeting construct for intron 1 or with the targeting construct only. Neomycin selection was carried out for one week and crystal violet staining was used to compare the number of live cells on the two plates.

7.4 Generation of Cnot3 conditional knockout mouse

The positive result obtained in ES cells demonstrated the high efficiency of the TALEN targeting. We applied this technology to generate a Cnot3 conditional knockout mouse. To achieve this purpose, fertilized eggs were micro-injected with RNA molecules coding for TALEN proteins and the DNA targeting constructs. The zygote would have a transient expression of TALENs in order to promote the recombination with the targeting constructs. The editing generated in the one cell stage would be propagated to every cell in the mouse. The fertilised eggs were generated in a background of CRE-ER^{T2} under the constitutive expression of the Rosa 26 promoter. The oocyte injections and all accompanying manipulations were carried out by the MRC CSC Transgenic Facility.

A total of 21 mice were generated from the oocyte injections of which two were heterozygous for the two LoxP sites (Figure 7.4A). One of these mice was bred successfully and gave the expected Mendellian level of transmission of the floxed allele (Figure 7.4B). Work is currently in progress to breed the line to homozygosity and to generate enough mice to carry out experiments. The TALEN RNAs and targeting constructs are also being re-injected to obtain a second mouse line, which will be used to verify important results obtained with the first targeted line and exclude any contribution from off-target mutations.

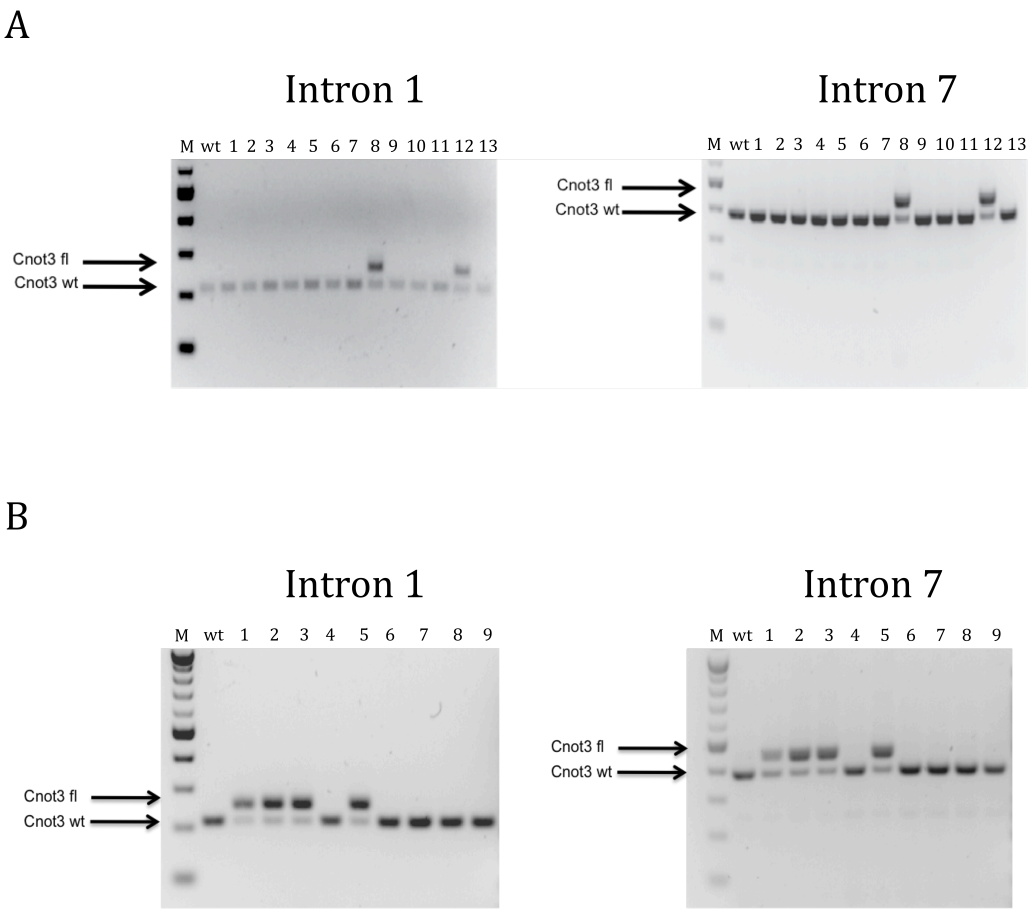


Figure 7.4: Genotyping of the *Cnot3* gene.
A) Genotyping of *Cnot3* intron 1 and intron 7 to verify the presence of LoxP sites. The genotyping was performed on the mice born after micro-injection of the TALENs and targeting construct. The order loading is the following: marker (M), a non floxed *Cnot3* wild type (wt) control and the remaining lanes are littermates. Samples were loaded in the same order on the gel for intron 1 and intron 7. **B)** F1 generation of mice born from the mouse number 8 on the gel in **A**. The order of loading is the following: marker (M), wt control and the remaining lanes are littermates. Samples are loaded in the same order in the gel for intron 1 and intron 7.

7.5 Summary

This chapter describes the strategy for the production of a Cnot3 conditional knockout mouse. TALEN targeting was used to generate two cuts in specific positions in the intron 1 and 7. This allowed a homologous recombination process for the insertion of two LoxP sites at these positions. The intron 1 TALEN was tested in ES cells showing a high efficiency of targeting construct integration in the genome. TALEN RNAs with two targeting constructs were micro-injected

to fertilised mouse eggs. The micro-injection experiment gave rise to of 2 targeted mice out of 21 animals generated. The progeny of one of these two mice has been bred successfully to generate heterozygous offspring. Work is now in progress to breed these mice to generate homozygous floxed *Cnot3* mice.

Note: The design and generation of TALEN plasmids has been carried out in collaboration with Dr. Mónica Román Trufero. The ES cell transfections and mouse breeding were carried out by Dr. Román Trufero. The oocyte injections and all associated manipulations were performed by the MRC CSC Transgenic Facility.

Chapter 8- Discussion

8.1 Overview

The overall theme of this thesis has been the behaviour of nuclear Cnot3 during cell cycle progression. Although the protein is present in the nucleus and in the cytoplasm, my analysis of Cnot3 has been focused on the nuclear compartment. The importance of studying the role of Cnot3 in transcriptional and post-transcriptional regulation has been highlighted by recent studies. Cnot3 was shown to be a tumor suppressor in T-cell acute lymphoblastic leukaemia (De Keersmaecker et al., 2013). It has also been implicated in a number of other human pathologies, including osteoporosis (Watanabe et al., 2014), obesity (Morita et al., 2011), impaired heart function (Neely et al., 2010) and retinitis pigmentosa (Venturini et al., 2012).

Cnot3 is part of the CCR4-NOT complex and is required for stability of the complex (Boland et al., 2013). This means that Cnot3 has a major role in RNA degradation (Watanabe et al., 2014) (Morita et al., 2011). The co-IP and mass spectrometry data described in this thesis have confirmed that Cnot3 interacts with other Cnot proteins (Cnot1, Cnot2, Cnot6, Cnot6L, Cnot7, Cnot8, Cnot10, Cnot11) in B cells. Although CCR4-NOT is involved in RNA metabolism, none of the subunits of the complex has an RNA binding motif. This could be part of a mechanism to target the deadenylase activity to specific mRNA targets. Instead of binding RNA directly, the complex requires RNA binding proteins, such as TTP (Lykke-Andersen and Wagner, 2005), to be recruited to the 3' end of mRNAs.

Cnot3 contains a NOT-box domain in the C-terminal region which is involved in interactions with other proteins (Figure 8.1). The NOT-box has been shown to be responsible for the interactions with different proteins, such as Cnot2 (Boland et al., 2013), TBP-interacting protein B (TIP120B) (Aoki et al., 2002), Aurora B. NOT-box proteins were first described in yeast as negative regulators of transcription (Collart and Struhl, 1994). Furthermore, a study in human cells reported that the NOT-box domain of CNOT2 and CNOT3 negatively affected transcription in a luciferase reporter assay. However, the same study also

showed that the full length CNOT3 protein did not have any repressive effect (Zwartjes et al., 2004).

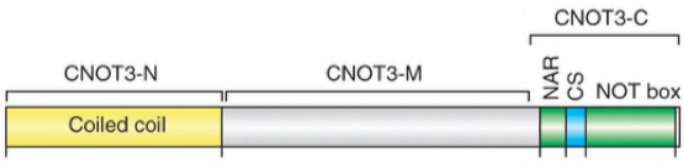


Figure 8.1: Schematic representation of the domain structure of human CNOT3.
The Figure shows the domains in the human CNOT3 protein. The protein consists of a coiled coil domain at the N terminal, an unstructured domain in the middle part and a C terminal domain. The C terminal domain contains a NOT1 anchor region (NAR), a Connector Sequence (CS) and the NOT-box domain.

In this thesis Cnot3 has also been shown to interact with Aurora B through the NOT-box domain, creating a connection between the CCR4-NOT complex and the CPC. The interactions with histones, chromatin remodelers, nucleolar factors and the presence of Cnot3 on active gene promoters suggest that Cnot3 play a role in transcriptional regulation. However, the data obtained to date cannot answer the question whether Cnot3 is an activator or a repressor. Characterization of Cnot3 depleted B cells using the conditional knockout mouse will allow this point to be investigated.

Many interactions were detected between Cnot3 and proteins involved in splicing. These data suggest that Cnot3 plays a role in RNA processing, but the precise task that the protein has in this co-transcriptional process is still unknown. Again, the analysis of the knockout mouse should allow this question to be addressed. From the analysis of our data and the studies published in literature, it seems reasonable to hypothesise that Cnot3 acts as an adaptor protein by interacting with a number different classes of proteins in the nucleus. The role of Cnot3 might be to recruit or mediate interactions among proteins that are involved in transcriptional and post-transcriptional regulation.

A recent paper reported that Cnot3 is important for maintaining the self-renewal program in ES cells (Hu et al., 2009). ChIP-seq analysis revealed extensive binding to promoters in ES cells and knockdown of Cnot3 resulted in upregulation of trophectoderm genes and differentiation into the trophectoderm

lineage. Based on motif analysis of ChIP-seq data, Hu et al. also reported that Cnot3 is a sequence-specific transcription factor that binds to a specific consensus sequence (Hu et al., 2009). Our efforts to verify this conclusion by analysing binding of Cnot3 to the sequence described by Hu et al. in EMSA assays were unsuccessful. Instead our results suggested that Cnot3 binds to DNA as a co-factor that interacts with DNA-binding factors (data not shown).

To gain further insights into the role of Cnot3 in gene regulation, a B cell system was developed that uses a controlled activation of resting B cells. This is a powerful tool to study the behaviour of Cnot3 during cell cycle progression in primary B cells. Activation of resting B cells by the stimulation of BCR and TLR4 receptors and the use of the DNA polymerase inhibitor aphidicolin allowed us to isolate cell populations that were highly enriched for different phases of the cell cycle. Using this system, I have analysed several different aspects of the behaviour of Cnot3 during the cell cycle.

8.2 Cnot3 interacts with the cell cycle regulator Aurora B

Data obtained by our lab showed that Aurora B is involved in regulating transcription in resting B cells (Frangini et al., 2013). The strong interaction between Cnot3 and Aurora B that was revealed by co-IP and the presence of Cnot3 on active gene promoters led us to investigate the role of Cnot3 in transcriptional regulation in B cells. In this thesis I have shown that Cnot3 interacts with Aurora B in a cell cycle dependent manner. A strong interaction was observed in resting B cells. The interaction decreased in early and late G1 and reached its lowest level in S-phase before increasing again in G2. The reduced interaction coincided with loss of binding of Cnot3 to gene promoters. However, experiments performed in Aurora B knockout mice showed that depletion of Aurora B does not affect binding of Cnot3 to promoters, indicating that loss of Cnot3 binding in S-phase is not directly linked to loss of the interaction with Aurora B. Another possibility is that binding of both proteins to the same region of chromatin promotes the interaction between them. Detection of the Cnot3-Aurora B interaction in resting B cells requires intensive digestion of the compact chromatin to release the bound proteins. This suggests that the

interacting Cnot3-Aurora B are bound to chromatin in the nucleus. However, digestion of resting B cell chromatin with Benzonase, which completely degrades DNA in the preparation, does not affect the interaction, indicating that it is a bona fide interaction and is not simply a consequence of co-localisation of the two proteins to the same region of DNA.

Aurora B and Cnot3 have both been shown to have a role in G1/S transition in other cell types (Song et al., 2007) (Mittal et al., 2011). The interaction that was observed between the two proteins in late G1 and in aphidicolin blocked cells, which are at the G1/S boundary, raises the possibility that the Cnot3-Aurora B interaction plays a role in the G1/S transition in B cells.

A strong interaction between Aurora B and Cnot3 proteins was detected in G2 cells. Cnot3 was also shown to interact with the CPC members INCENP and Borealin in G2. Interaction of Cnot3 with several other members of the CCR4-Not complex including Cnot1 and Cnot2 was also detected at this stage. This suggests that the CPC performs some of its functions in concert with sub-complexes of the CCR4-Not complex. The CPC controls the activity of many proteins through phosphorylation during mitosis and is directly involved in regulating the spindle assembly checkpoint (Sampath et al., 2004). A target of the CPC is MAD1, which is involved in spindle assembly. Localization of MAD1 to the spindle during mitosis is controlled by Aurora B (Matson and Stukenberg, 2014). A recent study has shown that Cnot3 is involved in correct mitotic progression by controlling the stability of MAD1 mRNA and the level of MAD1 protein. This result, together with our data, suggests that Cnot3 and the CPC could act together to ensure a proper mitotic division. Furthermore, during this phase Cnot3 is phosphorylated by CDK1, which promotes the G2 to M transition (Takahashi et al., 2012). Our Co-IP and MS analysis has confirmed that Cnot3 interacts with CDK1 in G2 (Appendix Table A).

8.3 The interaction of Cnot3 with histones suggests a role in transcriptional regulation

The co-IP and MS analysis revealed the presence of many histones among Cnot3 interactors. The absence of any enzymatic activity for Cnot3, suggests that the interaction with histones could be a mechanism to recruit other proteins to chromatin. Cnot3 interacts with core histones and many variants of these proteins, such as H2A, H2A.Z, H2B, H2A.V, H3.3, H3.3C, H4 (Appendix Table A). This indicates that Cnot3 is in contact with chromatin and suggests that it could be involved in recruiting modifications enzymes to chromatin.

In addition to the interactions with core histones, it is particularly interesting that Cnot3 interacts with many isoforms of the linker histone histone H1 and that this interaction is detected mainly in G1. The presence of histone H1 has been connected mainly with repression because it has been shown to promote a more closed chromatin structure (Robinson and Rhodes, 2006). However, a recent study has reported that histone H1.4 that is acetylated at lysine 34 is also found around the TSS of active genes. The presence of histone H1.4K34ac is correlated to the expression levels of the genes in MCF-7 cells (Kamieniarz et al., 2012).

In a peptide binding assay, we did not find any preference for Cnot3 to bind the acetylated form of the histone. A possible explanation for this could be that Cnot3 binds to unmodified H1 to promote the recruitment of chromatin factors. Furthermore, Cnot3 interacts with Nucleolin, which also interacts with histone H1 to promote decondensation of chromatin (Erard et al., 1988). Nucleolin has been described to have an activity that resembles the FACT complex and to enhance the activity of the remodelers SWI/SNF (Angelov et al., 2006). The interaction of Cnot3 with Nucleolin, histone H1, and also with the FACT complex subunits (Appendix Table A), could be explained by function of Cnot3 being to promote the passage of the elongation complex through the first nucleosome.

8.4 Cnot3 binds chromatin in a cell cycle dependent manner

The role of Cnot3 in transcriptional regulation has been studied in ES cells, where it has been proposed to form a self-renewal module with Trim28, c-myc and Zfx. In these cells Cnot3 has been shown to be an activator of a distinct class of genes. At the moment it is not possible to say whether Cnot3 is an activator or repressor in B cells. The genome wide analysis showed that Cnot3 binds to gene promoters in a cell cycle dependent manner. Cnot3 binding is particularly high in resting B cells and in G2 activated B cells. A generalised drop of binding is detected during S phase. The result obtained in S phase was also validated in a drug-free system. Binding of Pcna was detected at gene promoters indicating that the apparent loss of Cnot3 binding was not a ChIP artefact generated by differences in the properties of the chromatin at different stages of the cell cycle.

S-phase is a period of transition when chromatin undergoes changes because of DNA replication. Histones are subject to disruption and remodelling due to the passage of the replication fork. During B cell activation chromatin also becomes more generally sensitive to nuclease digestion compared to the other stages (our unpublished observations). These changes could lead to Cnot3 being displaced but we do not have any information about the detailed mechanism behind this at present. My analysis of the levels of primary transcripts revealed high levels of transcription during this phase, but also in G2 when significant levels of Cnot3 bindinga are detected at gene promoters. This makes it difficult to establish any clear correlation between binding of Cnot3 and transcription levels in S phase and G2. It should be noted, however, that the analysis of Cnot3 binding around the TSS in G2 showed a shift in binding towards the body of the gene compared to other phases of the cell cycle. This shift in binding could indicate a change in the functions of Cnot3 between the resting and G2 stages and might be connected to the hypothesis that Cnot3 works in concert with Xrn2 to control proximal promoter pausing and termination. Involvement of Cnot3 could also act in promoting Pol II passage through the first nucleosome would also explain the shift in binding when transcription is high in G2 cells.

Cnot3 is not only bound to promoter regions, but is present in distal regions where it binds to established and putative enhancer elements in a cell cycle

regulated manner. High levels of binding to enhancers are detected in resting and G2 cells. During early and late G1 and early S, Cnot3 the number of peaks in these regions is reduced whereas binding is retained to a greater degree on the promoter regions. Cnot3 binding is also found in the body of the gene, particularly within introns. It is possible that this binding is important for recruitment of SR or hnRNP proteins to exon/intron junctions and a role in splicing.

8.5 Involvement of Cnot3 with the RNA processing machinery

The co-IP and MS analysis detected many interactions of Cnot3 with SR proteins, hnRNPs, RNA helicases and small RNA associated proteins. SR and hnRNP proteins are known to have opposite roles during splicing. SR proteins promote the inclusion of exons (Long and Caceres, 2009), whereas the hnRNPs are usually inhibitors of exon inclusion (Han et al., 2010). Therefore, Cnot3 could be important in the decision between exon inclusion or exclusion and in alternative splicing. However, hnRNPs are also implicated in mRNA export to the cytoplasm. Cnot3 could direct the binding of hnRNPs to mediate mRNA export out of the nucleus.

The MS analysis also highlighted the interaction with proteins such as Cpsf1 and Fip1 that are involved in the process of pre-mRNA cleavage and stimulation (Kaufmann et al., 2004). It is also possible that the interaction of Cnot3 with these proteins facilitates the 3' end formation RNA. Moreover, the interaction of Cnot3 with Poly-A binding proteins (Pabps) could support this hypothesis due to the fact that Pabps stabilize the 3' end of the RNA after the cleavage to avoid degradation. Another component of RNA termination that has been found among the Cnot3 interactors in G2 is the exoribonuclease Xrn2. According to the Torpedo model, Xrn2 promotes termination by digesting the nascent transcript after cleavage at the Poly-A site, resulting in displacement of Pol II from the DNA (West et al., 2004). The interaction between Cnot3 and Xrn2 could also exert a role in the promoter region, as Xrn2 has been found at promoters of active genes, where it has been suggest that it controls promoter-proximal transcription. It has been hypothesised that Xrn2 ensures directionality of Pol II at the beginning of transcription by terminating transcription that is directed upstream (Brannan

et al., 2012). The possibility that Cnot3 is involved in this process will be investigated using the conditional Cnot3 knockout mouse.

8.6 Future directions: characterization of Cnot3 knockout mouse

The TALEN targeting approach has been a useful tool for generating a conditional Cnot3 knockout mouse. These mice will be used to investigate the functional role of Cnot3 in B cells. The hypotheses that have been formulated in this thesis can be tested in Cnot3 depleted *ex vivo* cultured B cells. Experiments using this system can be expected to clarify whether Cnot3 is an activator or a repressor in B cells.

Ex vivo experiments will make it possible to study Cnot3 ablation in the B cell system that I have set up. Cnot3 knockout in resting B cells will address the question of whether Cnot3 affects the quiescence program. The absence of Cnot3 in resting B cells will also be used to determine whether it affects Aurora B binding on active gene promoters. The data presented in this thesis suggests that Cnot3 could participate in the G1/S transition. This idea is supported by the study of Mittal et al., 2011 and the strong interaction between Cnot3 and Aurora B that I have observed in aphidicolin blocked cells. Cell cycle profiles will be compared between wild-type and knockout B cells to analyse progression from G1 to S phase. Depletion of Cnot3 by addition of tamoxifen at different time-points after B cell activation can also be used to examine whether Cnot3 is involved in the later stages of the cell cycle, including mitosis.

It will also be possible to study the role in transcriptional and post-transcriptional regulation by analysis of primary and fully processed transcripts at different stages of the cell cycle. Analysis of different classes of transcripts can used to determine whether Cnot3 affects transcription globally or, alternatively, whether it targets specific categories of genes. Additional questions that can be addressed using the $Cnot3^{-/-}$ B cells include whether Pol II activity is affected and whether Cnot3 affects directionality of Pol II transcription via the interaction with Xrn2. Analysis of active and repressive histone marks at gene promoters will provide information on whether Cnot3 affects the recruitment of chromatin modifiers.

Bibliography

Adams, R.R., Carmena, M., and Earnshaw, W.C. (2001). Chromosomal passengers and the (aurora) ABCs of mitosis. Trends Cell Biol *11*, 49-54.

Ahmad, K., and Henikoff, S. (2002a). Epigenetic consequences of nucleosome dynamics. Cell *111*, 281-284.

Ahmad, K., and Henikoff, S. (2002b). The histone variant H3.3 marks active chromatin by replication-independent nucleosome assembly. Mol Cell *9*, 1191-1200.

Akiyama, T., Ohuchi, T., Sumida, S., Matsumoto, K., and Toyoshima, K. (1992). Phosphorylation of the retinoblastoma protein by cdk2. Proc Natl Acad Sci U S A *89*, 7900-7904.

Albert, T.K., Hanzawa, H., Legtenberg, Y.I., de Ruwe, M.J., van den Heuvel, F.A., Collart, M.A., Boelens, R., and Timmers, H.T. (2002). Identification of a ubiquitin-protein ligase subunit within the CCR4-NOT transcription repressor complex. EMBO J *21*, 355-364.

Albert, T.K., Lemaire, M., van Berkum, N.L., Gentz, R., Collart, M.A., and Timmers, H.T. (2000). Isolation and characterization of human orthologs of yeast CCR4-NOT complex subunits. Nucleic Acids Res *28*, 809-817.

Allman, D., Lindsley, R.C., DeMuth, W., Rudd, K., Shinton, S.A., and Hardy, R.R. (2001). Resolution of three nonproliferative immature splenic B cell subsets reveals multiple selection points during peripheral B cell maturation. J Immunol *167*, 6834-6840.

Allman, D., and Pillai, S. (2008). Peripheral B cell subsets. Curr Opin Immunol *20*, 149-157.

Anderson, P., and Kedersha, N. (2006). RNA granules. J Cell Biol *172*, 803-808.

Aoki, T., Okada, N., Wakamatsu, T., and Tamura, T.A. (2002). TBP-interacting protein 120B, which is induced in relation to myogenesis, binds to NOT3. Biochem Biophys Res Commun *296*, 1097-1103.

Arellano, M., and Moreno, S. (1997). Regulation of CDK/cyclin complexes during the cell cycle. Int J Biochem Cell Biol *29*, 559-573.

Aslam, A., Mittal, S., Koch, F., Andrau, J.C., and Winkler, G.S. (2009). The Ccr4-NOT deadenylase subunits CNOT7 and CNOT8 have overlapping roles and modulate cell proliferation. Mol Biol Cell *20*, 3840-3850.

Azzouz, N., Panasenko, O.O., Colau, G., and Collart, M.A. (2009). The CCR4-NOT complex physically and functionally interacts with TRAMP and the nuclear exosome. PLoS One *4*, e6760.

Bagchi, S., Weinmann, R., and Raychaudhuri, P. (1991). The retinoblastoma protein copurifies with E2F-I, an E1A-regulated inhibitor of the transcription factor E2F. Cell *65*, 1063-1072.

Balatsos, N.A., Nilsson, P., Mazza, C., Cusack, S., and Virtanen, A. (2006). Inhibition of mRNA deadenylation by the nuclear cap binding complex (CBC). J Biol Chem *281*, 4517-4522.

Bannister, A.J., Zegerman, P., Partridge, J.F., Miska, E.A., Thomas, J.O., Allshire, R.C., and Kouzarides, T. (2001). Selective recognition of methylated lysine 9 on histone H3 by the HP1 chromo domain. Nature *410*, 120-124.

Bardwell, V.J., Zarkower, D., Edmonds, M., and Wickens, M. (1990). The enzyme that adds poly(A) to mRNAs is a classical poly(A) polymerase. Mol Cell Biol *10*, 846-849.

Bargaje, R., Alam, M.P., Patowary, A., Sarkar, M., Ali, T., Gupta, S., Garg, M., Singh, M., Purkanti, R., Scaria, V.*, et al.* (2012). Proximity of H2A.Z containing nucleosome to the transcription start site influences gene expression levels in the mammalian liver and brain. Nucleic Acids Res *40*, 8965-8978.

Bassing, C.H., Swat, W., and Alt, F.W. (2002). The mechanism and regulation of chromosomal V(D)J recombination. Cell *109 Suppl*, S45-55.

Batten, M., Groom, J., Cachero, T.G., Qian, F., Schneider, P., Tschopp, J., Browning, J.L., and Mackay, F. (2000). BAFF mediates survival of peripheral immature B lymphocytes. J Exp Med *192*, 1453-1466.

Belotserkovskaya, R., Oh, S., Bondarenko, V.A., Orphanides, G., Studitsky, V.M., and Reinberg, D. (2003). FACT facilitates transcription-dependent nucleosome alteration. Science *301*, 1090-1093.

Berek, C., Berger, A., and Apel, M. (1991). Maturation of the immune response in germinal centers. Cell *67*, 1121-1129.

Bernstein, B.E., Mikkelsen, T.S., Xie, X., Kamal, M., Huebert, D.J., Cuff, J., Fry, B., Meissner, A., Wernig, M., Plath, K.*, et al.* (2006). A bivalent chromatin structure marks key developmental genes in embryonic stem cells. Cell *125*, 315-326.

Bhatia, S., Pawar, H., Dasari, V., Mishra, R.K., Chandrashekaran, S., and Brahmachari, V. (2010). Chromatin remodeling protein INO80 has a role in regulation of homeotic gene expression in Drosophila. Genes Cells *15*, 725-735.

Blanchette, M., and Chabot, B. (1999). Modulation of exon skipping by high-affinity hnRNP A1-binding sites and by intron elements that repress splice site utilization. EMBO J *18*, 1939-1952.

Bogdanove, A.J., Schornack, S., and Lahaye, T. (2010). TAL effectors: finding plant genes for disease and defense. Curr Opin Plant Biol *13*, 394-401.

Boland, A., Chen, Y., Raisch, T., Jonas, S., Kuzuoglu-Ozturk, D., Wohlbold, L., Weichenrieder, O., and Izaurralde, E. (2013). Structure and assembly of the NOT module of the human CCR4-NOT complex. Nat Struct Mol Biol *20*, 1289-1297.

Bradsher, J., Coin, F., and Egly, J.M. (2000). Distinct roles for the helicases of TFIIH in transcript initiation and promoter escape. J Biol Chem *275*, 2532-2538.

Brannan, K., Kim, H., Erickson, B., Glover-Cutter, K., Kim, S., Fong, N., Kiemele, L., Hansen, K., Davis, R., Lykke-Andersen, J.*, et al.* (2012). mRNA decapping factors and the exonuclease Xrn2 function in widespread premature termination of RNA polymerase II transcription. Mol Cell *46*, 311-324.

Brown, K.M., and Gilmartin, G.M. (2003). A mechanism for the regulation of pre-mRNA 3' processing by human cleavage factor Im. Mol Cell *12*, 1467-1476.

Bryder, D., Rossi, D.J., and Weissman, I.L. (2006). Hematopoietic stem cells: the paradigmatic tissue-specific stem cell. Am J Pathol *169*, 338-346.

Busslinger, M. (2004). Transcriptional control of early B cell development. Annu Rev Immunol *22*, 55-79.

Buttinelli, M., Panetta, G., Rhodes, D., and Travers, A. (1999). The role of histone H1 in chromatin condensation and transcriptional repression. Genetica *106*, 117-124.

Cabart, P., Ujvari, A., Pal, M., and Luse, D.S. (2011). Transcription factor TFIIF is not required for initiation by RNA polymerase II, but it is essential to stabilize transcription factor TFIIB in early elongation complexes. Proc Natl Acad Sci U S A *108*, 15786-15791.

Cambier, J.C., Gauld, S.B., Merrell, K.T., and Vilen, B.J. (2007). B-cell anergy: from transgenic models to naturally occurring anergic B cells? Nat Rev Immunol *7*, 633-643.

Cermak, T., Doyle, E.L., Christian, M., Wang, L., Zhang, Y., Schmidt, C., Baller, J.A., Somia, N.V., Bogdanove, A.J., and Voytas, D.F. (2011). Efficient design and assembly of custom TALEN and other TAL effector-based constructs for DNA targeting. Nucleic Acids Res *39*, e82.

Cerutti, A., Cols, M., and Puga, I. (2013). Marginal zone B cells: virtues of innate-like antibody-producing lymphocytes. Nat Rev Immunol *13*, 118-132.

Cesta, M.F. (2006). Normal structure, function, and histology of the spleen. Toxicol Pathol *34*, 455-465.

Chang, C.T., Bercovich, N., Loh, B., Jonas, S., and Izaurralde, E. (2014). The activation of the decapping enzyme DCP2 by DCP1 occurs on the EDC4 scaffold and involves a conserved loop in DCP1. Nucleic Acids Res *42*, 5217-5233.

Chaudhury, A., Chander, P., and Howe, P.H. (2010). Heterogeneous nuclear ribonucleoproteins (hnRNPs) in cellular processes: Focus on hnRNP E1's multifunctional regulatory roles. RNA *16*, 1449-1462.

Chekulaeva, M., Mathys, H., Zipprich, J.T., Attig, J., Colic, M., Parker, R., and Filipowicz, W. (2011). miRNA repression involves GW182-mediated recruitment of CCR4-NOT through conserved W-containing motifs. Nat Struct Mol Biol *18*, 1218-1226.

Chen, B.R., Cheng, H.H., Lin, W.C., Wang, K.H., Liou, J.Y., Chen, P.F., and Wu, K.K. (2012). Quiescent fibroblasts are more active in mounting robust inflammatory responses than proliferative fibroblasts. PLoS One *7*, e49232.

Chen, Y.J., Dominguez-Brauer, C., Wang, Z., Asara, J.M., Costa, R.H., Tyner, A.L., Lau, L.F., and Raychaudhuri, P. (2009). A conserved phosphorylation site within the forkhead domain of FoxM1B is required for its activation by cyclin-CDK1. J Biol Chem *284*, 30695-30707.

Cho, S., Hoang, A., Sinha, R., Zhong, X.Y., Fu, X.D., Krainer, A.R., and Ghosh, G. (2011). Interaction between the RNA binding domains of Ser-Arg splicing factor 1 and U1-70K snRNP protein determines early spliceosome assembly. Proc Natl Acad Sci U S A *108*, 8233-8238.

Chou, M.Y., Rooke, N., Turck, C.W., and Black, D.L. (1999). hnRNP H is a component of a splicing enhancer complex that activates a c-src alternative exon in neuronal cells. Mol Cell Biol *19*, 69-77.

Chou, Z.F., Chen, F., and Wilusz, J. (1994). Sequence and position requirements for uridylate-rich downstream elements of polyadenylation signals. Nucleic Acids Res *22*, 2525-2531.

Chow, C.M., Georgiou, A., Szutorisz, H., Maia e Silva, A., Pombo, A., Barahona, I., Dargelos, E., Canzonetta, C., and Dillon, N. (2005). Variant histone H3.3 marks promoters of transcriptionally active genes during mammalian cell division. EMBO Rep *6*, 354-360.

Cinamon, G., Zachariah, M.A., Lam, O.M., Foss, F.W., Jr., and Cyster, J.G. (2008). Follicular shuttling of marginal zone B cells facilitates antigen transport. Nat Immunol *9*, 54-62.

Clapier, C.R., and Cairns, B.R. (2009). The biology of chromatin remodeling complexes. Annu Rev Biochem *78*, 273-304.

Collart, M.A., and Struhl, K. (1994). NOT1(CDC39), NOT2(CDC36), NOT3, and NOT4 encode a global-negative regulator of transcription that differentially affects TATA-element utilization. Genes Dev *8*, 525-537.

Coller, H.A., Sang, L., and Roberts, J.M. (2006). A new description of cellular quiescence. PLoS Biol *4*, e83.

Cong, R., Das, S., Ugrinova, I., Kumar, S., Mongelard, F., Wong, J., and Bouvet, P. (2012). Interaction of nucleolin with ribosomal RNA genes and its role in RNA polymerase I transcription. Nucleic Acids Res *40*, 9441-9454.

Connell-Crowley, L., Harper, J.W., and Goodrich, D.W. (1997). Cyclin D1/Cdk4 regulates retinoblastoma protein-mediated cell cycle arrest by site-specific phosphorylation. Mol Biol Cell *8*, 287-301.

Corden, J.L. (2007). Transcription. Seven ups the code. Science *318*, 1735-1736.

Cordin, O., and Beggs, J.D. (2013). RNA helicases in splicing. RNA Biol *10*, 83-95.

Costanzi, C., and Pehrson, J.R. (1998). Histone macroH2A1 is concentrated in the inactive X chromosome of female mammals. Nature *393*, 599-601.

D'Avino, P.P., Savoian, M.S., and Glover, D.M. (2005). Cleavage furrow formation and ingression during animal cytokinesis: a microtubule legacy. J Cell Sci *118*, 1549-1558.

Dantonel, J.C., Murthy, K.G., Manley, J.L., and Tora, L. (1997). Transcription factor TFIID recruits factor CPSF for formation of 3' end of mRNA. Nature *389*, 399-402.

Davidson, L., Kerr, A., and West, S. (2012). Co-transcriptional degradation of aberrant pre-mRNA by Xrn2. EMBO J *31*, 2566-2578.

De Keersmaecker, K., Atak, Z.K., Li, N., Vicente, C., Patchett, S., Girardi, T., Gianfelici, V., Geerdens, E., Clappier, E., Porcu, M.*, et al.* (2013). Exome sequencing identifies mutation in CNOT3 and ribosomal genes RPL5 and RPL10 in T-cell acute lymphoblastic leukemia. Nat Genet *45*, 186-190.

de la Mata, M., and Kornblihtt, A.R. (2006). RNA polymerase II C-terminal domain mediates regulation of alternative splicing by SRp20. Nat Struct Mol Biol *13*, 973-980.

de Vries, H., Ruegsegger, U., Hubner, W., Friedlein, A., Langen, H., and Keller, W. (2000). Human pre-mRNA cleavage factor II(m) contains homologs of yeast proteins and bridges two other cleavage factors. EMBO J *19*, 5895-5904.

Deaton, A.M., and Bird, A. (2011). CpG islands and the regulation of transcription. Genes Dev *25*, 1010-1022.

Defranco, A.L., Raveche, E.S., Asofsky, R., and Paul, W.E. (1982). Frequency of B lymphocytes responsive to anti-immunoglobulin. J Exp Med *155*, 1523-1536.

Dehay, C., and Kennedy, H. (2007). Cell-cycle control and cortical development. Nat Rev Neurosci *8*, 438-450.

Delogu, A., Schebesta, A., Sun, Q., Aschenbrenner, K., Perlot, T., and Busslinger, M. (2006). Gene repression by Pax5 in B cells is essential for blood cell homeostasis and is reversed in plasma cells. Immunity *24*, 269-281.

Dias, S., Mansson, R., Gurbuxani, S., Sigvardsson, M., and Kee, B.L. (2008). E2A proteins promote development of lymphoid-primed multipotent progenitors. Immunity *29*, 217-227.

Doma, M.K., and Parker, R. (2006). Endonucleolytic cleavage of eukaryotic mRNAs with stalls in translation elongation. Nature *440*, 561-564.

Earnshaw, W.C., and Cooke, C.A. (1991). Analysis of the distribution of the INCENPs throughout mitosis reveals the existence of a pathway of structural changes in the chromosomes during metaphase and early events in cleavage furrow formation. J Cell Sci *98 (Pt 4)*, 443-461.

Emami, K.H., Jain, A., and Smale, S.T. (1997). Mechanism of synergy between TATA and initiator: synergistic binding of TFIID following a putative TFIIA-induced isomerization. Genes Dev *11*, 3007-3019.

Erard, M.S., Belenguer, P., Caizergues-Ferrer, M., Pantaloni, A., and Amalric, F. (1988). A major nucleolar protein, nucleolin, induces chromatin decondensation by binding to histone H1. Eur J Biochem *175*, 525-530.

Esnault, C., Ghavi-Helm, Y., Brun, S., Soutourina, J., Van Berkum, N., Boschiero, C., Holstege, F., and Werner, M. (2008). Mediator-dependent recruitment of TFIIH modules in preinitiation complex. Mol Cell *31*, 337-346.

Evans, T., Rosenthal, E.T., Youngblom, J., Distel, D., and Hunt, T. (1983). Cyclin: a protein specified by maternal mRNA in sea urchin eggs that is destroyed at each cleavage division. Cell *33*, 389-396.

Ferri, F., Bouzinba-Segard, H., Velasco, G., Hube, F., and Francastel, C. (2009). Non-coding murine centromeric transcripts associate with and potentiate Aurora B kinase. Nucleic Acids Res *37*, 5071-5080.

Frangini, A., Sjoberg, M., Roman-Trufero, M., Dharmalingam, G., Haberle, V., Bartke, T., Lenhard, B., Malumbres, M., Vidal, M., and Dillon, N. (2013). The aurora B kinase and the polycomb protein ring1B combine to regulate active promoters in quiescent lymphocytes. Mol Cell *51*, 647-661.

Frischmeyer, P.A., van Hoof, A., O'Donnell, K., Guerrerio, A.L., Parker, R., and Dietz, H.C. (2002). An mRNA surveillance mechanism that eliminates transcripts lacking termination codons. Science *295*, 2258-2261.

Garapaty, S., Mahajan, M.A., and Samuels, H.H. (2008). Components of the CCR4-NOT complex function as nuclear hormone receptor coactivators via association with the NRC-interacting Factor NIF-1. J Biol Chem *283*, 6806-6816.

Garneau, N.L., Wilusz, J., and Wilusz, C.J. (2007). The highways and byways of mRNA decay. Nat Rev Mol Cell Biol *8*, 113-126.

Glotzer, M. (2009). The 3Ms of central spindle assembly: microtubules, motors and MAPs. Nat Rev Mol Cell Biol *10*, 9-20.

Glynne, R., Ghandour, G., Rayner, J., Mack, D.H., and Goodnow, C.C. (2000). B-lymphocyte quiescence, tolerance and activation as viewed by global gene expression profiling on microarrays. Immunol Rev *176*, 216-246.

Goldstrohm, A.C., and Wickens, M. (2008). Multifunctional deadenylase complexes diversify mRNA control. Nat Rev Mol Cell Biol *9*, 337-344.

Goodnow, C.C., Vinuesa, C.G., Randall, K.L., Mackay, F., and Brink, R. (2010). Control systems and decision making for antibody production. Nat Immunol *11*, 681-688.

Goto, H., Yasui, Y., Kawajiri, A., Nigg, E.A., Terada, Y., Tatsuka, M., Nagata, K., and Inagaki, M. (2003). Aurora-B regulates the cleavage furrow-specific vimentin phosphorylation in the cytokinetic process. J Biol Chem *278*, 8526-8530.

Grummt, I. (2003). Life on a planet of its own: regulation of RNA polymerase I transcription in the nucleolus. Genes Dev *17*, 1691-1702.

Gu, B., Eick, D., and Bensaude, O. (2013). CTD serine-2 plays a critical role in splicing and termination factor recruitment to RNA polymerase II in vivo. Nucleic Acids Res *41*, 1591-1603.

Gully, C.P., Velazquez-Torres, G., Shin, J.H., Fuentes-Mattei, E., Wang, E., Carlock, C., Chen, J., Rothenberg, D., Adams, H.P., Choi, H.H.*, et al.* (2012). Aurora B kinase phosphorylates and instigates degradation of p53. Proc Natl Acad Sci U S A *109*, E1513-1522.

Gupta, N., and DeFranco, A.L. (2007). Lipid rafts and B cell signaling. Semin Cell Dev Biol *18*, 616-626.

Hall, J.A., and Georgel, P.T. (2007). CHD proteins: a diverse family with strong ties. Biochem Cell Biol *85*, 463-476.

Han, S.P., Tang, Y.H., and Smith, R. (2010). Functional diversity of the hnRNPs: past, present and perspectives. Biochem J *430*, 379-392.

Hanakahi, L.A., Dempsey, L.A., Li, M.J., and Maizels, N. (1997). Nucleolin is one component of the B cell-specific transcription factor and switch region binding protein, LR1. Proc Natl Acad Sci U S A *94*, 3605-3610.

Happel, N., and Doenecke, D. (2009). Histone H1 and its isoforms: contribution to chromatin structure and function. Gene *431*, 1-12.

Harbour, J.W., Luo, R.X., Dei Santi, A., Postigo, A.A., and Dean, D.C. (1999). Cdk phosphorylation triggers sequential intramolecular interactions that progressively block Rb functions as cells move through G1. Cell *98*, 859-869.

Harper, J.W., Adami, G.R., Wei, N., Keyomarsi, K., and Elledge, S.J. (1993). The p21 Cdk-interacting protein Cip1 is a potent inhibitor of G1 cyclin-dependent kinases. Cell *75*, 805-816.

Hertz, M., and Nemazee, D. (1997). BCR ligation induces receptor editing in IgM+IgD- bone marrow B cells in vitro. Immunity *6*, 429-436.

Hirota, T., Lipp, J.J., Toh, B.H., and Peters, J.M. (2005). Histone H3 serine 10 phosphorylation by Aurora B causes HP1 dissociation from heterochromatin. Nature *438*, 1176-1180.

Honda, R., Korner, R., and Nigg, E.A. (2003). Exploring the functional interactions between Aurora B, INCENP, and survivin in mitosis. Mol Biol Cell *14*, 3325-3341.

Hu, G., Kim, J., Xu, Q., Leng, Y., Orkin, S.H., and Elledge, S.J. (2009). A genome-wide RNAi screen identifies a new transcriptional module required for self-renewal. Genes Dev *23*, 837-848.

Igarashi, H., Gregory, S.C., Yokota, T., Sakaguchi, N., and Kincade, P.W. (2002). Transcription from the RAG1 locus marks the earliest lymphocyte progenitors in bone marrow. Immunity *17*, 117-130.

Ip, J.Y., Schmidt, D., Pan, Q., Ramani, A.K., Fraser, A.G., Odom, D.T., and Blencowe, B.J. (2011). Global impact of RNA polymerase II elongation inhibition on alternative splicing regulation. Genome Res *21*, 390-401.

Ito, K., Inoue, T., Yokoyama, K., Morita, M., Suzuki, T., and Yamamoto, T. (2011). CNOT2 depletion disrupts and inhibits the CCR4-NOT deadenylase complex and induces apoptotic cell death. Genes Cells *16*, 368-379.

Izaurralde, E., Lewis, J., McGuigan, C., Jankowska, M., Darzynkiewicz, E., and Mattaj, I.W. (1994). A nuclear cap binding protein complex involved in pre-mRNA splicing. Cell *78*, 657-668.

Jambhekar, A., Emerman, A.B., Schweidenback, C.T., and Blower, M.D. (2014). RNA Stimulates Aurora B Kinase Activity during Mitosis. PLoS One *9*, e100748.

Jang, M.K., Mochizuki, K., Zhou, M., Jeong, H.S., Brady, J.N., and Ozato, K. (2005). The bromodomain protein Brd4 is a positive regulatory component of P-TEFb and stimulates RNA polymerase II-dependent transcription. Mol Cell *19*, 523-534.

Jayne, S., Zwartjes, C.G., van Schaik, F.M., and Timmers, H.T. (2006). Involvement of the SMRT/NCoR-HDAC3 complex in transcriptional repression by the CNOT2 subunit of the human Ccr4-Not complex. Biochem J *398*, 461-467.

Jiang, C., and Pugh, B.F. (2009). Nucleosome positioning and gene regulation: advances through genomics. Nat Rev Genet *10*, 161-172.

Jin, C., Zang, C., Wei, G., Cui, K., Peng, W., Zhao, K., and Felsenfeld, G. (2009). H3.3/H2A.Z double variant-containing nucleosomes mark 'nucleosome-free regions' of active promoters and other regulatory regions. Nat Genet *41*, 941-945.

Jones, C.I., and Newbury, S.F. (2010). Functions of microRNAs in Drosophila development. Biochem Soc Trans *38*, 1137-1143.

Jothi, R., Cuddapah, S., Barski, A., Cui, K., and Zhao, K. (2008). Genome-wide identification of in vivo protein-DNA binding sites from ChIP-Seq data. Nucleic Acids Res *36*, 5221-5231.

Kamieniarz, K., Izzo, A., Dundr, M., Tropberger, P., Ozretic, L., Kirfel, J., Scheer, E., Tropel, P., Wisniewski, J.R., Tora, L.*, et al.* (2012). A dual role of linker histone H1.4 Lys 34 acetylation in transcriptional activation. Genes Dev *26*, 797-802.

Kamon, M., Katano, M., Hiraki-Kamon, K., Hishida, T., Nakachi, Y., Mizuno, Y., Okazaki, Y., Suzuki, A., Hirasaki, M., Ueda, A.*, et al.* (2014). Identification of ccr4-not complex components as regulators of transition from partial to genuine induced pluripotent stem cells. Stem Cells Dev *23*, 2170-2179.

Kashima, I., Yamashita, A., Izumi, N., Kataoka, N., Morishita, R., Hoshino, S., Ohno, M., Dreyfuss, G., and Ohno, S. (2006). Binding of a novel SMG-1-Upf1-eRF1-eRF3 complex (SURF) to the exon junction complex triggers Upf1 phosphorylation and nonsense-mediated mRNA decay. Genes Dev *20*, 355-367.

Kaufmann, I., Martin, G., Friedlein, A., Langen, H., and Keller, W. (2004). Human Fip1 is a subunit of CPSF that binds to U-rich RNA elements and stimulates poly(A) polymerase. EMBO J *23*, 616-626.

Keller, W., Bienroth, S., Lang, K.M., and Christofori, G. (1991). Cleavage and polyadenylation factor CPF specifically interacts with the pre-mRNA 3' processing signal AAUAAA. EMBO J *10*, 4241-4249.

Kelly, A.E., and Funabiki, H. (2009). Correcting aberrant kinetochore microtubule attachments: an Aurora B-centric view. Curr Opin Cell Biol *21*, 51-58.

Kerr, S.C., Azzouz, N., Fuchs, S.M., Collart, M.A., Strahl, B.D., Corbett, A.H., and Laribee, R.N. (2011). The Ccr4-Not complex interacts with the mRNA export machinery. PLoS One *6*, e18302.

Khanna, R., and Kiledjian, M. (2004). Poly(A)-binding-protein-mediated regulation of hDcp2 decapping in vitro. EMBO J *23*, 1968-1976.

Kieffer-Kwon, K.R., Tang, Z., Mathe, E., Qian, J., Sung, M.H., Li, G., Resch, W., Baek, S., Pruett, N., Grontved, L.*, et al.* (2013). Interactome maps of mouse gene regulatory domains reveal basic principles of transcriptional regulation. Cell *155*, 1507-1520.

Kim, J., Guermah, M., and Roeder, R.G. (2010). The human PAF1 complex acts in chromatin transcription elongation both independently and cooperatively with SII/TFIIS. Cell *140*, 491-503.

Kimura, M., Ishiguro, A., and Ishihama, A. (1997). RNA polymerase II subunits 2, 3, and 11 form a core subassembly with DNA binding activity. J Biol Chem *272*, 25851-25855.

Kimura, M., Uchida, C., Takano, Y., Kitagawa, M., and Okano, Y. (2004). Cell cycle-dependent regulation of the human aurora B promoter. Biochem Biophys Res Commun *316*, 930-936.

Koodathingal, P., Novak, T., Piccirilli, J.A., and Staley, J.P. (2010). The DEAH box ATPases Prp16 and Prp43 cooperate to proofread 5' splice site cleavage during pre-mRNA splicing. Mol Cell *39*, 385-395.

Kornblihtt, A.R., Schor, I.E., Allo, M., Dujardin, G., Petrillo, E., and Munoz, M.J. (2013). Alternative splicing: a pivotal step between eukaryotic transcription and translation. Nat Rev Mol Cell Biol *14*, 153-165.

Kouzarides, T. (2007). Chromatin modifications and their function. Cell *128*, 693-705.

Kovesdi, D., Bell, S.E., and Turner, M. (2010). The development of mature B lymphocytes requires the combined function of CD19 and the p110delta subunit of PI3K. Self Nonself *1*, 144-153.

Kramer, A., and Utans, U. (1991). Three protein factors (SF1, SF3 and U2AF) function in pre-splicing complex formation in addition to snRNPs. EMBO J *10*, 1503-1509.

Krokan, H., Wist, E., and Krokan, R.H. (1981). Aphidicolin inhibits DNA synthesis by DNA polymerase alpha and isolated nuclei by a similar mechanism. Nucleic Acids Res *9*, 4709-4719.

Kruk, J.A., Dutta, A., Fu, J., Gilmour, D.S., and Reese, J.C. (2011). The multifunctional Ccr4-Not complex directly promotes transcription elongation. Genes Dev *25*, 581-593.

Kuehner, J.N., Pearson, E.L., and Moore, C. (2011). Unravelling the means to an end: RNA polymerase II transcription termination. Nat Rev Mol Cell Biol *12*, 283-294.

Kuhn, A.N., Li, Z., and Brow, D.A. (1999). Splicing factor Prp8 governs U4/U6 RNA unwinding during activation of the spliceosome. Mol Cell *3*, 65-75.

Kuhn, U., Gundel, M., Knoth, A., Kerwitz, Y., Rudel, S., and Wahle, E. (2009). Poly(A) tail length is controlled by the nuclear poly(A)-binding protein regulating the interaction between poly(A) polymerase and the cleavage and polyadenylation specificity factor. J Biol Chem *284*, 22803-22814.

Kulkarni, M., Ozgur, S., and Stoecklin, G. (2010). On track with P-bodies. Biochem Soc Trans *38*, 242-251.

Kumari, G., Ulrich, T., Krause, M., Finkernagel, F., and Gaubatz, S. (2014). Induction of p21CIP1 Protein and Cell Cycle Arrest after Inhibition of Aurora B Kinase Is Attributed to Aneuploidy and Reactive Oxygen Species. J Biol Chem *289*, 16072-16084.

Kupfer, H., Monks, C.R., and Kupfer, A. (1994). Small splenic B cells that bind to antigen-specific T helper (Th) cells and face the site of cytokine production in the Th cells selectively proliferate: immunofluorescence microscopic studies of Th-B antigen-presenting cell interactions. J Exp Med *179*, 1507-1515.

Lagrange, T., Kapanidis, A.N., Tang, H., Reinberg, D., and Ebright, R.H. (1998). New core promoter element in RNA polymerase II-dependent transcription: sequence-specific DNA binding by transcription factor IIB. Genes Dev *12*, 34-44.

Lampson, M.A., Renduchitala, K., Khodjakov, A., and Kapoor, T.M. (2004). Correcting improper chromosome-spindle attachments during cell division. Nat Cell Biol *6*, 232-237.

Langst, G., and Becker, P.B. (2001). Nucleosome mobilization and positioning by ISWI-containing chromatin-remodeling factors. J Cell Sci *114*, 2561-2568.

Laoukili, J., Alvarez, M., Meijer, L.A., Stahl, M., Mohammed, S., Kleij, L., Heck, A.J., and Medema, R.H. (2008). Activation of FoxM1 during G2 requires cyclin A/Cdk-dependent relief of autorepression by the FoxM1 N-terminal domain. Mol Cell Biol *28*, 3076-3087.

Lardelli, R.M., Thompson, J.X., Yates, J.R., 3rd, and Stevens, S.W. (2010). Release of SF3 from the intron branchpoint activates the first step of pre-mRNA splicing. RNA *16*, 516-528.

Laribee, R.N., Shibata, Y., Mersman, D.P., Collins, S.R., Kemmeren, P., Roguev, A., Weissman, J.S., Briggs, S.D., Krogan, N.J., and Strahl, B.D. (2007). CCR4/NOT complex associates with the proteasome and regulates histone methylation. Proc Natl Acad Sci U S A *104*, 5836-5841.

Lau, N.C., Kolkman, A., van Schaik, F.M., Mulder, K.W., Pijnappel, W.W., Heck, A.J., and Timmers, H.T. (2009). Human Ccr4-Not complexes contain variable deadenylase subunits. Biochem J *422*, 443-453.

Le Hir, H., Izaurralde, E., Maquat, L.E., and Moore, M.J. (2000). The spliceosome deposits multiple proteins 20-24 nucleotides upstream of mRNA exon-exon junctions. EMBO J *19*, 6860-6869.

Levine, M. (2011). Paused RNA polymerase II as a developmental checkpoint. Cell *145*, 502-511.

Lewis, J.D., and Izaurralde, E. (1997). The role of the cap structure in RNA processing and nuclear export. Eur J Biochem *247*, 461-469.

Li, X., and Nicklas, R.B. (1995). Mitotic forces control a cell-cycle checkpoint. Nature *373*, 630-632.

Lim, S., and Kaldis, P. (2013). Cdks, cyclins and CKIs: roles beyond cell cycle regulation. Development *140*, 3079-3093.

Liu, H.Y., Badarinarayana, V., Audino, D.C., Rappsilber, J., Mann, M., and Denis, C.L. (1998). The NOT proteins are part of the CCR4 transcriptional complex and affect gene expression both positively and negatively. EMBO J *17*, 1096-1106.

Long, J.C., and Caceres, J.F. (2009). The SR protein family of splicing factors: master regulators of gene expression. Biochem J *417*, 15-27.

Luger, K., Mader, A.W., Richmond, R.K., Sargent, D.F., and Richmond, T.J. (1997). Crystal structure of the nucleosome core particle at 2.8 A resolution. Nature *389*, 251-260.

Luke, B., Panza, A., Redon, S., Iglesias, N., Li, Z., and Lingner, J. (2008). The Rat1p 5' to 3' exonuclease degrades telomeric repeat-containing RNA and promotes telomere elongation in Saccharomyces cerevisiae. Mol Cell *32*, 465-477.

Lykke-Andersen, J., and Wagner, E. (2005). Recruitment and activation of mRNA decay enzymes by two ARE-mediated decay activation domains in the proteins TTP and BRF-1. Genes Dev *19*, 351-361.

Major, M.L., Lepe, R., and Costa, R.H. (2004). Forkhead box M1B transcriptional activity requires binding of Cdk-cyclin complexes for phosphorylation-dependent recruitment of p300/CBP coactivators. Mol Cell Biol *24*, 2649-2661.

Mandal, S.S., Chu, C., Wada, T., Handa, H., Shatkin, A.J., and Reinberg, D. (2004). Functional interactions of RNA-capping enzyme with factors that positively and negatively regulate promoter escape by RNA polymerase II. Proc Natl Acad Sci U S A *101*, 7572-7577.

Mandel, C.R., Bai, Y., and Tong, L. (2008). Protein factors in pre-mRNA 3'-end processing. Cell Mol Life Sci *65*, 1099-1122.

Martensson, I.L., Keenan, R.A., and Licence, S. (2007). The pre-B-cell receptor. Curr Opin Immunol *19*, 137-142.

Martin, A., Schneider, S., and Schwer, B. (2002). Prp43 is an essential RNA-dependent ATPase required for release of lariat-intron from the spliceosome. J Biol Chem *277*, 17743-17750.

Martin, F., and Kearney, J.F. (2000). B-cell subsets and the mature preimmune repertoire. Marginal zone and B1 B cells as part of a "natural immune memory". Immunol Rev *175*, 70-79.

Matson, D.R., and Stukenberg, P.T. (2014). CENP-I and Aurora B act as a molecular switch that ties RZZ/Mad1 recruitment to kinetochore attachment status. J Cell Biol *205*, 541-554.

Mauxion, F., Preve, B., and Seraphin, B. (2013). C2ORF29/CNOT11 and CNOT10 form a new module of the CCR4-NOT complex. RNA Biol *10*, 267-276.

Maxon, M.E., Goodrich, J.A., and Tjian, R. (1994). Transcription factor IIE binds preferentially to RNA polymerase IIa and recruits TFIIH: a model for promoter clearance. Genes Dev *8*, 515-524.

Mayas, R.M., Maita, H., and Staley, J.P. (2006). Exon ligation is proofread by the DExD/H-box ATPase Prp22p. Nat Struct Mol Biol *13*, 482-490.

Mayer, A., Heidemann, M., Lidschreiber, M., Schreieck, A., Sun, M., Hintermair, C., Kremmer, E., Eick, D., and Cramer, P. (2012). CTD tyrosine phosphorylation impairs termination factor recruitment to RNA polymerase II. Science *336*, 1723-1725.

McHeyzer-Williams, M.G., and Ahmed, R. (1999). B cell memory and the long-lived plasma cell. Curr Opin Immunol *11*, 172-179.

McLean, C.Y., Bristor, D., Hiller, M., Clarke, S.L., Schaar, B.T., Lowe, C.B., Wenger, A.M., and Bejerano, G. (2010). GREAT improves functional interpretation of cis-regulatory regions. Nat Biotechnol *28*, 495-501.

Michaud, S., and Reed, R. (1993). A functional association between the 5' and 3' splice site is established in the earliest prespliceosome complex (E) in mammals. Genes Dev *7*, 1008-1020.

Miller, A.L. (2011). The contractile ring. Curr Biol *21*, R976-978.

Minoshima, Y., Kawashima, T., Hirose, K., Tonozuka, Y., Kawajiri, A., Bao, Y.C., Deng, X., Tatsuka, M., Narumiya, S., May, W.S., Jr*., et al.* (2003). Phosphorylation by aurora B converts MgcRacGAP to a RhoGAP during cytokinesis. Dev Cell *4*, 549-560.

Mitchell, P., Petfalski, E., Shevchenko, A., Mann, M., and Tollervey, D. (1997). The exosome: a conserved eukaryotic RNA processing complex containing multiple 3'-->5' exoribonucleases. Cell *91*, 457-466.

Mittal, S., Aslam, A., Doidge, R., Medica, R., and Winkler, G.S. (2011). The Ccr4a (CNOT6) and Ccr4b (CNOT6L) deadenylase subunits of the human Ccr4-Not complex contribute to the prevention of cell death and senescence. Mol Biol Cell *22*, 748-758.

Mizuguchi, G., Tsukiyama, T., Wisniewski, J., and Wu, C. (1997). Role of nucleosome remodeling factor NURF in transcriptional activation of chromatin. Mol Cell *1*, 141-150.

Moore, M.J., and Sharp, P.A. (1993). Evidence for two active sites in the spliceosome provided by stereochemistry of pre-mRNA splicing. Nature *365*, 364-368.

Morel, A.P., Sentis, S., Bianchin, C., Le Romancer, M., Jonard, L., Rostan, M.C., Rimokh, R., and Corbo, L. (2003). BTG2 antiproliferative protein interacts with

the human CCR4 complex existing in vivo in three cell-cycle-regulated forms. J Cell Sci *116*, 2929-2936.

Morita, M., Oike, Y., Nagashima, T., Kadomatsu, T., Tabata, M., Suzuki, T., Nakamura, T., Yoshida, N., Okada, M., and Yamamoto, T. (2011). Obesity resistance and increased hepatic expression of catabolism-related mRNAs in Cnot3+/- mice. EMBO J *30*, 4678-4691.

Morita, M., Suzuki, T., Nakamura, T., Yokoyama, K., Miyasaka, T., and Yamamoto, T. (2007). Depletion of mammalian CCR4b deadenylase triggers elevation of the p27Kip1 mRNA level and impairs cell growth. Mol Cell Biol *27*, 4980-4990.

Morris, L., Allen, K.E., and La Thangue, N.B. (2000). Regulation of E2F transcription by cyclin E-Cdk2 kinase mediated through p300/CBP co-activators. Nat Cell Biol *2*, 232-239.

Murray, A.W., and Kirschner, M.W. (1989). Cyclin synthesis drives the early embryonic cell cycle. Nature *339*, 275-280.

Musacchio, A., and Salmon, E.D. (2007). The spindle-assembly checkpoint in space and time. Nat Rev Mol Cell Biol *8*, 379-393.

Nag, A., Narsinh, K., and Martinson, H.G. (2007). The poly(A)-dependent transcriptional pause is mediated by CPSF acting on the body of the polymerase. Nat Struct Mol Biol *14*, 662-669.

Nair, J.S., Ho, A.L., Tse, A.N., Coward, J., Cheema, H., Ambrosini, G., Keen, N., and Schwartz, G.K. (2009). Aurora B kinase regulates the postmitotic endoreduplication checkpoint via phosphorylation of the retinoblastoma protein at serine 780. Mol Biol Cell *20*, 2218-2228.

Nakamura, T., Yao, R., Ogawa, T., Suzuki, T., Ito, C., Tsunekawa, N., Inoue, K., Ajima, R., Miyasaka, T., Yoshida, Y.*, et al.* (2004). Oligo-astheno-teratozoospermia in mice lacking Cnot7, a regulator of retinoid X receptor beta. Nat Genet *36*, 528-533.

Nakayama, K.I., and Nakayama, K. (2006). Ubiquitin ligases: cell-cycle control and cancer. Nat Rev Cancer *6*, 369-381.

Neely, G.G., Kuba, K., Cammarato, A., Isobe, K., Amann, S., Zhang, L., Murata, M., Elmen, L., Gupta, V., Arora, S.*, et al.* (2010). A global in vivo Drosophila RNAi screen identifies NOT3 as a conserved regulator of heart function. Cell *141*, 142-153.

Nguyen, V.T., Kiss, T., Michels, A.A., and Bensaude, O. (2001). 7SK small nuclear RNA binds to and inhibits the activity of CDK9/cyclin T complexes. Nature *414*, 322-325.

Niiro, H., and Clark, E.A. (2002). Regulation of B-cell fate by antigen-receptor signals. Nat Rev Immunol *2*, 945-956.

Nikolov, D.B., and Burley, S.K. (1997). RNA polymerase II transcription initiation: a structural view. Proc Natl Acad Sci U S A *94*, 15-22.

Noelle, R.J., and Snow, E.C. (1991). T helper cell-dependent B cell activation. FASEB J *5*, 2770-2776.

Nutt, S.L., and Kee, B.L. (2007). The transcriptional regulation of B cell lineage commitment. Immunity *26*, 715-725.

Oki, T., Nishimura, K., Kitaura, J., Togami, K., Maehara, A., Izawa, K., Sakaue-Sawano, A., Niida, A., Miyano, S., Aburatani, H.*, et al.* (2014). A novel cell-cycle-indicator, mVenus-p27K-, identifies quiescent cells and visualizes G0-G1 transition. Sci Rep *4*, 4012.

Orphanides, G., Lagrange, T., and Reinberg, D. (1996). The general transcription factors of RNA polymerase II. Genes Dev *10*, 2657-2683.

Pan, Q., Shai, O., Lee, L.J., Frey, B.J., and Blencowe, B.J. (2008). Deep surveying of alternative splicing complexity in the human transcriptome by high-throughput sequencing. Nat Genet *40*, 1413-1415.

Papamichos-Chronakis, M., Watanabe, S., Rando, O.J., and Peterson, C.L. (2011). Global regulation of H2A.Z localization by the INO80 chromatin-remodeling enzyme is essential for genome integrity. Cell *144*, 200-213.

Pardee, A.B. (1974). A restriction point for control of normal animal cell proliferation. Proc Natl Acad Sci U S A *71*, 1286-1290.

Paull, T.T., Rogakou, E.P., Yamazaki, V., Kirchgessner, C.U., Gellert, M., and Bonner, W.M. (2000). A critical role for histone H2AX in recruitment of repair factors to nuclear foci after DNA damage. Curr Biol *10*, 886-895.

Pavletich, N.P. (1999). Mechanisms of cyclin-dependent kinase regulation: structures of Cdks, their cyclin activators, and Cip and INK4 inhibitors. J Mol Biol *287*, 821-828.

Peterlin, B.M., and Price, D.H. (2006). Controlling the elongation phase of transcription with P-TEFb. Mol Cell *23*, 297-305.

Pierce, S.K. (2002). Lipid rafts and B-cell activation. Nat Rev Immunol *2*, 96-105.

Pillai, S., and Cariappa, A. (2009). The follicular versus marginal zone B lymphocyte cell fate decision. Nat Rev Immunol *9*, 767-777.

Pinol-Roma, S., and Dreyfuss, G. (1992). Shuttling of pre-mRNA binding proteins between nucleus and cytoplasm. Nature *355*, 730-732.

Poltorak, A., He, X., Smirnova, I., Liu, M.Y., Van Huffel, C., Du, X., Birdwell, D., Alejos, E., Silva, M., Galanos, C.*, et al.* (1998). Defective LPS signaling in C3H/HeJ and C57BL/10ScCr mice: mutations in Tlr4 gene. Science *282*, 2085-2088.

Prelich, G., Tan, C.K., Kostura, M., Mathews, M.B., So, A.G., Downey, K.M., and Stillman, B. (1987). Functional identity of proliferating cell nuclear antigen and a DNA polymerase-delta auxiliary protein. Nature *326*, 517-520.

Proudfoot, N.J. (2011). Ending the message: poly(A) signals then and now. Genes Dev *25*, 1770-1782.

Pugh, B.F., and Tjian, R. (1991). Transcription from a TATA-less promoter requires a multisubunit TFIID complex. Genes Dev *5*, 1935-1945.

Raghunathan, P.L., and Guthrie, C. (1998). RNA unwinding in U4/U6 snRNPs requires ATP hydrolysis and the DEIH-box splicing factor Brr2. Curr Biol *8*, 847-855.

Ramanathan, Y., Rajpara, S.M., Reza, S.M., Lees, E., Shuman, S., Mathews, M.B., and Pe'ery, T. (2001). Three RNA polymerase II carboxyl-terminal domain kinases display distinct substrate preferences. J Biol Chem *276*, 10913-10920.

Ramirez-Carrozzi, V.R., Braas, D., Bhatt, D.M., Cheng, C.S., Hong, C., Doty, K.R., Black, J.C., Hoffmann, A., Carey, M., and Smale, S.T. (2009). A unifying model for the selective regulation of inducible transcription by CpG islands and nucleosome remodeling. Cell *138*, 114-128.

Resnick, J.L., Bixler, L.S., Cheng, L., and Donovan, P.J. (1992). Long-term proliferation of mouse primordial germ cells in culture. Nature *359*, 550-551.

Robinson, P.J., and Rhodes, D. (2006). Structure of the '30 nm' chromatin fibre: a key role for the linker histone. Curr Opin Struct Biol *16*, 336-343.

Rocak, S., and Linder, P. (2004). DEAD-box proteins: the driving forces behind RNA metabolism. Nat Rev Mol Cell Biol *5*, 232-241.

Ruchaud, S., Carmena, M., and Earnshaw, W.C. (2007). Chromosomal passengers: conducting cell division. Nat Rev Mol Cell Biol *8*, 798-812.

Ryan, K., Calvo, O., and Manley, J.L. (2004). Evidence that polyadenylation factor CPSF-73 is the mRNA 3' processing endonuclease. RNA *10*, 565-573.

Sainsbury, S., Niesser, J., and Cramer, P. (2013). Structure and function of the initially transcribing RNA polymerase II-TFIIB complex. Nature *493*, 437-440.

Sampath, S.C., Ohi, R., Leismann, O., Salic, A., Pozniakovski, A., and Funabiki, H. (2004). The chromosomal passenger complex is required for chromatin-induced microtubule stabilization and spindle assembly. Cell *118*, 187-202.

Santos-Rosa, H., Schneider, R., Bannister, A.J., Sherriff, J., Bernstein, B.E., Emre, N.C., Schreiber, S.L., Mellor, J., and Kouzarides, T. (2002). Active genes are tri-methylated at K4 of histone H3. Nature *419*, 407-411.

Sarma, K., and Reinberg, D. (2005). Histone variants meet their match. Nat Rev Mol Cell Biol *6*, 139-149.

Schamel, W.W., and Reth, M. (2000). Monomeric and oligomeric complexes of the B cell antigen receptor. Immunity *13*, 5-14.

Schreieck, A., Easter, A.D., Etzold, S., Wiederhold, K., Lidschreiber, M., Cramer, P., and Passmore, L.A. (2014). RNA polymerase II termination involves C-terminal-domain tyrosine dephosphorylation by CPF subunit Glc7. Nat Struct Mol Biol *21*, 175-179.

Scott, D.W. (2011). Transduced B cells: B is for 'beneficial'! Eur J Immunol *41*, 1528-1530.

Semlow, D.R., and Staley, J.P. (2012). Staying on message: ensuring fidelity in pre-mRNA splicing. Trends Biochem Sci *37*, 263-273.

Serrano, M., Hannon, G.J., and Beach, D. (1993). A new regulatory motif in cell-cycle control causing specific inhibition of cyclin D/CDK4. Nature *366*, 704-707.

Shahhoseini, M., Favaedi, R., Baharvand, H., Sharma, V., and Stunnenberg, H.G. (2010). Evidence for a dynamic role of the linker histone variant H1x during retinoic acid-induced differentiation of NT2 cells. FEBS Lett *584*, 4661-4664.

Sisken, J.E., and Morasca, L. (1965). Intrapopulation Kinetics of the Mitotic Cycle. J Cell Biol *25*, 179-189.

Song, J., Salek-Ardakani, S., So, T., and Croft, M. (2007). The kinases aurora B and mTOR regulate the G1-S cell cycle progression of T lymphocytes. Nat Immunol *8*, 64-73.

Soucek, T., Pusch, O., Hengstschlager-Ottnad, E., Adams, P.D., and Hengstschlager, M. (1997). Deregulated expression of E2F-1 induces cyclin A- and E-associated kinase activities independently from cell cycle position. Oncogene *14*, 2251-2257.

Spencer, S.L., Cappell, S.D., Tsai, F.C., Overton, K.W., Wang, C.L., and Meyer, T. (2013). The proliferation-quiescence decision is controlled by a bifurcation in CDK2 activity at mitotic exit. Cell *155*, 369-383.

Staley, J.P., and Guthrie, C. (1999). An RNA switch at the 5' splice site requires ATP and the DEAD box protein Prp28p. Mol Cell *3*, 55-64.

Stead, E., White, J., Faast, R., Conn, S., Goldstone, S., Rathjen, J., Dhingra, U., Rathjen, P., Walker, D., and Dalton, S. (2002). Pluripotent cell division cycles are driven by ectopic Cdk2, cyclin A/E and E2F activities. Oncogene *21*, 8320-8333.

Stewart, S., and Fang, G. (2005). Destruction box-dependent degradation of aurora B is mediated by the anaphase-promoting complex/cyclosome and Cdh1. Cancer Res *65*, 8730-8735.

Su, Y., Zhang, A.H., Li, X., Owusu-Boaitey, N., Skupsky, J., and Scott, D.W. (2011). B cells "transduced" with TAT-fusion proteins can induce tolerance and protect mice from diabetes and EAE. Clin Immunol *140*, 260-267.

Sudarsanam, P., and Winston, F. (2000). The Swi/Snf family nucleosome-remodeling complexes and transcriptional control. Trends Genet *16*, 345-351.

Takagaki, Y., and Manley, J.L. (2000). Complex protein interactions within the human polyadenylation machinery identify a novel component. Mol Cell Biol *20*, 1515-1525.

Takagaki, Y., Ryner, L.C., and Manley, J.L. (1989). Four factors are required for 3'-end cleavage of pre-mRNAs. Genes Dev *3*, 1711-1724.

Takahashi, A., Kikuguchi, C., Morita, M., Shimodaira, T., Tokai-Nishizumi, N., Yokoyama, K., Ohsugi, M., Suzuki, T., and Yamamoto, T. (2012). Involvement of CNOT3 in mitotic progression through inhibition of MAD1 expression. Biochem Biophys Res Commun *419*, 268-273.

Takeda, K., and Akira, S. (2004). TLR signaling pathways. Semin Immunol *16*, 3-9.

Tanaka, T.U., Rachidi, N., Janke, C., Pereira, G., Galova, M., Schiebel, E., Stark, M.J., and Nasmyth, K. (2002). Evidence that the Ipl1-Sli15 (Aurora kinase-INCENP)

complex promotes chromosome bi-orientation by altering kinetochore-spindle pole connections. Cell *108*, 317-329.

Tardaguila, M., Gonzalez-Gugel, E., and Sanchez-Pacheco, A. (2011). Aurora kinase B activity is modulated by thyroid hormone during transcriptional activation of pituitary genes. Mol Endocrinol *25*, 385-393.

Terada, Y., Tatsuka, M., Suzuki, F., Yasuda, Y., Fujita, S., and Otsu, M. (1998). AIM-1: a mammalian midbody-associated protein required for cytokinesis. EMBO J *17*, 667-676.

Tirode, F., Busso, D., Coin, F., and Egly, J.M. (1999). Reconstitution of the transcription factor TFIIH: assignment of functions for the three enzymatic subunits, XPB, XPD, and cdk7. Mol Cell *3*, 87-95.

Tolstorukov, M.Y., Goldman, J.A., Gilbert, C., Ogryzko, V., Kingston, R.E., and Park, P.J. (2012). Histone variant H2A.Bbd is associated with active transcription and mRNA processing in human cells. Mol Cell *47*, 596-607.

Toyoshima, H., and Hunter, T. (1994). p27, a novel inhibitor of G1 cyclin-Cdk protein kinase activity, is related to p21. Cell *78*, 67-74.

Trakala, M., Fernandez-Miranda, G., Perez de Castro, I., Heeschen, C., and Malumbres, M. (2013). Aurora B prevents delayed DNA replication and premature mitotic exit by repressing p21(Cip1). Cell Cycle *12*, 1030-1041.

Turner, B.M., Birley, A.J., and Lavender, J. (1992). Histone H4 isoforms acetylated at specific lysine residues define individual chromosomes and chromatin domains in Drosophila polytene nuclei. Cell *69*, 375-384.

Valadkhan, S., and Manley, J.L. (2000). A tertiary interaction detected in a human U2-U6 snRNA complex assembled in vitro resembles a genetically proven interaction in yeast. RNA *6*, 206-219.

van Dijk, E., Cougot, N., Meyer, S., Babajko, S., Wahle, E., and Seraphin, B. (2002). Human Dcp2: a catalytically active mRNA decapping enzyme located in specific cytoplasmic structures. EMBO J *21*, 6915-6924.

van Dijk, E., Le Hir, H., and Seraphin, B. (2003). DcpS can act in the 5'-3' mRNA decay pathway in addition to the 3'-5' pathway. Proc Natl Acad Sci U S A *100*, 12081-12086.

Van Hooser, A.A., Ouspenski, II, Gregson, H.C., Starr, D.A., Yen, T.J., Goldberg, M.L., Yokomori, K., Earnshaw, W.C., Sullivan, K.F., and Brinkley, B.R. (2001).

Specification of kinetochore-forming chromatin by the histone H3 variant CENP-A. J Cell Sci *114*, 3529-3542.

Venturini, G., Rose, A.M., Shah, A.Z., Bhattacharya, S.S., and Rivolta, C. (2012). CNOT3 is a modifier of PRPF31 mutations in retinitis pigmentosa with incomplete penetrance. PLoS Genet *8*, e1003040.

Vernino, L., McAnally, L.M., Ramberg, J., and Lipsky, P.E. (1992). Generation of nondividing high rate Ig-secreting plasma cells in cultures of human B cells stimulated with anti-CD3-activated T cells. J Immunol *148*, 404-410.

Vignali, M., Hassan, A.H., Neely, K.E., and Workman, J.L. (2000). ATP-dependent chromatin-remodeling complexes. Mol Cell Biol *20*, 1899-1910.

Wahl, M.C., Will, C.L., and Luhrmann, R. (2009). The spliceosome: design principles of a dynamic RNP machine. Cell *136*, 701-718.

Wang, Z., and Burge, C.B. (2008). Splicing regulation: from a parts list of regulatory elements to an integrated splicing code. RNA *14*, 802-813.

Watanabe, C., Morita, M., Hayata, T., Nakamoto, T., Kikuguchi, C., Li, X., Kobayashi, Y., Takahashi, N., Notomi, T., Moriyama, K.*, et al.* (2014). Stability of mRNA influences osteoporotic bone mass via CNOT3. Proc Natl Acad Sci U S A *111*, 2692-2697.

Weinberg, R.A. (1995). The retinoblastoma protein and cell cycle control. Cell *81*, 323-330.

West, S., Gromak, N., and Proudfoot, N.J. (2004). Human 5' --> 3' exonuclease Xrn2 promotes transcription termination at co-transcriptional cleavage sites. Nature *432*, 522-525.

White, R.J. (2011). Transcription by RNA polymerase III: more complex than we thought. Nat Rev Genet *12*, 459-463.

Will, C.L., and Luhrmann, R. (2011). Spliceosome structure and function. Cold Spring Harb Perspect Biol *3*.

Winkler, G.S., Mulder, K.W., Bardwell, V.J., Kalkhoven, E., and Timmers, H.T. (2006). Human Ccr4-Not complex is a ligand-dependent repressor of nuclear receptor-mediated transcription. EMBO J *25*, 3089-3099.

Wolf, J., and Passmore, L.A. (2014). mRNA deadenylation by Pan2-Pan3. Biochem Soc Trans *42*, 184-187.

Wong, J.M., and Bateman, E. (1994). TBP-DNA interactions in the minor groove discriminate between A:T and T:A base pairs. Nucleic Acids Res *22*, 1890-1896.

Xu, Y.Z., Newnham, C.M., Kameoka, S., Huang, T., Konarska, M.M., and Query, C.C. (2004). Prp5 bridges U1 and U2 snRNPs and enables stable U2 snRNP association with intron RNA. EMBO J *23*, 376-385.

Yamaguchi, Y., Takagi, T., Wada, T., Yano, K., Furuya, A., Sugimoto, S., Hasegawa, J., and Handa, H. (1999). NELF, a multisubunit complex containing RD, cooperates with DSIF to repress RNA polymerase II elongation. Cell *97*, 41-51.

Yamashita, A., Chang, T.C., Yamashita, Y., Zhu, W., Zhong, Z., Chen, C.Y., and Shyu, A.B. (2005). Concerted action of poly(A) nucleases and decapping enzyme in mammalian mRNA turnover. Nat Struct Mol Biol *12*, 1054-1063.

Yoshida, T., Ng, S.Y., Zuniga-Pflucker, J.C., and Georgopoulos, K. (2006). Early hematopoietic lineage restrictions directed by Ikaros. Nat Immunol *7*, 382-391.

Yusuf, I., and Fruman, D.A. (2003). Regulation of quiescence in lymphocytes. Trends Immunol *24*, 380-386.

Zamore, P.D., and Green, M.R. (1989). Identification, purification, and biochemical characterization of U2 small nuclear ribonucleoprotein auxiliary factor. Proc Natl Acad Sci U S A *86*, 9243-9247.

Zeitlin, S.G., Shelby, R.D., and Sullivan, K.F. (2001). CENP-A is phosphorylated by Aurora B kinase and plays an unexpected role in completion of cytokinesis. J Cell Biol *155*, 1147-1157.

Zetterberg, A., and Larsson, O. (1985). Kinetic analysis of regulatory events in G1 leading to proliferation or quiescence of Swiss 3T3 cells. Proc Natl Acad Sci U S A *82*, 5365-5369.

Zhang, Y., Liu, T., Meyer, C.A., Eeckhoute, J., Johnson, D.S., Bernstein, B.E., Nusbaum, C., Myers, R.M., Brown, M., Li, W.*, et al.* (2008). Model-based analysis of ChIP-Seq (MACS). Genome Biol *9*, R137.

Zheng, X., Dumitru, R., Lackford, B.L., Freudenberg, J.M., Singh, A.P., Archer, T.K., Jothi, R., and Hu, G. (2012). Cnot1, Cnot2, and Cnot3 maintain mouse and human ESC identity and inhibit extraembryonic differentiation. Stem Cells *30*, 910-922.

Zhu, J., Mayeda, A., and Krainer, A.R. (2001). Exon identity established through differential antagonism between exonic splicing silencer-bound hnRNP A1 and enhancer-bound SR proteins. Mol Cell *8*, 1351-1361.

Zwartjes, C.G., Jayne, S., van den Berg, D.L., and Timmers, H.T. (2004). Repression of promoter activity by CNOT2, a subunit of the transcription regulatory Ccr4-not complex. J Biol Chem *279*, 10848-10854.

Appendix

Table A: Cnot3 interactors in early G1 and G2.
591 proteins were detected by MS analysis after Cnot3 IPs carried out in early G1 and G2. The table reports the protein name, the protein score and Normalised MS intensities (fold over max). See Materials and Methods section 2.7.6 for details.

Normalised MS intensities (fold over max)										
0	0.1	0.2	0.3	0.4	0.5	0.6	0.7	0.8	0.9	1

Protein name	Protein score	Control	G1	G2
CNOT1_MOUSE	3528.449744			
DDX21_MOUSE	1393.945489			
TOP2A_MOUSE	1289.480389			
NUCL_MOUSE	1228.040559			
RRP5_MOUSE	1163.337728			
NPAT_MOUSE	1107.526525			
RL3_MOUSE	1093.419356			
PABP1_MOUSE	992.6687118			
TB182_MOUSE	988.8592707			
H12_MOUSE	922.245237			
U520_MOUSE	882.3503041			
H4_MOUSE	869.47			
CROCC_MOUSE	866.5340332			
PRP8_MOUSE	857.4147619			
RL4_MOUSE	841.2299151			
H2AY_MOUSE	827.2599151			
H14_MOUSE	824.4873388			
NOP56_MOUSE	795.9828795			
H13_MOUSE	787.573305			
NOP2_MOUSE	778.011932			
YBOX1_MOUSE	772.4920169			
MBB1A_MOUSE	732.608542			
MTMR5_MOUSE	731.7853219			
DHX9_MOUSE	717.1753219			
ACTH_MOUSE	708.2053219			
SON_MOUSE	675.4480675			
HNRPC_MOUSE	674.5953219			
H15_MOUSE	666.033305			
ROA3_MOUSE	658.563305			
H11_MOUSE	654.6265251			
RL6_MOUSE	646.7066101			
QCR2_MOUSE	644.63			
HNRPU_MOUSE	631.1532201			
TPR_MOUSE	628.8886264			
CNO10_MOUSE	612.8521862			

IQGA1_MOUSE	612.5225758			
RL7A_MOUSE	596.8166101			
TOP2B_MOUSE	577.7766095			
ROA2_MOUSE	576.3			
RLA0_MOUSE	567.8166101			
RS3A_MOUSE	566.2373388			
RL5_MOUSE	556.8166101			
RMXL1_MOUSE	552.5598302			
H2B1H_MOUSE	550.163305			
RBMX_MOUSE	545.1432201			
SRRM2_MOUSE	507.1702521			
RL7_MOUSE	503.9760506			
ANR17_MOUSE	490.6826607			
H33_MOUSE	489.8753219			
RS18_MOUSE	466.9266101			
WDR62_MOUSE	465.7066101			
NOP58_MOUSE	463.443305			
SMCA5_MOUSE	458.4164402			
RRBP1_MOUSE	456.4061305			
ROA1_MOUSE	454.3286269			
DDX3L_MOUSE	444.943305			
H2A2C_MOUSE	439.1966101			
UBF1_MOUSE	435.2599151			
IF4A3_MOUSE	434.5366101			
RL8_MOUSE	422.7			
RENT1_MOUSE	417.17			
H1T_MOUSE	413.903305			
FBRL_MOUSE	413.583305			
CAPR1_MOUSE	408.6299151			
H2B3B_MOUSE	407.483305			
RS6_MOUSE	400.723305			
RL30_MOUSE	398.41			
NPM_MOUSE	398.243305			
LYAR_MOUSE	389.7287118			
H3C_MOUSE	388.793305			
MDC1_MOUSE	388.2588811			
IMA1_MOUSE	386.903305			
ARP3_MOUSE	384.7099151			
RLA2_MOUSE	380.99			
HELZ2_MOUSE	376.2132201			
AZI1_MOUSE	370.2232201			
RN219_MOUSE	367.5686269			
RS14_MOUSE	363.6553219			
EF2_MOUSE	362.3820169			
H2AX_MOUSE	361.4			
NAT10_MOUSE	361.041932			
RL26_MOUSE	359.353305			
DDX3Y_MOUSE	359.1			
TOP1_MOUSE	357.1614574			
HNRPQ_MOUSE	354.1820169			
TBA1C_MOUSE	351.63			
CNO11_MOUSE	350.58			

TR150_MOUSE	348.983305			
NPA1P_MOUSE	347.6286269			
RBM14_MOUSE	346.123305			
RL9_MOUSE	340.163305			
COR1A_MOUSE	340.11			
RL14_MOUSE	339.903305			
DDX24_MOUSE	337.3653219			
ALDH2_MOUSE	335.97			
MYO1G_MOUSE	334.9953219			
BCLF1_MOUSE	332.3920169			
H2B1A_MOUSE	327.45			
PRP19_MOUSE	327.19			
H2B2E_MOUSE	326.87			
HNRL2_MOUSE	325.64			
HP1B3_MOUSE	324.3687118			
CPSF1_MOUSE	324.2			
G3BP1_MOUSE	322.9166101			
RS9_MOUSE	320.2853219			
RUVB1_MOUSE	315.453305			
RS2_MOUSE	308.96			
RAVR1_MOUSE	308.173305			
PARP1_MOUSE	305.2366101			
RS8_MOUSE	304.4			
ACINU_MOUSE	303.6687118			
YBOX3_MOUSE	299.223305			
FLNA_MOUSE	296.8186269			
RL24_MOUSE	296.2866101			
RCD1_MOUSE	295.183305			
CNOT6_MOUSE	293.48			
RSSA_MOUSE	292.233305			
DKC1_MOUSE	289.263305			
RRP1B_MOUSE	288.463305			
RL23A_MOUSE	284.3787118			
GEMI5_MOUSE	283.7153219			
ARHG6_MOUSE	283.563305			
RL19_MOUSE	282.5587118			
RL18_MOUSE	281.883305			
RL28_MOUSE	280.0374237			
CNOT2_MOUSE	278.8120169			
MYO1C_MOUSE	276.9486269			
SRSF7_MOUSE	276.43			
GBLP_MOUSE	275.813305			
RL12_MOUSE	275.223305			
RL10A_MOUSE	275.0386269			
SRSF1_MOUSE	274.8932201			
EBP2_MOUSE	272.3786269			
PAIRB_MOUSE	269.7420169			
SYF1_MOUSE	267.46			
U5S1_MOUSE	267.16			
LBR_MOUSE	266.1787118			
TRA2B_MOUSE	265.2366101			
RS17_MOUSE	263.393305			

RL17_MOUSE	261.9			
SAFB1_MOUSE	260.3840337			
RS27A_MOUSE	260.073305			
LARP1_MOUSE	258.5			
HNRPK_MOUSE	258.4787118			
NOL6_MOUSE	256.79			
SCRIB_MOUSE	256.223305			
DDX17_MOUSE	252.9166101			
RL10_MOUSE	252.89			
PCBP1_MOUSE	249.426695			
TBB2B_MOUSE	245.39			
TBB4A_MOUSE	244.58			
DHX15_MOUSE	241.3765251			
CHD4_MOUSE	241.3239488			
K2C6A_MOUSE	240.493305			
DDX18_MOUSE	240.153305			
RL31_MOUSE	239.82			
PININ_MOUSE	237.9066101			
SF3B3_MOUSE	237.863305			
CLH1_MOUSE	237.8487118			
RL37A_MOUSE	236.42			
RS7_MOUSE	234.43			
ROAA_MOUSE	233.73			
HNRPD_MOUSE	233.15			
AURKB_MOUSE	233.0321846			
HNRPL_MOUSE	232.9666101			
RL35_MOUSE	232.6366101			
RL36A_MOUSE	230.6131352			
SRSF3_MOUSE	230.603305			
RL34_MOUSE	230.113305			
PRC2A_MOUSE	226.9873388			
RL21_MOUSE	226.52			
PTBP1_MOUSE	225.26			
HDGR2_MOUSE	223.8587118			
UTP20_MOUSE	222.7994406			
DDX47_MOUSE	222.79			
RS5_MOUSE	222.753305			
CBX3_MOUSE	218.93			
MOV10_MOUSE	218.93			
ROA0_MOUSE	215.06			
CAZA1_MOUSE	213.94			
DDX51_MOUSE	213.666695			
RS13_MOUSE	211.3087118			
SMCA1_MOUSE	211.2066101			
ECHA_MOUSE	209.933305			
MTA2_MOUSE	207.9127456			
CNOT8_MOUSE	206.993305			
UHRF1_MOUSE	205.9166101			
H2AV_MOUSE	203.933305			
UBP2L_MOUSE	203.18			
DNJC9_MOUSE	202.2166101			
WDR46_MOUSE	202.083305			

CG050_MOUSE	201.8			
MK67I_MOUSE	201.563305			
UBB_MOUSE	200.5866929			
HNRPF_MOUSE	200.4901678			
CDC5L_MOUSE	200.3987118			
TCPD_MOUSE	199.433305			
RL27_MOUSE	198.633305			
TCPE_MOUSE	197.493305			
CNO6L_MOUSE	194.893305			
GNL3_MOUSE	194.7487118			
HNRH2_MOUSE	194.6			
C8AP2_MOUSE	193.7873388			
RL10L_MOUSE	193.7			
RN213_MOUSE	192.3865251			
PR40A_MOUSE	192.1420169			
SP16H_MOUSE	191.7987118			
AQR_MOUSE	191.6420169			
SAFB2_MOUSE	191.6366101			
RL35A_MOUSE	191.42			
YBOX2_MOUSE	191.32			
H2AZ_MOUSE	189.56			
LARP4_MOUSE	188.08			
ARP3B_MOUSE	187.97			
PP1A_MOUSE	187.0187118			
FXR1_MOUSE	185.4353219			
GLYR1_MOUSE	184.0766101			
ABEC3_MOUSE	182.353305			
RL18A_MOUSE	181.18			
IF4G1_MOUSE	180.6174237			
NHP2_MOUSE	178.68			
LA_MOUSE	178.3966101			
FMR1_MOUSE	178.0387118			
ARP2_MOUSE	177.68			
WDR3_MOUSE	176.43			
HNRDL_MOUSE	176.403305			
PTN6_MOUSE	176.33			
KAP2_MOUSE	176.3			
PP1G_MOUSE	174.64			
ELYS_MOUSE	173.7			
KI20A_MOUSE	172.94			
EDC4_MOUSE	171.4387118			
CI114_MOUSE	169.5687118			
CHTOP_MOUSE	169.445237			
PYR1_MOUSE	169.3720169			
RL22_MOUSE	168.27			
K1C15_MOUSE	168			
SFPQ_MOUSE	167.673305			
RL27A_MOUSE	167.15			
LSP1_MOUSE	166.7687118			
MATR3_MOUSE	165.94			
XRN2_MOUSE	164.9920169			
RUVB2_MOUSE	161.4587118			

OASL1_MOUSE	161.14			
SSRP1_MOUSE	160.9887118			
BAZ1B_MOUSE	160.7166101			
THOC2_MOUSE	159.92			
PCNT_MOUSE	157.3873388			
SYNE1_MOUSE	156.7648453			
ILF2_MOUSE	155.78			
RS25_MOUSE	155.71			
DDX1_MOUSE	155.563305			
RBBP4_MOUSE	155.243305			
ISY1_MOUSE	155.16			
DDX6_MOUSE	154.803305			
C1TM_MOUSE	153.853305			
RBM25_MOUSE	152.33			
RL13A_MOUSE	151.353305			
BAZ1A_MOUSE	151.2566101			
RS15A_MOUSE	150.1			
U3IP2_MOUSE	149.183305			
SPB1_MOUSE	148.54			
SRSF5_MOUSE	147.38			
RS12_MOUSE	146.84			
RL36_MOUSE	146.09			
K0020_MOUSE	145.6299151			
IMB1_MOUSE	144.29			
MTMR1_MOUSE	143.043305			
NH2L1_MOUSE	142.91			
NOG1_MOUSE	142.503305			
DHX8_MOUSE	140.7040337			
TRIPC_MOUSE	138.1721018			
CNOT7_MOUSE	138.08			
KAPCA_MOUSE	137.55			
GIT2_MOUSE	137.24			
PRDX1_MOUSE	135.24			
HNRH1_MOUSE	134.25			
CEP85_MOUSE	134.1199151			
CRNL1_MOUSE	134.1066101			
MRT4_MOUSE	134.0720169			
PGAM5_MOUSE	133.45			
CDC73_MOUSE	133.2432201			
SRSF4_MOUSE	132.5520169			
ZC11A_MOUSE	132.283305			
CTR9_MOUSE	132.063305			
NCOR1_MOUSE	131.9532201			
H2A3_MOUSE	131.143305			
RL29_MOUSE	130.063305			
SF3B1_MOUSE	129.7266101			
AGO2_MOUSE	129.59			
EIF3A_MOUSE	128.8265251			
CN166_MOUSE	128.11			
TCPA_MOUSE	126.9453219			
RU2A_MOUSE	126.6720169			
RS10_MOUSE	126.6			

H2B2B_MOUSE	126.1820169			
GFAP_MOUSE	125.71			
CH60_MOUSE	125.483305			
IF6_MOUSE	125.2			
EIF3F_MOUSE	124.96			
SNW1_MOUSE	124.7799151			
TNR6A_MOUSE	123.933305			
DOCK2_MOUSE	123.9234728			
PP1B_MOUSE	122.71			
SYNE2_MOUSE	122.1528641			
DNLI3_MOUSE	121.9221846			
PLRG1_MOUSE	121.7766101			
UIF_MOUSE	121.42			
KAPCB_MOUSE	120.4174237			
RL15_MOUSE	120.16			
RALY_MOUSE	119.7666101			
EVPL_MOUSE	119.2632201			
HYOU1_MOUSE	119.12			
SMC1B_MOUSE	118.9499151			
SAMH1_MOUSE	118.78			
LPPRC_MOUSE	118.673305			
RBM28_MOUSE	118.67			
LACTB_MOUSE	118.033305			
RCC2_MOUSE	117.523305			
SAP18_MOUSE	116.943305			
RS26_MOUSE	116.48			
ELAV1_MOUSE	115.07			
ARC1B_MOUSE	115.0687118			
GAR1_MOUSE	114.78			
WDR43_MOUSE	114.55			
CN37_MOUSE	113.143305			
CD11B_MOUSE	113.0466101			
LAR4B_MOUSE	112.8866101			
CAPZB_MOUSE	112.81			
PCBP2_MOUSE	112.04			
NUFP2_MOUSE	111.91			
DHX30_MOUSE	111.62			
CK5P2_MOUSE	110.603305			
DYH17_MOUSE	109.9607407			
SAHH_MOUSE	109.1266101			
FXR2_MOUSE	109			
ATX2L_MOUSE	108.77			
PRKDC_MOUSE	108.5366101			
RL32_MOUSE	108.51			
DDX49_MOUSE	107.99			
MCM5_MOUSE	106.473305			
DDX27_MOUSE	106.31			
M4K4_MOUSE	106.0486269			
CBX1_MOUSE	105.99			
KV3A7_MOUSE	105.773305			
RBM39_MOUSE	104.5			
MED12_MOUSE	104.103305			

VIGLN_MOUSE	102.953305			
INCE_MOUSE	102.483305			
LAMA2_MOUSE	102.1287118			
SRP14_MOUSE	101.86			
DDX54_MOUSE	101.62			
DYH2_MOUSE	101.2927456			
PR38A_MOUSE	101.0820169			
GON4L_MOUSE	100.7299151			
GOGA4_MOUSE	100.6708965			
RLA1_MOUSE	100.6			
RALYL_MOUSE	100.493305			
PIWL1_MOUSE	100.4866101			
LMNA_MOUSE	100.46			
SURF6_MOUSE	99.97661006			
ASPM_MOUSE	99.62240498			
ABCAD_MOUSE	99.52523699			
SRS10_MOUSE	99.1853219			
RS28_MOUSE	98.81			
RPGF2_MOUSE	98.68201687			
RNPS1_MOUSE	97.7			
TBL3_MOUSE	97.42742369			
UTP15_MOUSE	97.39			
VPS53_MOUSE	97.37991508			
ALDR_MOUSE	97.04			
LORF2_MOUSE	96.59862693			
CHD2_MOUSE	96.32540682			
DX39A_MOUSE	96.2			
LAMA1_MOUSE	96.14			
EPIPL_MOUSE	95.94519895			
PSMD3_MOUSE	95.72330503			
TCPZ_MOUSE	95.37			
1433T_MOUSE	94.95			
PESC_MOUSE	94.76330503			
LARP7_MOUSE	94.43			
EIF3C_MOUSE	94.34330503			
ACSF2_MOUSE	94.1			
DX39B_MOUSE	94.03			
HYDIN_MOUSE	93.7853219			
SSA27_MOUSE	93.51			
RAC2_MOUSE	92.76			
NOL9_MOUSE	92.66330503			
TLN1_MOUSE	92.43			
BAG6_MOUSE	92.28			
IF4A1_MOUSE	92.14			
NUSAP_MOUSE	91.03			
ROCK2_MOUSE	90.80540682			
SYDC_MOUSE	90.58			
GCC2_MOUSE	90.51661006			
PLEC_MOUSE	90.39832017			
DDB1_MOUSE	90.32330503			
TT23L_MOUSE	90.11862693			
CMC1_MOUSE	90.01330503			

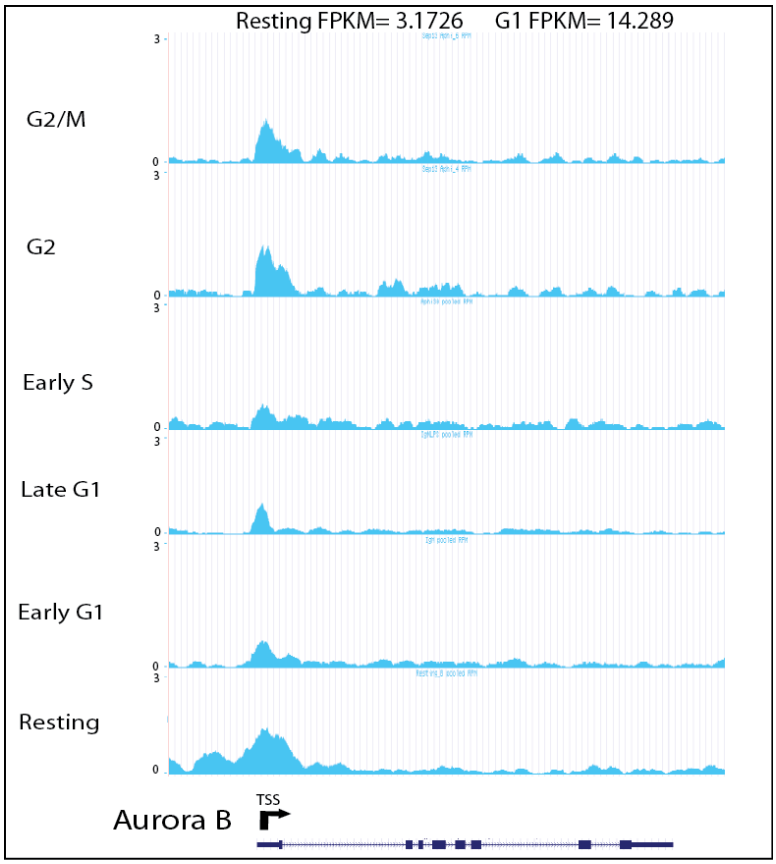
DDX52_MOUSE	89.90661006			
GNAL_MOUSE	89.46661006			
RS24_MOUSE	89.39330503			
LYST_MOUSE	88.86			
CHM4B_MOUSE	87.50330503			
MICA3_MOUSE	87.3953219			
HDAC2_MOUSE	87.34072872			
DDX56_MOUSE	87.30330503			
SLTM_MOUSE	87.18661006			
TBB1_MOUSE	87.06			
NONO_MOUSE	86.98			
SYVC_MOUSE	86.89201687			
FHAD1_MOUSE	86.65862693			
NACC1_MOUSE	86.61			
RBBP7_MOUSE	86.53330503			
ZN512_MOUSE	86.53			
CKP2L_MOUSE	86.44862693			
CTRO_MOUSE	86.43733877			
PELP1_MOUSE	86.35			
CE290_MOUSE	86.06862693			
CMYA5_MOUSE	85.68338788			
CAZA2_MOUSE	85.61			
SYNEM_MOUSE	85.44			
DYH12_MOUSE	85.37055889			
LDHA_MOUSE	85.24			
SMC2_MOUSE	85.06201687			
ITPR2_MOUSE	84.78201687			
MAST4_MOUSE	84.76072872			
UCKL1_MOUSE	84.62330503			
ATX7_MOUSE	84.52322011			
RRS1_MOUSE	84.5			
THOC5_MOUSE	84.28330503			
SNUT1_MOUSE	84.06661006			
CCNL2_MOUSE	83.74			
DHX36_MOUSE	83.35330503			
AURKA_MOUSE	82.83661006			
SAS10_MOUSE	82.78			
RP1_MOUSE	82.75733877			
ERC2_MOUSE	82.65991508			
EXOS5_MOUSE	82.6			
MGT4A_MOUSE	82.42			
CDAN1_MOUSE	82.39330503			
U2AF1_MOUSE	82.38			
ESF1_MOUSE	82.36201687			
KI21B_MOUSE	82.28862693			
GVIN1_MOUSE	82.18484738			
KIF27_MOUSE	82.11742369			
CTTB2_MOUSE	82.09			
CLK1_MOUSE	82.03661006			
GNAI2_MOUSE	81.94871184			
DYHC2_MOUSE	81.76652514			
MRCKA_MOUSE	81.75201687			

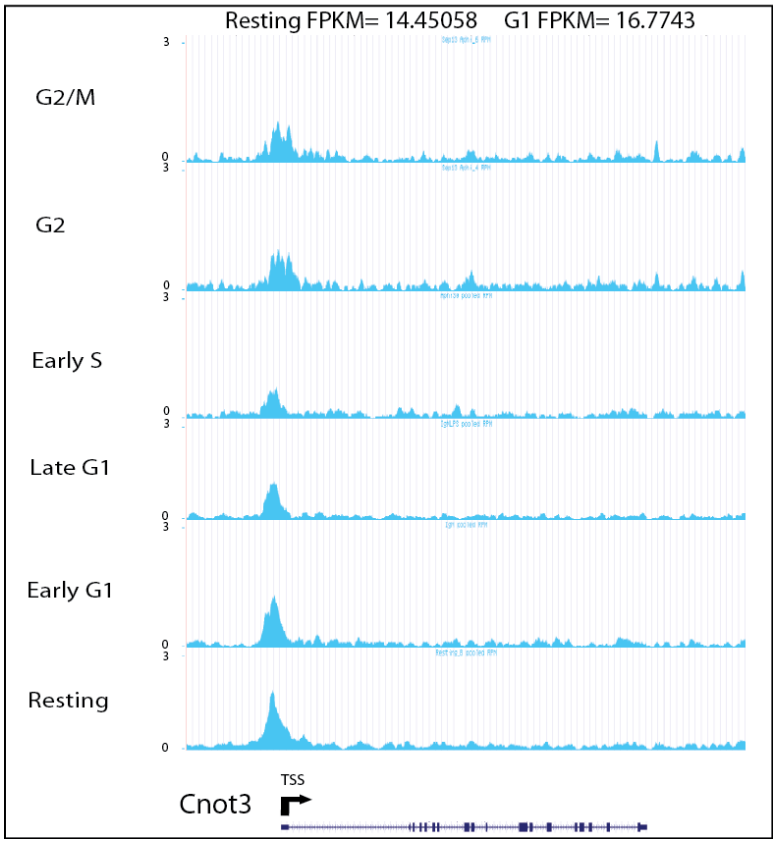
THOC4_MOUSE	81.67			
ZN292_MOUSE	80.99193196			
SPTN1_MOUSE	80.82944056			
GPR98_MOUSE	80.56661006			
CSDE1_MOUSE	80.56330503			
MAP11_MOUSE	80.54			
EIF3D_MOUSE	80.37			
S12A2_MOUSE	80.26201687			
TEFM_MOUSE	80.20330503			
HIP1_MOUSE	80			
PRP6_MOUSE	79.68330503			
CUL1_MOUSE	79.33330503			
TLN2_MOUSE	78.89733877			
DSRAD_MOUSE	78.78330503			
RRP12_MOUSE	78.76330503			
SSF1_MOUSE	78.71			
RTN4_MOUSE	78.68			
FCRLA_MOUSE	78.63330503			
CCD38_MOUSE	78.30871184			
GIT1_MOUSE	78.26			
CENPJ_MOUSE	78.21201687			
TNIK_MOUSE	77.91991508			
FIP1_MOUSE	77.84			
RPF2_MOUSE	77.77330503			
SPKAP_MOUSE	77.74330503			
SCLT1_MOUSE	77.43523699			
MYOM1_MOUSE	77.29201687			
RBM33_MOUSE	77.11			
ETAA1_MOUSE	76.99193196			
APC_MOUSE	76.43114917			
H2AW_MOUSE	76.3			
HDAC1_MOUSE	76.13			
4ET_MOUSE	75.98669497			
CCD86_MOUSE	75.83			
KRT86_MOUSE	75.81			
ADA12_MOUSE	75.61661006			
EP300_MOUSE	75.49661006			
PCBP3_MOUSE	75.36094755			
PERQ2_MOUSE	75.35			
LRIF1_MOUSE	75.32944056			
NOC2L_MOUSE	75.22			
NUCB2_MOUSE	75.15			
FBF1_MOUSE	75.12330503			
TIF1B_MOUSE	74.99661006			
WWC2_MOUSE	74.86330503			
FR1OP_MOUSE	74.8			
DNJA1_MOUSE	74.68			
MY18A_MOUSE	74.64201687			
HS105_MOUSE	74.63661006			
CBX5_MOUSE	74.47330503			
CKAP5_MOUSE	74.34983017			
K2022_MOUSE	74.26871184			

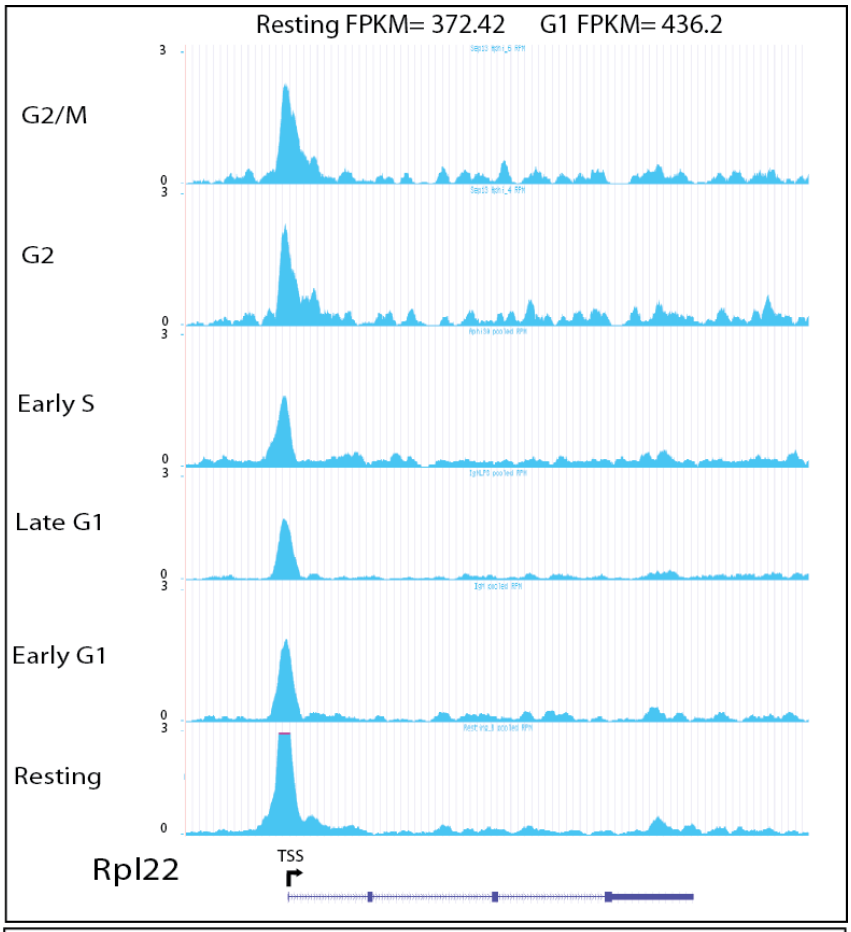
SMD1_MOUSE	74.2			
TCPQ_MOUSE	74.2			
SR140_MOUSE	73.71862693			
COCA1_MOUSE	73.71201687			
BLM_MOUSE	73.68016777			
FAT3_MOUSE	73.43201687			
DOCK8_MOUSE	73.3053219			
UT14A_MOUSE	73.08			
ZCCHV_MOUSE	72.62			
RS30_MOUSE	72.58			
RRP8_MOUSE	72.47			
CDK1_MOUSE	72.45			
RFC1_MOUSE	72.40871184			
SRRM1_MOUSE	72.39871184			
FBLL1_MOUSE	72.27			
IGSF2_MOUSE	72.24330503			
CBP_MOUSE	72.18661006			
LRWD1_MOUSE	72.07			
RIMB3_MOUSE	72.05330503			
TPX2_MOUSE	71.67661006			
CIP2A_MOUSE	71.63991508			
UBN1_MOUSE	71.60330503			
RTCB_MOUSE	71.59			
ANFY1_MOUSE	71.44			
FLNB_MOUSE	71.35			
TCF20_MOUSE	71.33			
BIG3_MOUSE	71.25661006			
MAP7_MOUSE	71.19733877			
TTLL7_MOUSE	71.11991508			
PTRF_MOUSE	71.09871184			
TRRAP_MOUSE	71.08330503			
IGFN1_MOUSE	70.97733877			
ODF2L_MOUSE	70.97661006			
LAMC1_MOUSE	70.91201687			
M3K6_MOUSE	70.88330503			
DPOLB_MOUSE	70.73661006			
GOGA5_MOUSE	70.7			
RS29_MOUSE	70.7			
RCL1_MOUSE	70.58			
ZEP1_MOUSE	70.50661006			
ZN638_MOUSE	70.5053219			
IQGA2_MOUSE	70.45			
GRWD1_MOUSE	70.42330503			
DMD_MOUSE	70.36854201			
F178A_MOUSE	70.36661006			
OBSCN_MOUSE	70.30089648			
NOG2_MOUSE	70.25871184			
EME1_MOUSE	70.23330503			
NEST_MOUSE	69.97330503			
RFIP1_MOUSE	69.71201687			
DDX50_MOUSE	69.69871184			
ALMS1_MOUSE	69.69072872			

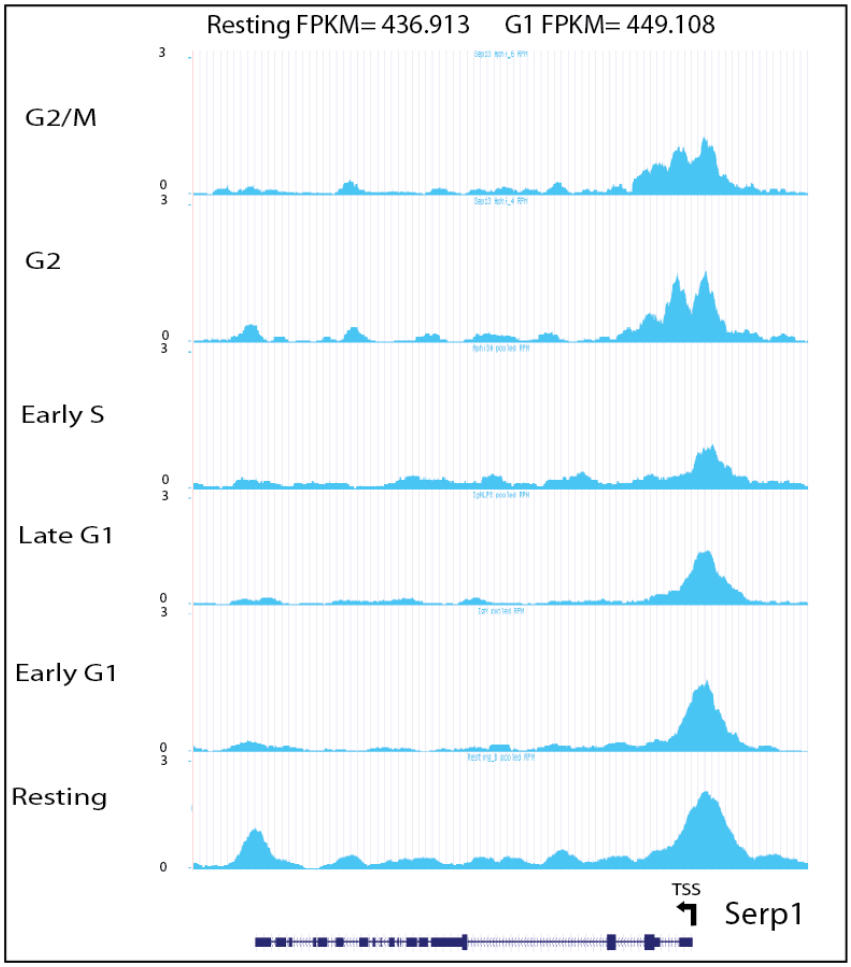
CLK4_MOUSE	69.46			
EIF3H_MOUSE	69.12			
DESP_MOUSE	68.97355922			
DDX20_MOUSE	68.72			
RGRF1_MOUSE	68.45330503			
KMT2D_MOUSE	68.34338788			
TIAM2_MOUSE	68.33330503			
DPOE1_MOUSE	68.14661006			
EEA1_MOUSE	67.99871184			
CTND2_MOUSE	67.96330503			
RAI14_MOUSE	67.94991508			
THADA_MOUSE	67.83330503			
SDHA_MOUSE	67.81			
RB6I2_MOUSE	67.80330503			
K1109_MOUSE	67.64322011			
RYR1_MOUSE	67.63330503			
CNTRL_MOUSE	67.62887961			
GNAS2_MOUSE	67.42330503			
KI26B_MOUSE	67.25733877			
TNR6B_MOUSE	67.25			
TTC3_MOUSE	67.2353219			
APC2_MOUSE	67.1853219			
G3BP2_MOUSE	67.16			
UTP18_MOUSE	67.15			
HAUS1_MOUSE	66.9053219			
RBP2_MOUSE	66.80742369			
NINL_MOUSE	66.65661006			
TCPH_MOUSE	66.64661006			
IPYR2_MOUSE	66.57			
SP110_MOUSE	66.51330503			
TDIF2_MOUSE	66.41330503			
PLSL_MOUSE	66.39			
ARPC3_MOUSE	66.30330503			
K1731_MOUSE	66.27201687			
VP13C_MOUSE	66.18742369			

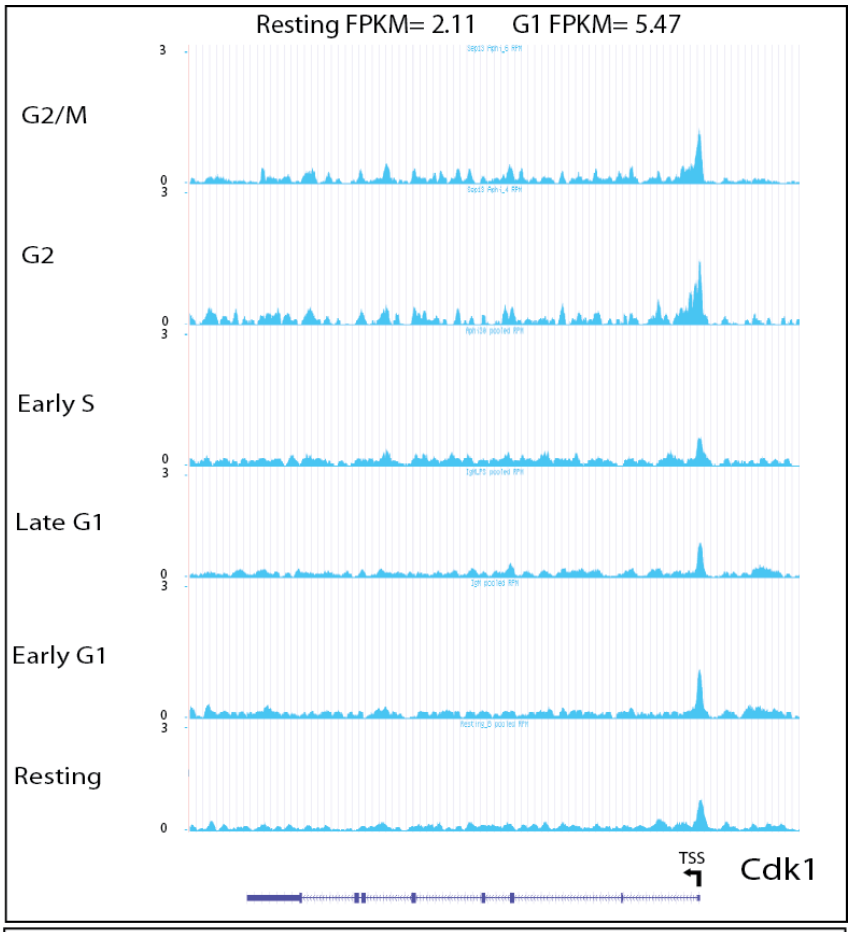
Figure B: Snapshots of ChIP-seq tracks of Cnot3 binding during cell cycle progression.
The figures show snapshots of ChIP-seq tracks for Cnot3 binding in resting, early and late G1, early S, G2 and G2/M. FPKM values are reported in each chart.

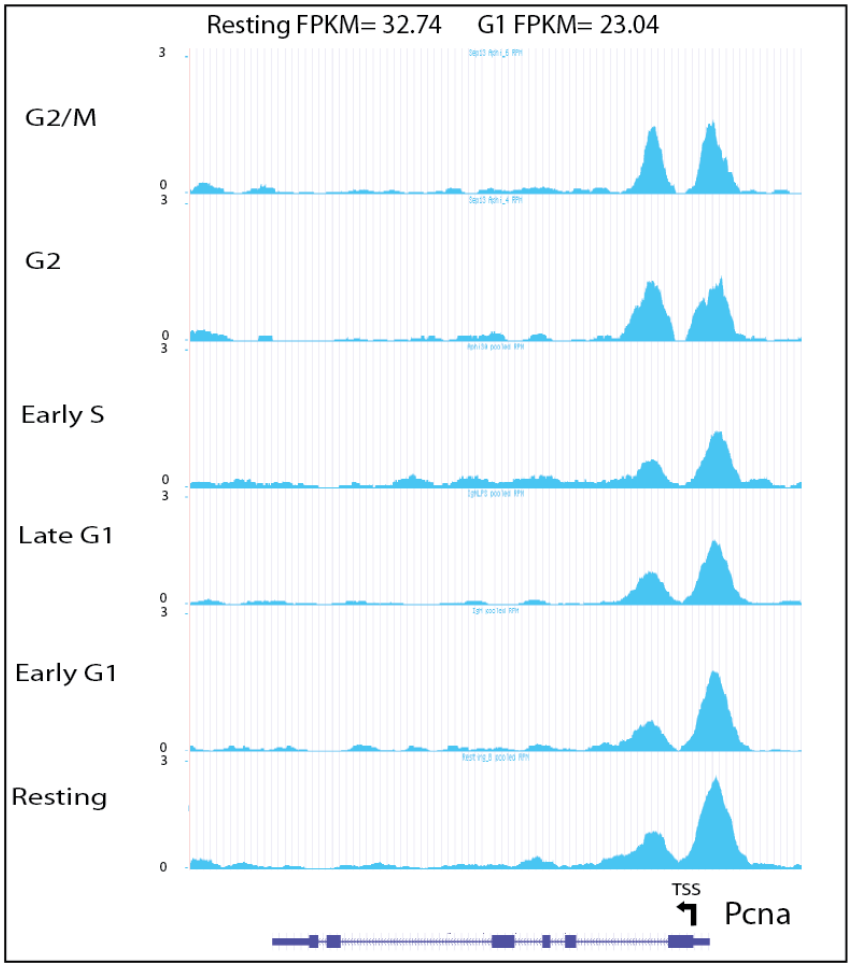


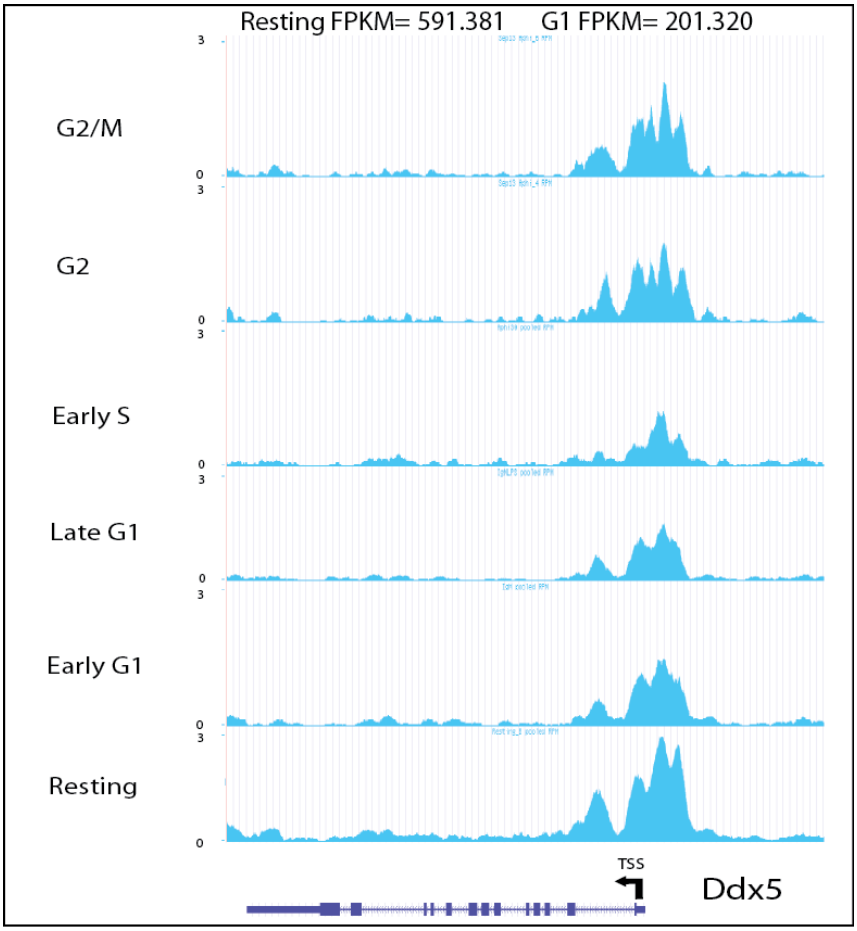


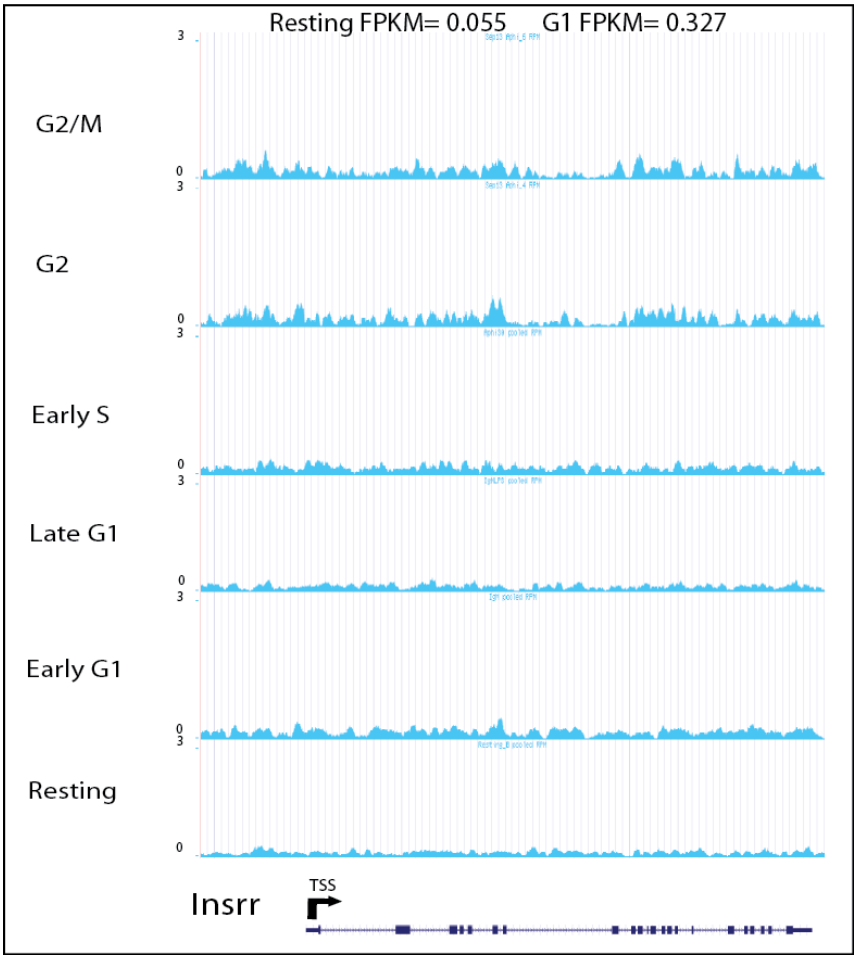

Resting FPKM= 372.42
G1 FPKM= 436.2
G2/M
G2
Early S
Late G1
Early G1
Resting
Rpl22
TSS


Resting FPKM= 436.913
G1 FPKM= 449.108
G2/M
G2
Early S
Late G1
Early G1
Resting
TSS
Serp1


Resting FPKM= 2.11
G1 FPKM= 5.47
G2/M
G2
Early S
Late G1
Early G1
Resting
TSS
Cdk1


Resting FPKM= 32.74
G1 FPKM= 23.04
G2/M
G2
Early S
Late G1
Early G1
Resting
TSS
Pcna


Resting FPKM= 591.381
G1 FPKM= 201.320
G2/M
G2
Early S
Late G1
Early G1
Resting
TSS
Ddx5


Resting FPKM= 0.055
G1 FPKM= 0.327
G2/M
G2
Early S
Late G1
Early G1
Resting
TSS
Insrr